NASA CR 66186

EXPERIMENTAL STUDY OF DYNAMIC EFFECTS OF CREW MOTION IN A MANNED ORBITAL RESEARCH LABORATORY (MORL)

OCTOBER 1966

Prepared under Contract No. NAS 1-5937
by Douglas Aircraft Company, Inc.
Missile and Space Systems Division
Huntington Beach, California
for
NATIONAL AERONAUTICS AND SPACE ADMINISTRATION

NASA CR 66186

EXPERIMENTAL STUDY OF DYNAMIC EFFECTS OF CREW MOTION IN A MANNED ORBITAL RESEARCH LABORATORY (MORL)

OCTOBER 1966

by W.F. FUHRMEISTER
J.L. FOWLER

Prepared under Contract No. NAS 1-5937
by Douglas Aircraft Company, Inc.
Missile and Space Systems Division
Huntington Beach, California
for
NATIONAL AERONAUTICS AND SPACE ADMINISTRATION

CONTENTS

FIGURES

TABLES

SUMMARY

The Experimental Study of Dynamic Effects of Crew Motion in a Manned Orbital Research Laboratory (MORL) was conducted by Douglas Aircraft Company, Inc., Missile and Space Systems Division, for the NASA Langley Research Center.

The program objectives were to define the routine crew motions in a spacecraft, select a simulation scheme, design and fabricate all equipment required for simulation, perform a test series to record the disturbance profiles resulting from these motions, and reduce and analyze the data obtained from the simulation.

The four general categories of crew motion investigated were: (1) body segment motion, (2) exercise, (3) translation, and (4) console operation. The maximum, nominal, and minimum disturbance levels which could be achieved by the test subjects were recorded during the locomotion and console tasks. Only the nominal disturbance level was recorded during simulation of the various exercises and body segment motions. The body segment motions investigated included single pendulum arm motion, double pendulum arm motion, head motion, waist bending, and leg motion. The exercises simulated included trunk bending, neck bending, rowing, pedal ergometer, oscillating acceleration, trunk rotation, and full-length body exercise. Translation involved the investigation of free soaring, guided soaring, velcro walking, and compression walking. Console operation was limited to torquing, sliding, and push-pull operations.

The zero-g simulation scheme basically consists of a counterbalanced pendulous support of the test subject. The suspended subject performs the selected crew motions while in contact with an instrumented platform. The crew motions performed on the platform produce forces and moments which are transmitted through the platform to a six-component force balance. This force balance transforms the three orthogonal forces and three orthogonal moments induced by the subject into electrical signals. These signals are transmitted to the data reduction system which transforms the electrical signals into tabulated data, plotted data, and an analytical expression defining the best fit curve to the plotted data.

After the simulation scheme was selected, the simulation hardware was designed and fabricated. This hardware consists of a velcro walk strip, velcro shoes, foot restraint, hand rails, full-length body exercise machine, pedal ergometer, compression walking simulator, waist restraint, and a control console.

The experimental test program was initiated following fabrication of the simulation equipment. Two subjects were selected to perform the crew motions. Each crew motion was performed three times by each subject.

This ensured that the results were repeatable and that should data be lost during one test, data of the crew motion would be available from the remaining two tests. Data from one of the three tests of each crew motion are presented in this report. These data are presented graphically in the results section and are also presented as a Fourier series in Appendix C.

The test results indicate a large range of forces, cyclic in nature, for the various crew motions performed. In the body segment motion tests, typical forces transmitted to the standing surface are between 3 lb for the double pendulum arm motion and 9 lb for the bending at the waist motion. The predominate periods for these cyclic disturbances are approximately 0.9 sec and 1.7 sec, respectively. The locomotion tests indicate that quiet velcro walking could be performed without transmitting more than 10 lb of force to the walking surface, while for the free soaring locomotion a normal force up to 350 lb can be attained. The predominate sinusoidal periods for these two locomotion tests are 1.0 and 0.5 sec, respectively. For the console operation tests, the disturbance force is nearly the same for the torquing, push-pull, or sliding operations. For a minimum level of the torquing operation, a normal force to the console of 3 lb is produced. For the maximum level, this force is increased to 10 lb. The predominate periods for these cyclic disturbances of the console operation are in the range of 0.2 to 1.0 sec. The range of disturbing forces for the exercises is between 3 lb for the neck bending exercise and 100 lb for the oscillating acceleration exercise. Table 1 shows the range of the disturbance imparted to the standing surface for the various crew motions performed. To investigate the controllability (attitude hold and rate stabilization) of a space station, the various distrubances must be completely described. This description consists of the amplitude and time history of the disturbances. Of the major disturbances--gravity gradient, aerodynamic, and crew motion--influencing MORL attitude, only crew motion does not lend itself to simple analytical or predictable expressions.

With the amplitude and frequency characteristics of the various crew motion disturbances presented in this report, the controllability of a space station can be determined more thoroughly.

All but four of the tests are based on producing disturbances in the local horizontal plane. This primarily avoids the suspension force errors. For these tests the data for the x and y components of force and the z component of moment is calculated to be 6% data. The errors in the suspension force, F_z, will result in errors for the x and y components of moment. However, from all the tests performed, the moments which were referenced to the center of the platform (near the subject's feet) were small compared to the moments produced from the forces acting at a nominal distance. This nominal distance is 6 to 8 ft of separation between the man and the center of mass of a space station. It is illustrated that the moments produced from pure angular accelerations of the various body segments are negligible when compared to the moments produced by the segment forces acting at nominal distances.

TABLE I

CREW MOTION RANGE OF DISTURBANCES

Motion	Standing surface peak distrubance range (lb)
Single pendulum arm motion	2.6 to 3
Double pendulum arm motion	3.2 to 4
Leg motion	4 to 7.6
Bending at waist	8 to 9
Console operation	3 to 13
Guided locomotion	6 to 50
Velcro walking	10 to 50
Compression walking	10 to 74
Free soaring	30 to 350
Pedal ergometer exercise	19 to 20
Trunk bending exercise	13 to 33
Full length body exercise	40 to 62
Oscillating acceleration exercise	98 to 110

The test results indicate that for MORL fine pointing requirements, the crew member may have to be isolated from the spacecraft. This would be accomplished with vibration isolators between the astronaut and the spacecraft to reduce the disturbance transmitted to the spacecraft.

Similar crew motion tests should be conducted for the subject wearing a space suit. This study would simulate the extra vehicular activity (EVA) and would be valuable for use in the orbtial astronomy support facility program.

INTRODUCTION

As spacecraft develop to a point at which they can accommodate more crew members, effects of the crew motions on the spacecraft attitude become increasingly critical. This criticallity was defined in the MORL study. The crew motion effect on the spacecraft's performance will determine which experiments can be adequately handled by the laboratory's control system and which experiments would require separate control or isolation from the laboratory's motion. To define thoroughly the performance capability of a spacecraft being perturbed by crew motions, knowledge of the complete spectrum of the actual distrubances is required.

This report presents the results of a 7-1/2-month Douglas study performed to investigate the distrubance profiles of routine crew motions in a simulated shirt-sleeve, zero-g environment. The investigation included both the analytical prediction of crew motion distrubance profiles and the performance of a test series in a simulated zero-g environment to record the crew motion distrubance profiles.

Simulation of the zero-g environment can be accomplished by supporting the individual body segments with a force equal to and opposite the magnitude of the force resulting from gravity. This can be accomplished in several ways. The subject can be immersed in a water tank and weighed to the point of neutral buoyancy. Another method is to suspend the subject in a servo-controlled gimbal system. Still another method is to suspend the body segments of the subject with cables extending over pulleys and attached to counterweights.

The hydrostatic tank simulation technique is not applicable whenever dynamic data are required. The viscosity of the water reduces both the frequency and magnitude of the distrubance forces. The servo-controlled gimbal system was eliminated primarily because of the cost and development time associated with its implementation.

The counterbalanced pendulous support technique selected for this simulation offers the advantage of being simple, yet provides zero-g simulation with 6% accuracy for limited body motions.

The balance of the report presents the simulation technique, the crew motions simulated, the test results, and the conclusions and recommendations made as a result of the study.

SYMBOLS

F	force, pounds
I	moment of inertia, slug-ft^2
L	pendulum arm length, ft
M	moment, lb-ft
t	time, seconds
W	weight, pounds
x, y, z	rectangular Cartesian coordinates
δ	pendulum displacement, ft
θ	angular displacement x-y plane, radians
$\emptyset$	angular displacement y-z plane, radians
$\dot{\theta}$	angular rate x-y plane, radians per second
$\ddot{\theta}$	angular acceleration x-y plane, radians per second^2

SUBSCRIPTS

i	along i axis
x	along x axis
y	along y axis
z	along z axis
n_i	hinge axis parallel to the i axis
n_x	hinge axis parallel to the x axis
n_y	hinge axis parallel to the y axis
n_z	hinge axis parallel to the z axis
LAL	left arm, lower
LAU	left arm, upper
LLL	left leg, lower
LLU	left leg, upper
T	trunk
RAL	right arm, lower
RAU	right arm, upper
RLL	right leg, lower
RLU	right leg, upper

SIMULATION TECHNIQUE

The experimental setup for the simulation scheme shown in fig. 1 and fig. 2 basically consists of a counterbalanced pendulous support of the test subject to allow contact with an instrumented platform. The platform simulates an interior surface of the space station and is held vertically and attached to the outer sleeve of a six-component force balance. The adapter of the balance is attached to a rigid sting, which in turn is supported by a base fabricated of heavy steel pipe.

The subject's body suspension system includes two arm supports, two leg supports, a torso sling, and a pelvic sling. The arm supports are circular padded members which fit snugly around the arm. Velcro strips on both ends of the support provide adjustment capability to various arm sizes and also are easily connected and disconnected. The left arm support is connected directly to the suspension cable. However, the right arm support is first connected to a U-shaped aluminum rod, which in turn is connected to a suspension cable. The U-shaped rod permits arm motion without interference with the suspension cable, while still maintaining vertical support of the center of mass of the arm. Both leg supports are similar to the arm supports, the only difference being the circular size of the supports. Again, the left leg support is attached directly to the suspension cable, while the right leg support is attached with U-shaped aluminum rod. This rod permits leg motion without interference with the suspension cable while still maintaining a vertical support of the center of mass of the leg. Support for the torso of the subject is provided by an aluminum L-shaped bracket to which a padded sling has been attached. This sling is riveted to the bracket at one end and attaches with a velcro strip to the other end of the bracket, permitting easy adjustment to various chest sizes. The L-shaped aluminum bracket is attached to an offset aluminum rod which allows left arm movement without interference with the torso support cable. A rigidly supported helmet is attached to the L-shaped bracket, as shown in fig. 1. Longitudinal adjustment is provided by two interlocking bolts. Support for the pelvic region is provided by a padded sling attached directly to the suspension cable.

The six suspension cables which attach to the body-segment supports are strung over ball bearing aircraft control pulleys to the respective counterbalance weights. These pulleys are 54 ft above the subject and thus minimize the pendulum effect discussed in the error analysis section of Appendix A.

The platform upon which the simulated crew motions are performed is a 3 x 6 ft surface which has a honeycomb core and aluminum skin material. The two desirable characteristics of this material, stiffness and small weight, were required for the accurate transmission of the distrubance profiles to the force balance. Errors introduced by this platform are presented in the error analysis section of Appendix A.

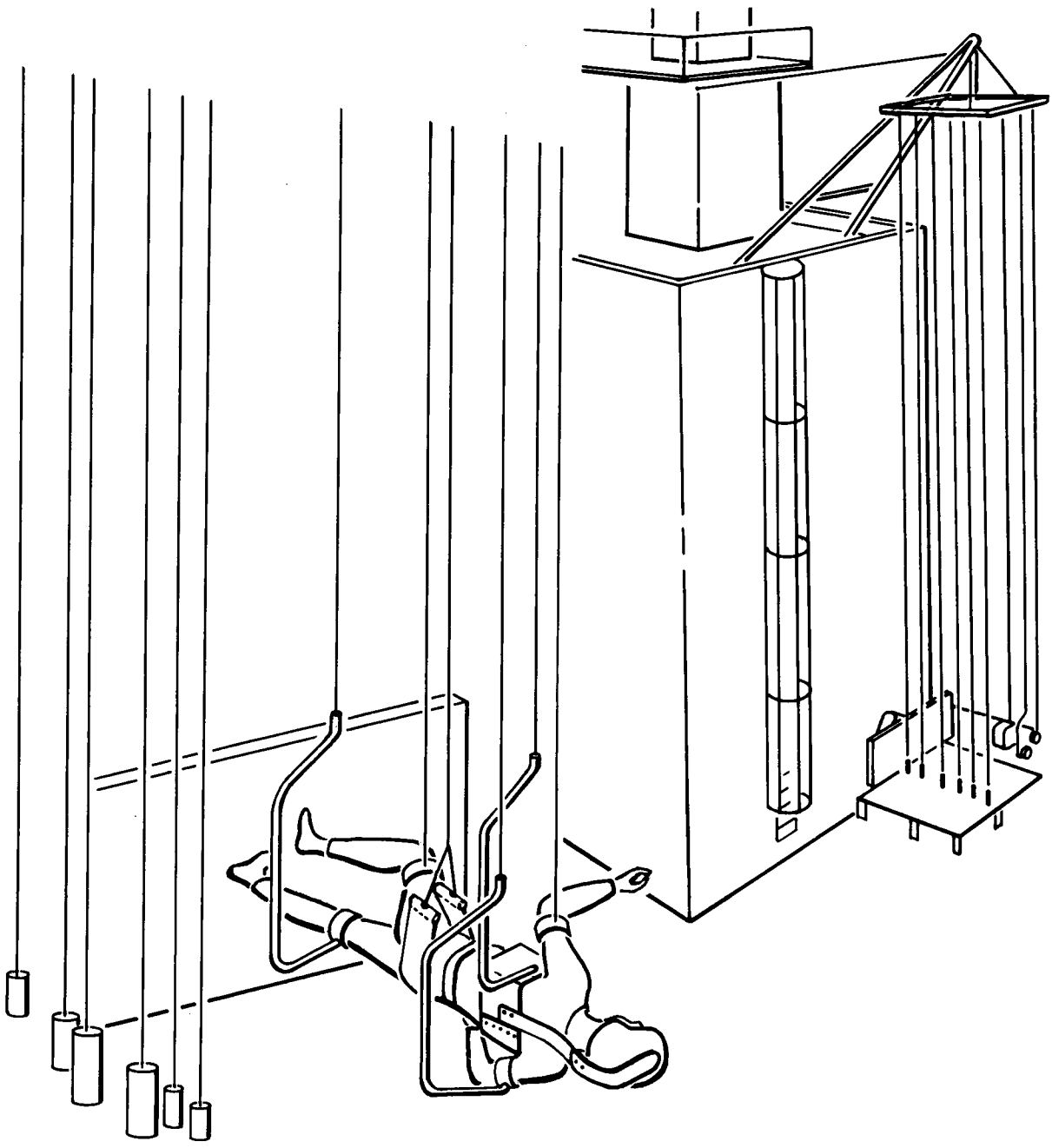

Figure 1. Test Setup

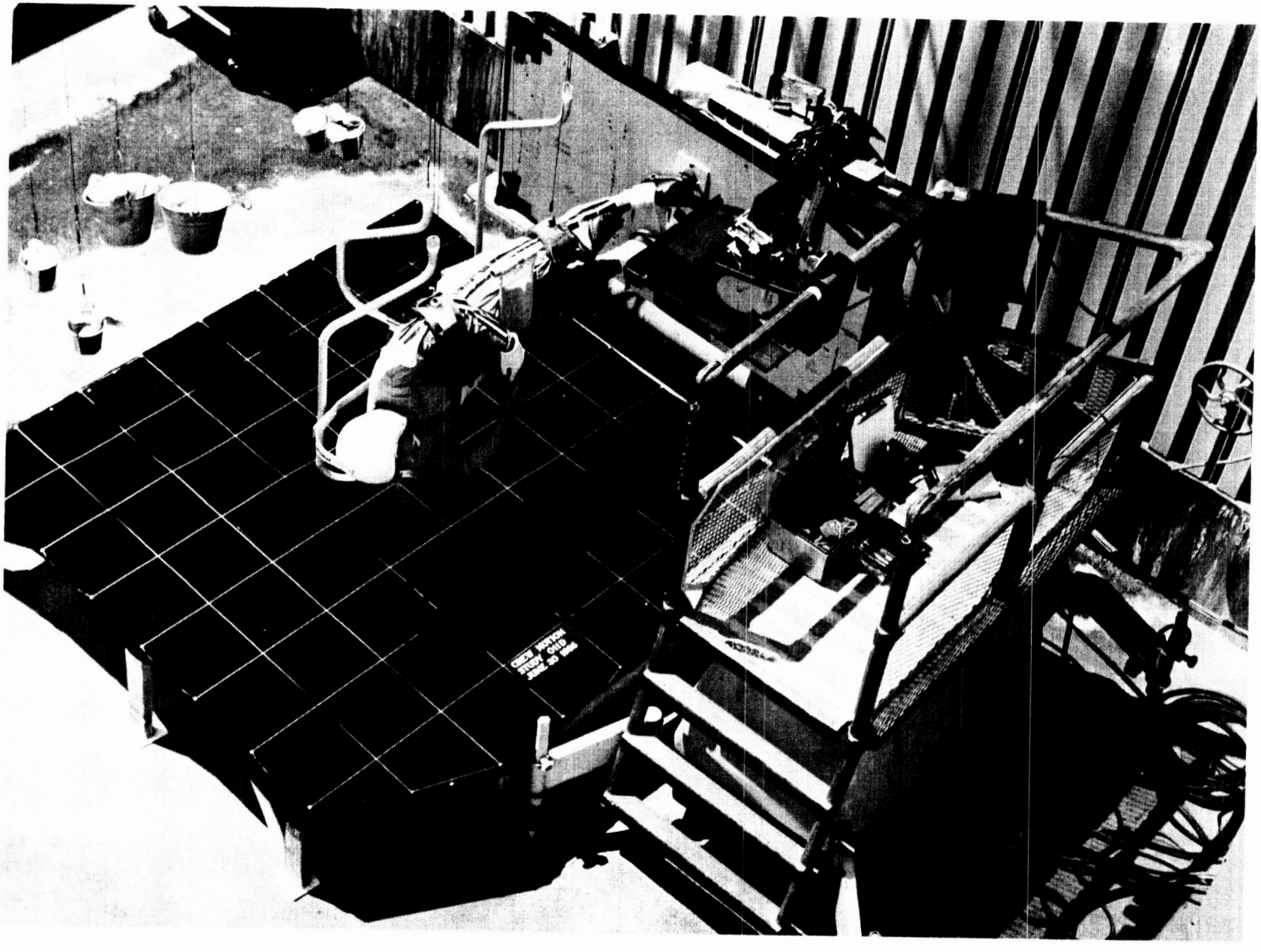

Figure 2. Experimental Setup

All of the simulated spacecraft equipment is attached to this platform during the appropriate portion of the test series. This spacecraft equipment includes a velcro walk strip, velcro shoes, foot restraints, hand rail, locomotion restraint, full-length body exercise machine, compression walking simulator, pedal ergometer, control console, waist restraint, and toe restraint.

The velcro walk strip is an 18 x 66 in. surface of nylon velcro pile. Strips of the velcro are cemented to an aluminum backing with velcro bonding adhesive. This aluminum base is readily attached with six bolts to the platform.

Velcro shoes were designed to be used for walking on the velcro walk strip. These shoes are basketball shoes with a new bonded velcro sole. The velcro sole is constructed by first bonding 3/4-in. urethane foam to the sole of the basketball shoe. Next, an aluminum heel and half sole are bonded to the urethane foam. Nylon velcro hook is then bonded to the aluminum half sole and heel. This construction allows maximum contact of the velcro surfaces yet permits the flexibility required for walking.

Foot restraints are used for attaching the test subject's feet to the force platform. The foot restraint is an elastic toe strap to which a 1-in. wide adjustable heel strap has been attached. The toe of the shoe is inserted into the toe strap and is held in this position by enclosing the subject's heel with the heel strap. The foot restraints are mounted on a 24 x 6-in. aluminum surface, which permits easy installation of the restraint on the force platform. The subject, when restrained by the foot restraints, is held to the force platform, yet has freedom to rock on his toes. This rocking freedom is required to minimize the possibility of damage to the subject's ankle.

Additional support for the subject is provided by the hand rail. This hand rail is an aluminum rod bent into the shape of a U and attached to the force table. The subject is provided a 68-in.-long support, 37-1/2 in. from the force table, when the hand rail is attached.

Support for the subject is also provided by the locomotion restraint. This restraint is identical to the hand rail, except that the support is provided 4 in. from the force table instead of 37 1/2 in.

The full-length body exercise machine (shown in fig. 87 in the exercise section of this report) contains the base plate, stanchion, stanchion brace, handle bar, and negator springs. The base plate provides a means of attaching the exercise machine to the force platform. Attached to the base plate are the stanchion, stanchion brace, and negator springs. The stanchion is an 88-in. long aluminum rod which acts as a guide for the handle bar. The handle bar rides freely on the stanchion. Attached to the handle bar are the negator spring cables, which continuously supply a 22 to 25 lb pull on the handle bar toward the base plate. The stanchion is further supported by the attachment of the stanchion brace to the stanchion and base plate. The full-length body exercise machine is designed to provide both flexibility and isotonic-type exercises.

Implementation of the compression walking simulator is achieved by attaching a 30 x 36 in. plywood bounce board to the stanchion of the full-length body exercise machine. The bounce board is located 80 in. from the force platform for the compression walking and oscillating acceleration tests and 84 in. from the force platform (corresponding to the floor-to-ceiling height in the MORL) for the nominal and minimum distrubance free soaring tests.

The pedal ergometer (shown in fig. 83 in the exercise section) is essentially a bicycle which the subject pedals. The resistance of the pedal motion is adjustable and was set at 150 W during this experiment.

The control console, waist restraint, and toe restraint are shown in fig. 56 in the console operation section of this report. Mounted on the left side of the control console are the hand wheel, slide bar, and phone jack receptacle.

The subject is supported at the console by the waist and toe restraints. The waist restraint is a belt to which two swiveled bars are attached. These bars extend from the subject's hips to the control console rail and are fastened around the rail. Both ends of the bars are hinged and swiveled to allow freedom of lateral and longitudinal rotation of the subject about the rail. Additional support is provided by the toe restraint, which is a flat velcro surface for foot support.

A black velveteen surface with 1 ft^2 white grid lines was laid underneath the suspended subject to provide a contrasting surface for motion picture and multiple-exposure camera documentation of the test series. The multiple-exposure camera recorded 24 sequential motions per second on the same negative. The cameras were located 16 ft above the subject.

The crew motions performed on the platform produce forces and moments which are transmitted through the platform to a six-component force balance shown in fig. 3. This force balance transforms the three orthogonal forces and three orthogonal moments induced by the subject into electrical signals. The accuracy of the balance is increased by calibrating the balance prior to the test series. This calibration procedure involves the loading of each component separately while measuring the output from all six components.

These calibration data are used to produce a 6 x 6 matrix that is used to reduce the raw data obtained from the crew motion experiments. These 6 x 6 matrixes minimize the cross-coupling and nonlinearity effects of the force balance.

Additional improvement is provided by referencing initial force and moment data to zero, thus eliminating the effect of the equipment, etc., attached to the force balance.

The reduced data are referenced to the surface of the force platform, as shown in figs. 4, 5, and 6 in the simulation technique section.

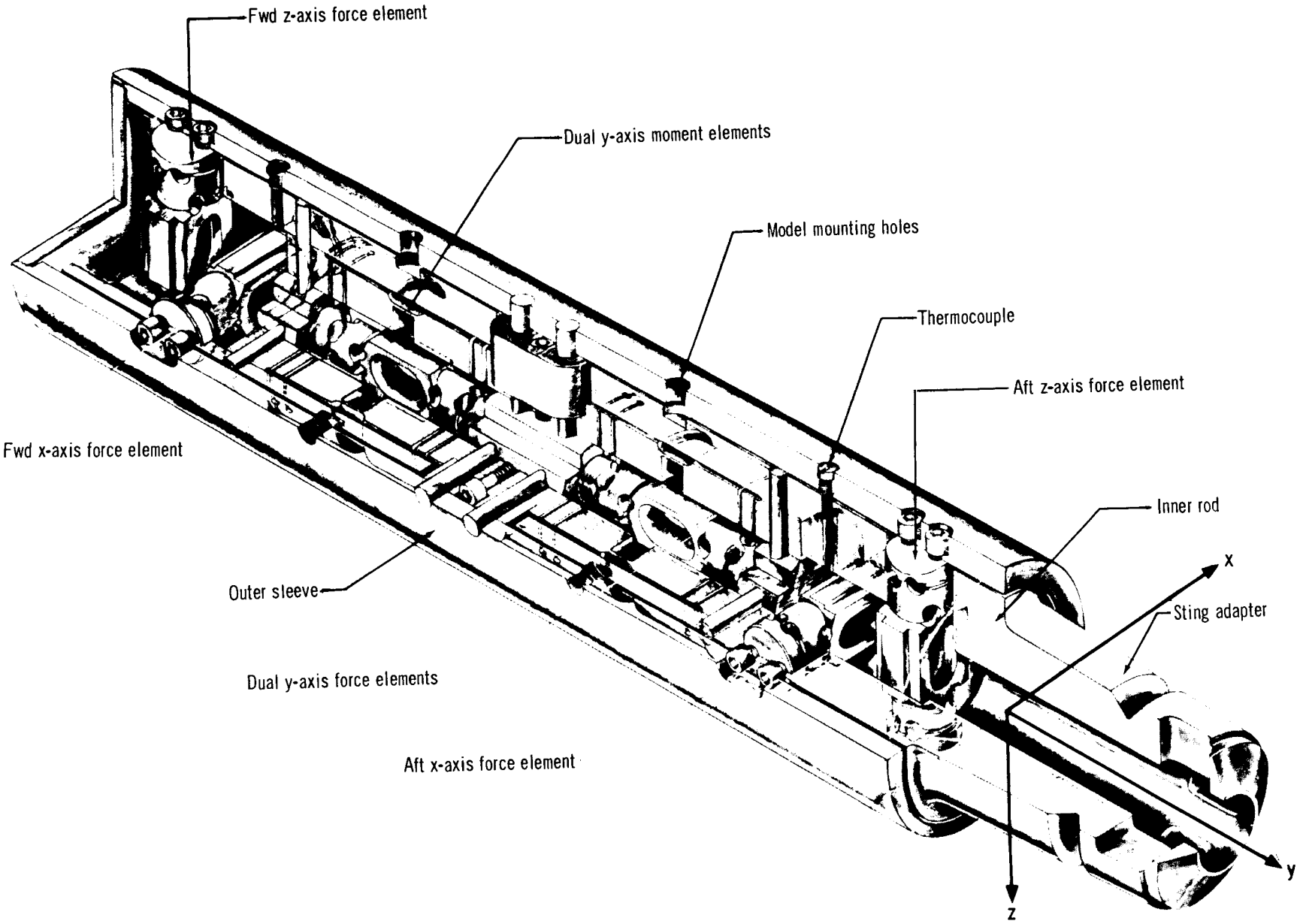

Figure 3. Six-Component Internal Strain Gage Balance

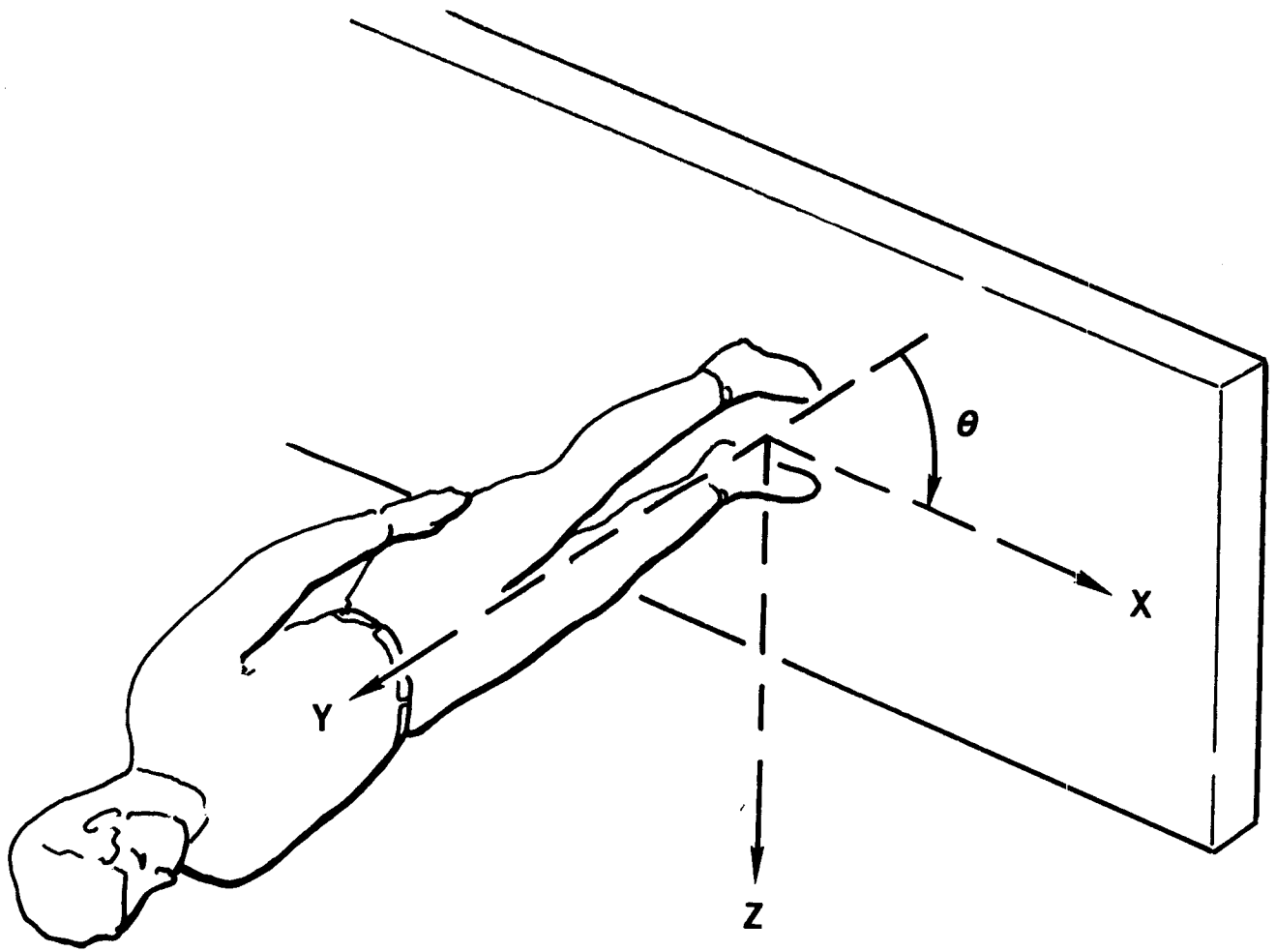

Figure 4. Orientation Diagram

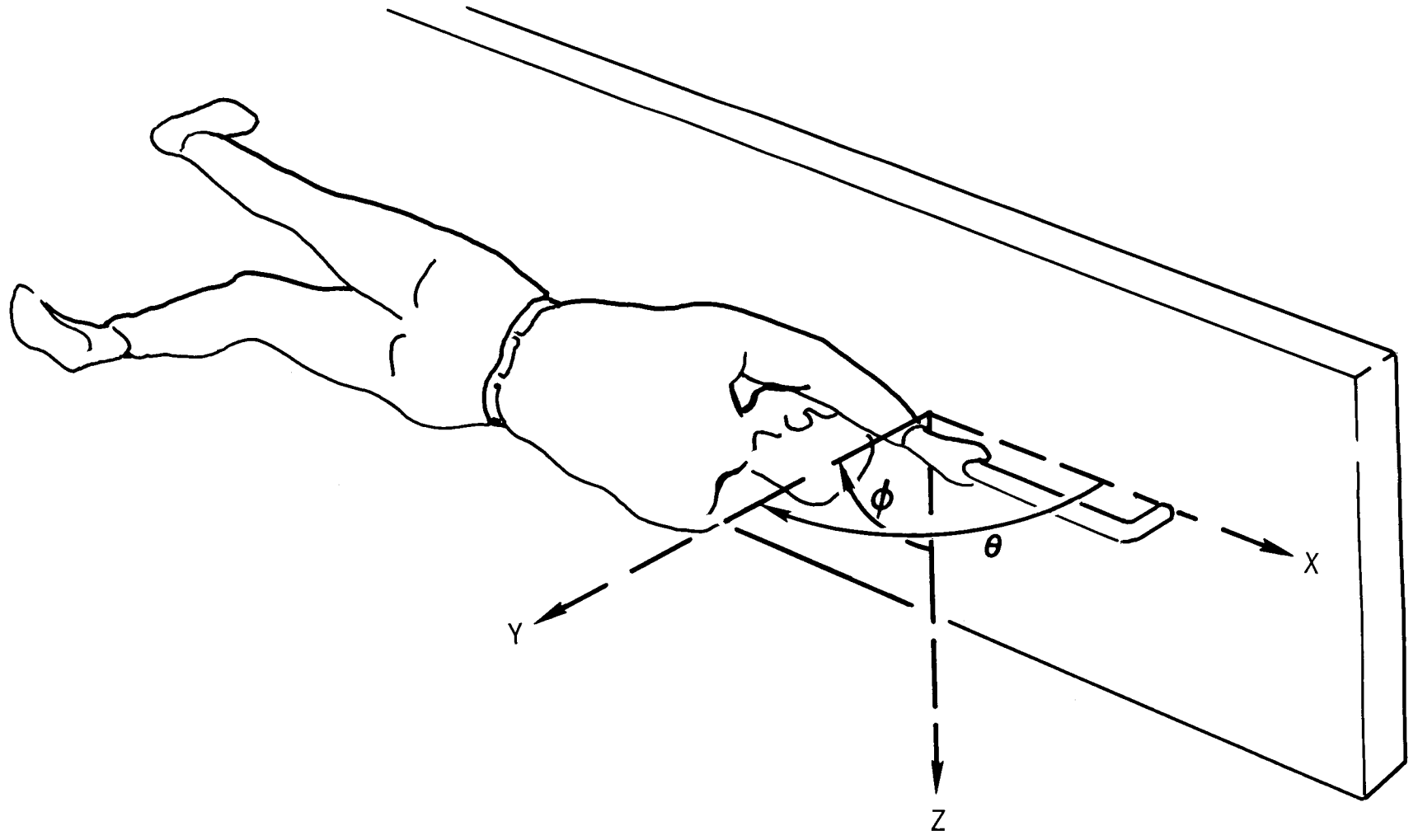

Figure 5. Orientation Diagram

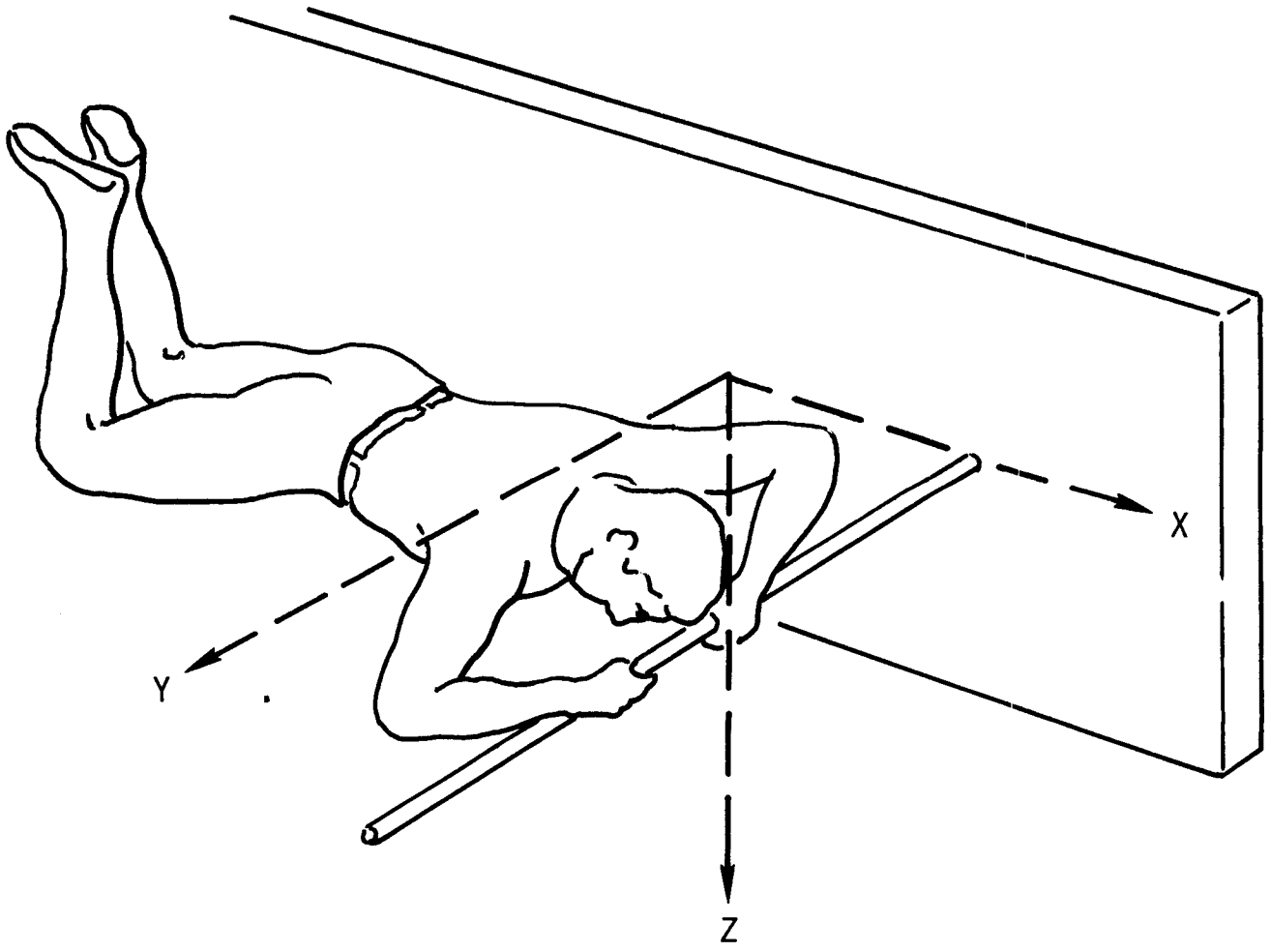

Figure 6. Orientation Diagram

Data produced from these experiments are processed by a high-speed data gathering system which has a total sampling capacity of 10 000 samples a second. The raw data are recorded and reduced by an SDS 930 Computer. Reduced data consist of tabulated data, plotted data, and a Fourier series defining the best-fit curve to the plotted data. Only the plotted data and the Fourier series representing the plotted data are presented in this report.

PRESENTATION OF RESULTS

Test Description

A test description of the various crew motion activities performed by the two subjects follows. The physical body measurements of the two subjects are presented in Appendix D. The crew motion activity is divided into four categories: (1) body segment motion, (2) locomotion, (3) console operation, and (4) exercise.

The body segment motion involves simple segment motions, such as an arm or leg swing. An analytical study was performed for these body segment motions to compare with the test results. A discussion of this comparison is presented in Appendix B. Combinations of several body segment motions can be formed to describe more complex activities, such as walking.

The locomotion tests consisted of soaring, guided locomotion (using hand restraints), and velcro walking. The locomotion tests, unlike the body segment tests were performed at three different levels of intensity: (1) minimum, (2) nominal, and (3) maximum. The minimum level of locomotion is used to determine minimum disturbances during critical times of tight attitude control of a spacecraft. During routine spacecraft operation, the normal distrubance levels are representative of the crew motion distrubance profiles. The maximum crew motion disturbance profiles represent the probable force and moment levels which would be experienced in emergency situations.

The console operation consists of three different tasks a crew member would have to perform in a typical orbiting spacecraft mission. These tasks are turning hand wheels, operating sliding controls, and push-pull or phone jack operations. The console operation, like the locomotion tests, is performed at minimum, nominal, and maximum levels of intensity.

There are three basic types of exercises the crew performs for conditioning: (1) flexibility, (2) strength, and (3) endurance exercises.

A description of the test measurements and procedures is presented in the following paragraphs.

Test Measurements and Procedures

The forces and torques induced from the crew motion activity are measured by a six-component force balance. These three orthogonal forces and three orthogonal moments are referenced to the center of the platform,

which is the floor directly under the subject's feet for most of the tests. Figs. 4, 5, and 6 show the orientation of the subject and the corresponding coordinate system for the complete series of tests. The reference angles shown in figs. 4 and 5 are used to describe the positions of the various body segments for some of the tests. These positions will be described later in more detail. In nearly all of these tests an attempt was made to keep the body segment motion in a single plane; usually this was the local horizontal or x-y plane, as shown in figs. 4, 5, and 6.

With this single-plane restriction for a body segment motion, a general form for the induced moments about the reference axes is given by the following:

$$M_x = I_{n_x} \ddot{\theta}_{n_x} + y F_{n_z} - z F_{n_y} \quad (1)$$

$$M_y = I_{n_y} \ddot{\theta}_{n_y} + z F_{n_x} - x F_{n_z} \quad (2)$$

$$M_z = I_{n_z} \ddot{\theta}_{n_z} + x F_{n_y} - y F_{n_x} \quad (3)$$

where

M_i = moment in lb-ft about the i^{th} reference axis as shown in figs. 4, 5, or 6.

I_{n_i} = moment of inertia in slug-ft^2 for the particular body segment about the axis of rotation parallel to the i^{th} axis

$\ddot{\theta}_{n_i}$ = angular acceleration in rad/sec^2 of the particular body segment about the hinge axis parallel to the i^{th} axis

F_{n_i} = force in LB produced along the hinge axis parallel to the i^{th} axis from the particular body segment motion

(x, y, z) = component distance in ft from the hinge point of the body segment rotation to the center of the reference axis

The hinge point forces, F_{n_x}, F_{n_y}, and F_{n_z}, are the same as those measured which are termed F_x, F_y, and F_z, respectively. Most of the tests involve body segment motions in the local horizontal plane, hence the z component of force measured is an error source including the imbalance of the suspension system and the effects of small out-of-plane (horizontal) motions. These two sources of error are not separable because the out-of-plane motion is not measured. From eqs. (1), (2), and (3), it is noted that the z component of force appears in two of the measured moments M_x and M_y. Also, for the segment motion in the local horizontal plane, the angular accelerations $\ddot{\theta}_{n_x}$ and $\ddot{\theta}_{n_y}$ will be zero. Therefore, the first two moment equations are

primarily dependent upon the x and y components of force and the z distance from the reference point to the hinge point of the movable body segment. For manned spacecraft application, this reference point is the spacecraft center of mass. Hence, the magnitudes of these two torques are primarily a function of the man's position in the spacecraft and the x and y components of force. From eq. (3), the z-axis moment contains the body-segment angular acceleration term. For the tests performed which involved body segment motions, the forces are dependent upon the angular acceleration and angular rates of the body segments. Hence, if the forces are small, the angular accelerations of the body segments will be small. Therefore, a large moment is induced primarily by increasing the lever arm of the applied forces. The results of these tests illustrate that the moments caused by angular accelerations of the body segment inertias are negligible when compared to the moments produced by the inertia forces acting at a nominal distance (6 to 8 ft). This nominal distance of 6 or 8 ft is approximately the shortest distance a crew member can be placed from the MORL spacecraft center of mass. For most of the results presented, the moment data are omitted. Only for tests in which the moments could have some value, other than illustrating that these moments are small, will they be presented.

Before each test series the force balance is zeroed electrically and calibrated. The test series are comprised of three repetitions of each type of crew motion performed. This zeroing and calibration is done while the subject is in the initial position for the test and is motionless. Some of the tests require attachment of equipment to the platform, which, in effect, loads platform. This loading is then zeroed electrically before each test series.

Before the plotted data are shown, an important point regarding their general characteristics should be noted: because the support mechanism is a counterbalanced pendulous support, any translation of the body center of mass in the local horizontal plane from the static position of the pendulous support will induce a restoring force in the local horizontal plane. This force is equal to the pendulum angular deflection of the body center of mass multiplied by the body weight. Although this pendulous error force is a small percentage of the total disturbance force (see Appendix A), its effect on some of the test data is easily observed. Before the effects of the pendulous support on the test data are illustrated a basic principle must be pointed out. In a true zero-g enrivonment, the vector quantity of the impulse (force x time) required to accelerate a mass from rest and then decelerate the mass back to rest is zero. Hence, in the crew motion tests in which body segments were accelerated and then motions terminated, the disturbing forces and moments would integrate to zero with respect to time if there were no external disturbing forces. As previously described, this simulation is not free of external disturbances. For example, a walking motion is used to describe the effects of the pendulous support. In performing the walking motion, the subject's displacement is centered, as close as possible, over the force balance measurement unit. Therefore, as the subject moves from the starting position to the terminating position, the pendulous error force has the shape of a cosine function for a half cycle (the points of maximum defection being the starting and terminating points with the zero point of the function being

the position over the force balance). Obviously, integrating a half cycle of a cosine function over a complete period produces a value of zero for the integral. This, however, is not the case in the simulation testing. It was mentioned that at the start of each test, the force balance is zeroed and calibrated. Hence, for walking, the gravity component at the start of the test is zeroed electrically. This, in effect, puts a bias on the cosine curve of the pendulous error force. Integrating this does not yield the integral value of zero.

Hence, any test in which the center of mass of the subject is displaced from the static position of the pendulum will yield bias forces and moments in which the time integrals are not zero. These data can be useful because the necessary disturbances for each test are given in an equation form, which is of more use to the engineer for analyses studies. This equation form is the first eight terms of the Fourier series. A digital computer is used to evaluate the terms of the Fourier series for each test.

The bias force caused by the pendulum support can be removed from the Fourier series approximation for a given test by setting the integral of the series to zero and solving for a new constant term in the Fourier series. This preserves the harmonics and phase shifts of the sinusoidal terms in the series which represent the data for the given test.

A discussion of the results of the various tests follows. Each test, whether performed at a minimum, nominal, or maximum level is performed three times by each of the two subjects.

BODY SEGMENT MOTION

The body segment motion series of tests involve simple segment motion in only one plane. These motions include single pendulum arm swing, double pendulum arm swing, head motion, bending at the waist, and leg motion. The coordinate system shown in fig. 4 is used to define the forces and moments for the series of tests. As shown in fig. 4, the subject's longitudinal axis is aligned with the y-axis of the coordinate system. Test results for the body segment motions are discussed in the following paragraphs.

Single Pendulum Arm Motion

The single pendulum arm motion is a body segment motion in which the arm swing is done without bending the elbow, as shown in fig. 7. The initial position of the left hand is at the thigh. The left arm is rotated until it is normal to and in front of the body. Fig. 8 shows the two force components, F_x and F_y measured for Subject A. The total time of the motion is noted to be about 1 sec. The force component F_y (the force normal to the platform) has a maximum value of approximately 3 lb and exhibits a fairly smooth curve. As the arm is raised, the reaction on the body is in a downward (-y) and backward (-x) direction. Both the x and y force components start in a negative direction. The x component is smaller and irregular compared to the y component of force. Because the arm is rotated about an axis parallel to the z axis, the force in the direction parallel to the platform or x axis resulting from the arm motion will be partially negated by a body motion in the opposite direction. The subject has some limited freedom of rotation about the z axis. The body attempts to negate any angular momentum because of a segment rotation about an axis parallel to the z axis. Hence, the peak z-axis moment obtained during this test was small--1 lb-ft.

The double negative peak in the F_y plot is a particular characteristic of this subject. It indicates two separate arm-acceleration periods.

The positive portion of the F_y plot is produced by the deceleration of the arm. For the positive portion of F_y, the double peak effect is not nearly as pronounced as in the negative portion.

The moments about the x and y axes were small. The subject would have to be within 1 ft of the spacecraft center of mass for the moments caused by the angular acceleration of the arm to be as large as the moments resulting from the cross-product of the inertia forces and distances.

Fig. 9 shows the single pendulum arm motion done by Subject B. The time for this arm motion is approximately 1.1 sec, 10% longer than the time used by Subject A. Consequently, the amplitudes of the forces are not

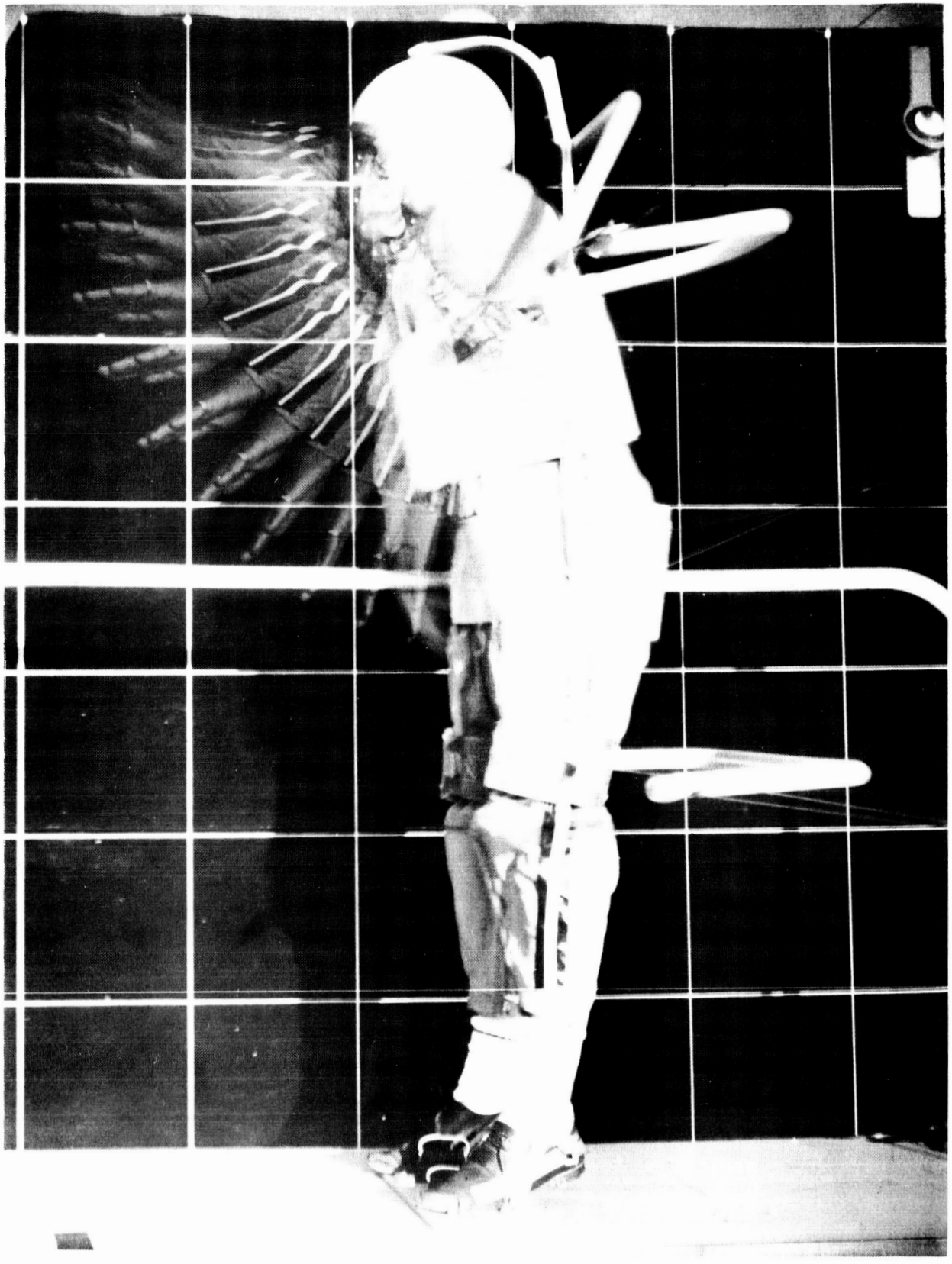

Figure 7. Single Pendulum Arm Motion

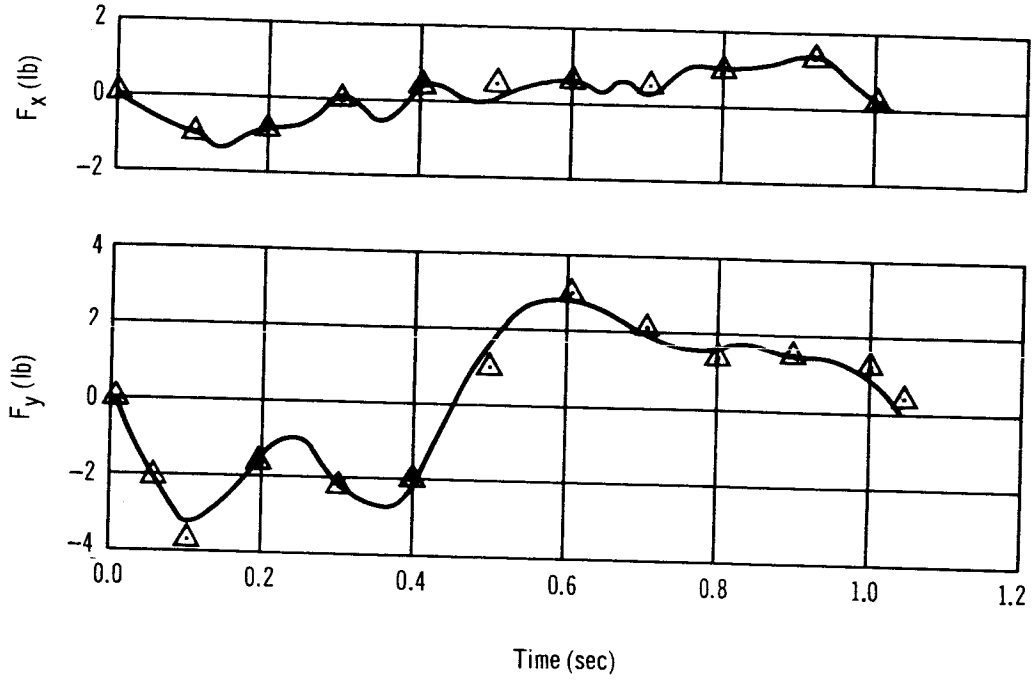

Figure 8. Single Pendulum Arm Motion Disturbance Profile – Subject A

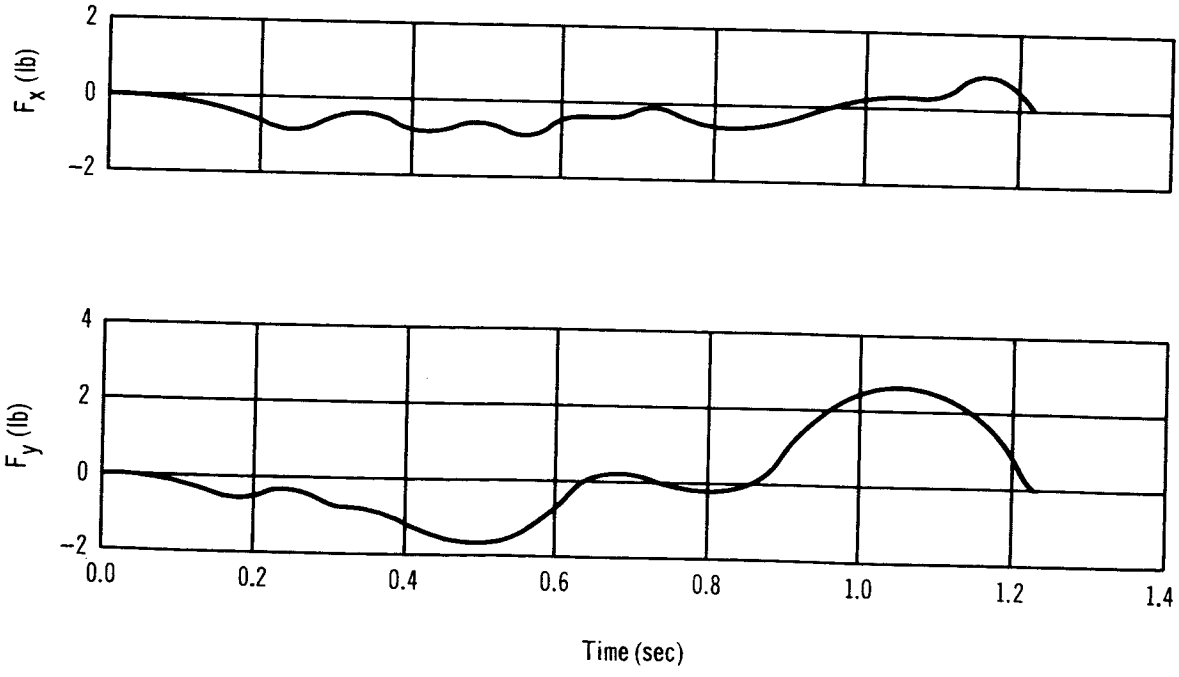

Figure 9. Single Pendulum Arm Motion Disturbance Profile – Subject B

as large because of the smaller acceleration. Subject B does not have the pronounced double-peak effect as has Subject A for the acceleration of the arm. The x component of force and the moments are small, as explained for Subject A.

To predict the forces and torques resulting from single pendulum arm motion, a mathematical model was derived utilizing the results of the NASA Man's Analytical Inertia Determination (MAID) program for determining the body segments mass and inertia properties.

The force equations for the single pendulum arm motion are given in Appendix B as eqs. (B29) and (B30) as are the parameters of the segments and the assumed rate profile.

Substituting the assumed angular acceleration and its derivatives into eqs. (B29) and (B30), the peak amplitudes for these two forces are approximately 2 lb each. The results of the simulation showed the maximum y components of force to be 3 and 2.6 lb for the two subjects. The maximum x components of force obtained from the simulation of the arm motion tests is approximately 1.4 lb. From the simulation data of the single pendulum arm motion, the acceleration of the arm appears to be variable. The slopes of the force curves at the start and the end of the motion are small, which indicates a small initial arm acceleration. The test arm motion was completed in approximately 2 sec, which indicates higher accelerations later in the arm motion. The analytical description results in a discontinuous force profile because the assumed acceleration consists of a constant acceleration-constant deceleration profile. Hence, the wave shape of the predicted and actual forces only can be compared on the basis of initial- and terminal-force directions.

The x component of force computed is larger than that measured, as previously explained.

The mathematical expressions, in the form of Fourier series, eight terms are given for the x and y components of the forces in figs. 8 and 9. The equations are presented in Appendix C. The terms of the Fourier Serier were evaluated and plotted for the single pendulum arm motion of Subject A on fig. 8 to show the fit accuracy. As shown in fig. 8 there is practically no error associated with the use of the Fourier series for this motion.

Double Pendulum Arm Motion

The double pendulum arm motion is the same as the single pendulum arm motion except the arm is allowed to rotate at the elbow during the swing. The left arm is rotated in the x-y plane (fig. 4) until the elbow is normal to and in front of the chest, and the fingers touch the left shoulder. Fig. 10 shows a multiple-exposure photograph of this crew motion. This movement required approximately 1 sec.

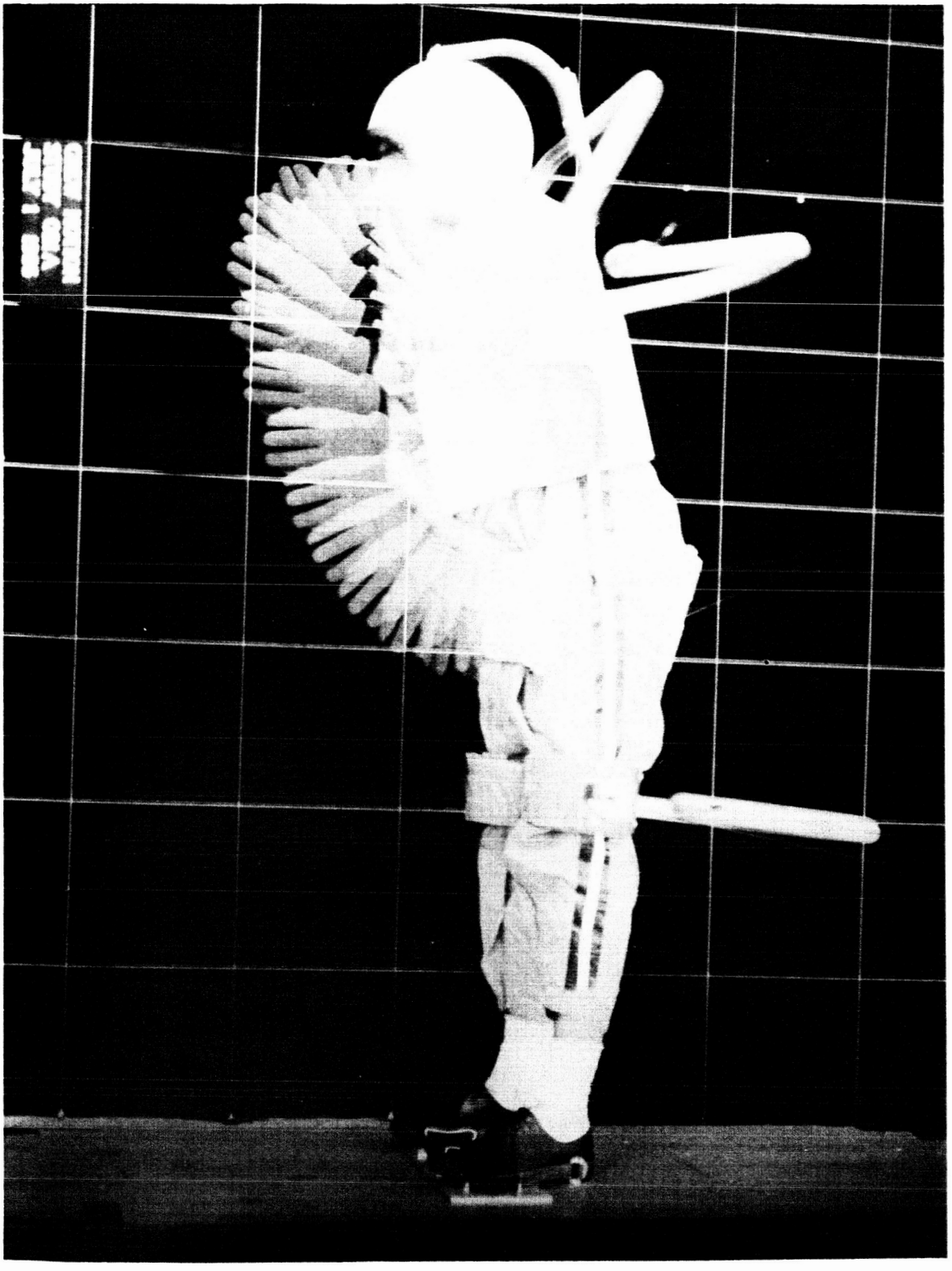

Figure 10. Double Pendulum Arm Motion

Fig. 4 shows the reference angle, θ, for describing the various body segment motions when the subject was suspended perpendicular to the force table. Time histories of the torso, right and left upper arms, right and left lower arms, right and left upper legs, and the right and left lower legs were recorded with a motion picture camera during several of the crew motions. The Euler angles, with the same reference as θ, defining each of those segments and the translational movement of the head were then plotted as a function of time for the selected crew motion.

Fig. 11 presents the Euler-angle description for the double pendulum arm motion. Only two plots are required to describe the motion, namely, the left arm lower, θ_{LAL}, and the left arm upper, θ_{LLU}. The remaining body segments that remained motionless during this test are defined by the following notations: trunk Euler angle, θ_T; left leg upper, θ_{LLU}; left leg lower, θ_{LLL}; right arm upper, θ_{RAU}; right arm lower, θ_{RAL}; right leg upper, θ_{RLU}; and right leg lower, θ_{RLL}. Fig. 11 shows the Subject A rotated the lower arm 160° in 0.8 sec and at a fairly constant rate of 4.2 rad/sec during the time interval of 0.3 to 0.8 sec. The upper arm delayed 0.5 sec after the lower arm first motion and then rotated 65°. The average rate of upper arm movement is approximately the same as the lower arm, 4.2 rad/sec.

Fig. 12 shows the x and y components of the forces produced by the double pendulum arm motion of Subject A. Again, the moment data are omitted because they are insignificant if the subject is several feet from the spacecraft center of mass or reference point. The maximum amplitude of the y component of force is approximately 4 lb. Also, the x component of force is small, as explained for the single pendulum arm motion test.

The initial positive peak of the force F_y appeared in all three tests for Subject A. It is possible that the subject straightened his arm initially before starting the swinging motion. The first negative peak is the acceleration of the lower segment of the arm. The upper segment of the arm did not move until approximately 0.4 sec later. (This was determined from the motion picture data by plotting the arm-segment motions for this particular test.) The second positive peak in the F_y plot results from deceleration of the two arm segments.

Fig. 13 shows the force data for Subject B in performing the double pendulum arm motion. The y component does not contain the harmonics noted for the same test with Subject A (fig. 12). The y component of force for Subject B is smooth and has a maximum amplitude of 4.5 lb. The negative peaking that occurs after 0.8 sec is caused by the deceleration of the lower arm when the upper arm is nearly parallel to the platform. At this position, the lower arm is moving in a negative or downward direction. The maximum moments obtained during this body segment motion for both subjects is 2 lb-ft about the z axis. The phenomenon of near negation of the z-axis moment was described in the single pendulum arm motion tests.

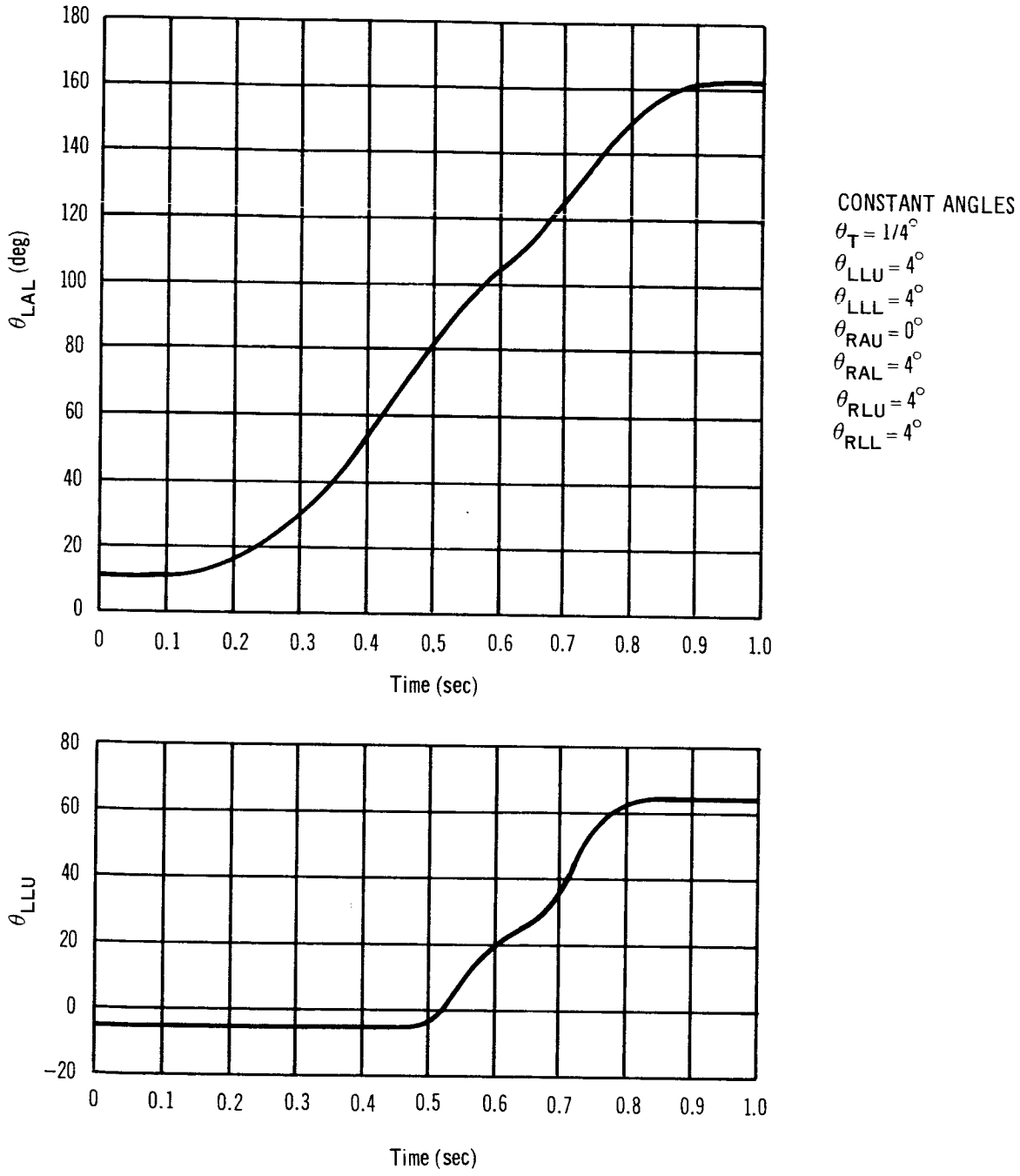

Figure 11. Double Pendulum Arm Motion Euler Angles – Subject A

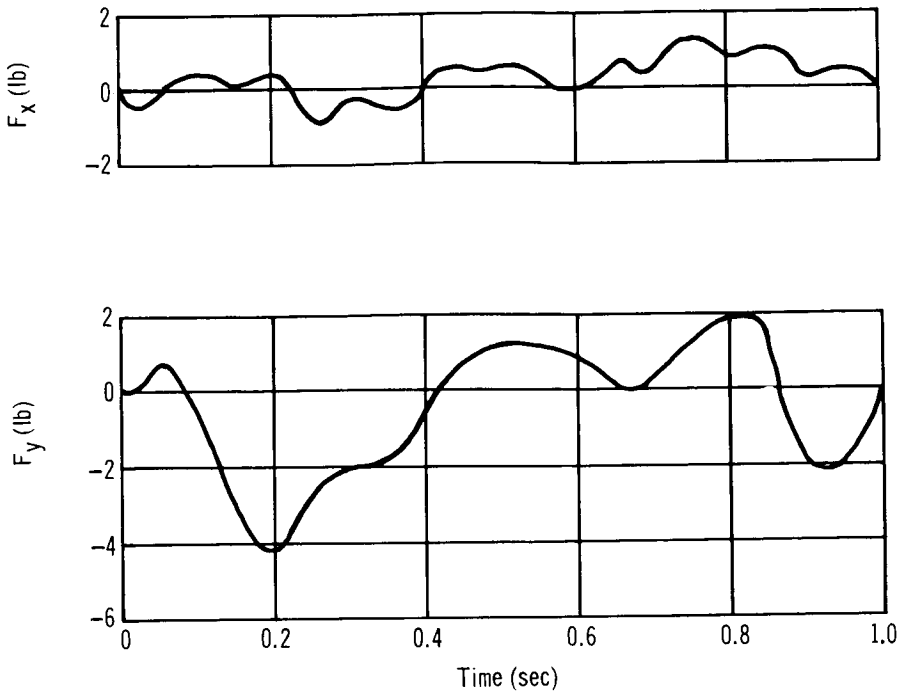

Figure 12. Double Pendulum Arm Motion Disturbance Profile – Subject A

The mathematical model for the double pendulum arm motion is given in Appendix B. With this mathematical model and the rate profile of the arm motion shown in fig. 11, the actual as opposed to the predicted forces can be compared. The following rate profiles of the upper and lower arm are obtained from fig. 11:

(1) Lower Arm

$\theta_{LAL} = 10°$ for $t = 0$

$\ddot{\theta}_{LAL} = 20.6$ rad/sec^2 for $0.12 \leq t \leq 0.32$ sec

$\dot{\theta}_{LAL} = 4.14$ rad/sec for $0.32 < t \leq 0.8$ sec

$\ddot{\theta}_{LAL} = -34.3$ rad/sec^2 for $0.8 < t \leq 0.92$ sec

(2) Upper Arm

$\theta_{LAU} = -6°$ for $t = 0$

$\ddot{\theta}_{LAU} = 50$ rad/sec^2 for $0.45 \leq t \leq 0.53$ sec

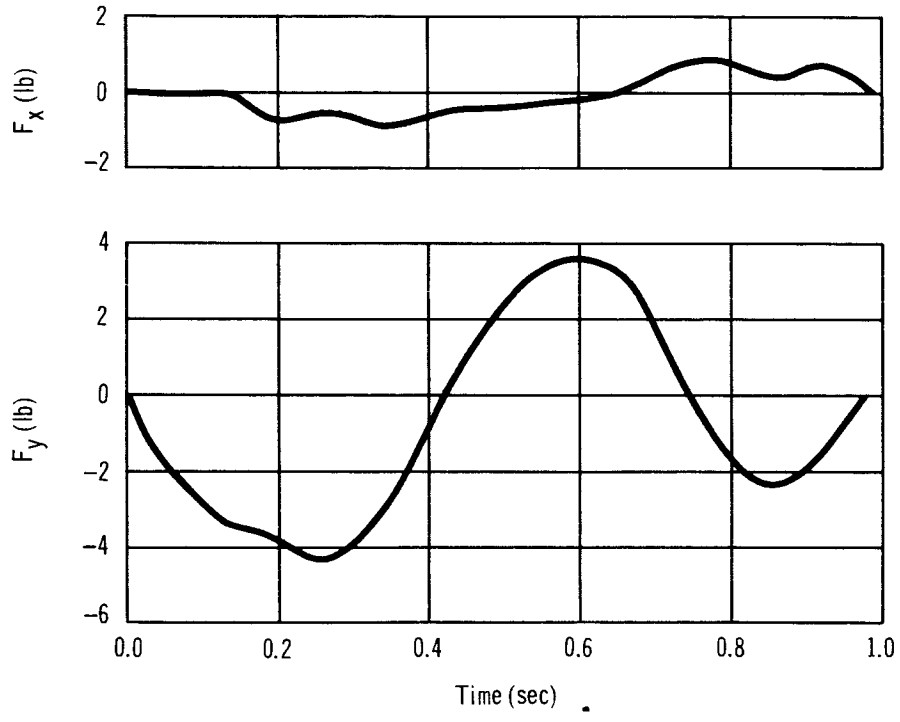

Figure 13. Double Pendulum Arm Motion Disturbance Profile – Subject B

$$\dot{\theta}_{LAU} = 4 \text{ rad/sec for } 0.53 < t \leq 0.77 \text{ sec}$$

$$\ddot{\theta}_{LAU} = -57.2 \text{ rad/sec}^2 \text{ for } 0.77 < t \leq 0.84 \text{ sec}$$

Substituting these rate profiles into eqs. (B16) and (B17) of Appendix B, along with the arm parameters given in Appendix D, the predicted forces are obtained. As illustrated in fig. 12, Subject A produced a maximum disturbing force of 4 lb. The results of the mathematical model produce a maximum force of 2 lb with the lower arm movement and a maximum force of 12 lb with the movement of the upper arm. The 12-lb maximum force produced by the upper arm is dependent only on the angular acceleration caused by the upper arm profile shown in fig. 11. If the given segment profiles of the upper and lower arms are reasonably accurate, the difference between the predicted force and the actual force can be accounted for by a small movement of the torso when performing the arm motion. Because the mass of the arm is small (0.31 slugs), a small torso movement would reduce the force caused by the arm motion. These small body motions are not detectable from the motion picture data.

It should be noted that the models for the segment motion basically are used to size the force balance unit and to ensure the order of magnitude of the actual test data.

The equations derived for the test data of the double pendulum arm motion are given in Appendix C.

Head Motion

For this body segment motion, the subject is in a standing position with his arms at his side, his head rotated to the right and his feet fixed firmly to the platform. He then rotates his head from right to left, which completes this motion.

Fig. 14 shows the force components produced by the head motion of Subject A. The rotation of the head took approximately 0.85 sec. This head movement, it should be noted, is a fairly small disturbance. The maximum forces are on the order of 1.5 lb. The z component of force is not a true representation of the force because it contains the suspension-force error, which was described in the previous section on test measurements and procedures.

The equations derived for the head motion are presented in Appendix C. The distrubances of Subject B while performing this test were small and were in the threshold of the measurement capability of the force balance; therefore, the data are not given.

Bending at the Waist

For waist bending motion the subject is in a standing position with his arms at his sides. He then bends at the waist, keeping his hands at his side until his upper torso has rotated approximately 90° in the x-y plane (fig. 4).

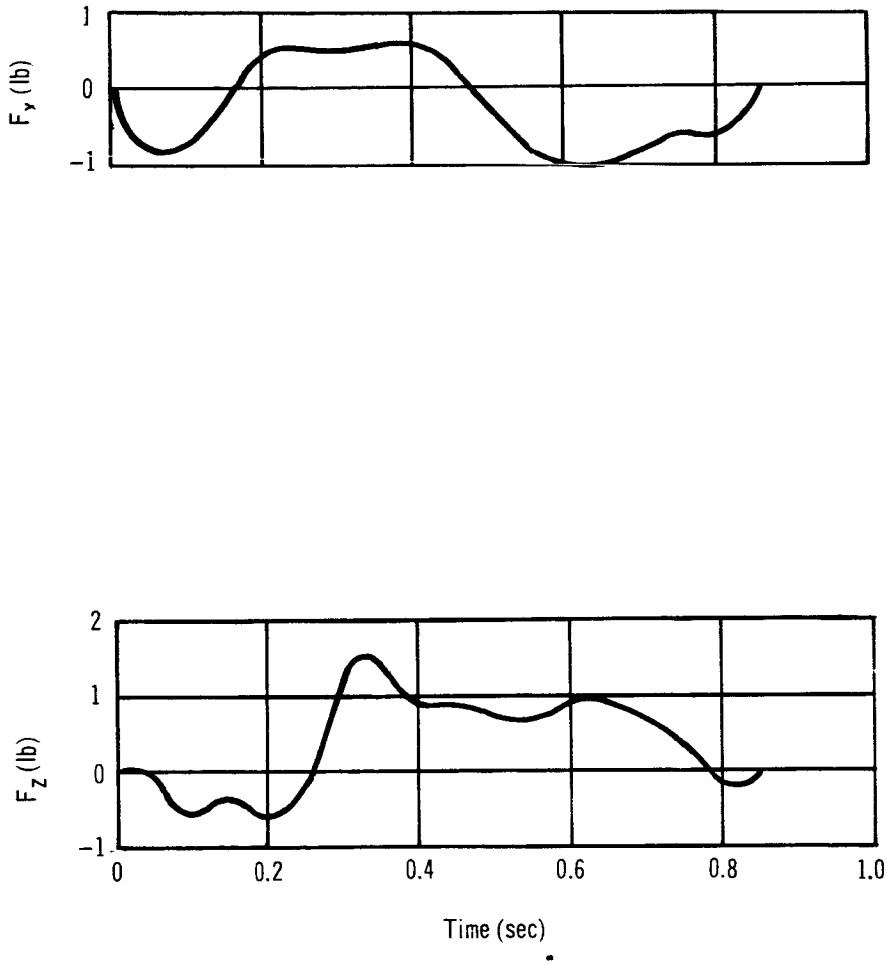

Figure 14. Head Motion Disturbance Profiles – Subject A

Fig. 15 is a multiple exposure photograph of the waist bending motion. The upper torso rotated 65° and the legs rotated 9° in the opposite direction.

Fig. 16 presents the Euler-angle description for this motion. Three plots are required to describe this motion: (1) the right and left legs (both segments), (2) the torso, and (3) the right and left arms. This time history shows that Subject A rotated his torso 65° and his lower torso or leg rotated 9° in the opposite direction. The arms were nearly rigid with the upper torso. This motion requires approximately 1.4 sec.

Fig. 17 is a plot of the x and y components of the force for Subject A. The positive portion of the F_y plot results from the acceleration of the upper torso, which produced a maximum force of 9 lb. The negative portion, which peaked around at approximately 9 lb, is produced by the deceleration of the upper torso in halting the movement. The initial positive peak of the x component of force is produced by the rocking back of the lower torso bending at the waist. This causes the total body center of mass to be behind (-x direction) the feet. After the lower torso has stopped, the reaction force of the upper torso, which is in a negative x direction, dominates. The maximum x component of force is, as noted 5 lb. The variation in suspension force during this motion is approximately 5 lb of the total suspended weight of 175 lb. Again, the moment data are insignificant, because they are only approximately 10 lb-ft for this motion.

For this motion, it was noted that each time the subject performed the motion the forces became higher, the motion duration time became shorter, and the force curves became smoother. This indicates a limbering-up or warm-up period for the subject performing the motion.

The forces for Subject B performing this motion are shown in fig. 18. Peak amplitudes for the y component are +8 and -9 lb, which are nearly the same as those for Subject A. Subject B took approximately 0.3 sec longer to accomplish the z motion than did Subject A.

The mathematical model used to describe this body segment motion was set up on the basis of the lower torso being fastened rigidly to the platform with pure rotation of the upper torso. The forces obtained from this model are given in Appendix B as eqs. (B19) and (B20). Substituting the torso parameters in these equations, the following are obtained:

$$F_x = 2.84 \left(\ddot{\theta}_T \cos \theta_T - \dot{\theta}_T^2 \sin \theta_T\right) \text{ in lb} \tag{4}$$

$$F_y = 2.84 \left(\ddot{\theta}_T \sin \theta_T + \dot{\theta}_T^2 \cos \theta_T\right) \text{ in lb} \tag{5}$$

The description of the torso rotation, θ_1, is obtained as follows from fig. 16:

$$\ddot{\theta}_T = 2.31 \text{ rad/sec}^2 \text{ for } 0 \le t \le 0.7 \text{ sec}$$

$$\theta_T = -2.31 \text{ rad/sec}^2 \text{ for } 0.7 < t \le 1.4 \text{ sec}$$

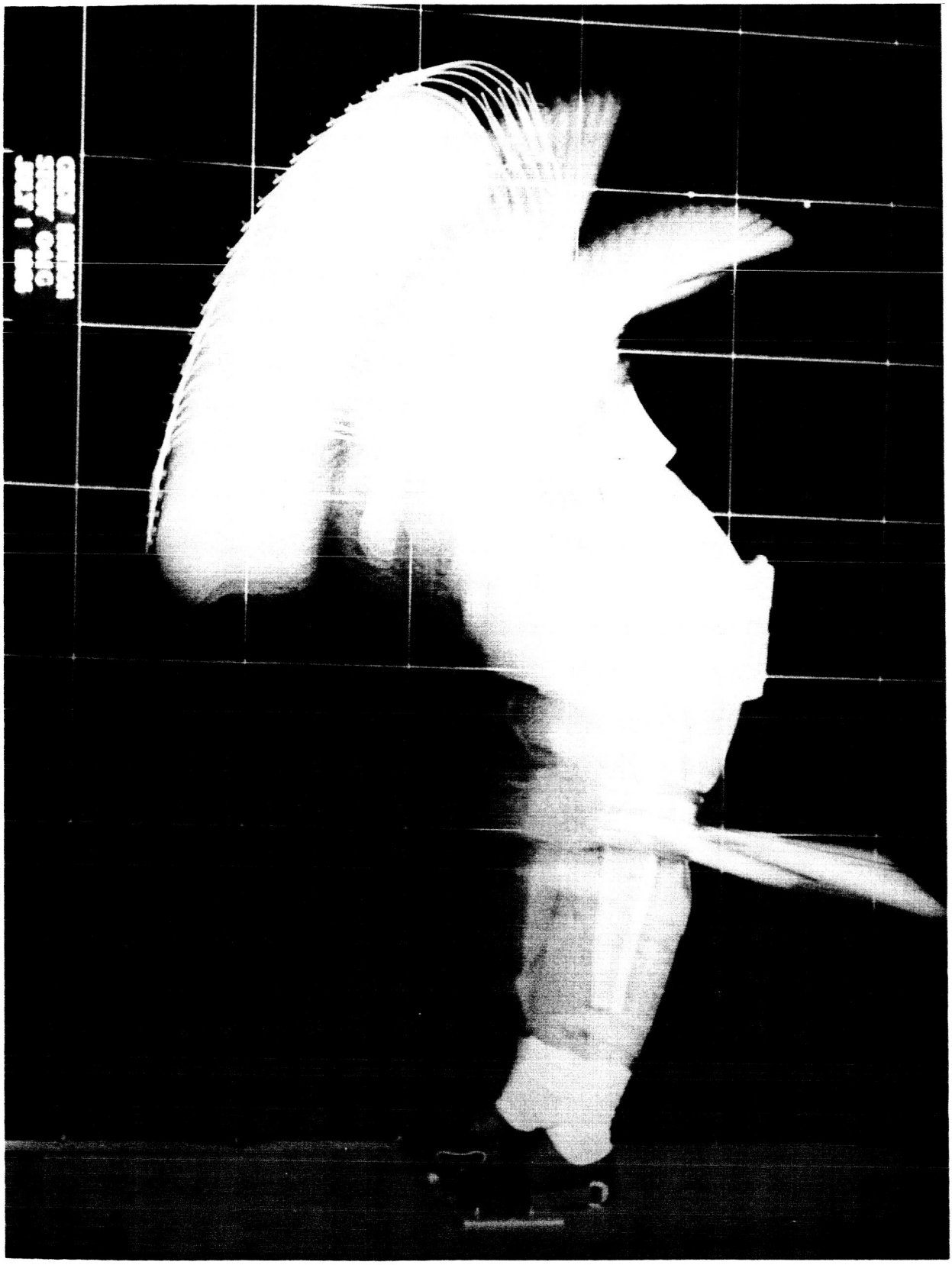

Figure 15. Bending at the Waist

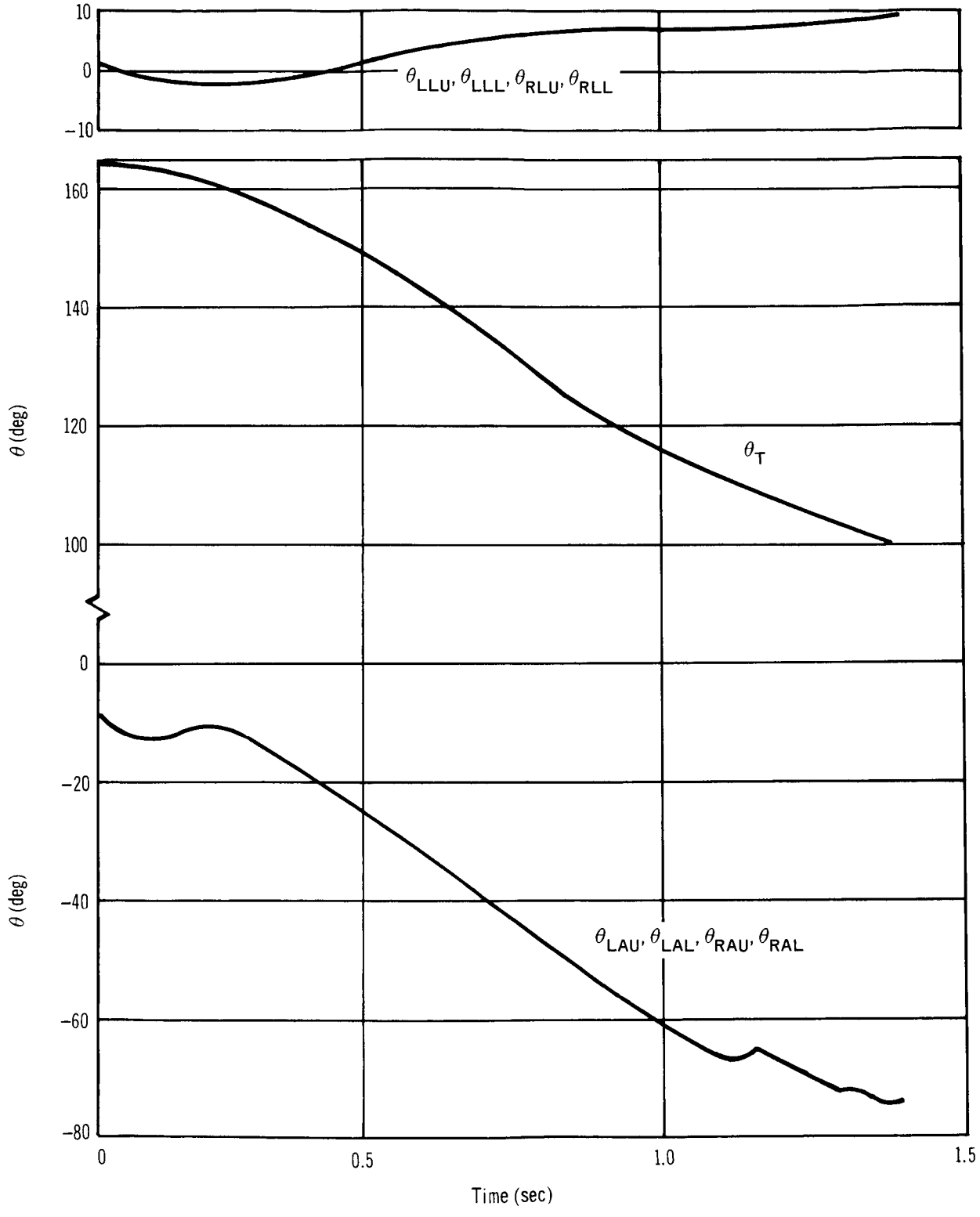

Figure 16. Bending at Waist Euler Angles – Subject A

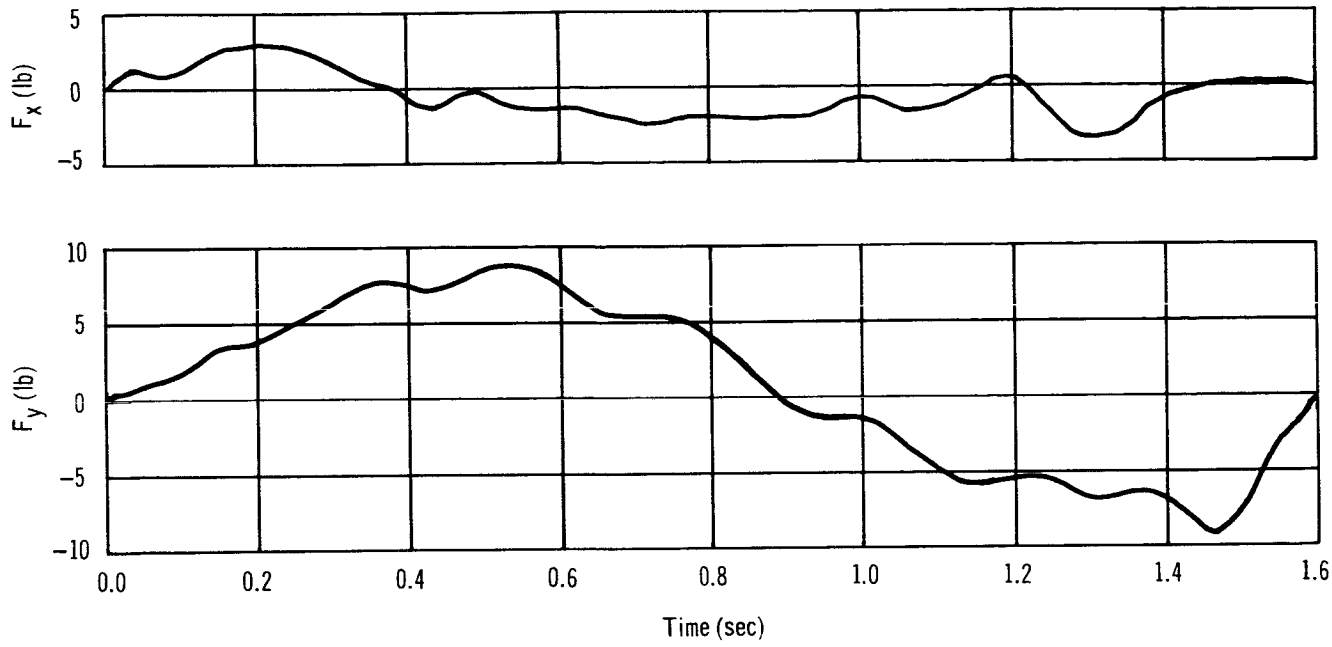

Figure 17. Bending at Waist Disturbance Profiles – Subject A

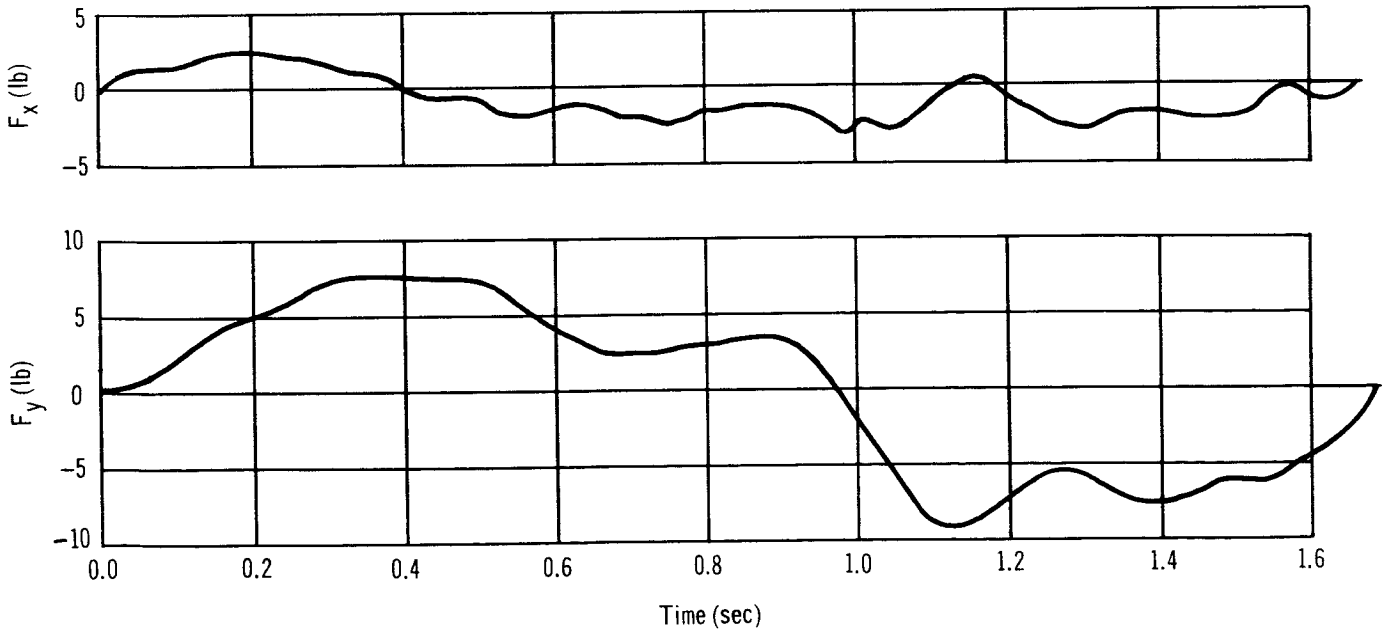

Figure 18. Bending at Waist Disturbance Profiles – Subject B

Essentially, this is constant acceleration and constant deceleration for the torso. Substituting this rate profile into eqs. (4) and (5), the maximum x- and y-component forces each are approximately 10 lb. From the test data of Subject B, the maximum x and y components of force are 3 and 9 lb, respectively. As in the previous tests, the transmission of force in a parallel direction to the standing surface will be small compared to the force transmitted normal to the standing surface. The predicted normal force, F_y, for this test agrees with the test data. Because the upper torso, which is the larger mass, is rotated, any movements of the smaller body segments have a smaller influence on the normal force of the waist bending.

The equations derived for the test data of bending at the waist motion are presented in Appendix C.

Leg Motion

For leg-motion segment motion, the left leg is lifted approximately 10 in., as in walking, from the platform. The time required for this movement is 0.5 sec. The leg motion is similar to the double pendulum arm motions; the major difference is that the lower leg is rotated in a direction opposite to that of the upper leg.

Fig. 19 is a multiple-exposure photograph of the motion. The left upper leg rotated 55° and the lower leg rotated 35° in the opposite direction.

Fig. 20 is the Euler-angle time history of the left leg, upper, θ_{LLU}, and the left leg, lower, θ_{LLL}. The other body segments were essentially motionless during this test.

The disturbances from the leg motion for Subject A are shown in fig. 21. As the leg is raised, or accelerated, a reaction force is produced in the negative y direction. During the acceleration of the leg, the maximum y force produced is 5.8 lb. As the leg is decelerated, the reaction force, F_y, changes direction. The maximum deceleration force produced in the y direction is 7.6 lb. The total time of the leg motion is approximately 1 sec. The x component of force is at most 1 lb during the leg motion, which is a smaller percentage of x-axis force transmission than the arm motions produce because of the opposite segment motions of the leg segments. As in the previous motions, the moment data of the leg segment angular accelerations and, therefore, it is omitted.

Fig. 22 shows the disturbances of the leg motion for Subject B, who performed the leg motion in approximately the same time as Subject A, with a smaller disturbance. This indicates that Subject B did not pick up his leg as high as did Subject A.

The mathematical model for predicting the forces of the leg motion was again the double pendulum model [see eqs. (B16) and (B17) Appendix B].

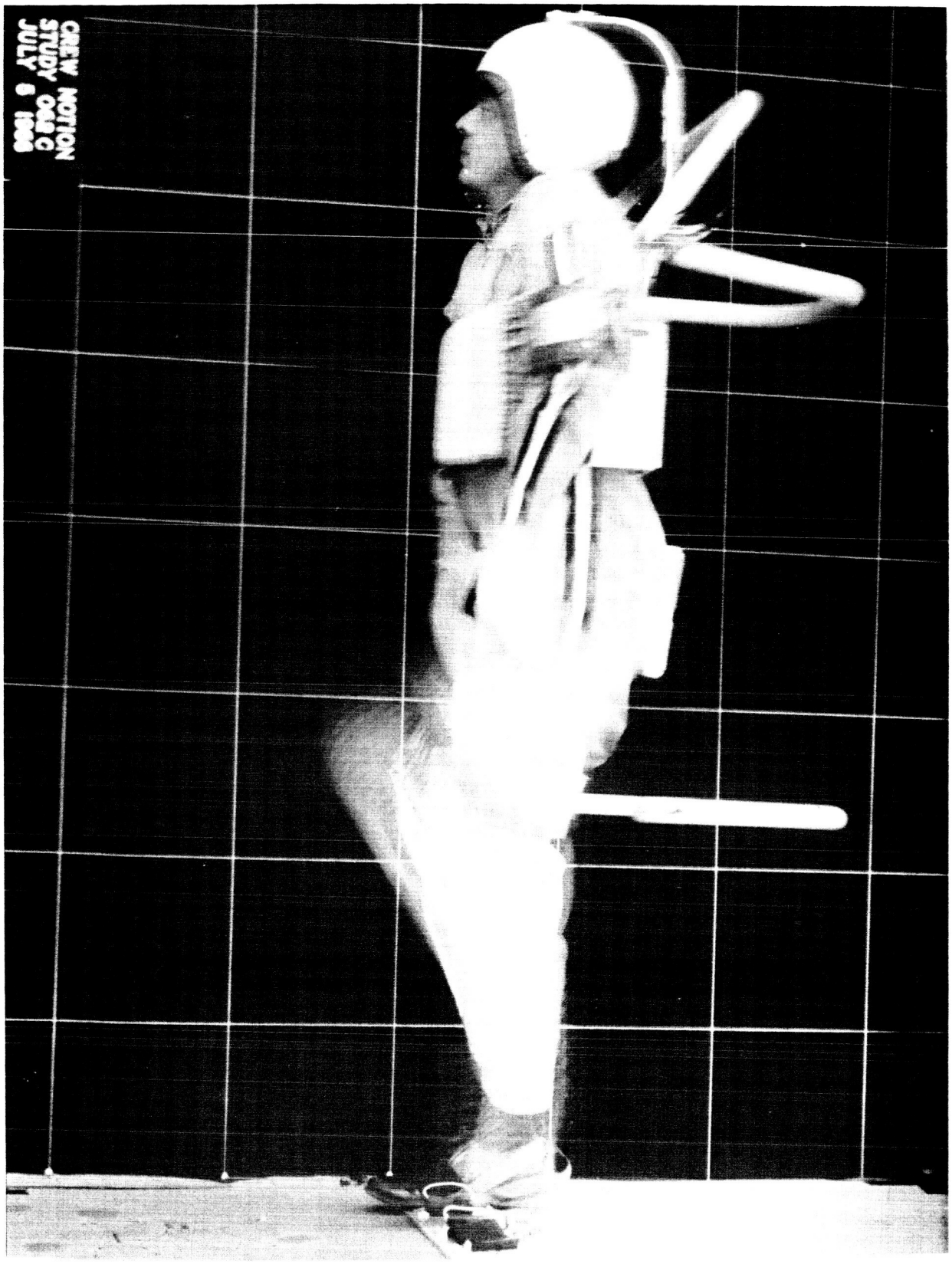

Figure 19. Leg Motion

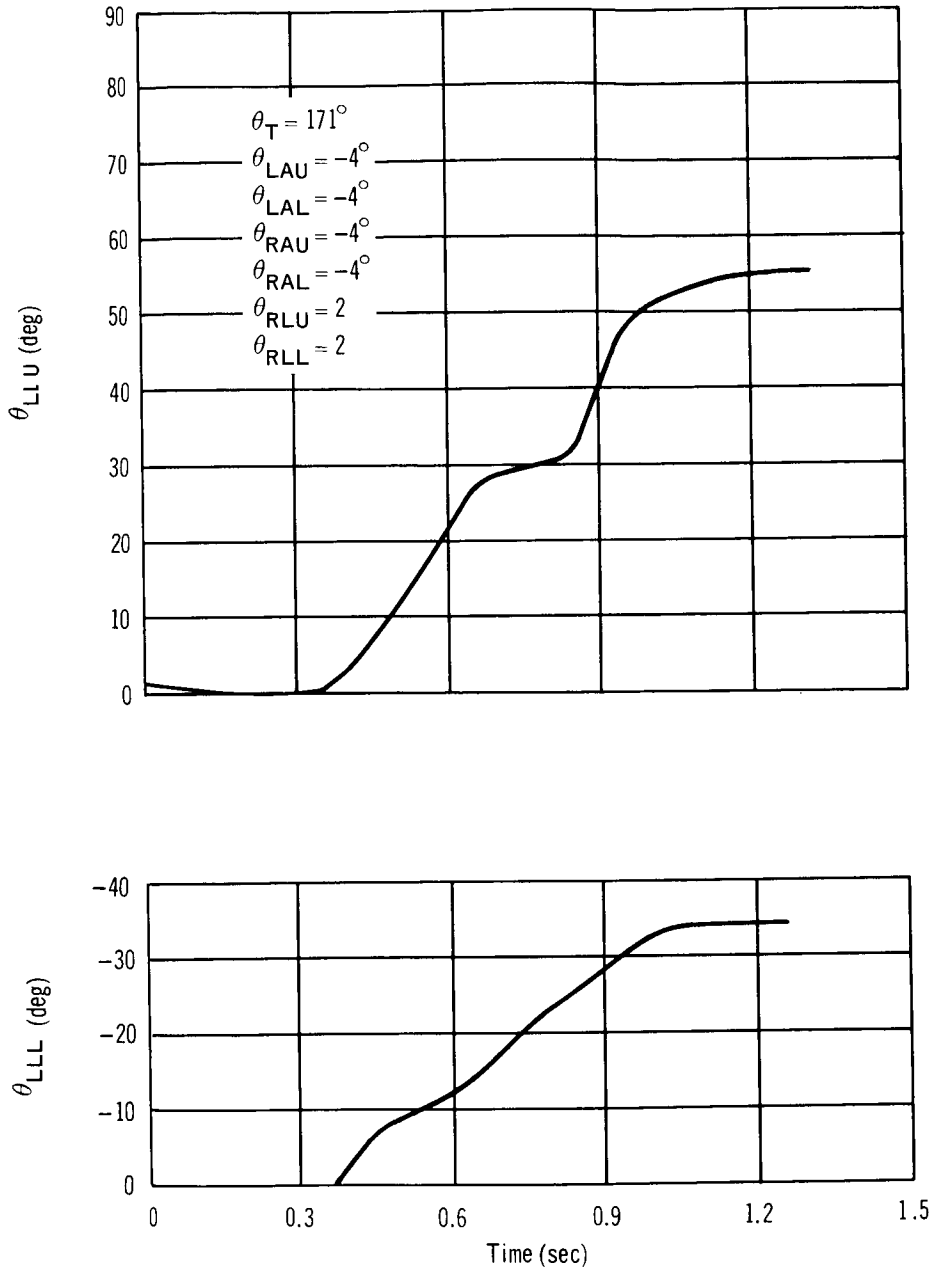

Figure 20. Leg Motion Euler Angles – Subject A

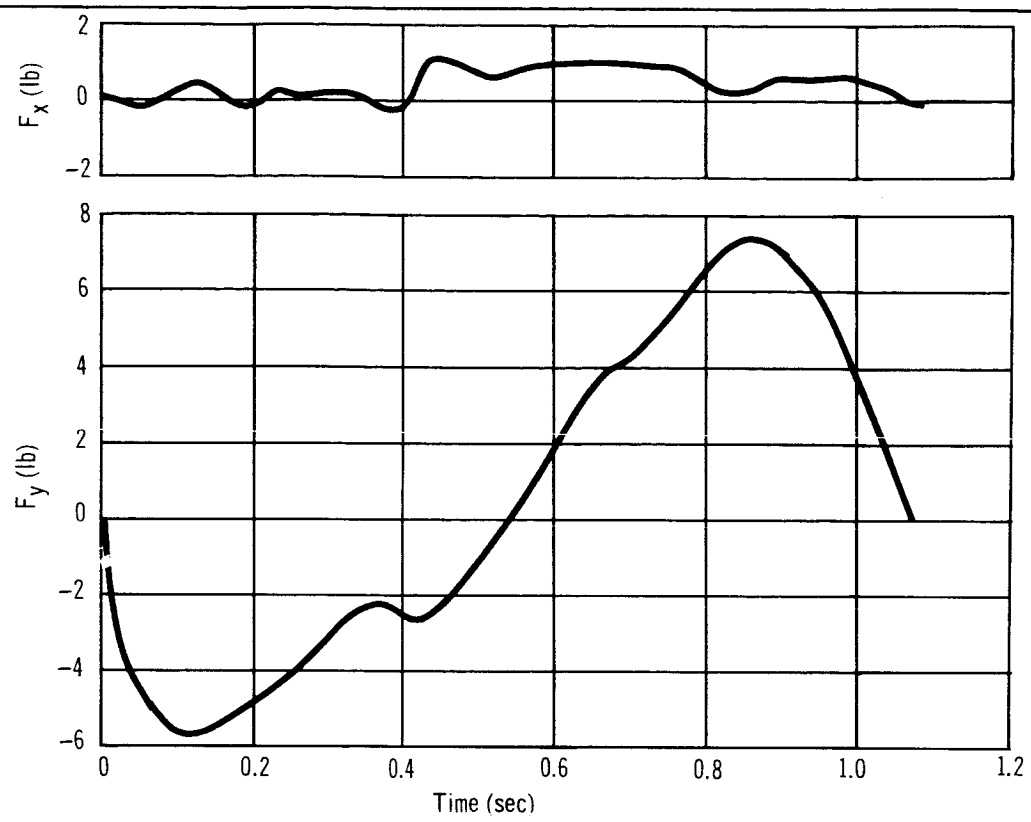

Figure 21. Leg Motion Disturbance Profiles – Subject A

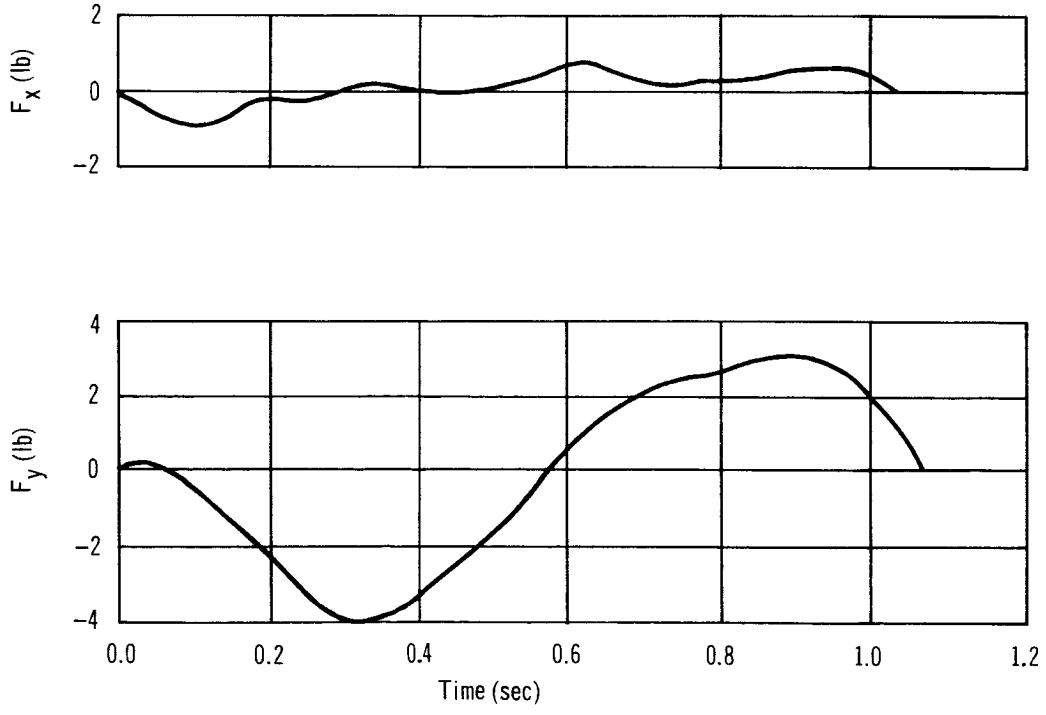

Figure 22. Leg Motion Disturbance Profiles – Subject B

The disturbing forces are computed by substituting the leg profiles, given in fig. 20, in these equations. The upper leg segment profile shown in fig. 20 indicates a deceleration/acceleration motion in the middle of the leg segment motion. The calculation of the forces for the leg segment motion using the profile of fig. 20 is laborious. Hence, a simpler leg segment profile will be used to illustrate the magnitude of the forces. This profile is derived as follows:

(1) Upper Leg

$$\ddot{\theta}_{LLU} = 3.84 \text{ rad/sec}^2 \text{ for } 0 \leq t \leq 0.5 \text{ sec}$$

$$\ddot{\theta}_{LLU} = -3.84 \text{ rad/sec}^2 \text{ for } 0.5 < t \leq 1.0 \text{ sec}$$

(2) Lower Leg

$$\ddot{\theta}_{LLL} = -2.97 \text{ rad/sec}^2 \text{ for } 0 \leq t \leq 0.45 \text{ sec}$$

$$\ddot{\theta}_{LLL} = +2.97 \text{ rad/sec}^2 \text{ for } 0.45 < t \leq 0.9 \text{ sec}$$

This profile is used in the force equations for the leg motion that follow.

$$F_x = 1.06 (\ddot{\theta}_{LLU} \cos \theta_{LLU} - \dot{\theta}^2_{LLU} \sin \theta_{LLU}) + 0.281 (\ddot{\theta}_{LLL} \cos \theta_{LLL} - \dot{\theta}^2_{LLL} \sin \theta_{LLL}) \quad (6)$$

$$F_y = 1.06 (\ddot{\theta}_{LLU} \sin \theta_{LLU} + \dot{\theta}^2_{LLU} \cos \theta_{LLU}) + 0.281 (\ddot{\theta}_{LLL} \sin \theta_{LLL} + \dot{\theta}^2_{LLL} \cos \theta_{LLL}) \quad (7)$$

(The numerical constants represent the leg parameters obtained from the MAID Program generated by NASA and are given in Appendix D.)

The results of these equations and assumed leg profiles yield x and y components of force of approximately 5 lb each. The forces exerted by Subject B, fig. 22, are 1 and 4 lb for the x and y axes, respectively. Here again, the x-axis force is low compared to the predicted value.

The equations derived for the test data of the leg motion are given in Appendix C.

LOCOMOTION

Locomotion may be conveniently devided into two classes: (1) guided motion and (2) free soaring. Guided motion is the translation of the body utilizing either continuous or intermittent contact with the vehicle for purposes of controlling body attitude and velocity. The types of guided motion simulated during this study include: (1) velcro walking, (2) compression walking, and (3) guided soaring. Free soaring is the translation of the body in which no contact is made with the laboratory, except at initiation and termination of motion.

The disturbance profiles for the velcro walking, compression walking, and free soaring are referenced to the coordinate system shown in fig. 4. The guided soaring perpendicular to the platform disturbance profile is referenced to the coordinate system of fig. 6. Guided soaring parallel to the platform is referenced to the coordinate system of fig. 5.

For the guided locomotion, it should be noted, the force parallel to the direction of movement contains two error sources: (1) the component of gravity induced when the subject moves from static pendulous support position and (2) the rotation of the subject when linear motion is terminated. For each foot of displacement of the subject from the static pendulous position, a bias force of 3. 2 lb will be present in the direction of motion, on the basis of the 54-ft pendulum length. In one particular test of the guided locomotion, the subject translated at least 2 ft from the static pendulous position which would produce an approximate 6. 5 lb bias in the direction of motion. When the subject terminates the linear translation, a body rotation is induced. The amount of rotation depends on the location of the subject's center of mass with respect to the locomotion surface and the level of intensity or speed of translation. Individual locomotion simulation and test results are described in the following paragraphs.

Velcro Walking

To enable a person to walk in a zero-g field, an adehesive material could be used on shoes and walking surface. Such a material is velcro. To perform the velcro walk, the subject plants both feet firmly on the velcro walk strip, grasps the hand rail with his right hand, moves his left foot by rotating around the ball of the foot, and then lifts the foot free of the velcro. He then advances the left foot approximately 8 in., moving forward in the plus-x direction, and repeats the process with the right foot. Velcro walking is done at three levels of intensity: minimum, nominal, and maximum. For the minimum level, the subject does not use the hand rail.

Fig. 23 is a multiple exposure photograph of the velcro walk at a nominal rate.

Figs. 24, 25 and 26 present the Euler angles for the various body segments and the in-plane translation of the head for the velcro walk. From fig. 24 there was practically no rotation of the torso and left arm. The subject held his left arm to his side. Fig. 25 shows the motion of the right arm which the subject used to grasp the handrail. Fig. 26 indicates that the subject took approximately a 20-in. step in approximately 2 sec.

Fig. 27 shows the force profiles for Subject A in performing the nominal velcro walk. The initial positive force F_y, is produced as the foot is pulled to free it from the velcro. Freeing of the foot from the velcro takes a maximum force of 3 lb in this case. After the foot is free from the velcro, which takes approximately 0.2 sec, the leg is moved in a normal stepping manner. This leg motion produces the first negative peak in F_y and the second of succeeding positive peak. The same wave form is noted for the leg motion as was shown in fig. 21. The high frequency, or spiking, negative peak, approximately 1.2 sec, is caused by the impacting of the foot on the velcro strip to complete the first step. The leg motion of the right foot then starts with the next negative peak and is completed in approximately 1.8 sec. The data indicate that the right foot was set down on the platform with the utmost of ease at the completion of the step.

The maximum y component of force is approximately 15 lb for the nominal velcro walk.

During the walking motion, the x component of force is almost always negative. Initially, the right foot pushes back (-x direction) for approximately 1.0 sec. At approximately 1.3 sec, the left foot is then pushing back. Also during this time the right hand, by grasping the rail, is applying a negative F_x force. The curve for the x component of force is biased and, therefore, the integral of the force is not zero at the termination of the motion. As previously mentioned, this is the result of the gravity component induced from the translation and the residual rotation of the body at the completion of the movement.

In these guided motion tests an attempt was made to center the subject's translation with respect to the force balance. That is, if the subject translates 2 ft along the platform, the starting position is 1 ft aft of the force balance, assuming the static position of the subject performing the motion is centered over the force balance. This would induce a positive force of approximately 3.2 lb in the x direction (parallel to the platform) at the start of the test. Because the force balance is zeroed and calibrated at the start of each test series, the reading of the x component of the force balance has a negative initial error of 3.2 lb. If the subject performs the locomotion centered over the force balance, then the following procedure may be used to correct the x component of force. With the starting position of the pendulum support deflected away from the static position, the gravity component of force in the plus-x direction is expressed as $-W \sin \delta / L$. The amplitude, W, is the suspended weight, L the length of the pendulum arm (54 ft), and δ

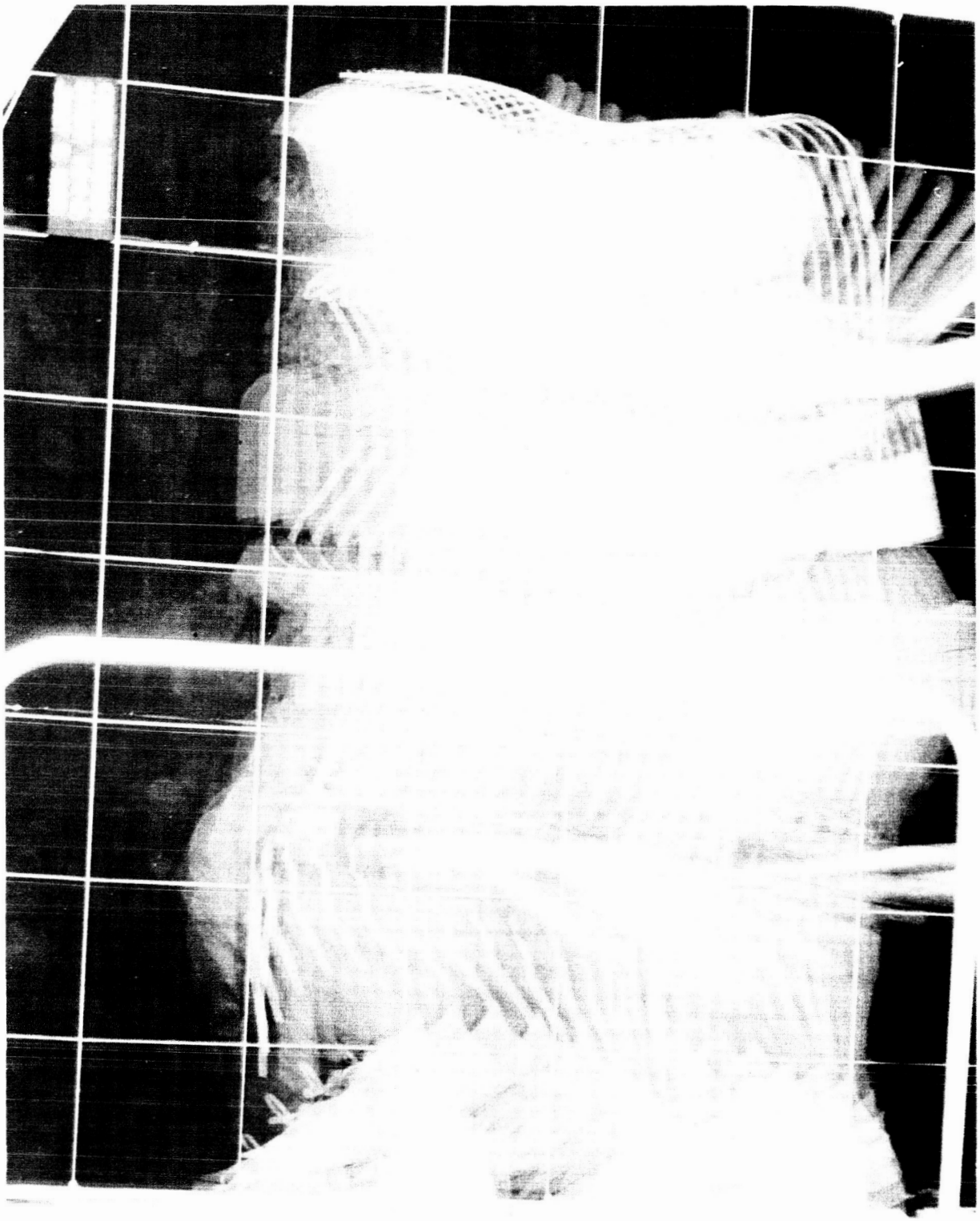

Figure 23. Velcro Walking

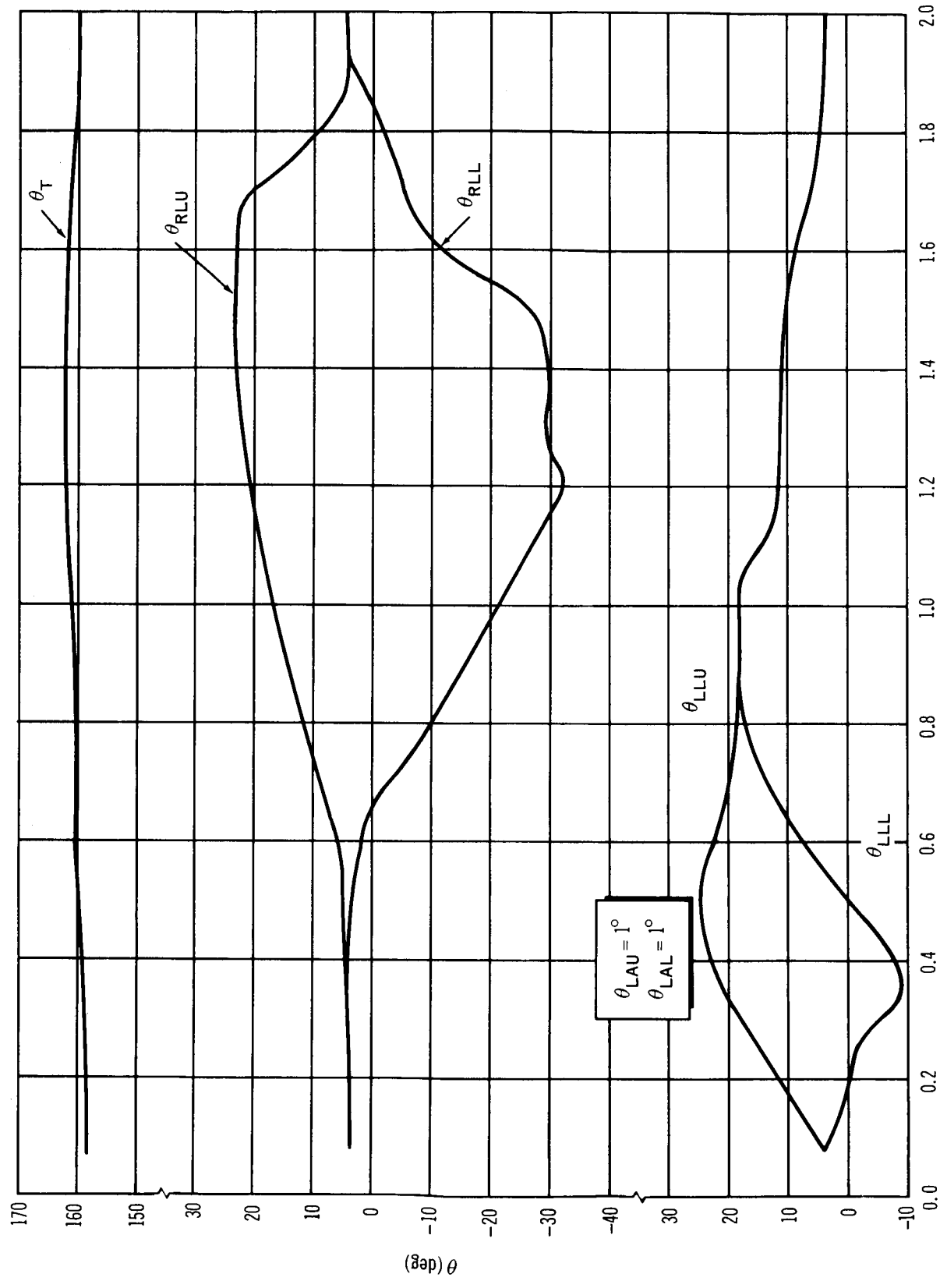

Figure 24. Velcro Walking Euler Angles – Subject A

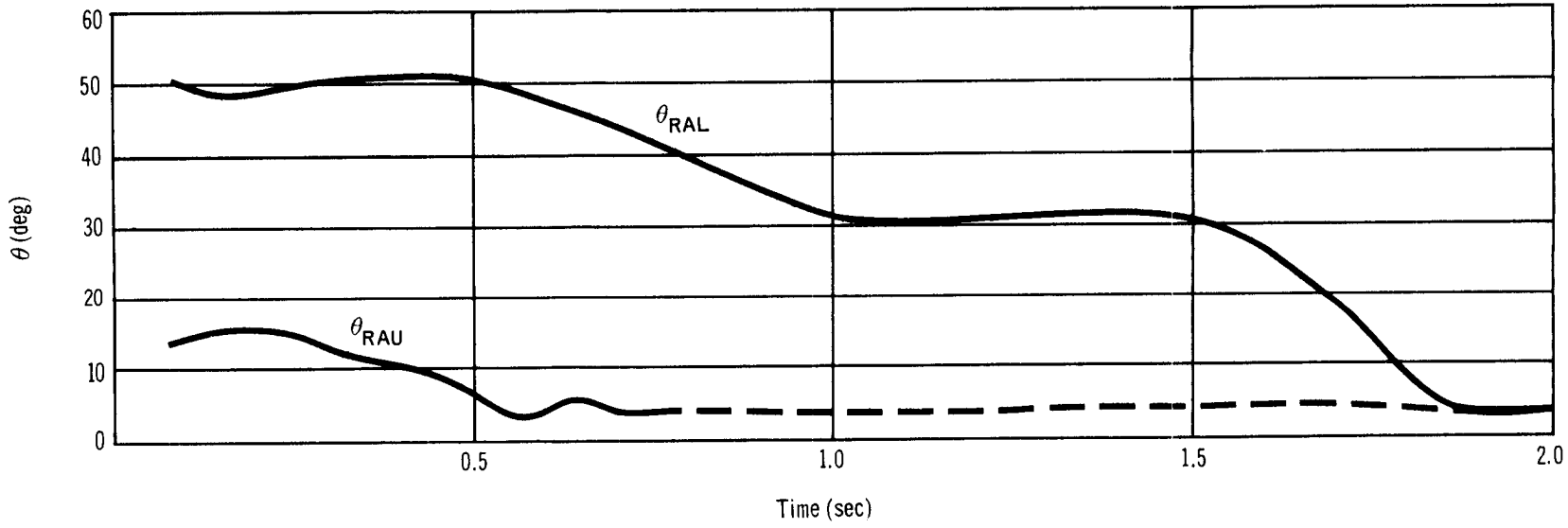

Figure 25. Velcro Walking Euler Angles – Subject A

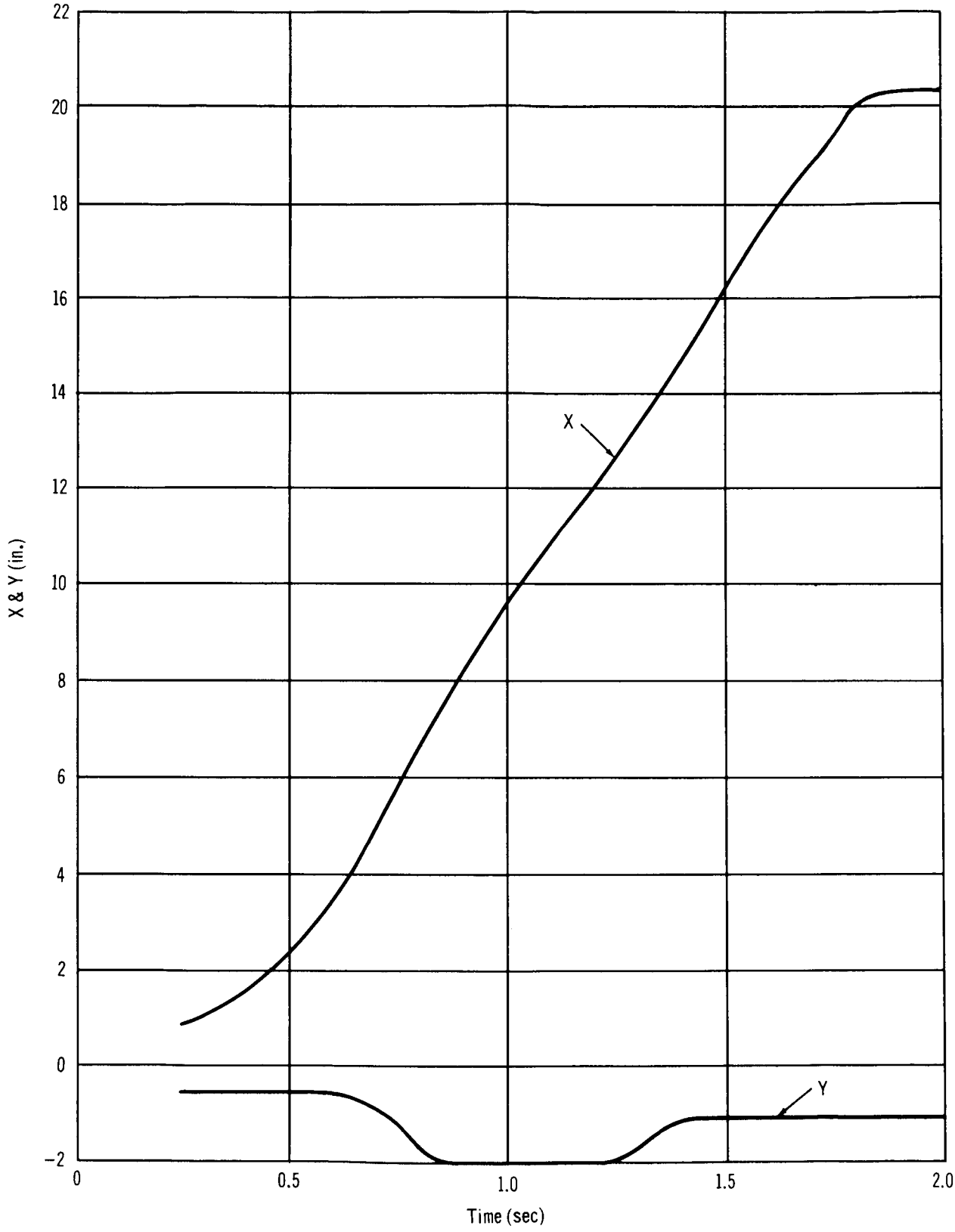

Figure 26. Velcro Walking Displacement – Subject A

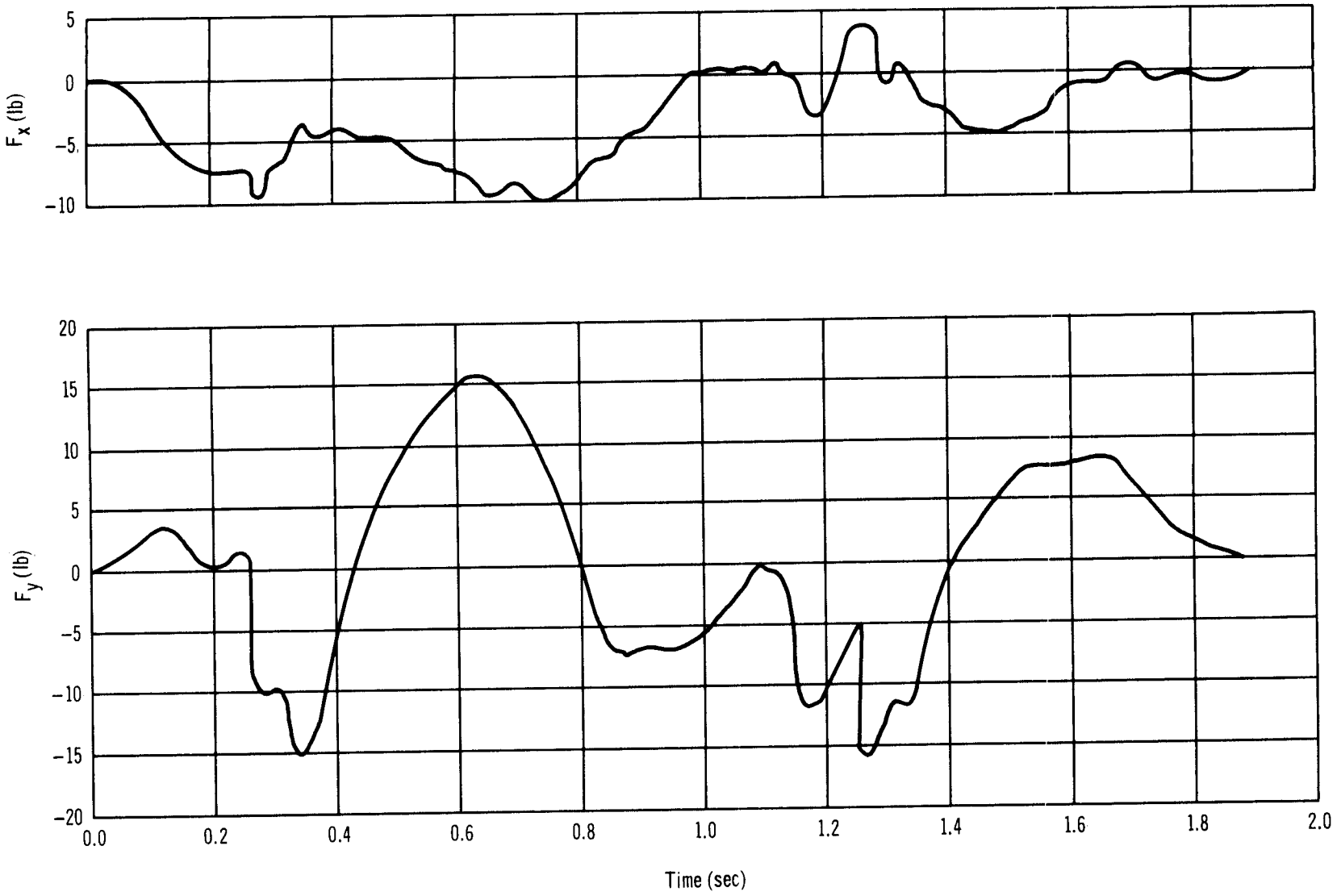

Figure 27. Velcro Walking Nominal Disturbance Profile – Subject A

is the x-axis displacement in feet from the center of the force balance. Because the force balance is zeroed at the beginning of the test, the error component becomes W sin δ/L. (The sign of δ is obtained from the direction of displacement along the x axis.) This curve represents the abcissa of the line of zero force for negating the gravity component when superimposed on the plotted data for the x component of force. In superimposing this zero-force curve on the plot, the integral of the x component of force will be more nearly zero. If the initial and final positions with respect to the force balance are known, the effect of the gravity component can be removed. These positions were not noted during the guided locomotion tests and therefore the data were not corrected.

The forces produced by Subject B in performing the velcro walk are shown in fig. 28. Subject B stepped quicker and, consequently, harder than Subject A for the nominal case. The maximum y component of force is 28 lb, which occurred at the time of impact of the right foot, approximately 1.4 sec. Subject B took approximately 9 lb to free his left foot (first positive peak) from the velcro. The left foot impact is near 0.9 sec.

Figures 29 and 30 show the minimum level of velcro walking for Subjects A and B, respectively. It took Subject A 0.6 sec longer to complete the walk than Subject B. The leg motion forces produced by Subject A are only about half those produced by Subject B. The impact forces of the steps, occurring approximately 1.4 and 1.9 sec after first motion for Subject A and 0.25 and 1.4 sec after first motion for Subject B, are approximately equal, 10 lb.

In performing the minimum velcro walk, the hand rail was not used. This constrained the subject's walk to a small step. Any movement in the x direction of the total center of mass of the body produces a restoring force, thereby limiting the subject's step. (This is the pendulum action of the counterbalance system.) To perform the velcro walk without the use of hand holds in a true zero-g environment, a moment must be produced by the flexture of the ankle so that the body rotates in the direction of the walk. This compensates for the tendency of the torso to move in a direction opposite to the direction of motion. The ease of performance of the walk is determined by the moment the astronaut can induce by flexing his ankle.

The transmissibility of this moment to the spacecraft is determined by the construction of the shoes. The shoes must have a rigid sole such that the heel cannot be peeled off, but must be lifted from the velcro walk. This will provide the maximum moment transmissibility to the walking strip. Even with the astronaut wearing a shoe of optimum design, this induced moment appears to be so small that velcro walking without the use of a hand hold will be laborious, if not impossible. The errors introduced by the pendulum length, location of the walking surface, etc., limit the feasibility of the velcro walking simulation.

Figs. 31 and 32 show the disturbances for Subjects A and B, respectively, performing the maximum velcro walk. Subject A produced forces of 50 lb in the x and y components, while Subject B produced 32 lb of force in these components. Here again, the curve of F_x should be modified in the manner previously outlined for a more realistic force profile.

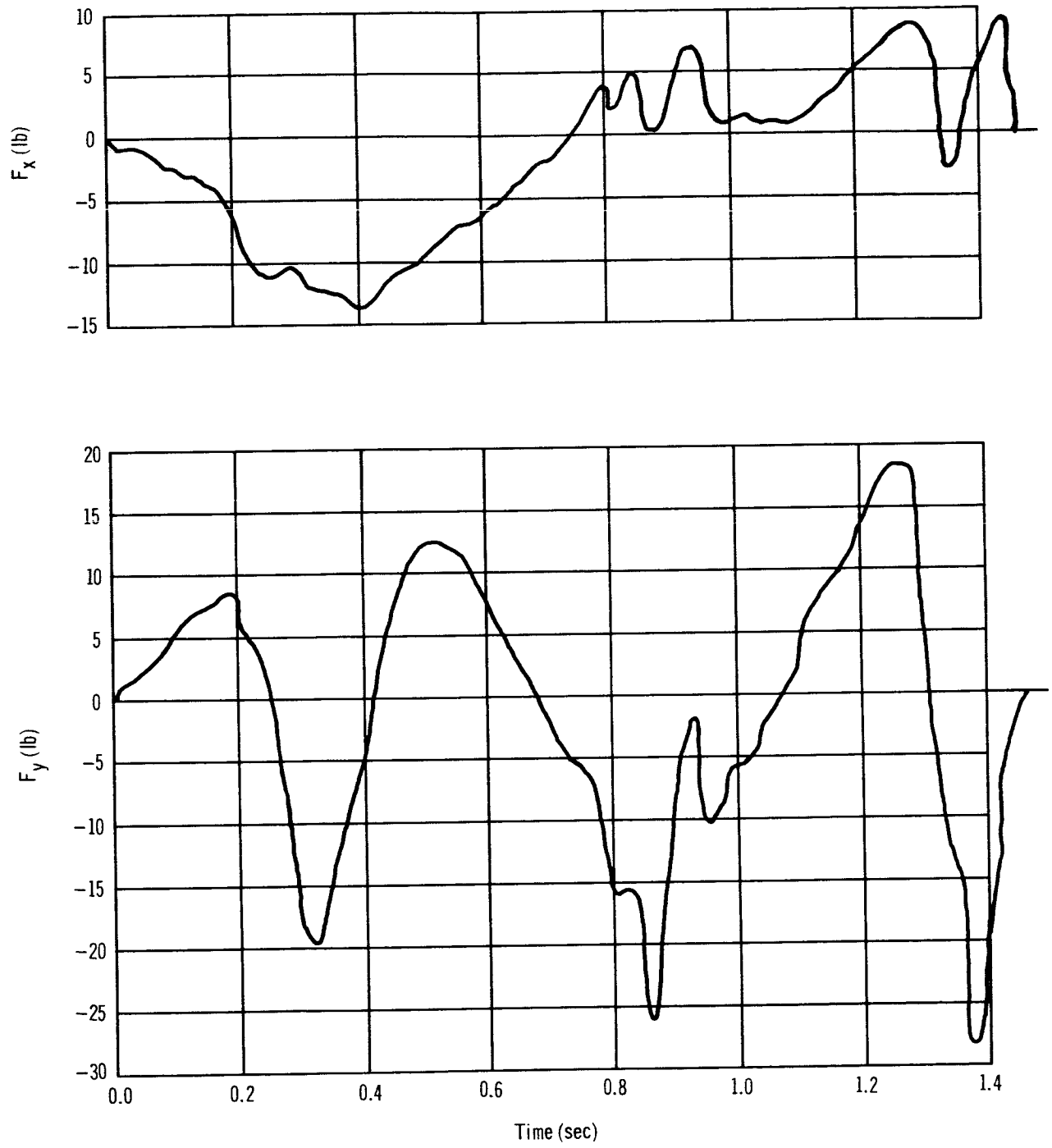

Figure 28. Velcro Walking Nominal Disturbance Profile – Subject B

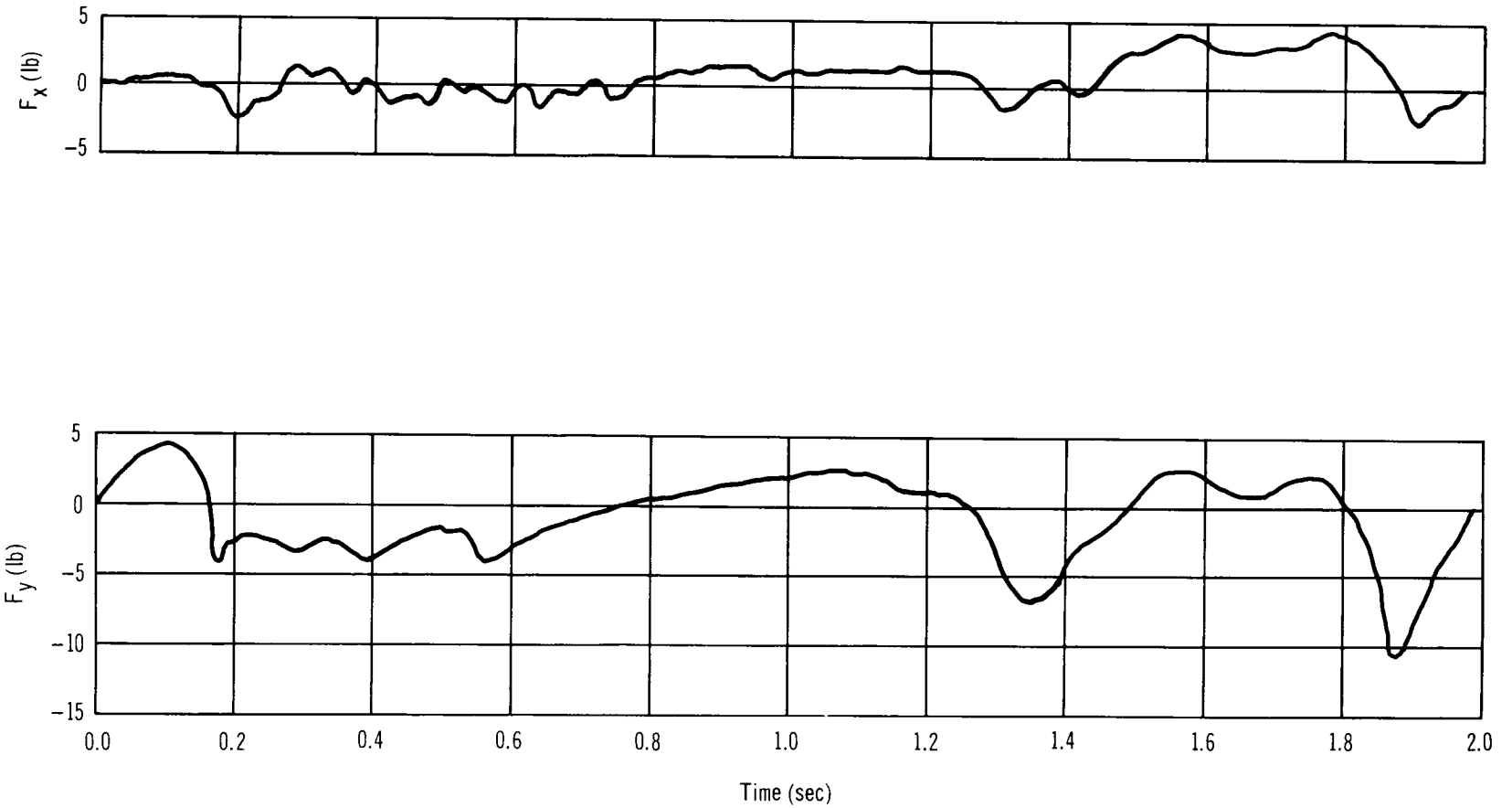

Figure 29. Velcro Walking Minimum Disturbance Profile – Subject A

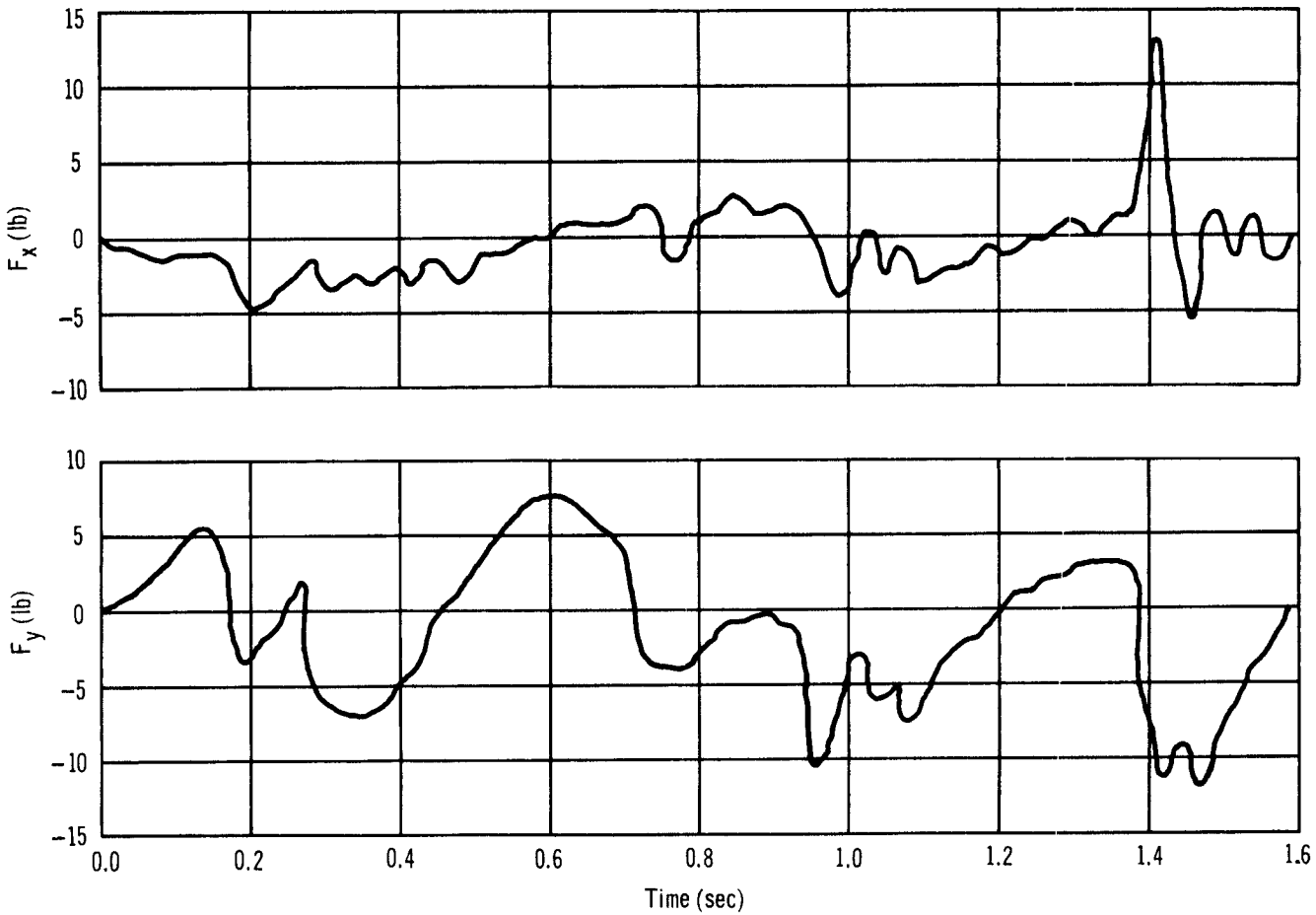

Figure 30. Velcro Walking Minimum Disturbance Profile – Subject B

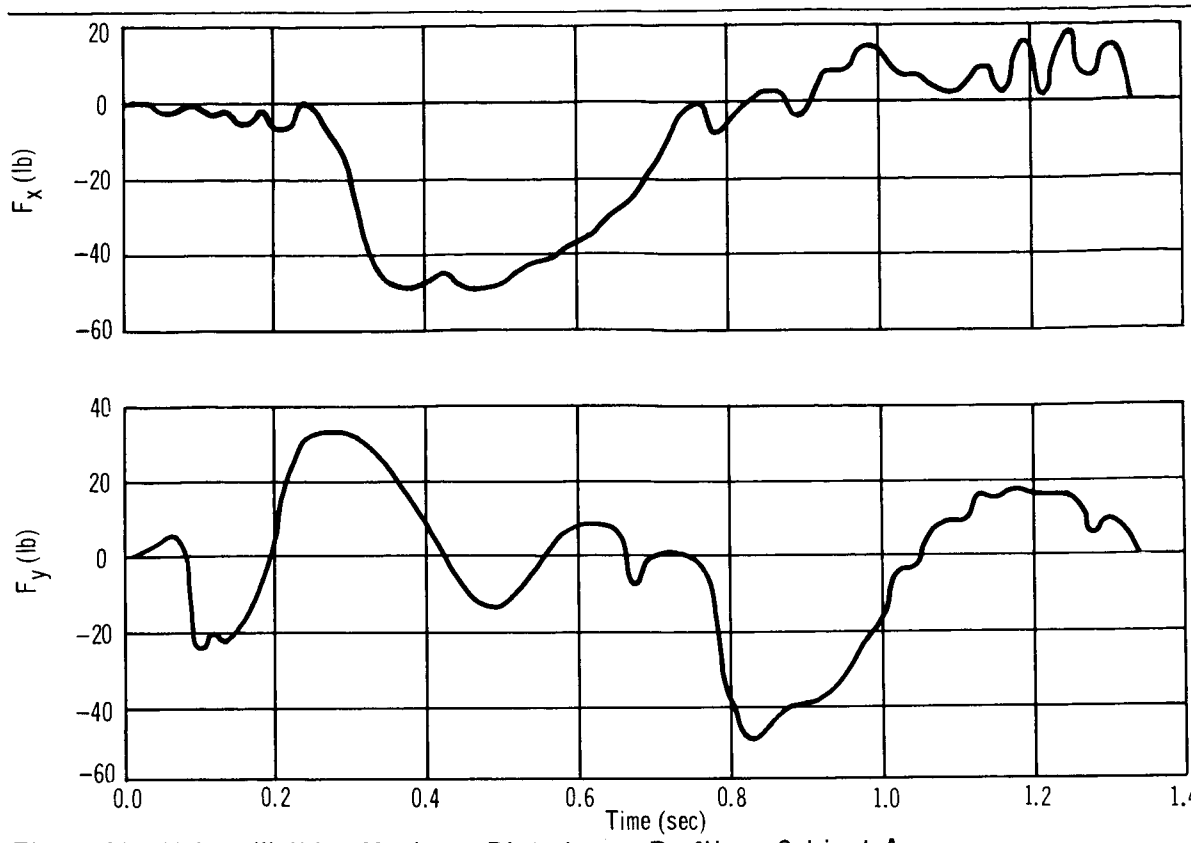

Figure 31. Velcro Walking Maximum Disturbance Profile – Subject A

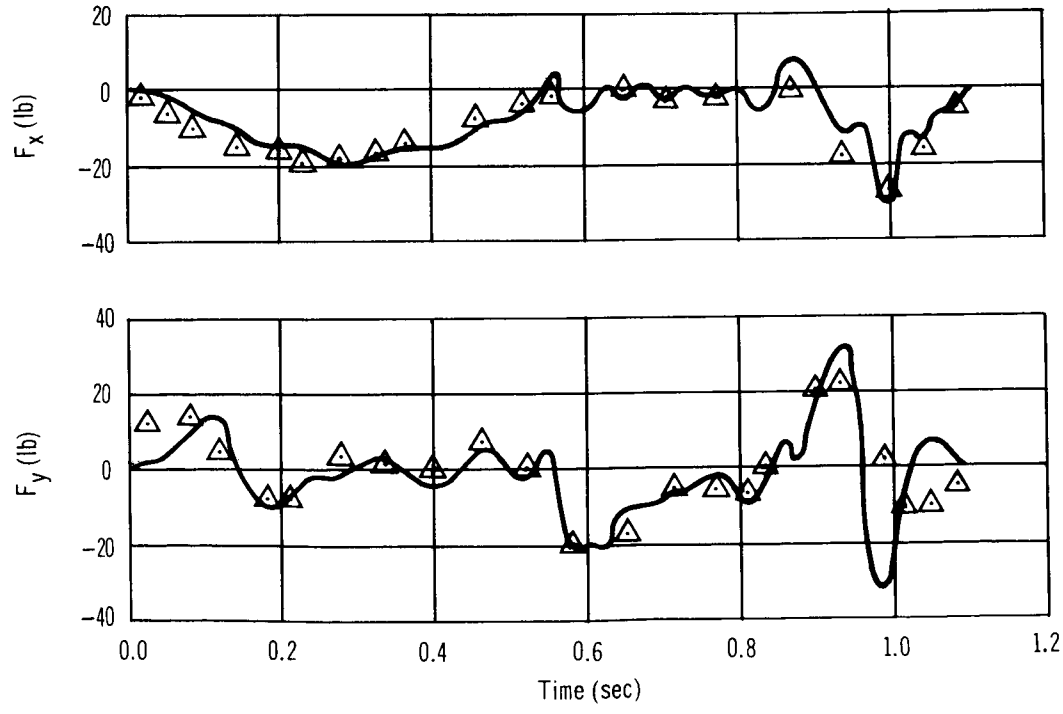

Figure 32. Velcro Walking Maximum Disturbance Profile – Subject B

During this maximum condition, the maximum suspension force, F_z, was 11% of Subject A's weight and 20% of Subject B's weight. In all the tests that involved translations in x and/or y, these relatively high suspension forces were present. These forces are caused by the out-of-plane motion by the subject and the pendulum action of the suspension system. These out-of-plane motions by the subject can be induced by an initial tilting of the subject out of the horizontal plane; therefore, the subject's feet are higher or lower than his head. During the testing, such tilting was carefully minimized. In some cases tilting probably was induced by the subject after the motion was started. The force data F_x and F_y, presented for these tests, might be 15% greater in amplitude to account for the out-of-plane motion. The general shape of the curves would not be affected. These forces are large enough in magnitude so that the moment data resulting from body segment angular accelerations are negligible.

The equations of the forces for the velcro walking are given in Appendix C. The terms of the Fourier series are evaluated and plotted in fig. 32 for the maximum velcro walking of Subject B. The higher frequency terms present in the F_x and F_y data were not reproduced, as shown in fig. 32.

Free Soaring

In performing free soaring locomotion, the subject in the standing position pushes off from the platform by flexing the left foot, traveling in the plus y direction (note fig. 4). This is done at three levels of intensity: (1) minimum, (2) nominal, and (3) maximum. For the minimum and nominal levels, a bounce board is positioned over the subject's head and attached to the force platform by means of a bar. After the subject pushes off the force platform, he impacts on the bounce board with his hands and then pushes off to return to the platform. The maximum level of intensity is attained by the subject being in a crouched position and then flexing both legs as rapidly as possible. This is done without the bounce board attached.

Fig. 33 is a plot of the downward force, F_y, for the three levels of intensity of the free soaring for Subject A. In the nominal case, the push off with the left leg takes place over the first 0.35 sec and produces a normal force on the platform of 92 lb. The second peaking, between 0.5 sec and 1.0 sec, occurs when the subject impacts on the bounce board with his hands. The area under this portion of the curve, which represents linear impulse, is greater than the pushoff impulse because it represents the impact and a return pushoff to the platform. The forces transmitted to the x and z axes for this motion are 7% and 10% of the y axis, respectively. These small misalignment forces are omitted because they do not affect the test. The total time of the impulse obtained with the leg for the nominal case is 0.35 sec. Integrating the pushoff force curve gives approximately 15.5 lb-sec of impulse, which results in a soaring velocity of approximately 3 ft/sec for this 175-lb subject.

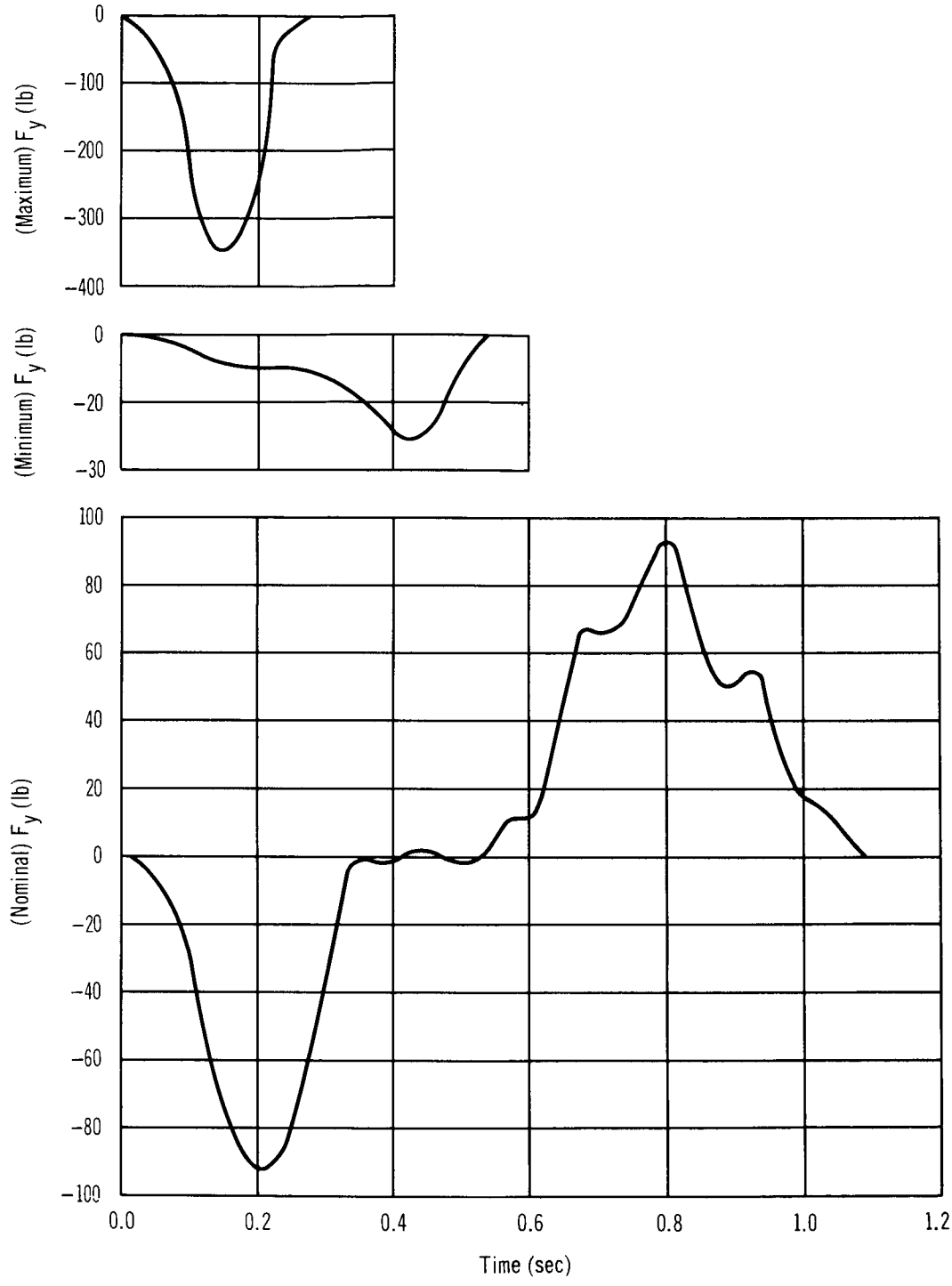

Figure 33. Free Soaring Disturbance Profiles – Subject A

In the minimum case, the maximum force is approximately 32 lb with a total time of application of approximately 0.55 sec. The shape of this force curve is quite different than the nominal or maximum case. Again, the forces transmitted to the x and z axes were small and therefore omitted. Also, the impact on the bounce board is omitted because it is not significant.

The subjects had some assistance in performing the maximum case of free soaring. They grasped the full-length body exercise supporting rod for stability prior to first movement. This, in effect, spring loads the subject and accordingly permits a maximum force level to be exerted on the platform. In the maximum case, a peak of 350 lb was produced in the free soaring exercise. The total impulse, which is the area under the curve, is 42 lb-sec. In defining the MORL attitude hold capability, the case of a six-slug crew member soaring at 5 ft/sec was used. This yields an impulse of 30 lb-sec, which is about 28% lower than the impulse obtained by the performance of Subject A. The soaring velocity obtained by Subject A, who weighs 175 lb, is computed as 7.7 ft/sec.

Fig. 34 shows the force curves of Subject B free soaring at the three levels of intensity. The main point of interest is that Subject B was only able to exert 56% of the force that Subject A produced.

All of the free soaring tests performed gave very smooth curves for the F_y-force component. Also, the shorter the time of application, the higher was the force exerted.

The equations for these forces are given in Appendix C.

Compression Walking

For the compression walking, an overhead bounce board is attached to the platform. The subject then walks, using the hand and foot pressure on the bounce board and force platform, respectively. The compression walking is done at three levels of intensity: (1) nominal, (2) minimum, and (3) maximum.

The nominal case of compression walking is presented in figs. 35 and 36 for Subjects A and B, respectively. In both cases, the force transmitted to the x axis is small compared to the normal component, F_y, of force. In comparing the y-axis force profiles, there is a marked difference between Subjects A and B. Subject A appears to have a much smoother walking ability than Subject B. Subject B produced impulse forces up to 50 lb, while Subject A produced results of 24 lb. It appears that Subject A pushed down with his foot and up with his hand about the same time, thus minimizing the y-axis force transmitted. From the total time of the walking, both subjects performed at about the same rate.

Noting the plot for Subject B, the y-axis force has the same similar characteristics as noted in the velcro walking exercises. The first negative and positive peaks (one cycle) are produced in raising the leg. (Breaking loose of the foot from the velcro is not apparent because of the scale.) The

next negative and positive peaks are caused by lowering the leg. The large negative pulse is then the foot impacting on the platform, 0.52 sec. From this time on, two body segment motions take place. These are the arm repositioning for the movement of the hand on the bounce board and the raising of the right leg. The right foot then impacts at 1.0 sec.

The minimum levels of compression walking are shown in fgs. 37 and 38 for Subject A and B, respectively. In both cases for the minimum exercise, the x component of force shows the bias effect produced by the pendulum support. Again, Subject A has a smoother walk. However, he produces the largest impact force, approximately 14 lb compared to the 11-lb maximum produced by Subject B. In comparing the nominal and the minimum cases, the disturbances resulting from compression walking, namely F_y, can be reduced by at least half by walking slower and smoother.

The maximum intensity of compression walking is shown in figs. 39 and 40. The peak y-component force impulses are noted to be 74 lb at 0.74 sec and 46 lb at 0.66 sec for Subjects A and B, respectively.

The equations of the forces are given in Appendix C for the three intensity levels.

Locomotion Normal to the Force Table

During this test, the subject is oriented as shown in fig. 6. The subject grasps the locomotion rod with both hands, keeping the rod perpendicular to and 12 in. from his chest. The subject translates by releasing the rod with the right hand and then moving the right hand a comfortable distance from the body, grasping the rod at the termination of the movement. The left hand is then released and moved a comfortable distance toward the right hand. This locomotion is in the plus-y direction. This type of locomotion is performed at three levels of intensity: (1) nominal, (2) minimum, and (3) maximum.

Figs. 41 and 42 show the nominal level of disturbance for Subjects A and B. For this particular locomotion, the subject's translation motion is in the y direction. Hence, the same pendulum effect will be present in the plot of the y component of force as was present in the x component of force of the walking tests. To remove the gravity component of force and account for the zeroing of the force balance at the start of the test, the curve of $W \sin \delta/L$ is again used to describe the zero-force line for the y component of force. The derivation of this curve is given in the velcro walk motion. This assumes that the starting and terminating positions for the motion are equal in deflection from the static position of the pendulum. If this is not the case, then the curve of the zero-force line can be modified to satisfy the conditions.

In modifying the y component of force by the equation for the zero-force curve, $W \sin \delta/L$, the y component of force would be initially negative, which indicates an acceleration of the subject away from the force table. The y force would then decrease to zero (the subject stops accelerating) and continue to increase in the positive direction. The positive direction indicates a deceleration of the subject to terminate his movement.

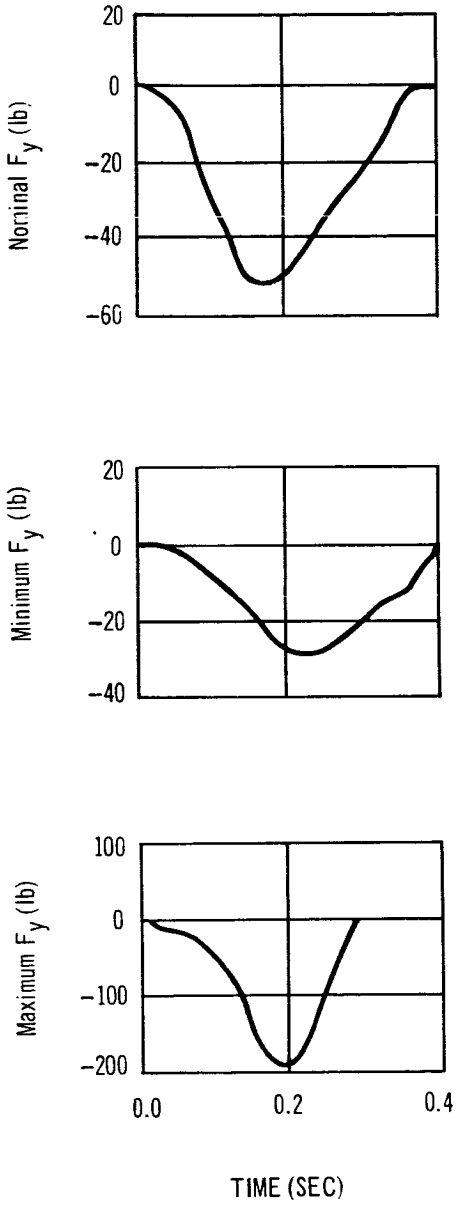

Figure 34. Free Soaring Disturbance Profiles – Subject B

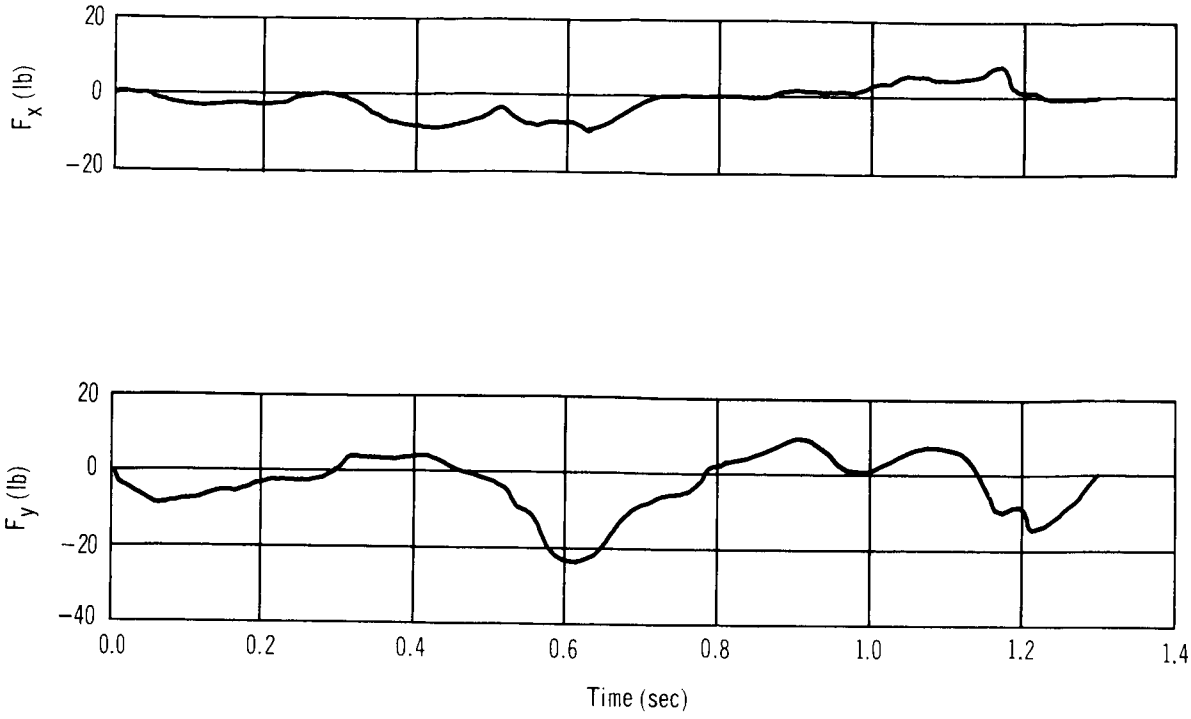

Figure 35. Compression Walking Nominal Disturbance Profile – Subject A

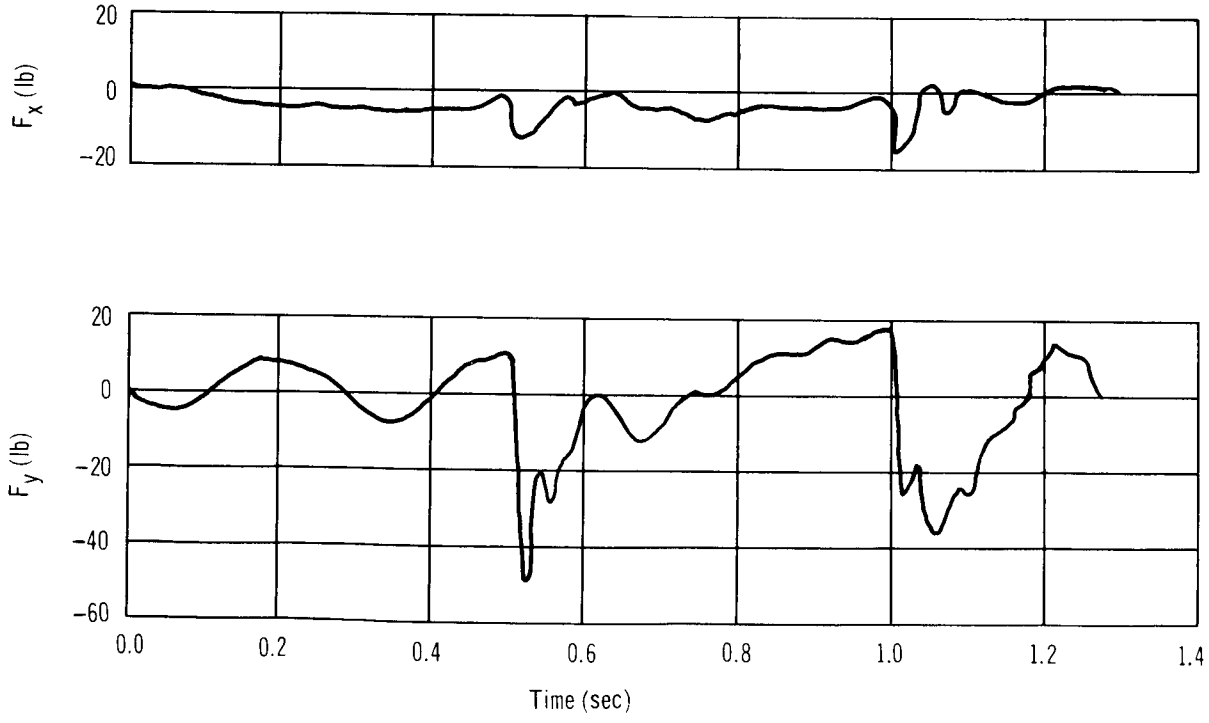

Figure 36. Compression Walking Nominal Disturbance Profile – Subject B

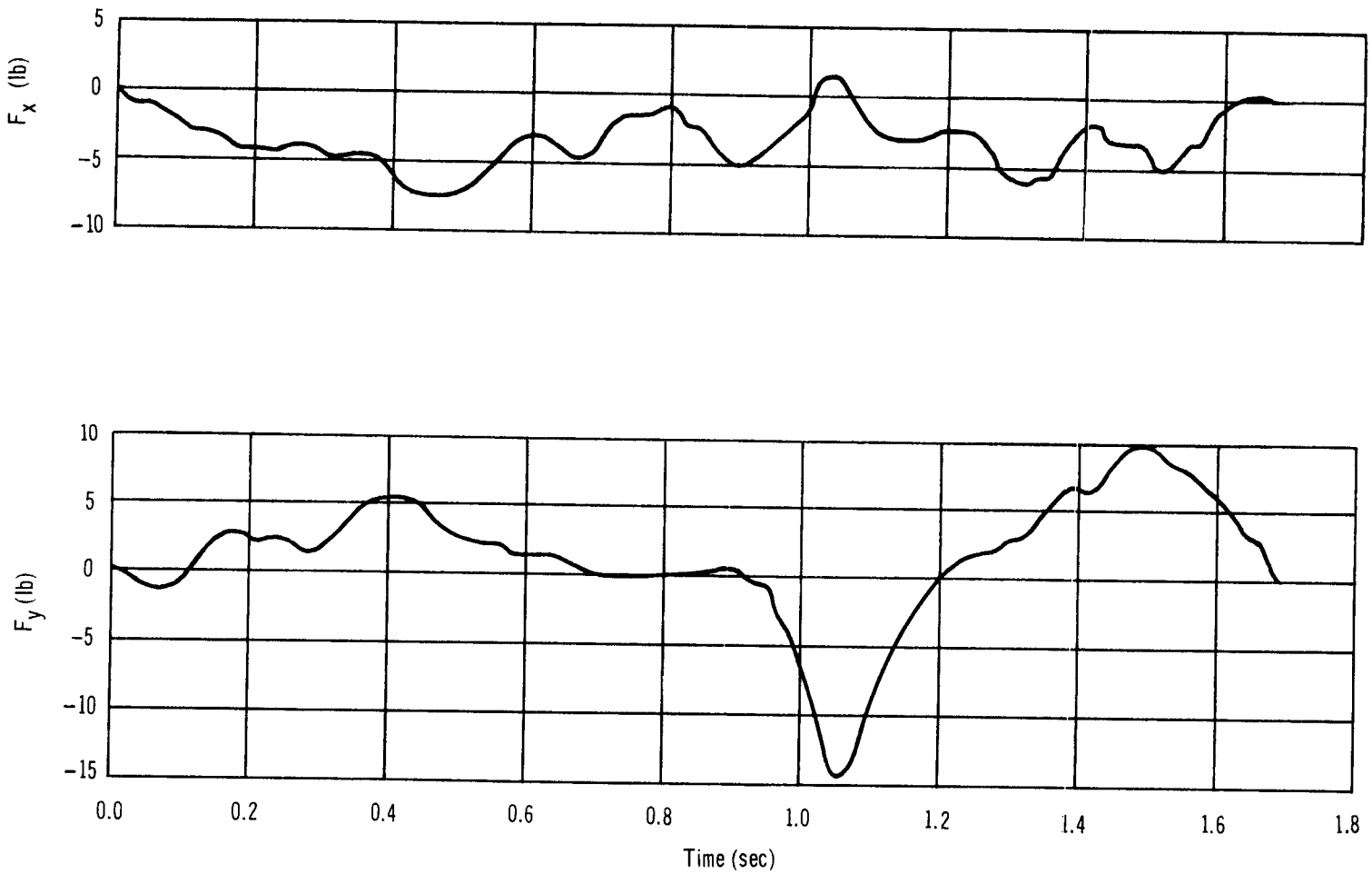

Figure 37. Compression Walking Minimum Disturbance Profile – Subject A

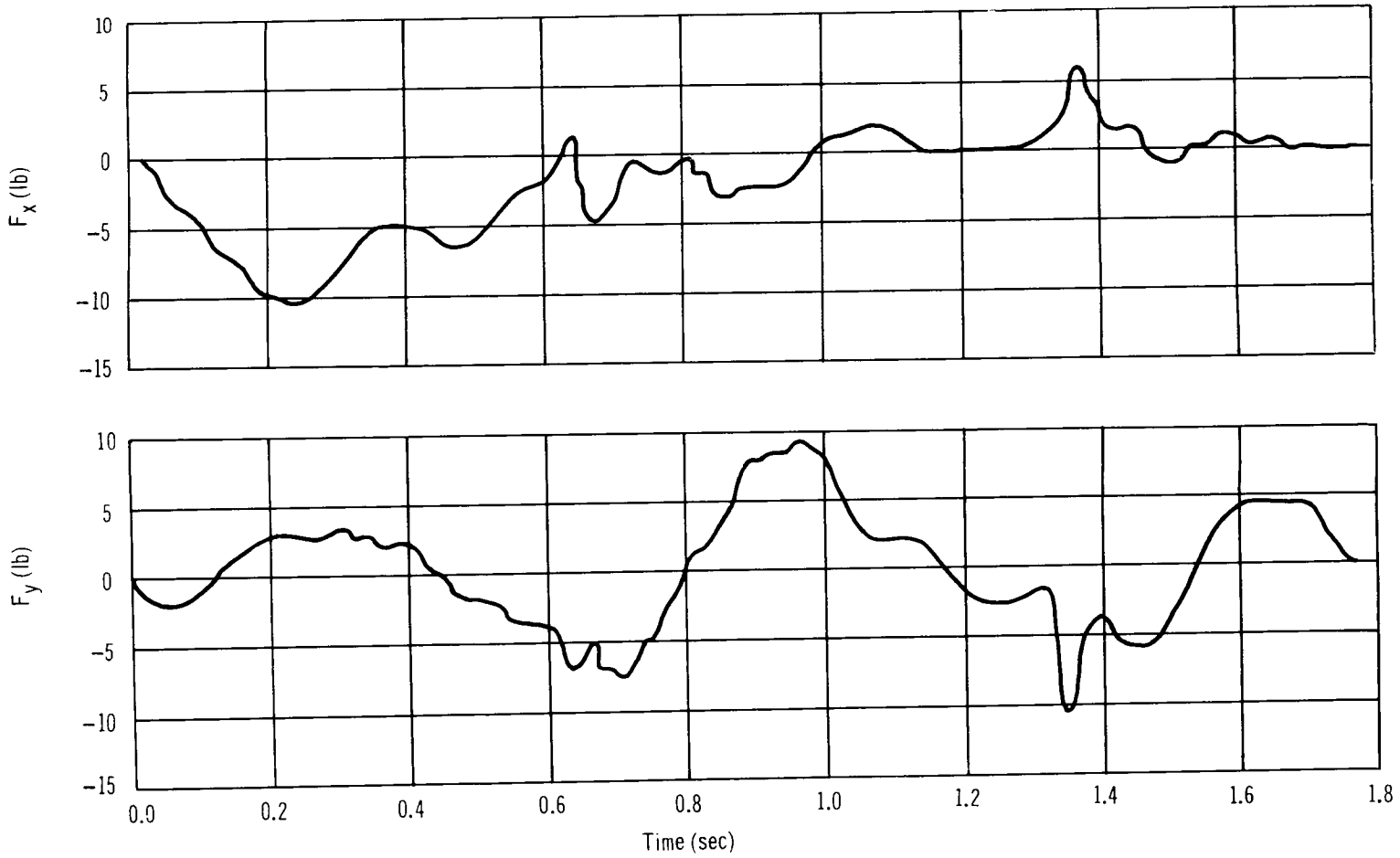

Figure 38. Compression Walking Minimum Disturbance Profile – Subject B

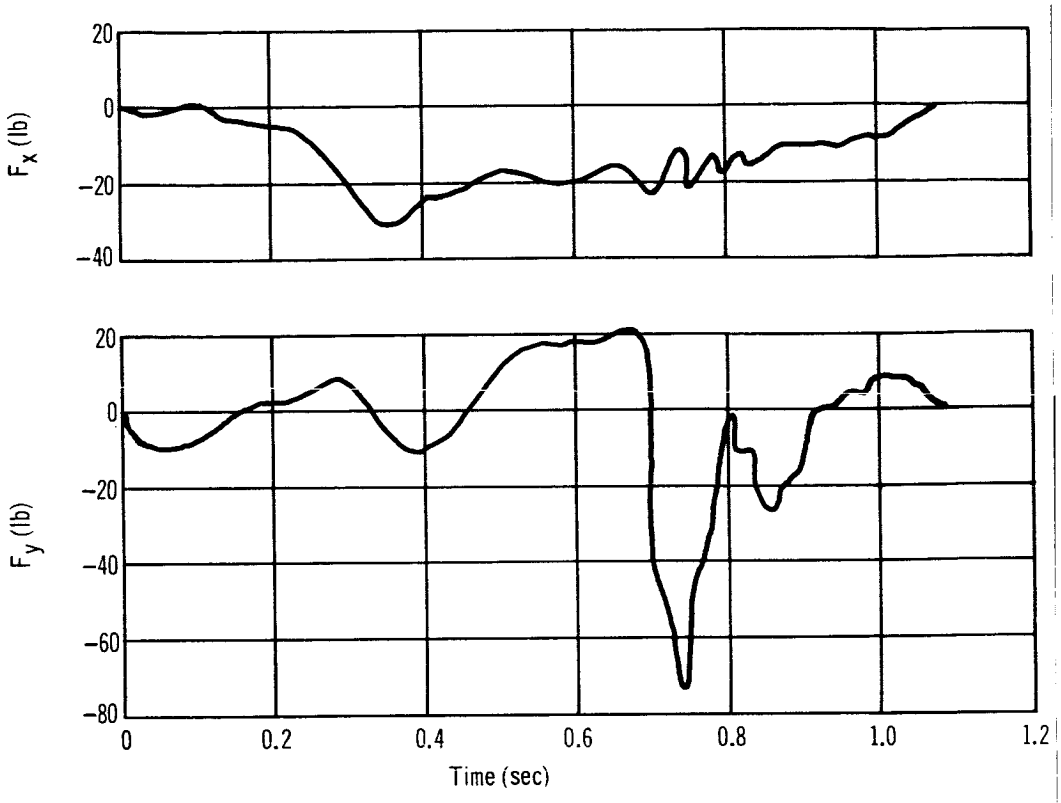

Figure 39. Compression Walking Maximum Disturbance Profile – Subject A

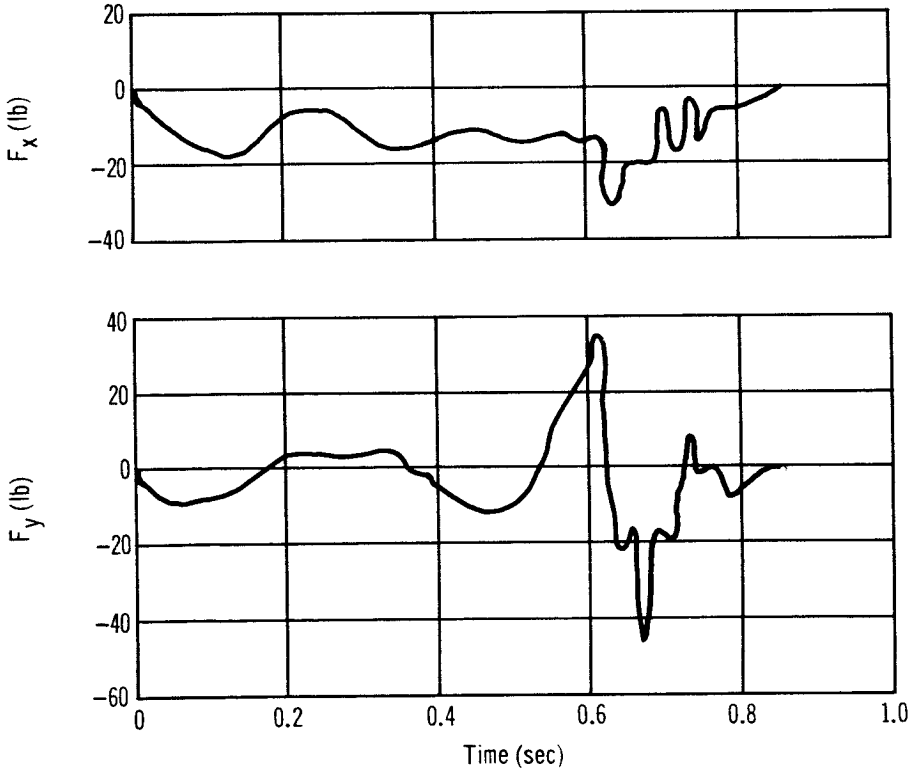

Figure 40. Compression Walking Maximum Disturbance Profile – Subject B

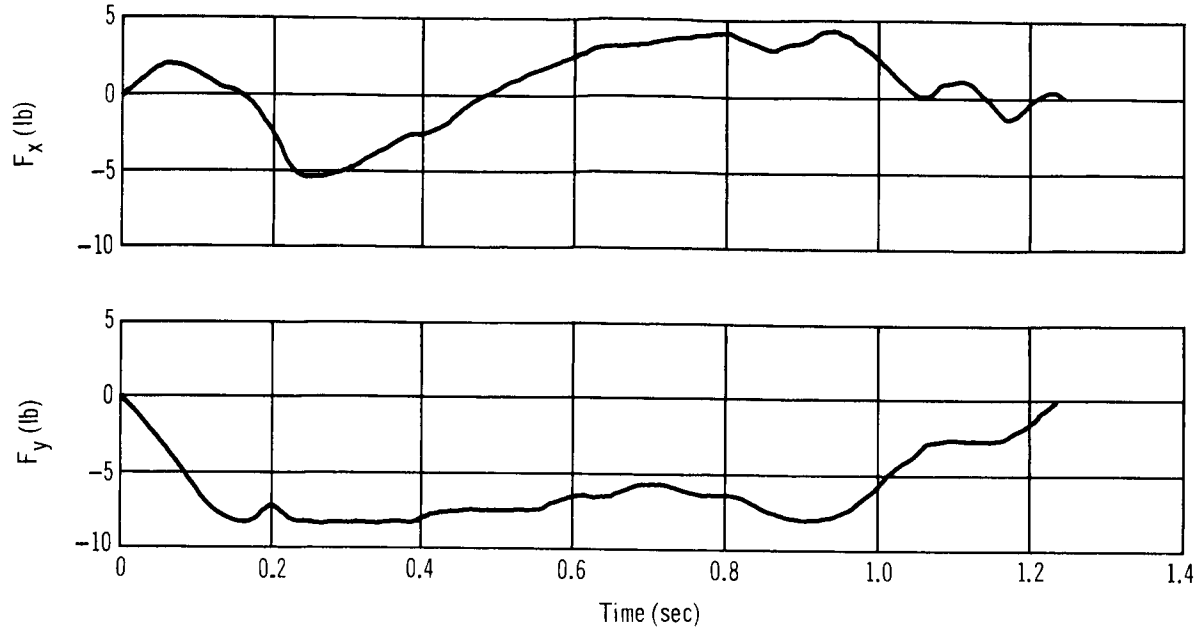

Figure 41. Guided Locomotion Normal to Force Table Nominal Disturbance Profile – Subject A

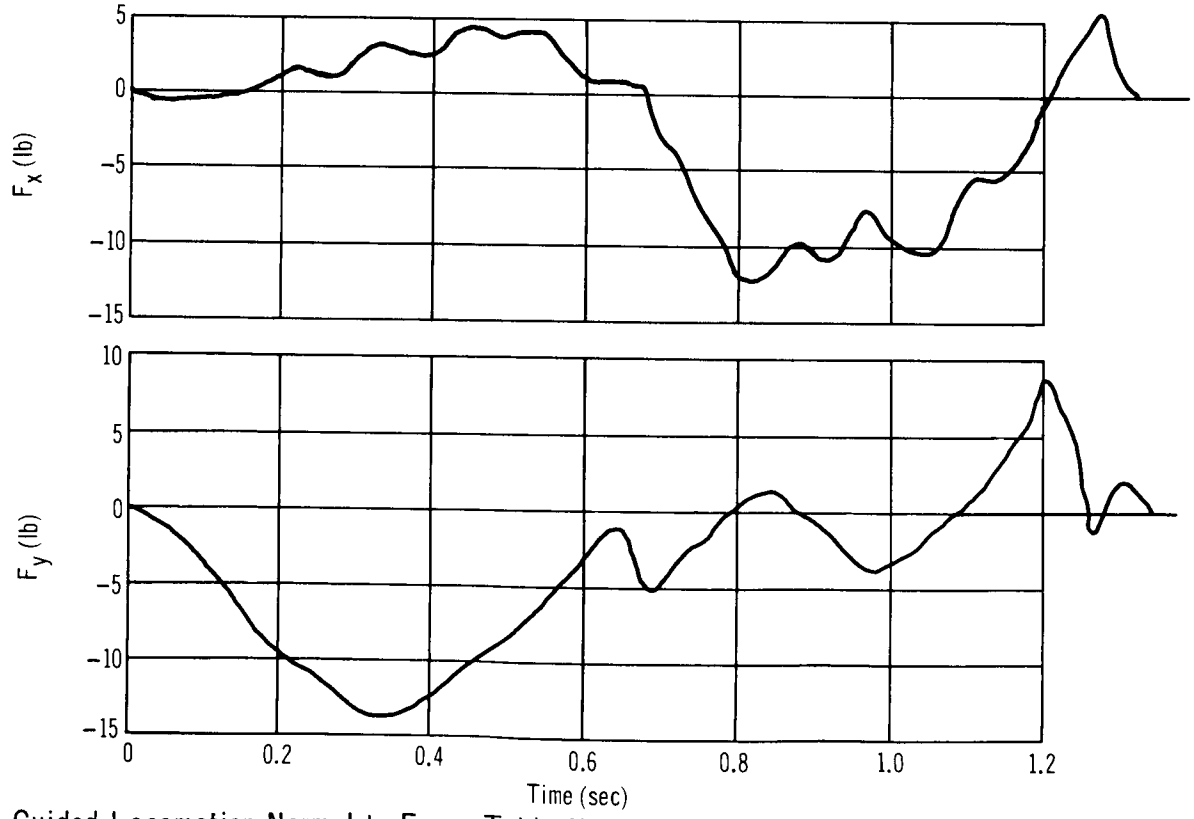

Figure 42. Guided Locomotion Normal to Force Table Nominal Disturbance Profile – Subject B

The x component of force is produced by a small swaying, or body rotation, about the z axis as the subject moved along the bar. The flexing of the bar is also contained in the x component of force.

The movement of Subject B (fig. 42) was not as smooth as that of Subject A. This is illustrated by the higher frequency component in the force data for Subject B. The x component for Subject B is approximately twice the magnitude, 12 lb, as that for Subject A.

The minimum level of intensity of this locomotion is shown in figs. 43 and 44 for Subjects A and B, respectively. Again, Subject A exhibited a smooth movement, as evidenced by the fairly smooth plot of F_y. The magnitude of forces obtained for the minimum level are nearly the same as those shown for the nominal level. The time to complete the motion for the minimum case is approximately 0.7 sec longer than the nominal case. Again, the error source caused by the gravity component is quite predominate in the y component of force.

Subject B again performed in the same manner for the minimum case as he did in the nominal case. The disturbances he induced were somewhat less than the nominal case.

The maximum level of intensity for the motion is shown in figs. 45 and 46. The forces that both subjects produced are twice as large as those in the nominal case.

The equations derived for these disturbances of the locomotion normal to the force table are given in Appendix C.

Locomotion Parallel to the Force Table

The guided locomotion parallel to the force table is performed by the subject initially grasping the locomotion bar with both hands, the right hand 18 in. forward of the left hand. The subject translates by releasing the bar with the left hand and moving the left hand a comfortable distance forward of the right hand, grasping the bar at the termination of the movement. Then the right hand is released and moved a comfortable distance forward of the left hand. This locomotion is performed in the plus-x direction (see fig. 5). As in all the locomotion tests, this one is also performed at the nominal, minimum, and maximum levels of intensity.

Fig. 47 is a multiple-exposure photograph of the locomotion parallel to the force table.

Fig. 48 is a time history of the Euler angles describing the various body segment motions for this locomotion test. These plots show that the legs were held together with no bending at the knees. During the last second of the motion, the legs were held fairly rigid to the torso. The variation of the torso angle is approximately 14° during this motion. Because the arms are used as the source of locomotion, there is a large variation in the Euler angles describing their relative position.

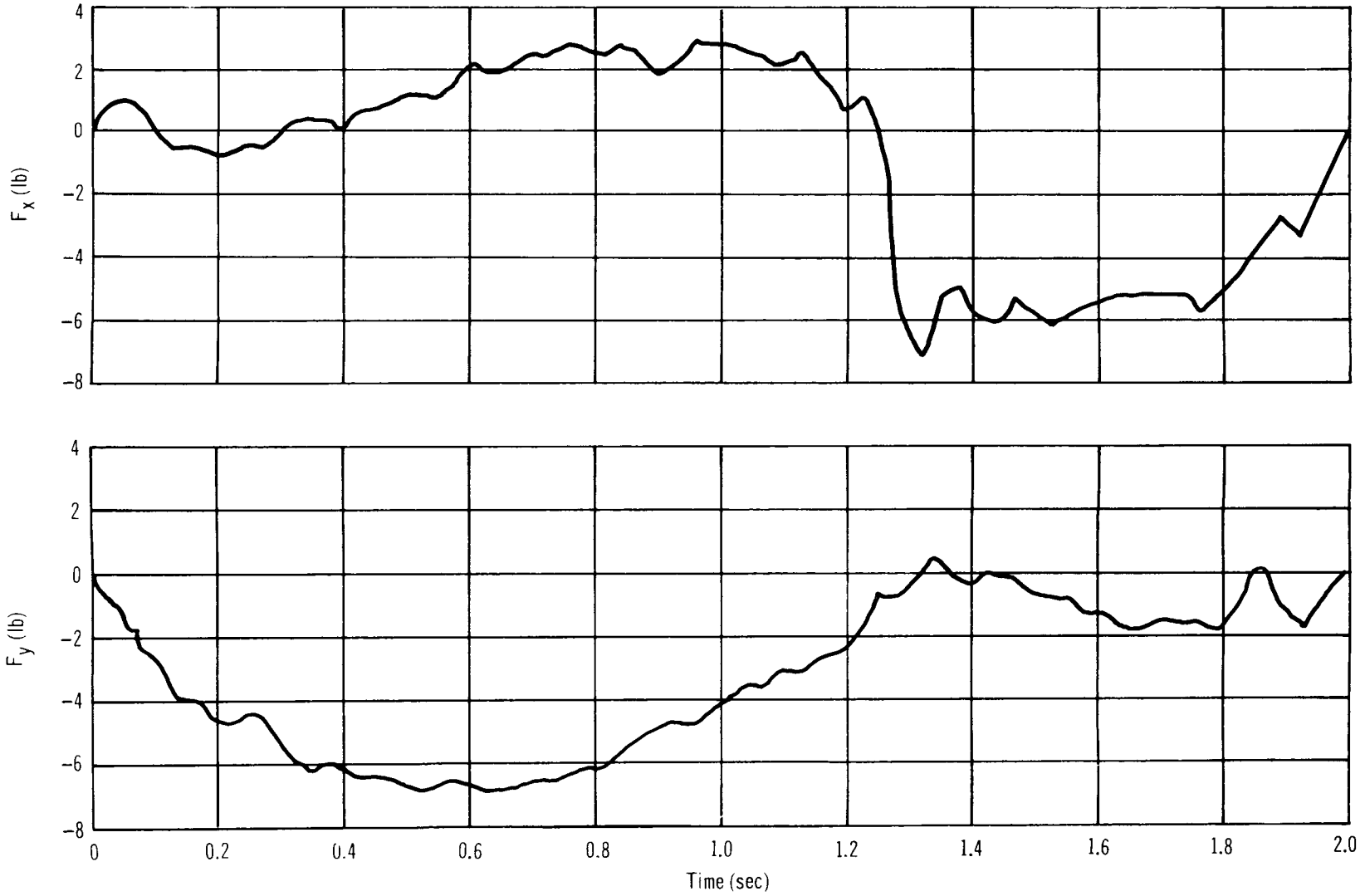

Figure 43. Locomotion Normal to Force Table Minimum Disturbance Profile – Subject A

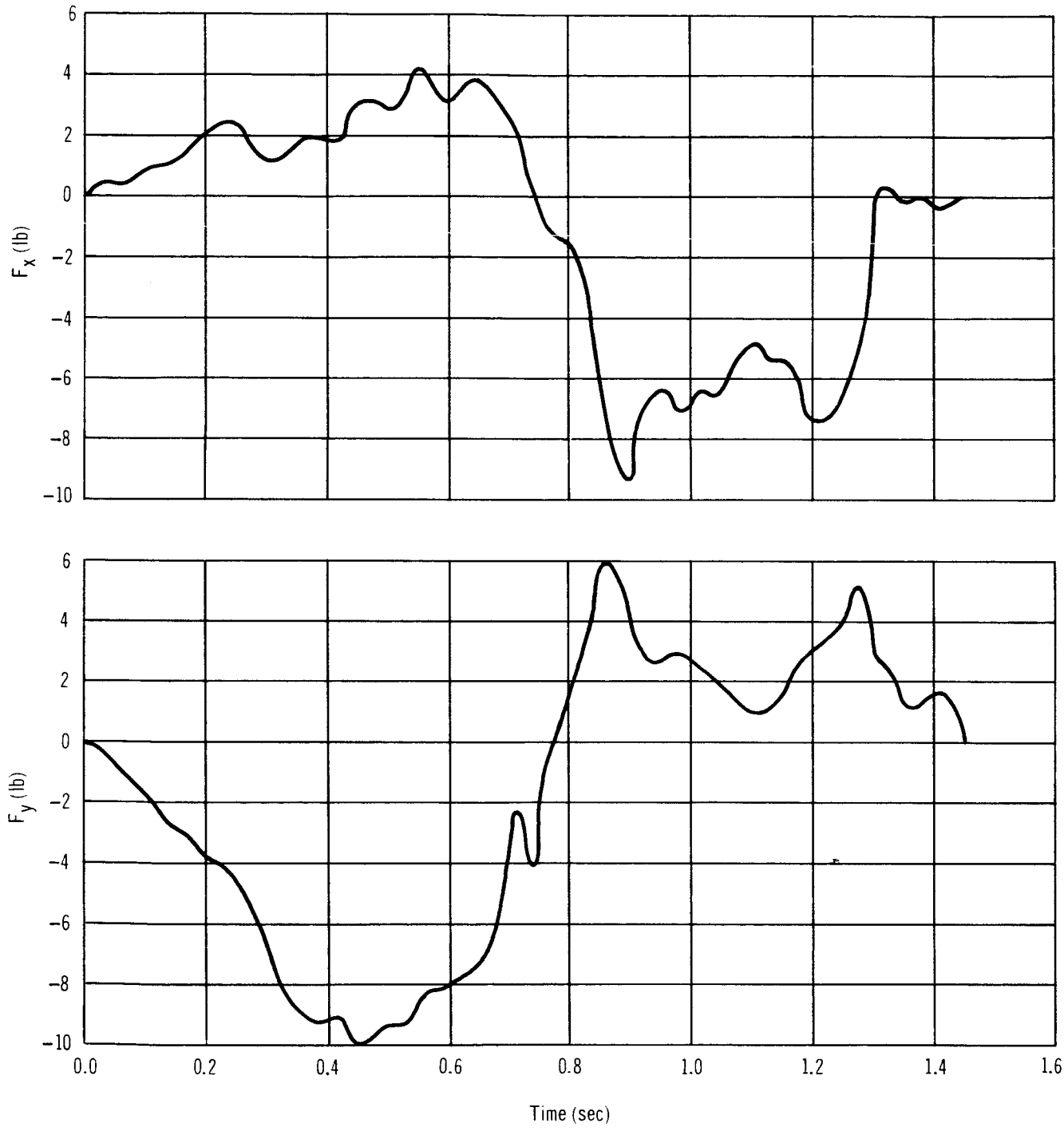

Figure 44. Guided Locomotion Normal to Force Table Minimum Disturbance Profile – Subject B

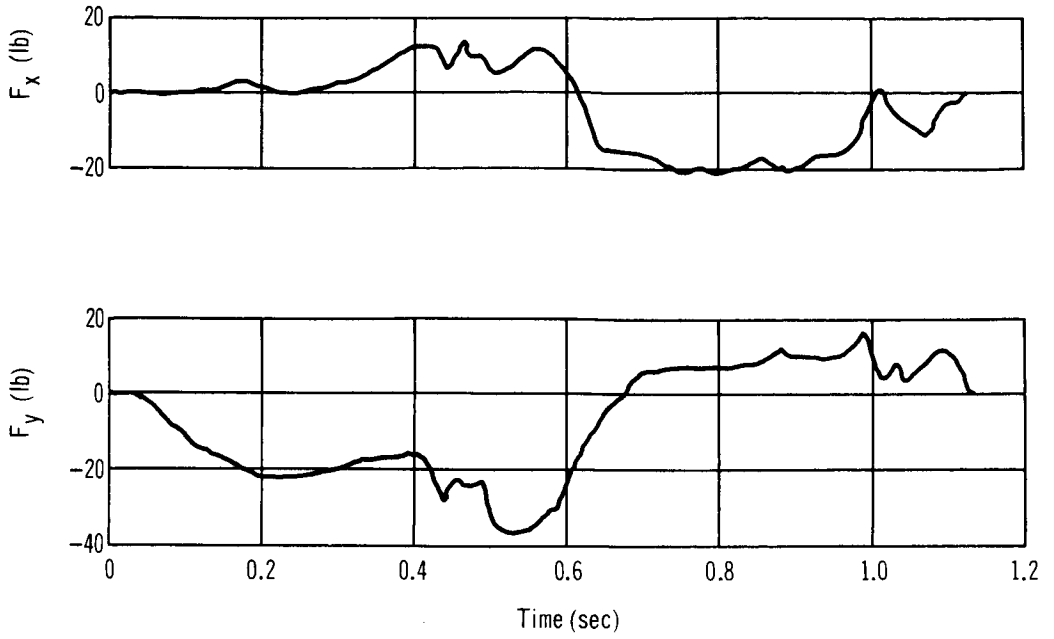

Figure 45. Guided Locomotion Normal to Force Table Maximum Disturbance Profile – Subject A

Fig. 49 is the time history of the linear displacement of the subject for this locomotion. The subject translated nearly 4 ft parallel to the platform, keeping his head at a nearly constant distance away from it. The velocity of the motion is obtained by computing the slope of the x displacement, which is found to be approximately 2.5 ft/sec and is fairly constant throughout most of the test. The subject here performs a smooth motion for this locomotion test.

The nominal level of intensity is shown in figs. 50 and 51 for Subjects A and B, respectively. In this locomotion test, as in velcro walking, the x component of force contains the gravity component of the pendulum support. It was pointed out previously that for equal deflections about the static position of the pendulum support, the component of force resulting from gravity can be eliminated by superimposing the curve of $W \sin \delta / L$ for the line of zero force of the x component of force. In both figs. 50 and 51, the peak x components of force occur within 0.3 sec of the initial movement. Because the subject's velocity is approximately 2.5 ft/sec, as obtained from fig. 49, the total movement during 0.3 sec is 0.75 ft. For the pendulum support length of 54 ft, this 0.75-ft deflection produces a 2.3-lb error in the x component of force. Noting fig. 50, this amounts to an error of approximately 11% for the peak x component of force. Hence, the maximum amplitudes of the x component of force, which is the acceleration force, is reasonably close, but its profile needs modifying to remove gravity effects.

As in the previous locomotion test, Subject A had a smoother motion. The maximum y component of force Subject A produced is only 3 lb, compared to 10 lb produced by Subject B. The motions for the two subjects are within 0.1 sec of each other.

From figs. 52 and 53 for the minimum level of intensity, Subject A was slow, 2.2 sec, compared to the time of Subject B, 1.8 sec. The magnitude of the x component of force in both cases is roughly the same. Also, they are somewhat less than those shown in the nominal case.

For the maximum intensity level shown in fig. 54, Subject A exerted a large pulling force, F_x, of 66 lb. This peak is fairly close to the starting time as it was for the nominal case of this locomotion. Hence, the peak magnitude is within 10% of the value indicated. Subject B, fig. 55, shows similar characteristics with a somewhat smaller pulling force, 50 lb.

The equations derived for these tests are given in Appendix C.

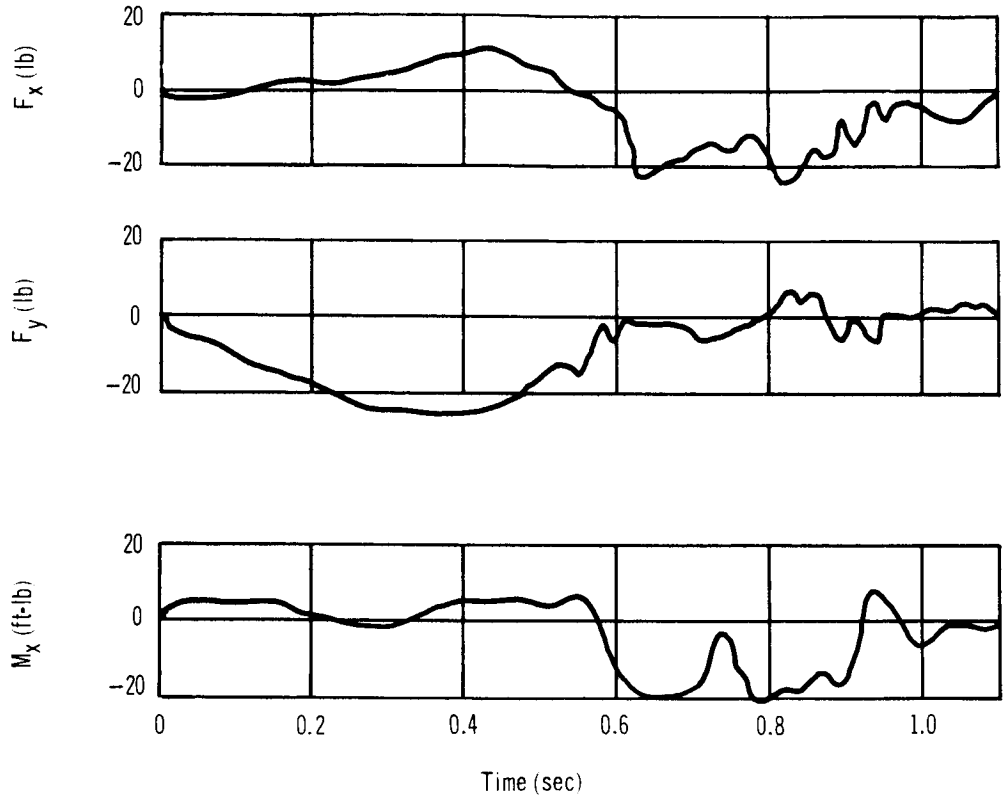

Figure 46. Guided Locomotion Normal to Force Table Maximum Disturbance Profile – Subject B

Figure 47. Locomotion Parallel to Force Table

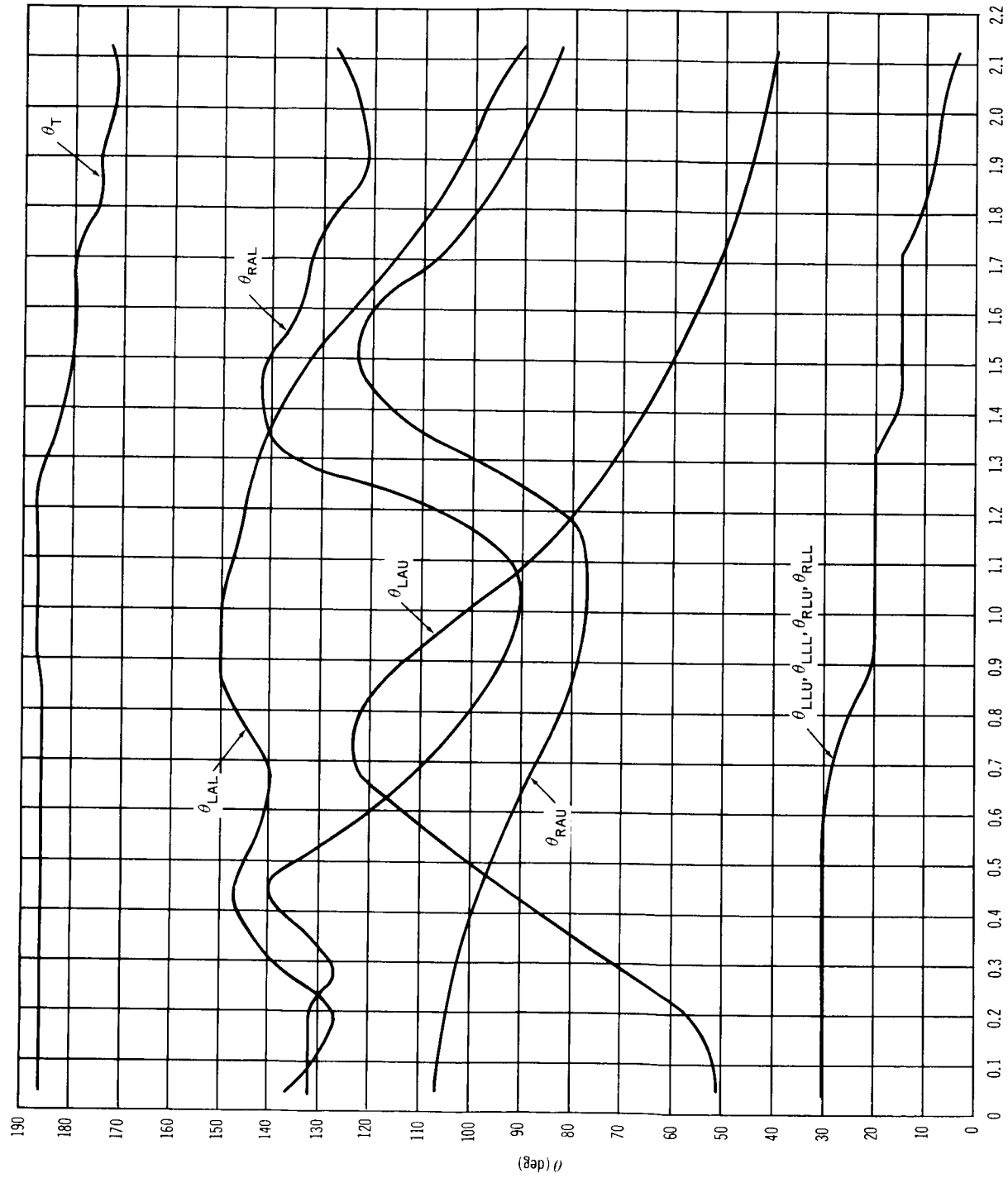

Figure 48. Guided Locomotion Parallel to Force Table Euler Angles – Subject A

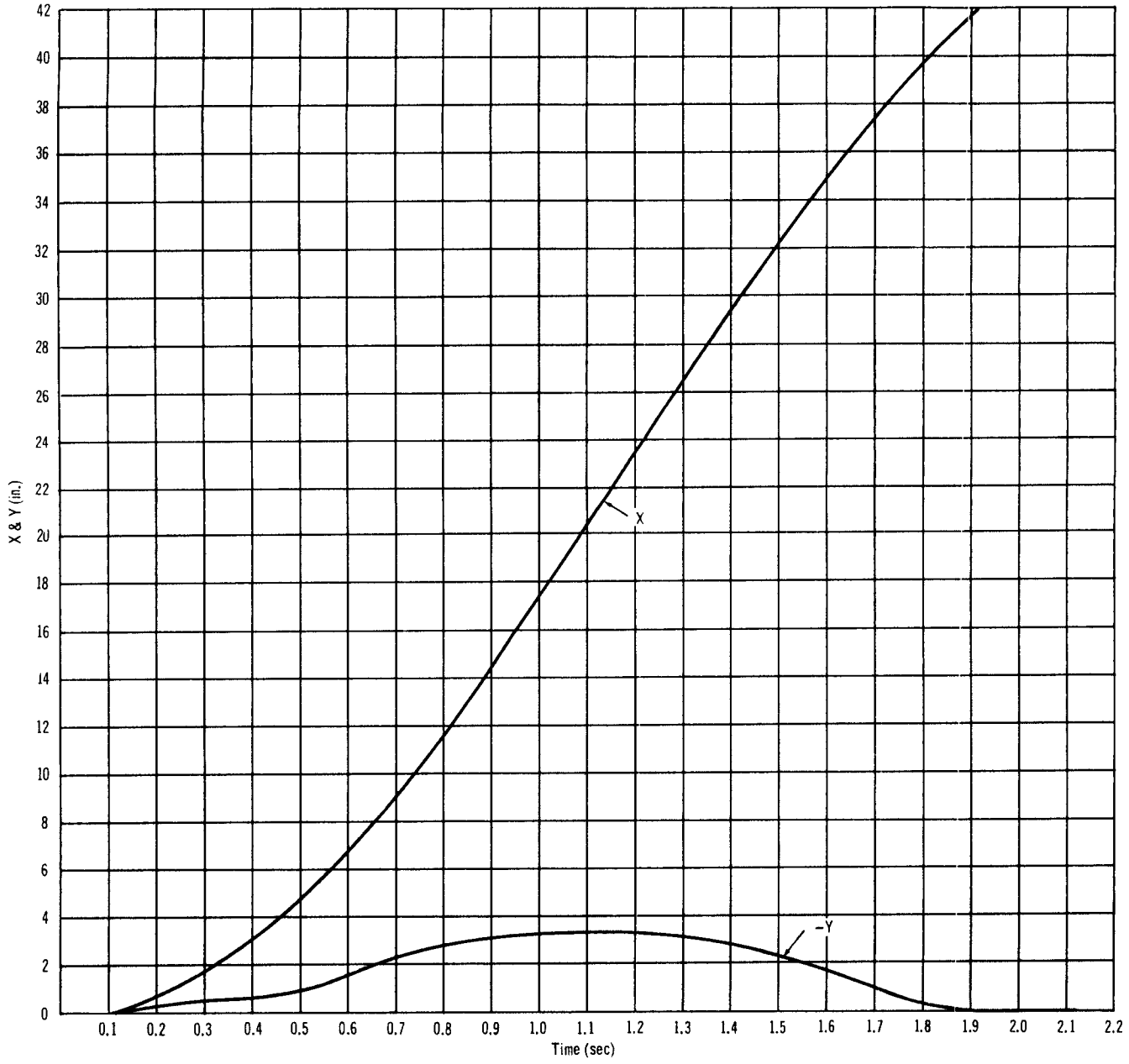

Figure 49. Guided Locomotion Parallel to Force Table Displacement – Subject A

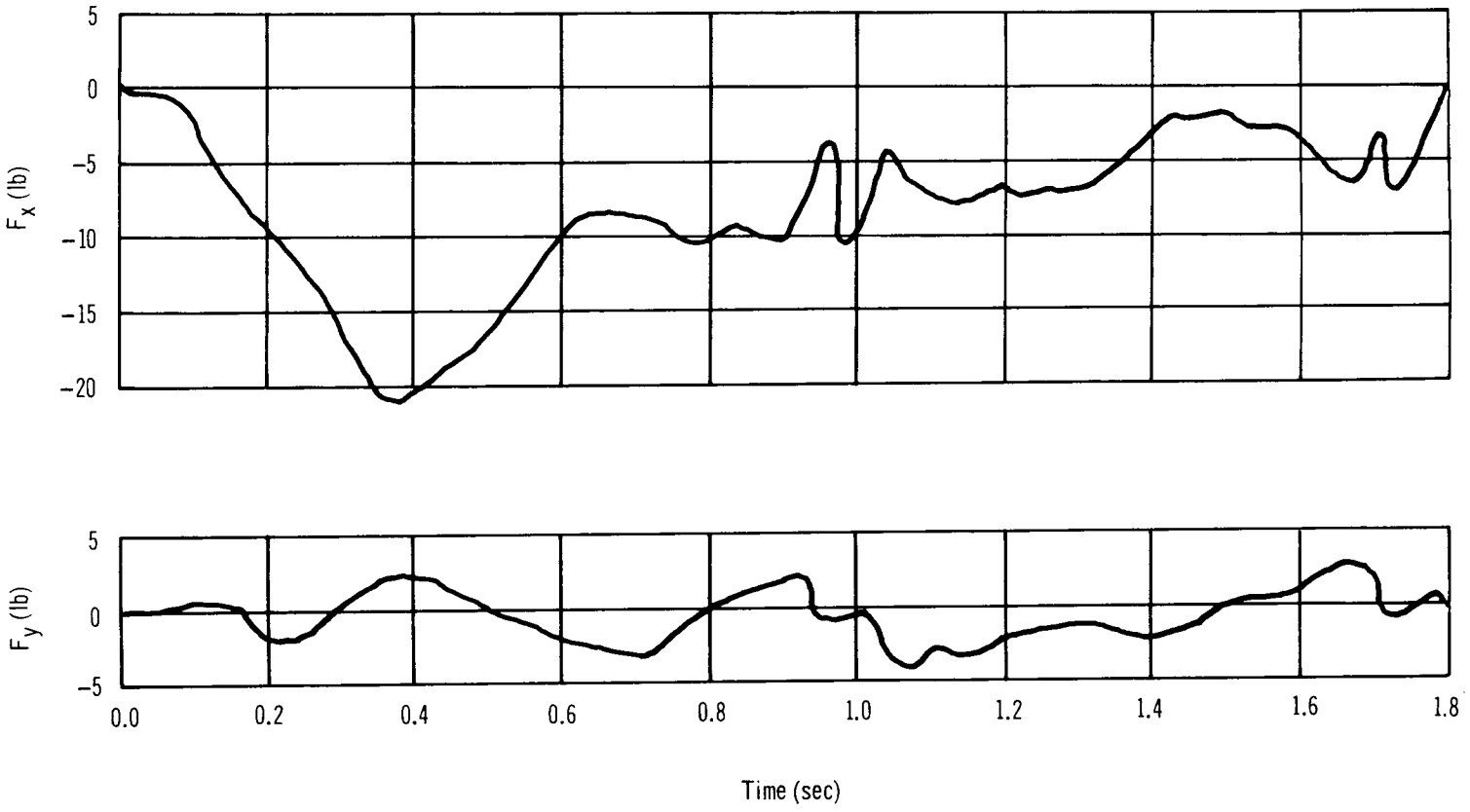

Figure 50. Guided Locomotion Parallel to Force Table Nominal Disturbance Profile – Subject A

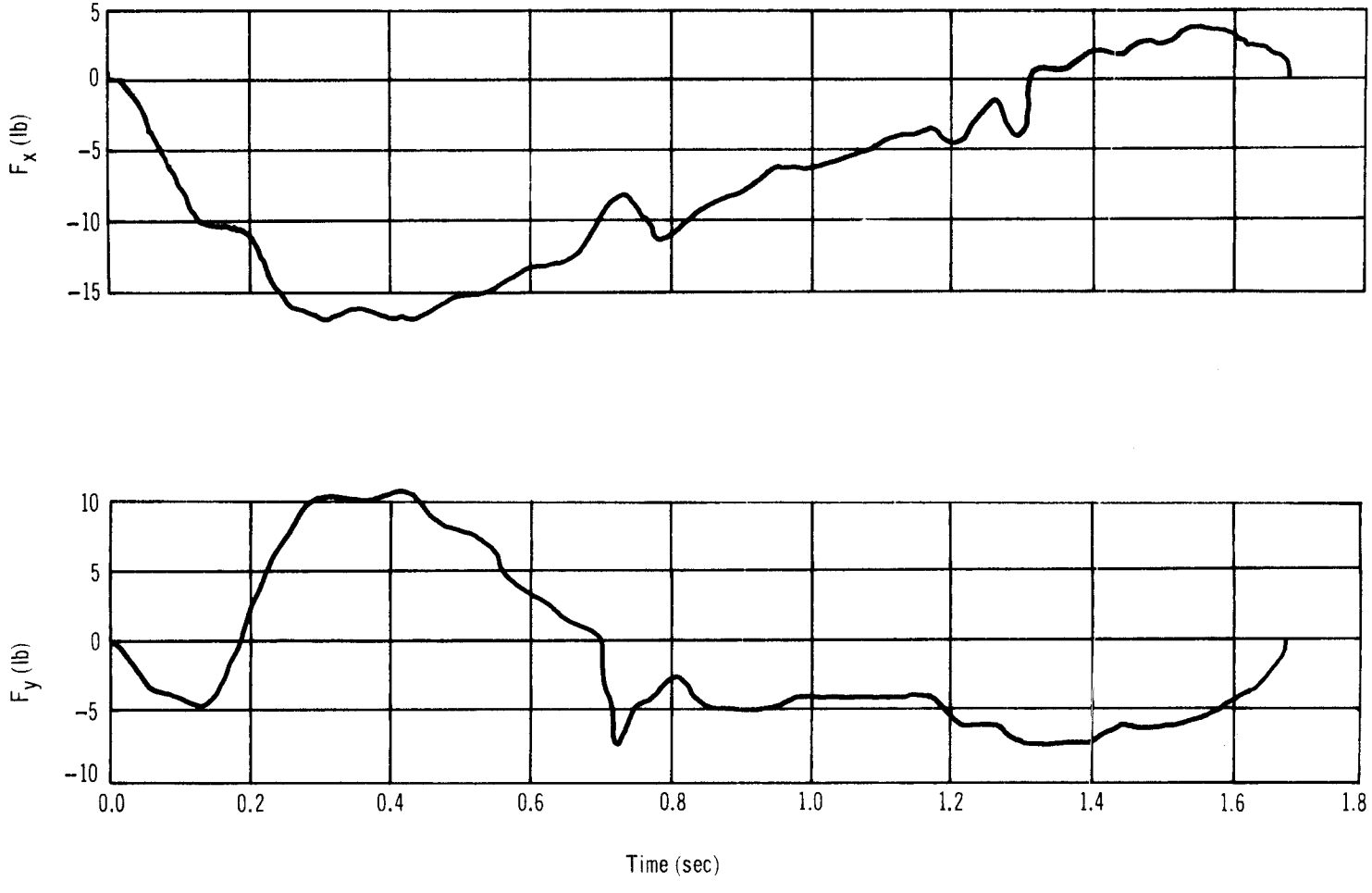

Figure 51. Guided Locomotion Parallel to Force Table Nominal Disturbance Profile – Subject B

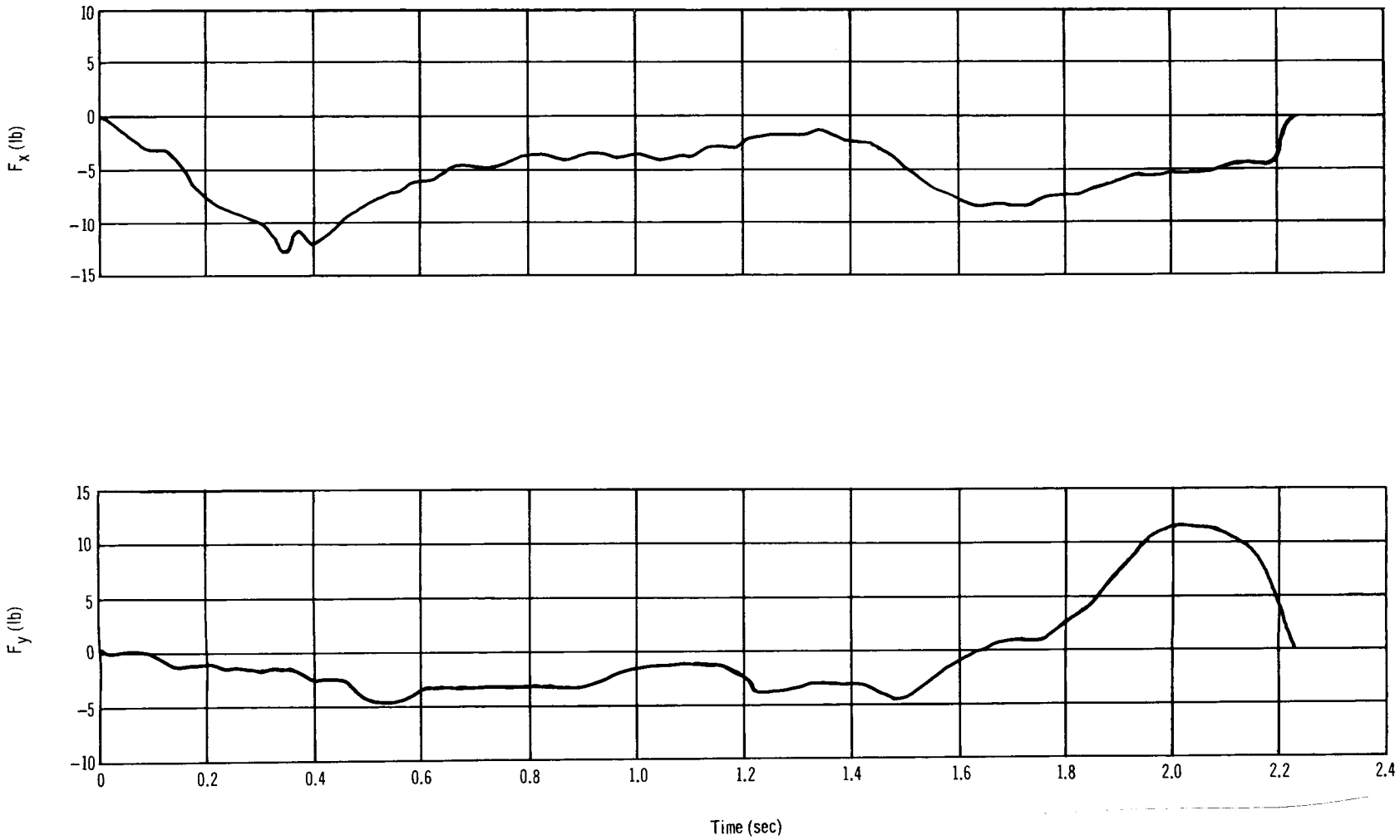

Figure 52. Guided Locomotion Parallel to Force Table Minimum Disturbance Profile – Subject A

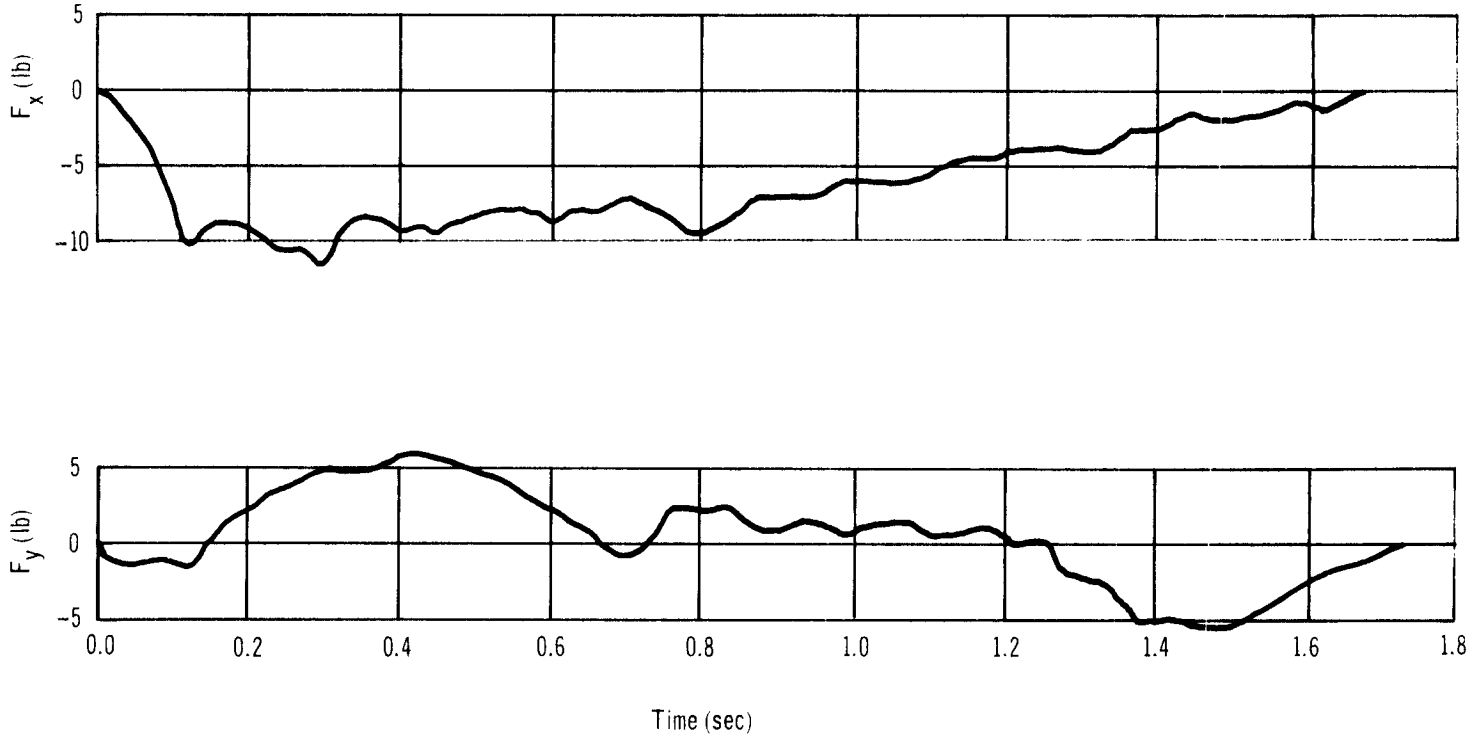

Figure 53. Guided Locomotion Parallel to Force Table Minimum Disturbance Profile – Subject B

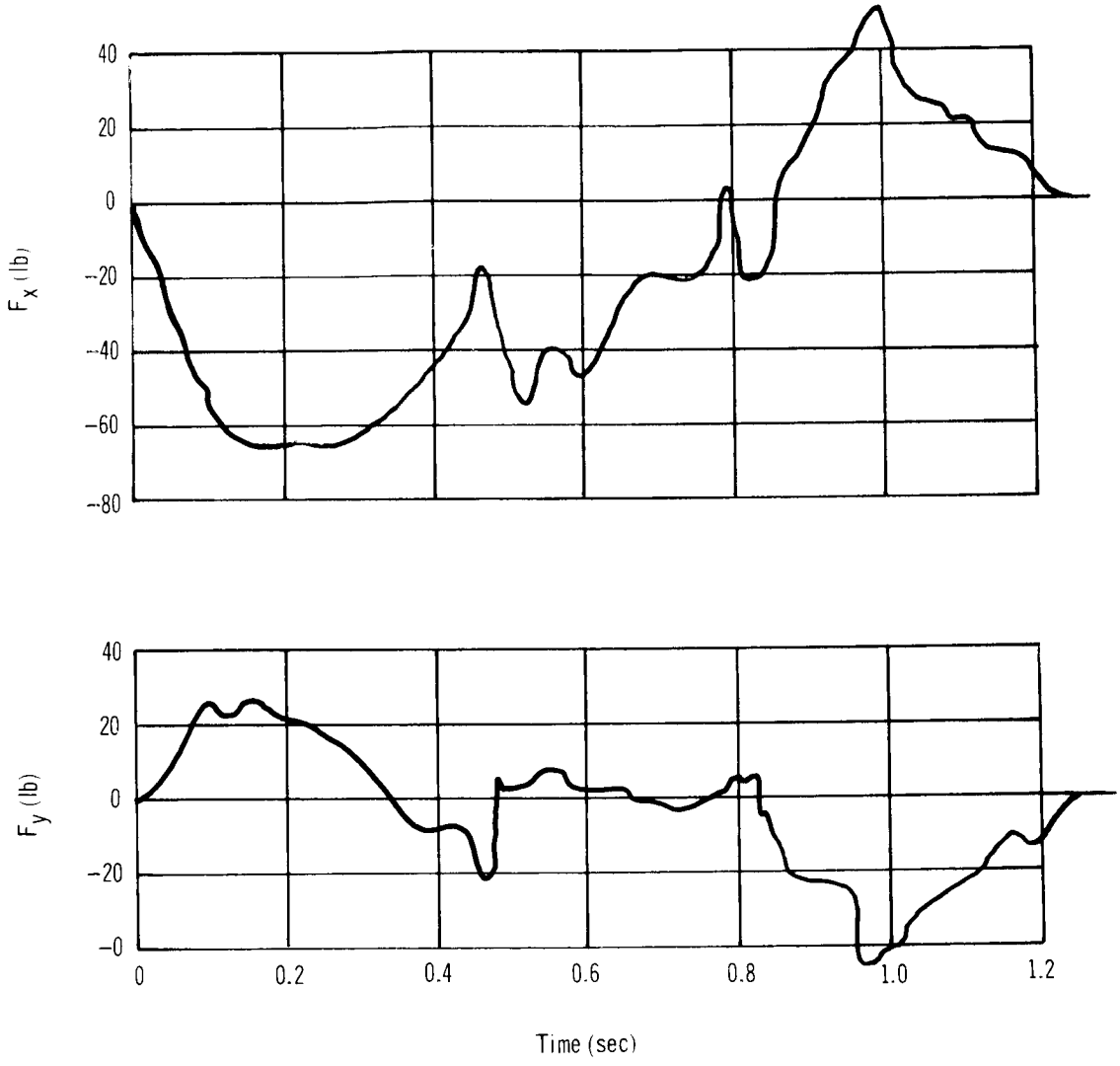

Figure 54. Guided Locomotion Parallel to Force Table Maximum Disturbance Profile – Subject A

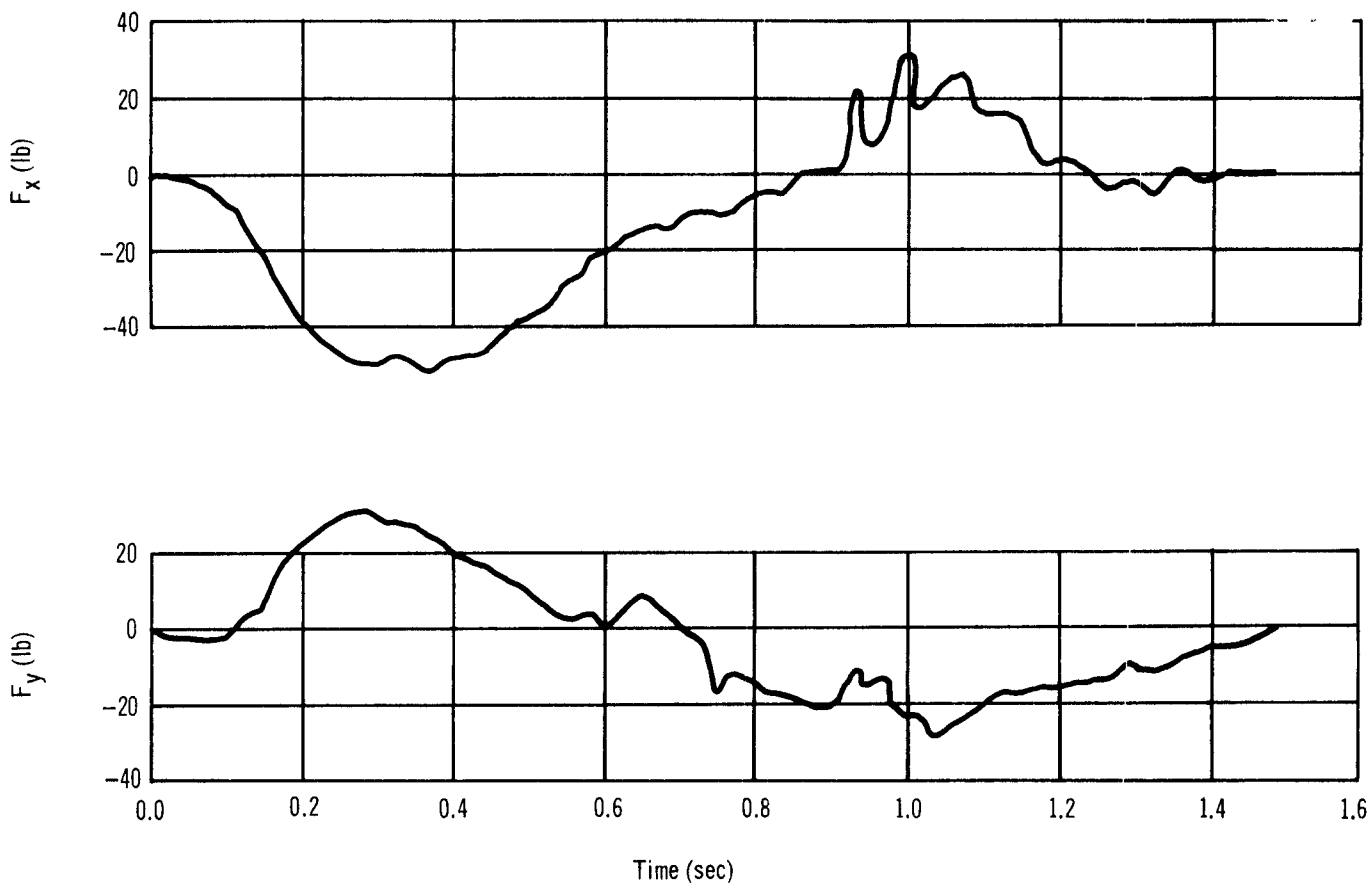

Figure 55. Locomotion Parallel to Force Table Maximum Disturbance Profile – Subject B

CONSOLE OPERATION

Three typical console operations were simulated during this experiment: (1) turning a hand wheel, (2) operation of sliding controls, and (3) a push-pull or phone-jack operation. A more detailed list of console operations was not considered because the disturbance profiles are generated primarily by the body segment traveling to and from the console. The actual console operation imparts a disturbance which represents the relative ease with which the operation is performed. For properly designed consoles, this disturbance will be negligible.

The console operation is performed with only one restraint configuration. In this configuration, the crew member is standing at the console with his feet attached to the floor by velcro strips. A waist restraint, in the form of a belt with a bar attached to each side of the belt and connecting to the console, holds the operator at a comfortable distance for console operation.

The console operation disturbance profiles are referenced to the coordinate system shown in fig. 5.

A description of each individual console operation simulation and test results are presented in the following paragraphs. Each type of console operation is performed at three levels of intensity: (1) nominal, (2) minimum, and (3) maximum.

Console Operation Torquing

Console operation torquing is a crew motion similar to the arm swing motion previously discussed. The subject initially has both hands resting on his thighs. He moves his left hand to the control console wheel. The subject grasps the wheel and rotates it 360° clockwise, then releases the wheel, and returns his hand to the original position.

Fig. 56 is a multiple exposure photograph of Subject B performing the nominal torquing console operation.

The Euler angle description for the various body segments performing this console operation is presented in fig. 57. Only the upper, θ_{LAU}, and lower, θ_{LAL}, arm motions are plotted because the remaining body segments were partially motionless. The Euler angle, ϕ_{LAL}, about the x axis shown in this figure is the result predicted on the basis of body segment length, diameter of the torquing wheel, and time required to rotate the wheel 360°.

Figure 56. Console Operation Torquing

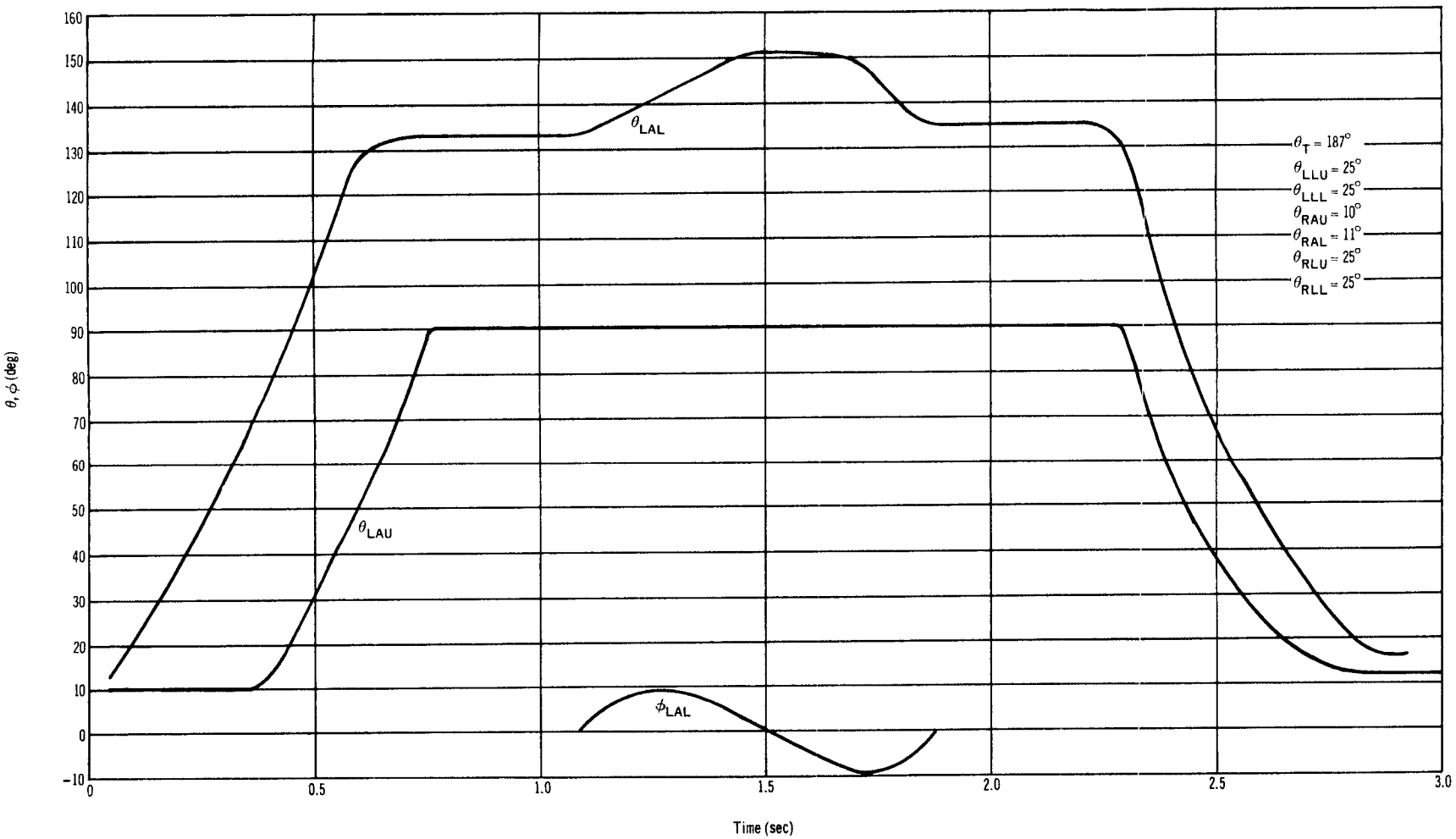

Figure 57. Console and Operation Torquing Euler Angles – Subject A

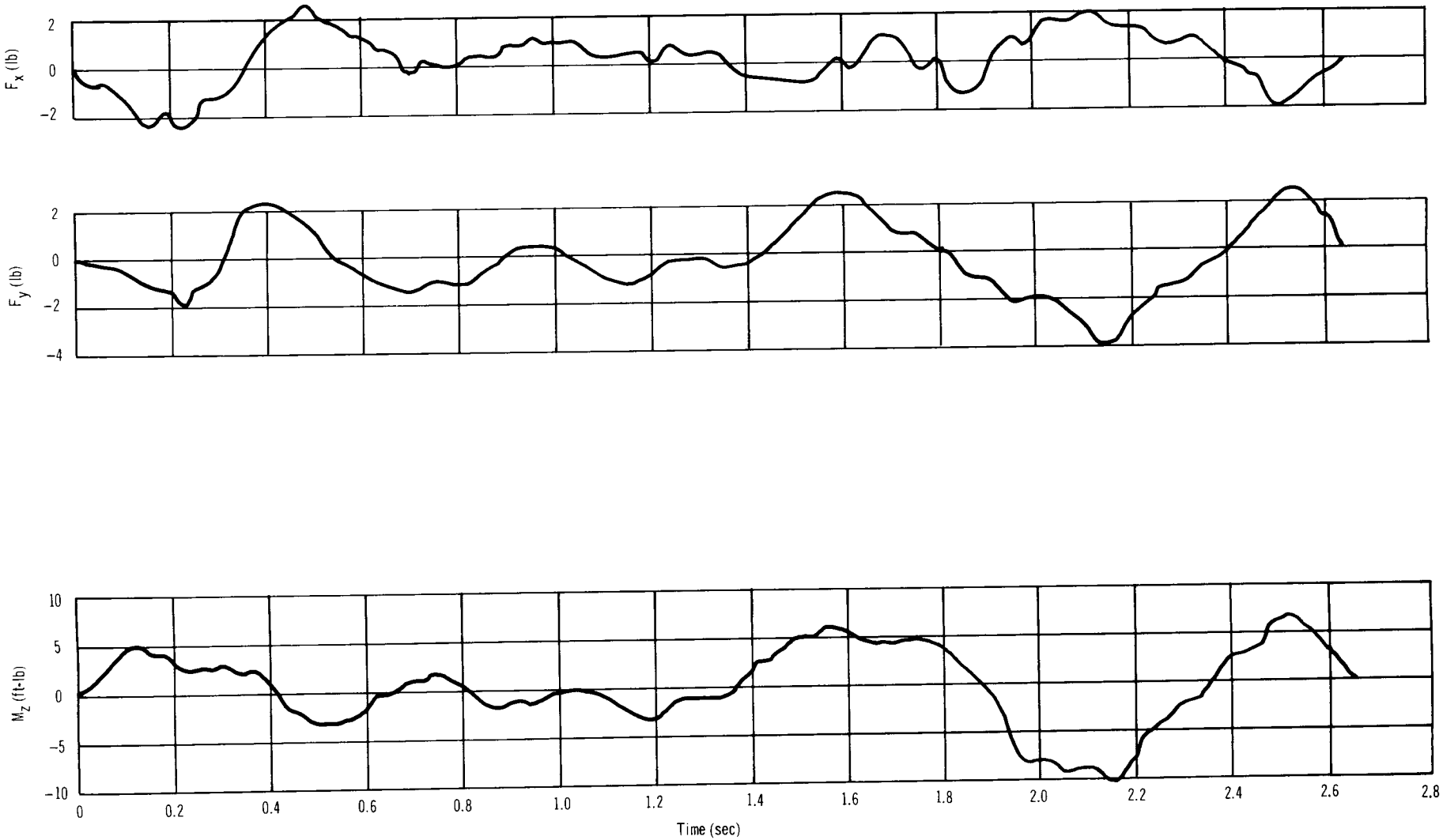

Figure 58. Console Operation Torquing Nominal Disturbance Profiles – Subject A

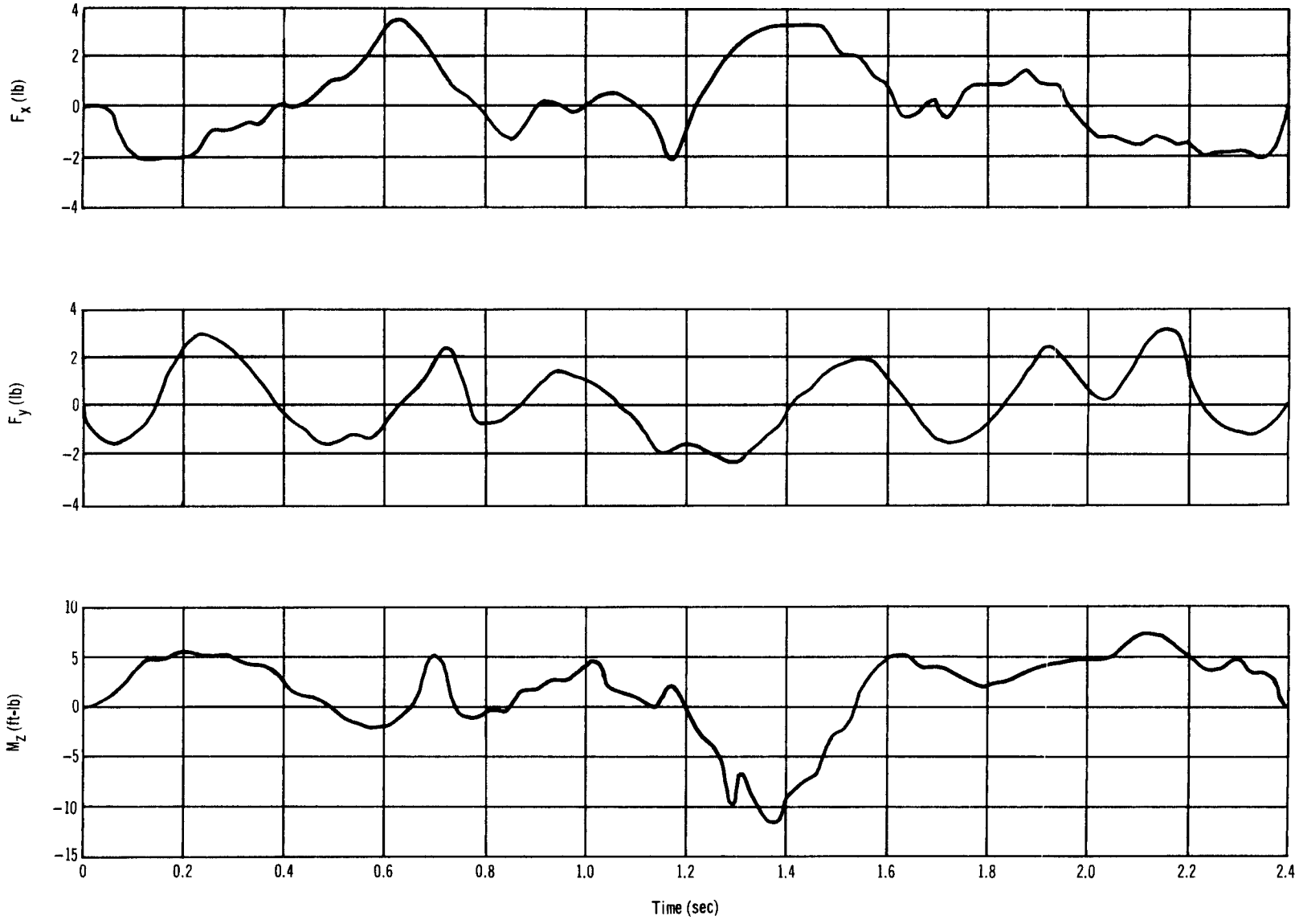

Figure 59. Console Operation Torquing Nominal Disturbance Profile – Subject B

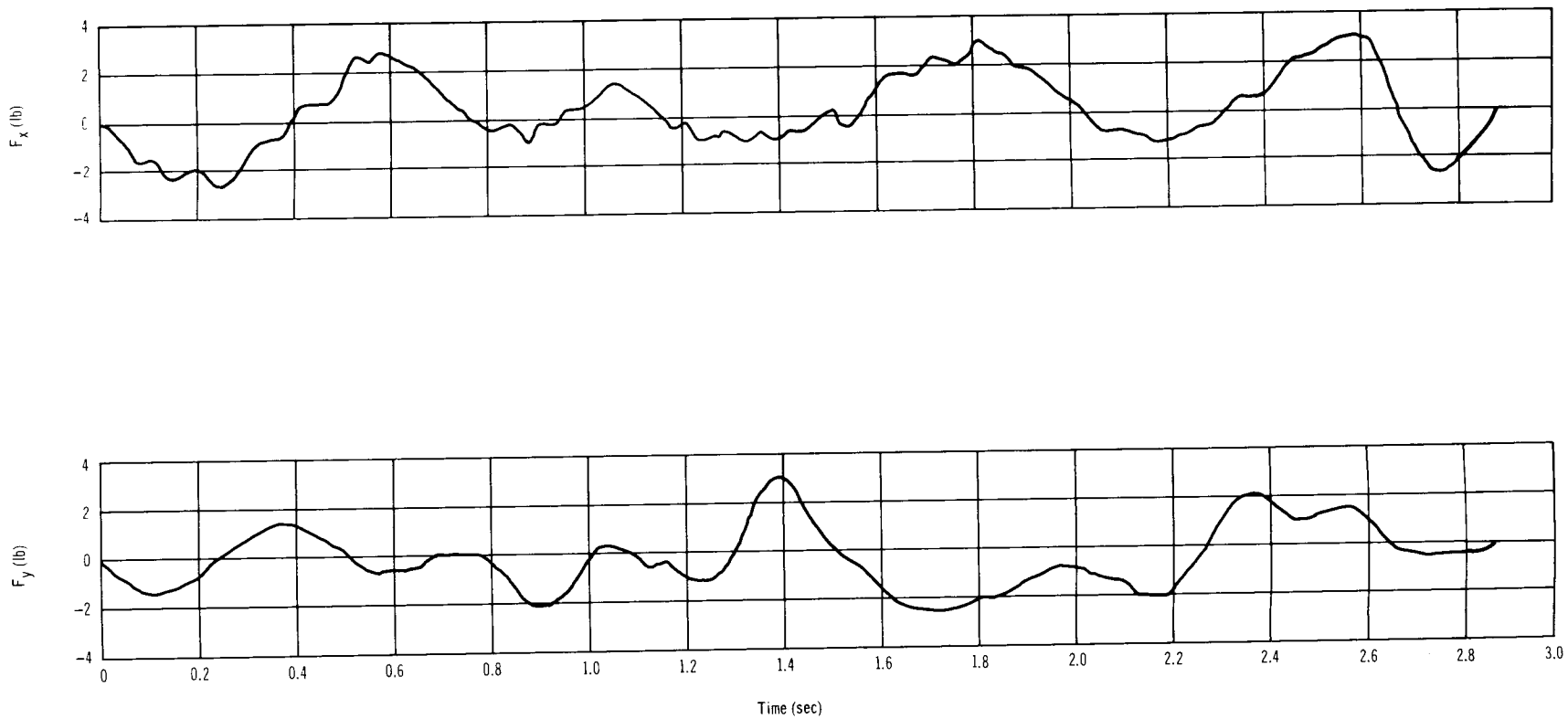

Figure 60. Console Operation Torquing Minimum Disturbance Profile – Subject A

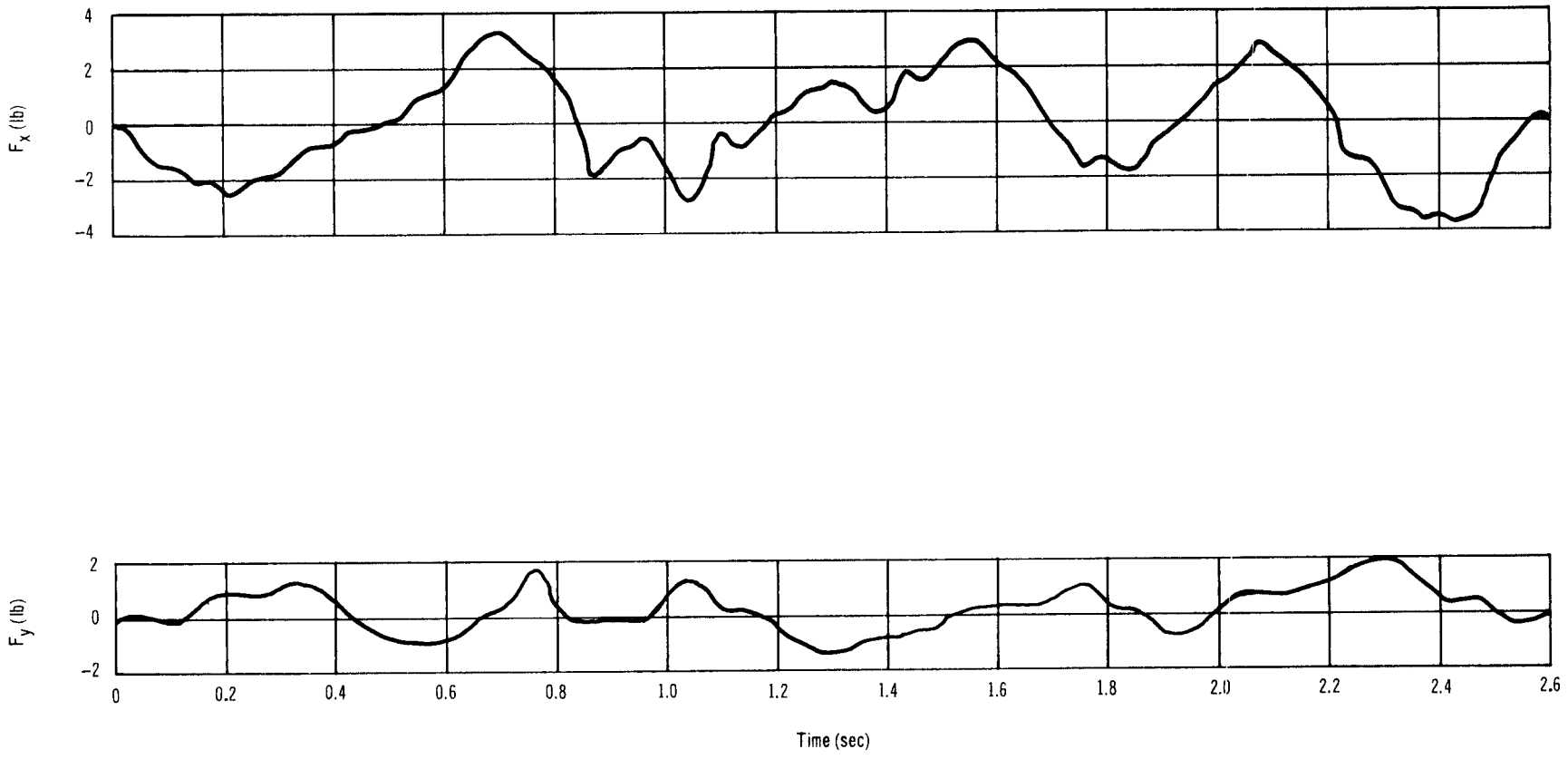

Figure 61. Console Torquing Minimum Disturbance Profile – Subject B

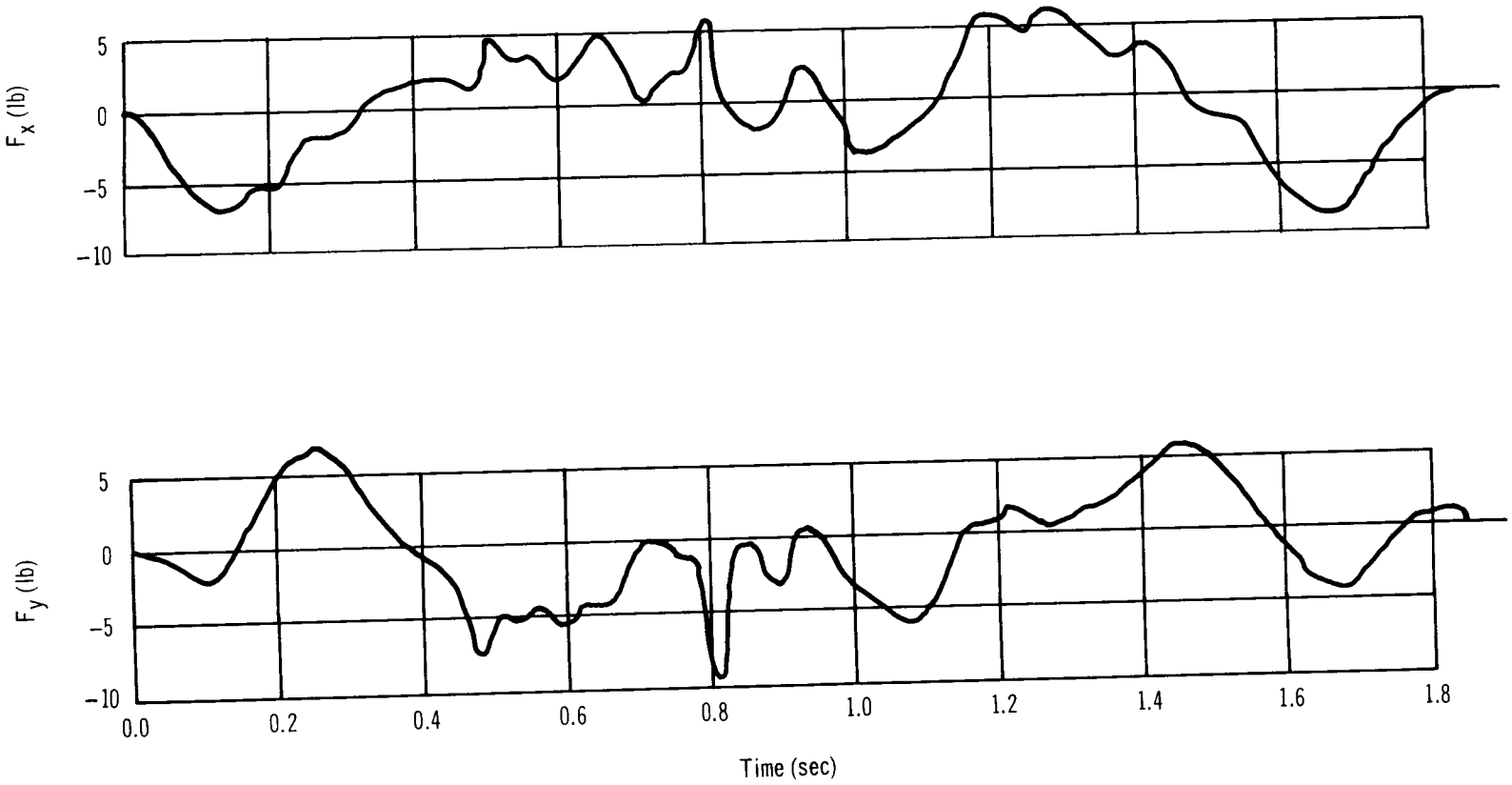

Figure 62. Console Operation Torquing Maximum Disturbance Profile – Subject A

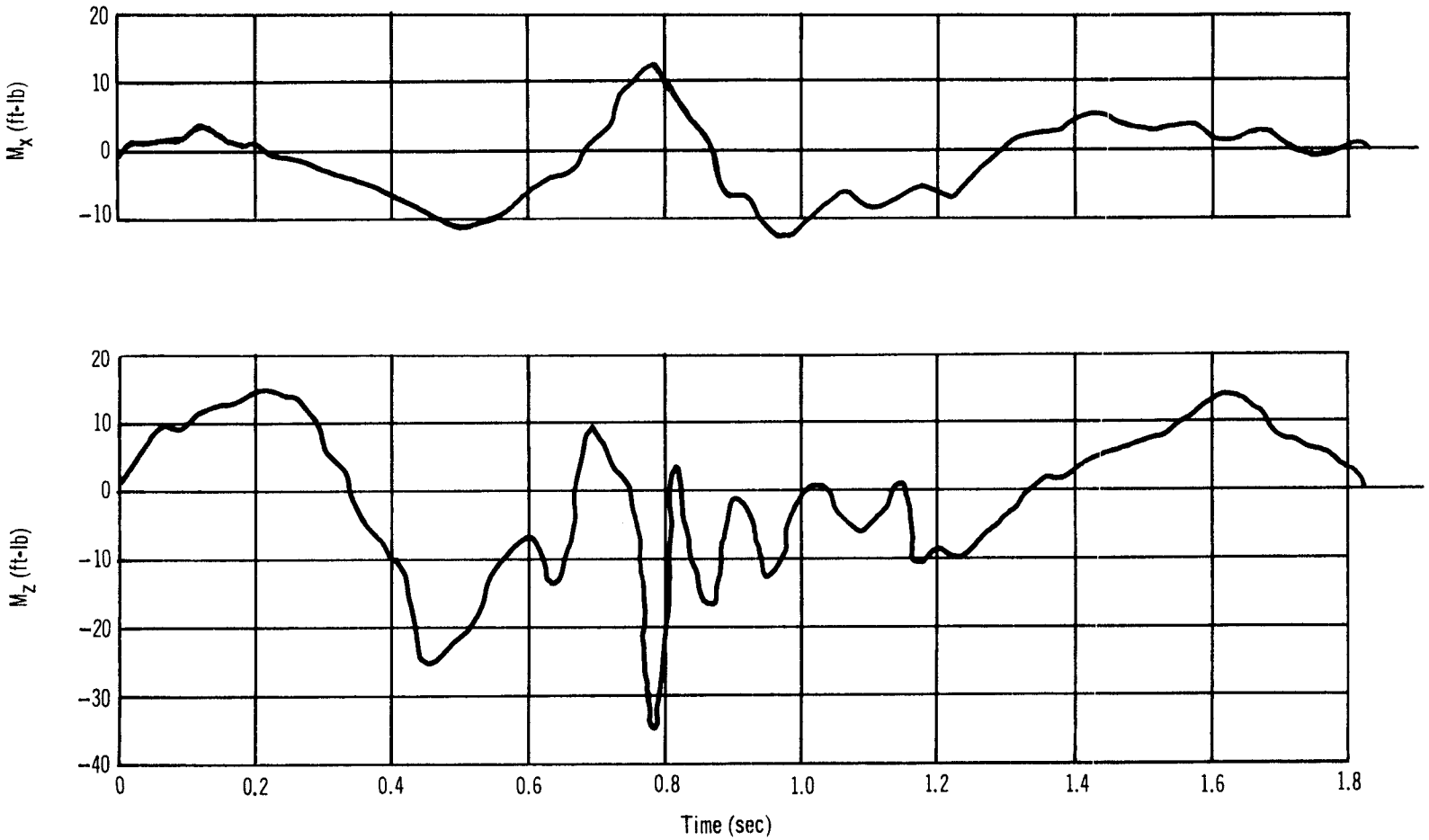

Figure 63. Console Operation Torquing Maximum Disturbance Profile – Subject A

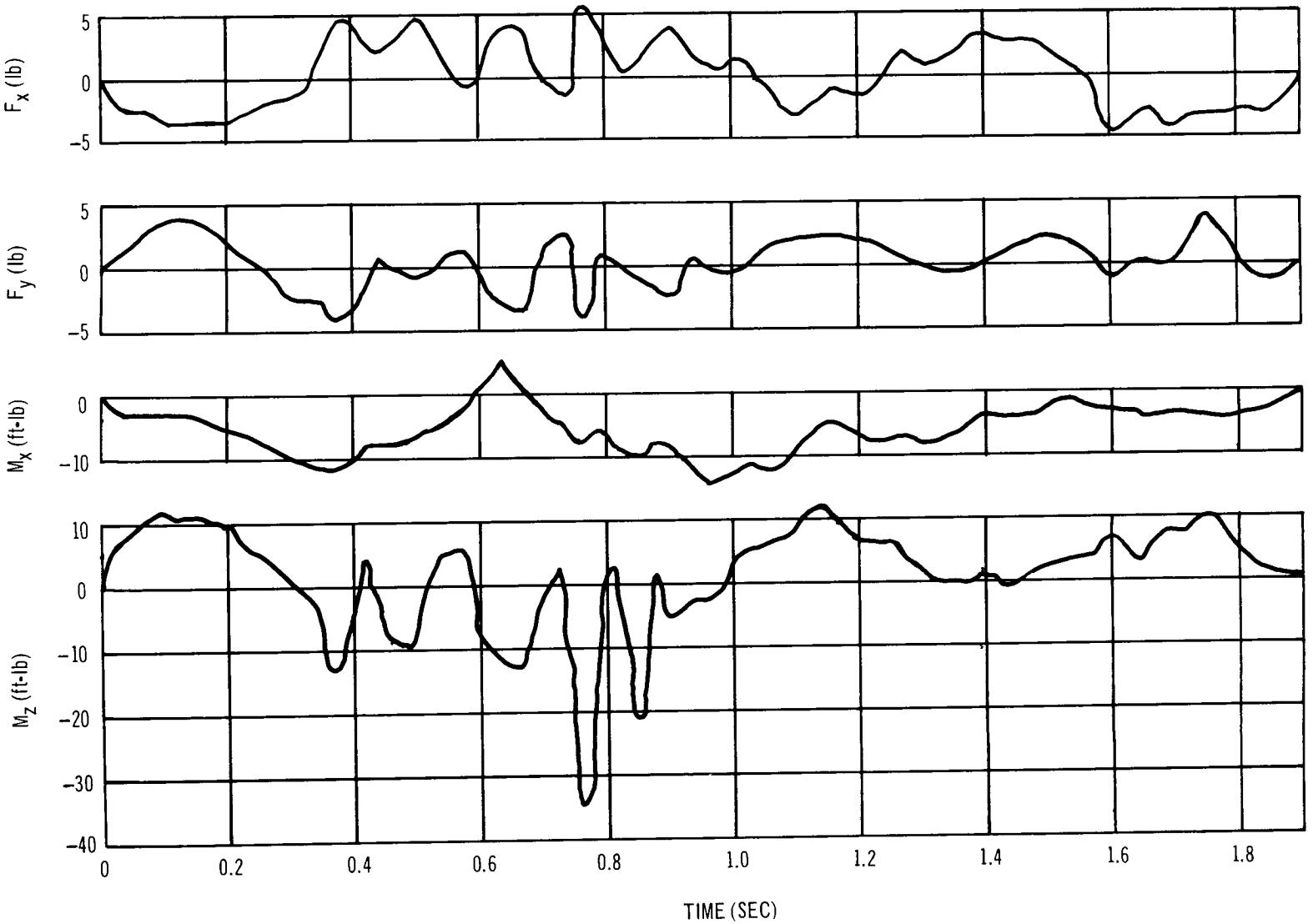

Figure 64. Console Operation Torquing Maximum Disturbance Profile – Subject B

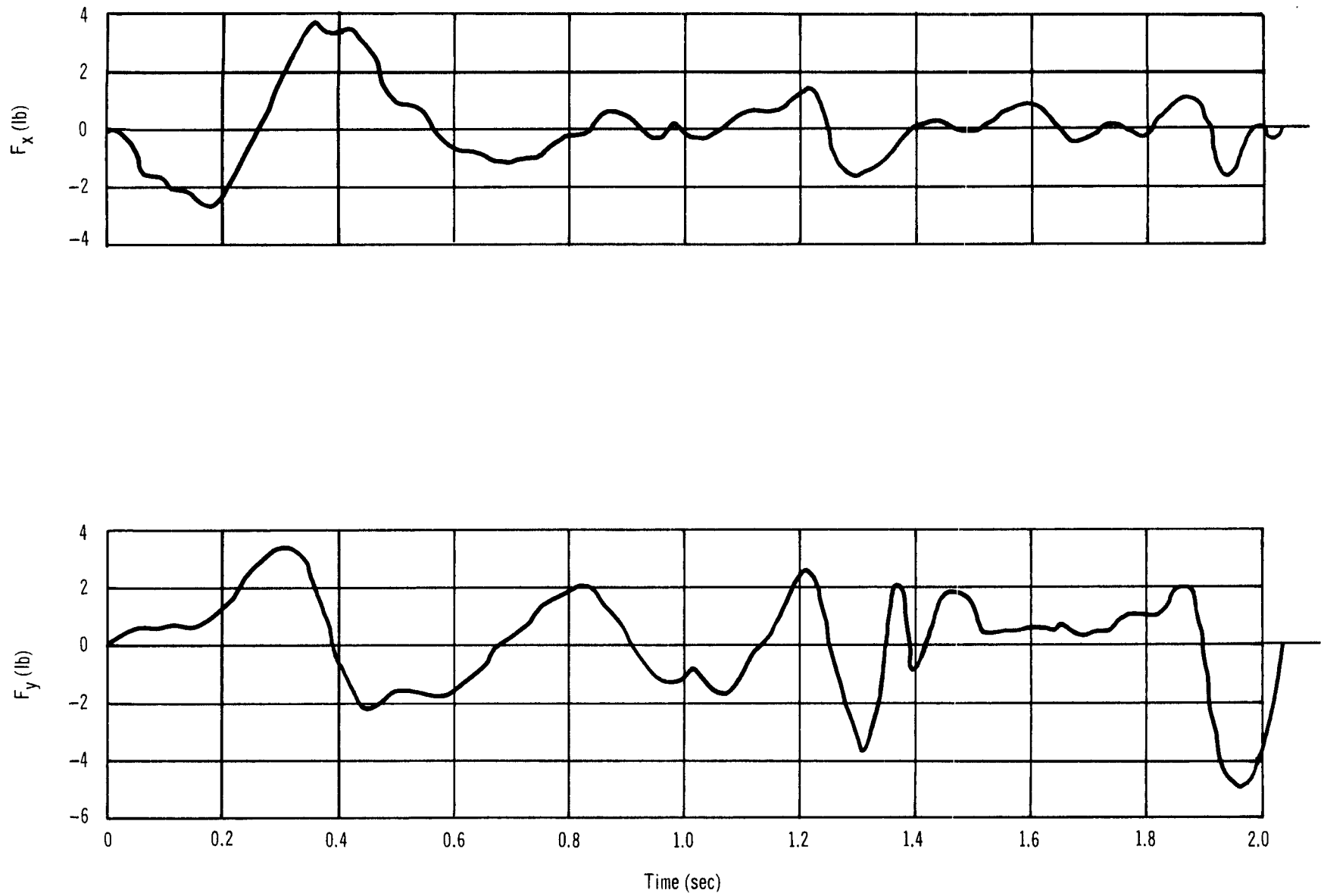

Figure 65. Console Operation Push-Pull Nominal Disturbance Profile – Subject A

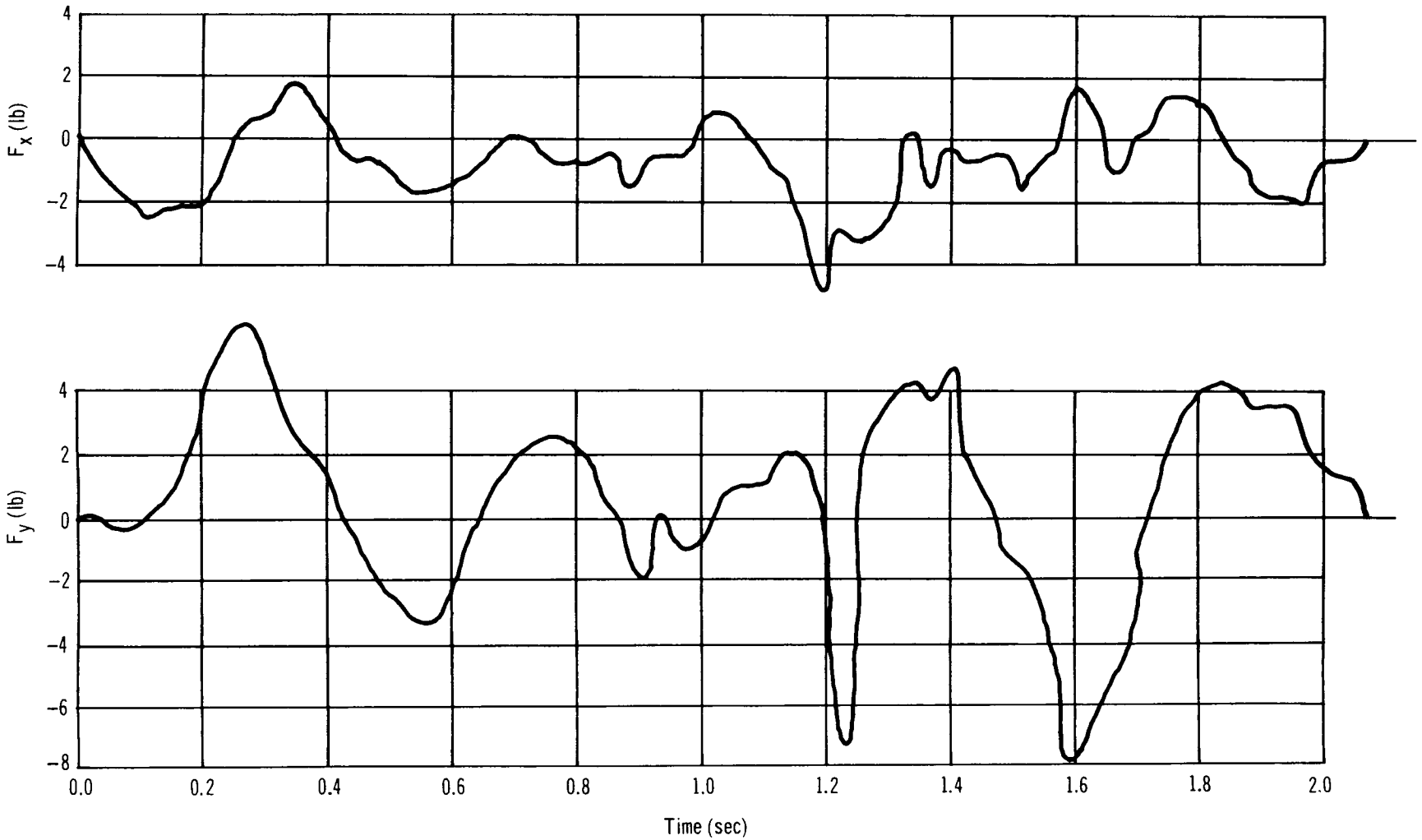

Figure 66. Console Operation Push-Pull Nominal Disturbance Profile – Subject B

The nominal level for the console operation is shown in figs. 58 and 59. Noting fig. 58 for Subject A, the first 0.7 sec are caused by the arm motion in moving up to the console. The x component of force here corresponds to the y component of force shown in fig. 8 for the arm motion, which is the result of reorientation of the man with respect to the force platform. For the console operation tests, both the x and y components of force have approximately equal transmission ability. This is caused by the restraint configuration which stops the operator from rotating. From 0.7 sec to approximately 1.9 sec, the particular console operation, torquing in this case, takes place. From 1.9 sec to termination is the disturbance resulting from lowering of the arm at the side. Maximum forces for Subject A are 2.6 lb and 4 lb for the x and y components, respectively. In the same test, Subject B produced forces of 3.6 lb and 3 lb for the x and y axes, respectively.

The minimum intensity for this test is shown in figs. 60 and 61 for Subjects A and B. Here, the force levels are approximately the same as in the nominal case. The force profiles are smoother because the subjects were instructed to make their motions as smooth as possible.

Figs. 62, 63, and 64 show the disturbance profiles for the maximum intensity of Subjects A and B. The maximum forces and moments for both subjects are nearly the same, the maximum force being about 7 lb for the y axis with a maximum moment of 35 lb-ft for the z axis. It should be noted that these moments are dependent upon the geometry of the console with respect to the force balance.

The equations derived for the forces are given in Appendix C.

Push-Pull Console Operation

The push-pull console operation is a test designed to simulate the crew member of a spacecraft inserting the intercom phone jack into a wall receptacle. Initially, the subject has both hands resting on his thighs with the left hand holding the phone jack. He moves the left hand toward the wall receptacle and inserts the phone jack. The phone jack is then removed and the hand returned to the initial position, resting on the thigh.

Figs. 65 and 66 show the nominal case of the push-pull operation for Subjects A and B. The first 0.5 sec is the disturbance from the arm motion swinging up. The same disturbance profile as in the previous console operation is noted for the x axis. Also, the force magnitudes are approximately the same. The phone jack is inserted at 1.3 sec for Subject A and 1.2 sec for Subject B, as can be seen in the spiked characteristic of the y component of force. For this test, the actual console operation produces a larger disturbance than the arm motion.

Figs. 67 and 68 show the minimum level of intensity for the push-pull operation. Again, the prominent spike characteristics of the y component of force are the times which the phone jack was inserted and removed. The force produced by the arm motion is less than that illustrated in the nominal case.

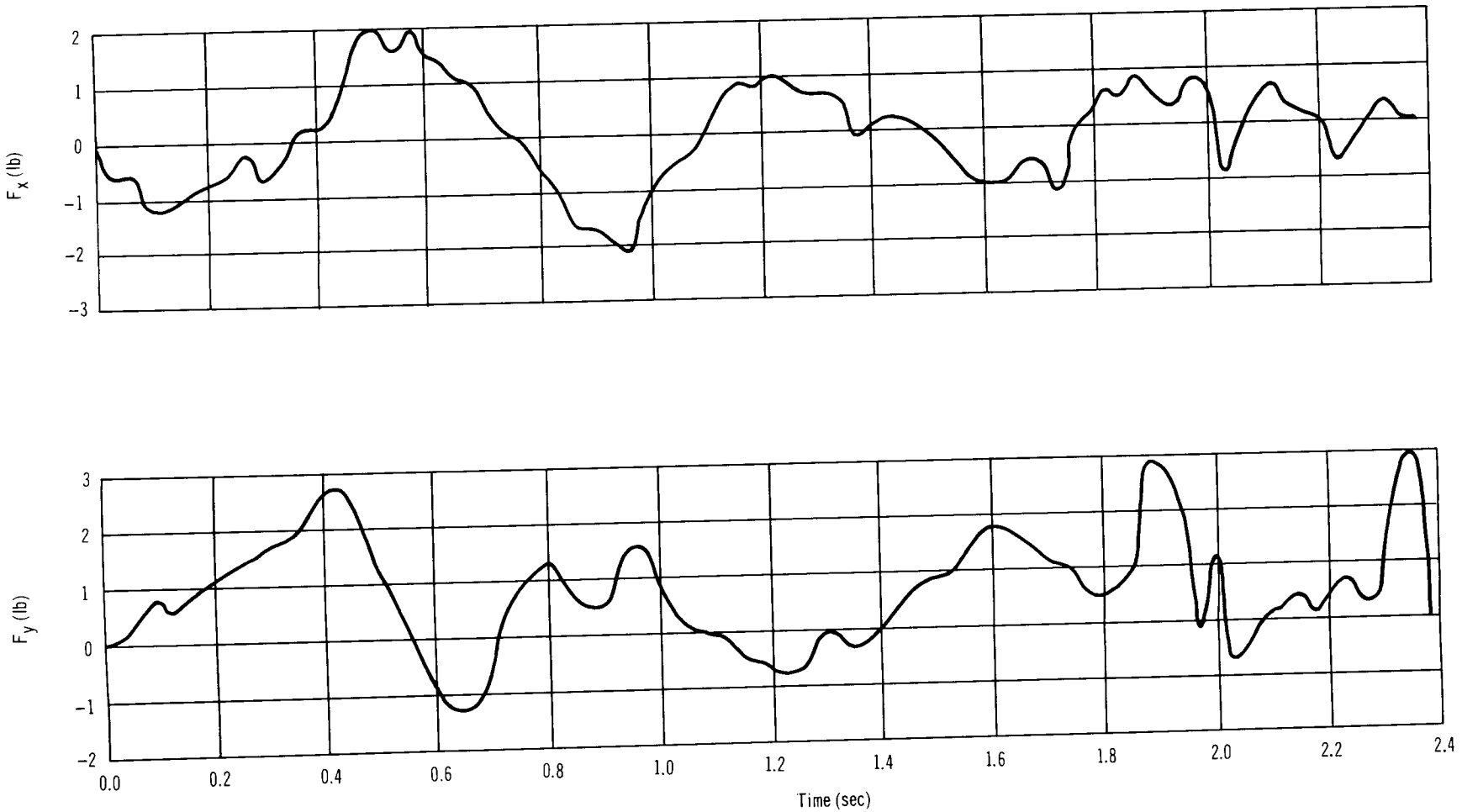

Figure 67. Console Operation Push-Pull Minimum Disturbance Profile – Subject A

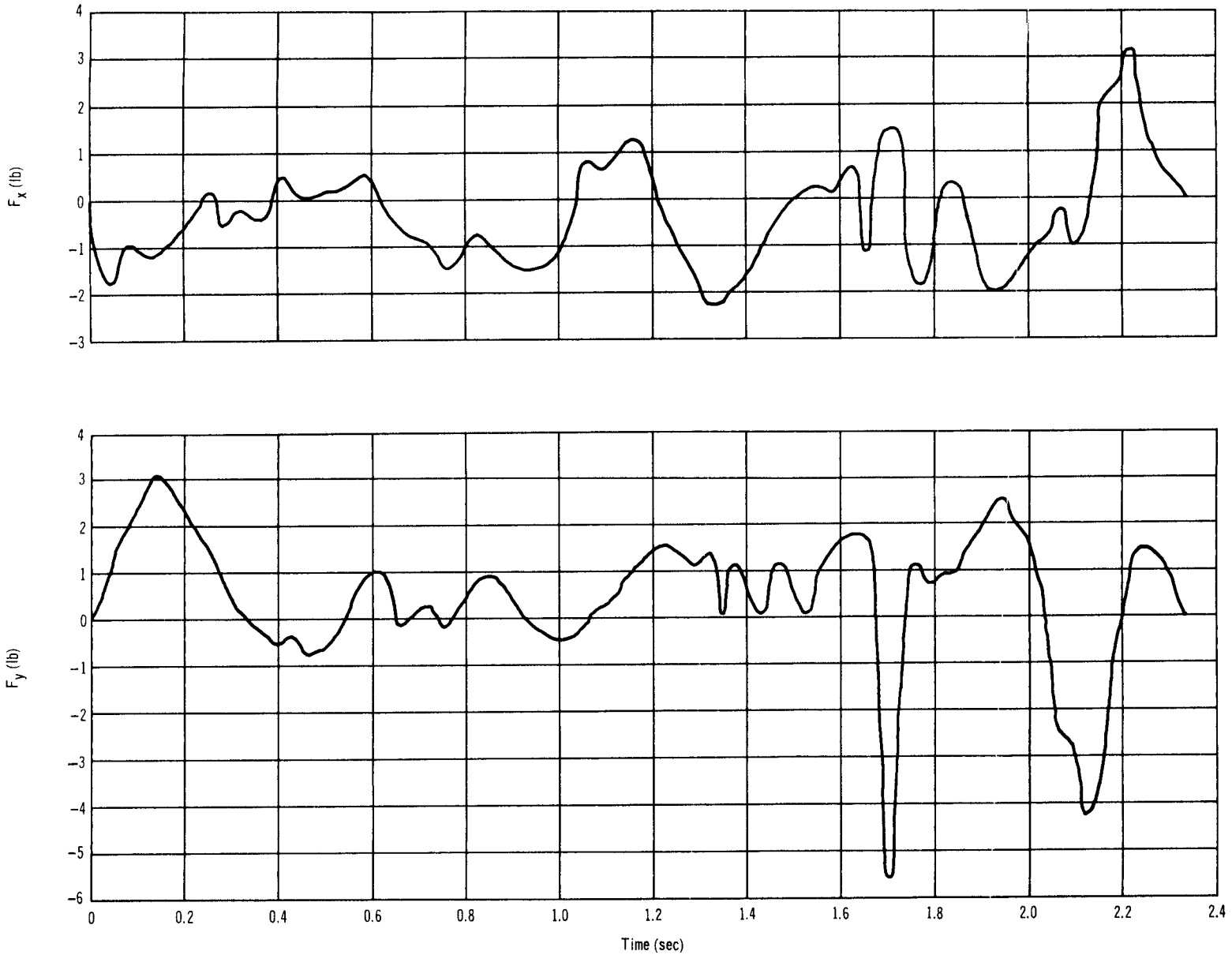

Figure 68. Console Operation Push-Pull Minimum Disturbance Profile – Subject 6

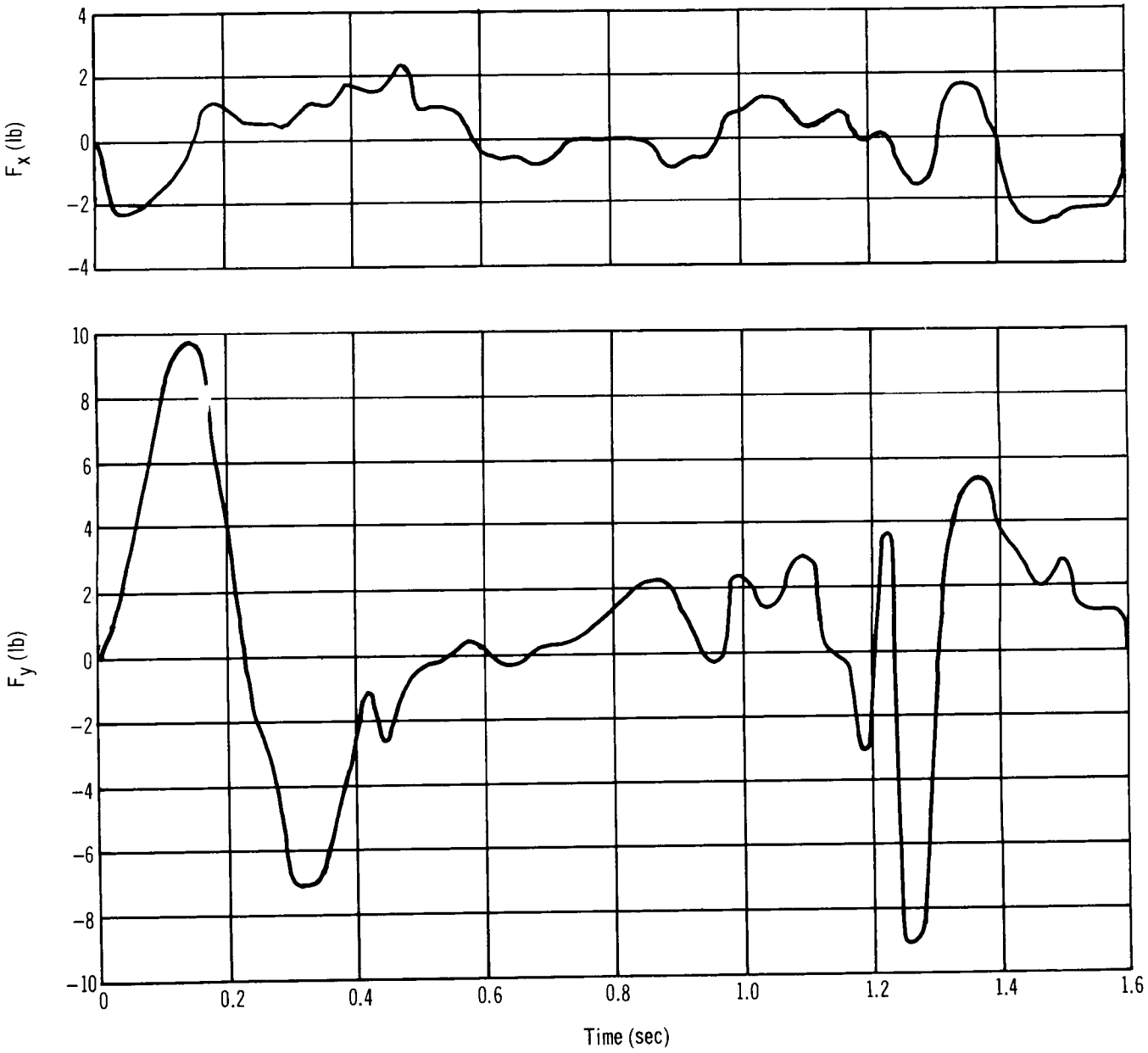

Figure 69. Console Operation Push-Pull Maximum Disturbance Profile – Subject A

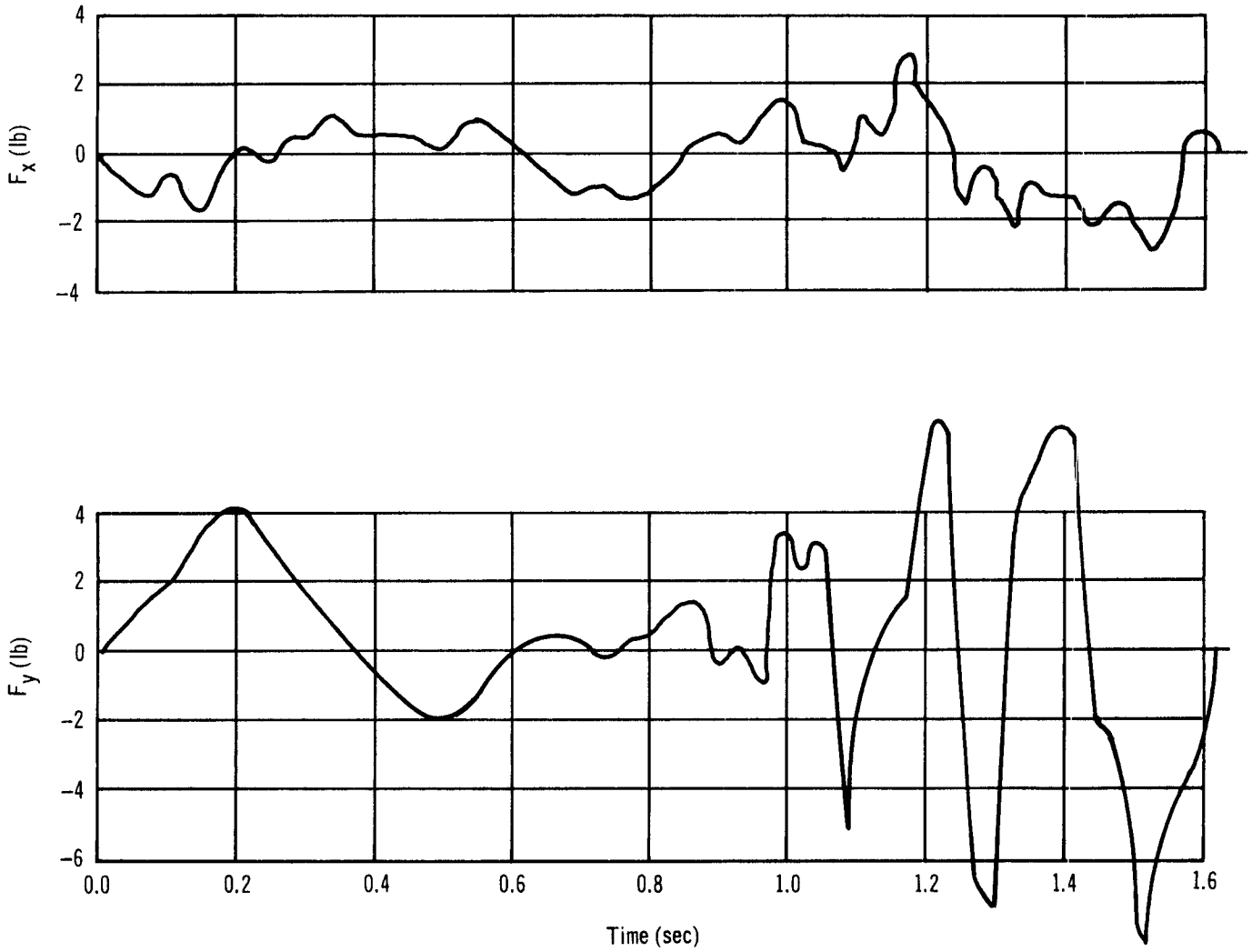

Figure 70. Console Operation Push-Pull Maximum Disturbance Profile – Subject B

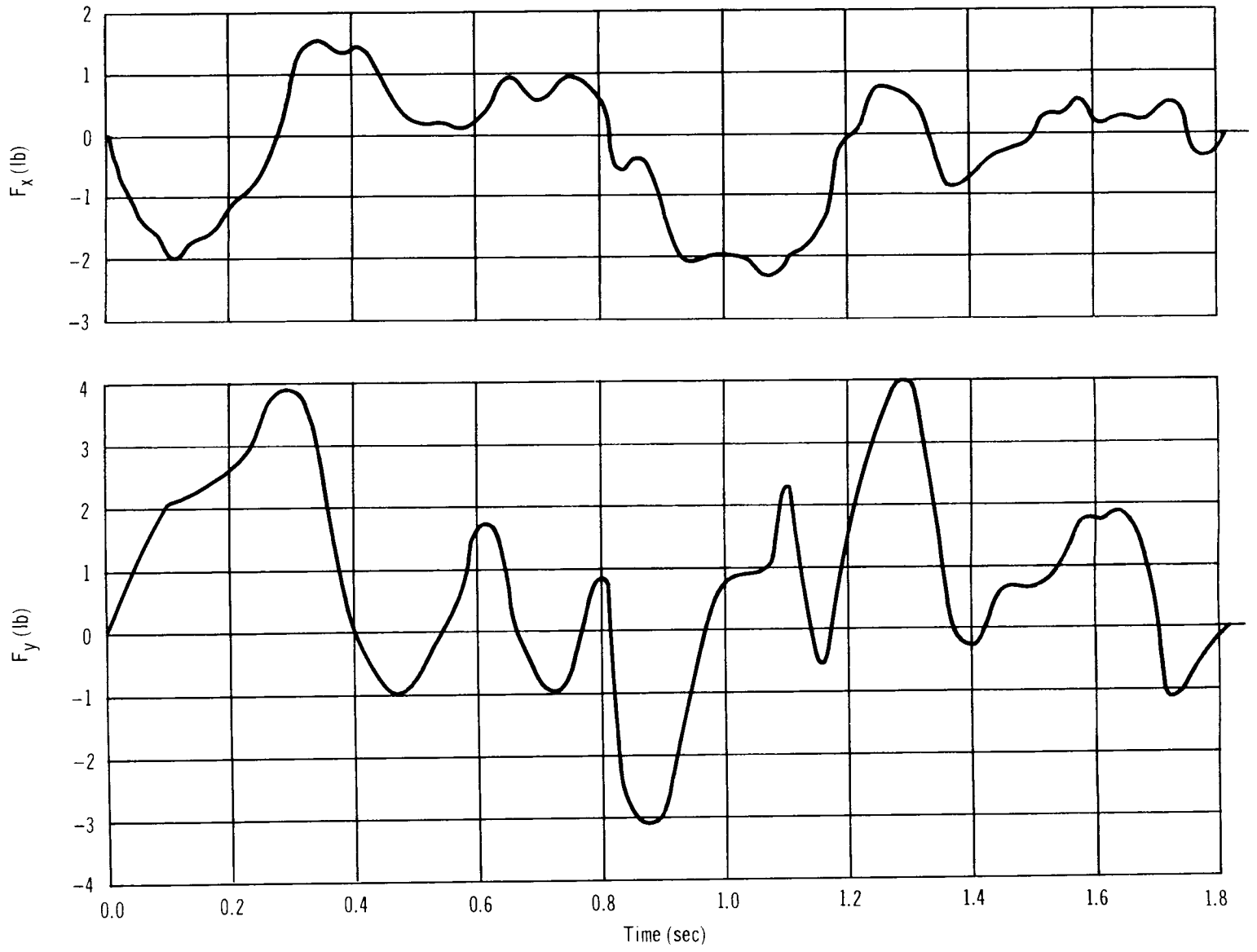

Figure 71. Console Operation Lateral Sliding Nominal Disturbance Profile – Subject A

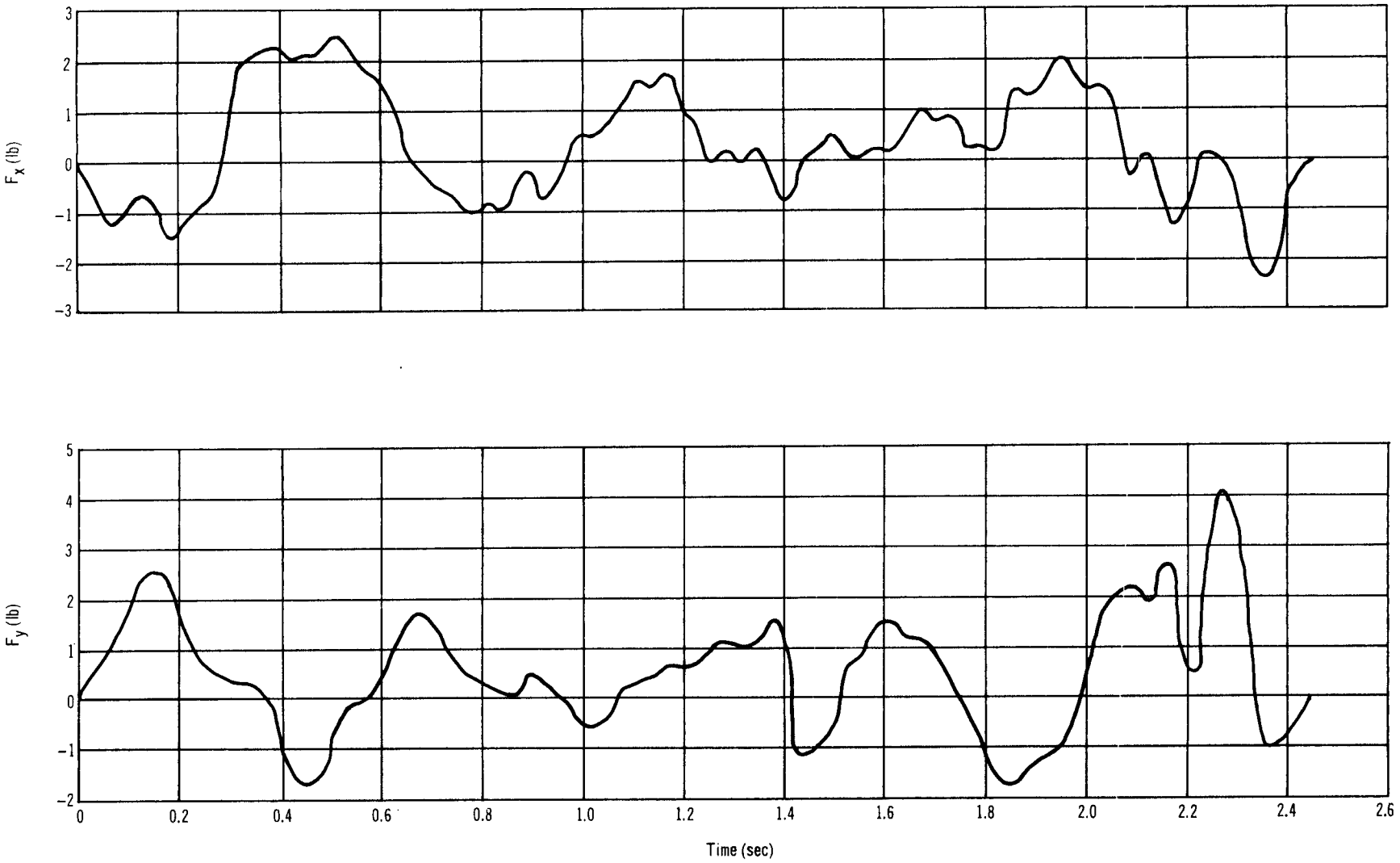

Figure 72. Console Operation Sliding Nominal Disturbance Profile – Subject B

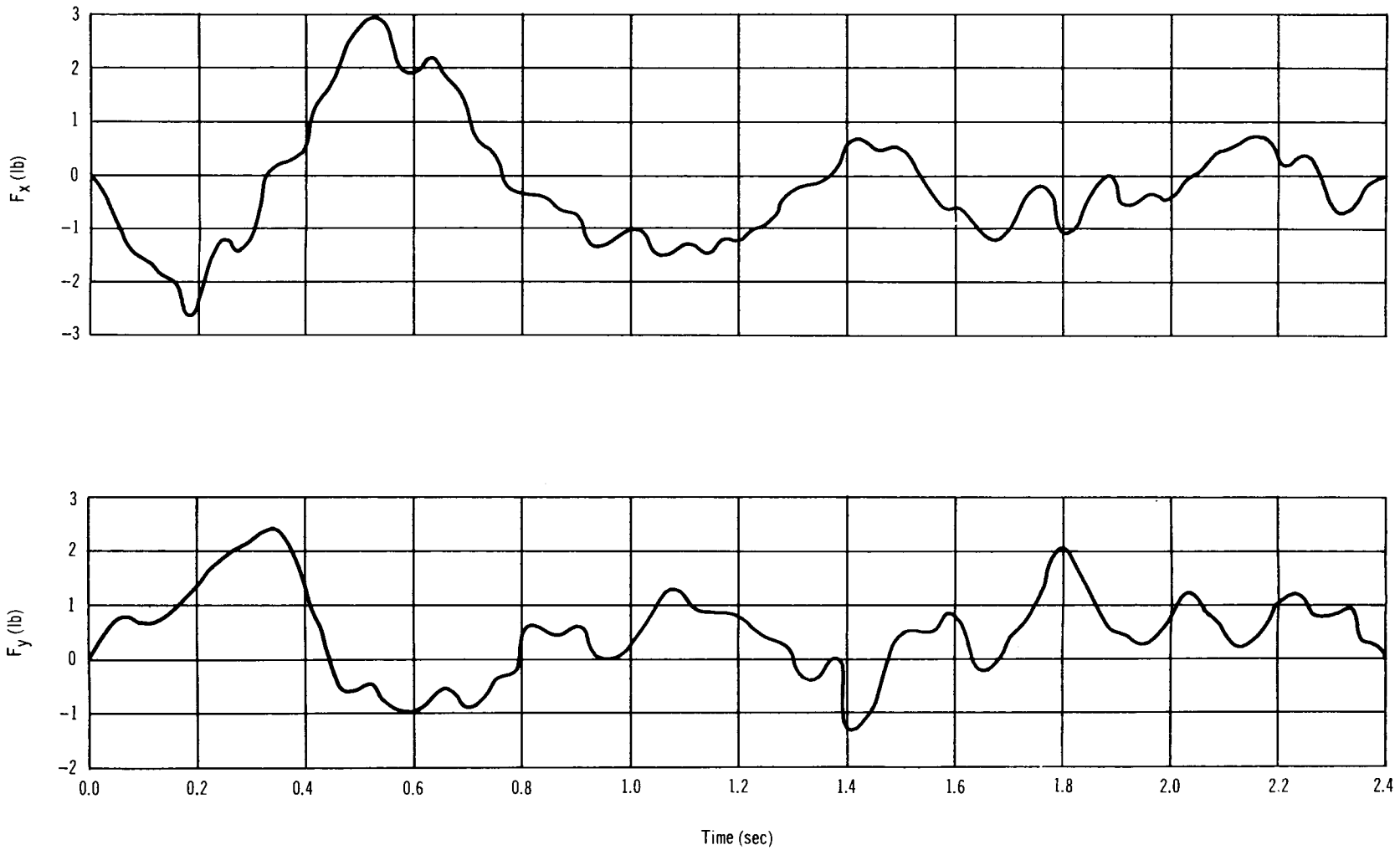

Figure 73. Console Operation Lateral Sliding Minimum Disturbance Profile – Subject A

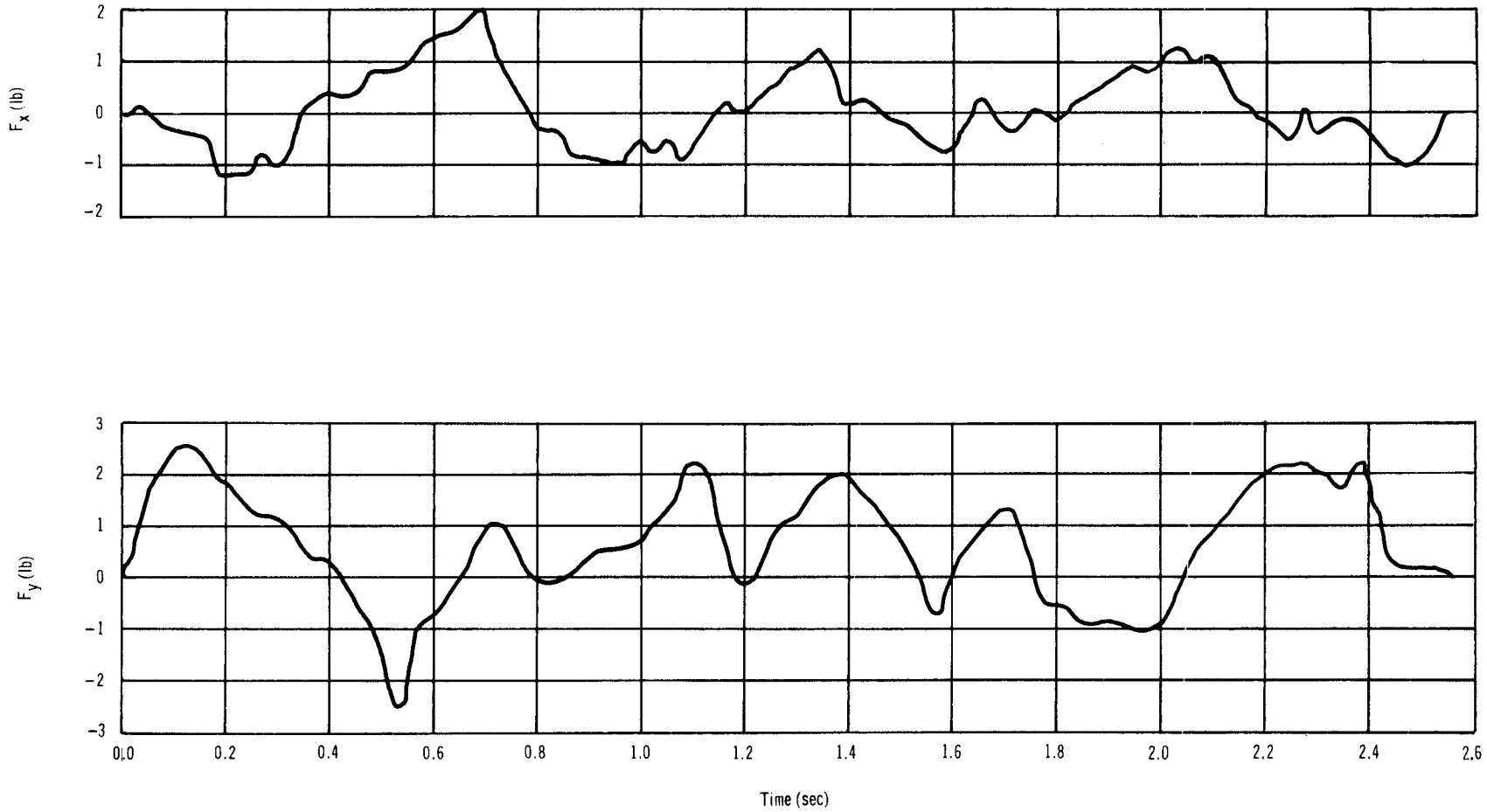

Figure 74. Console Operation Sliding Minimum Disturbance Profile – Subject B

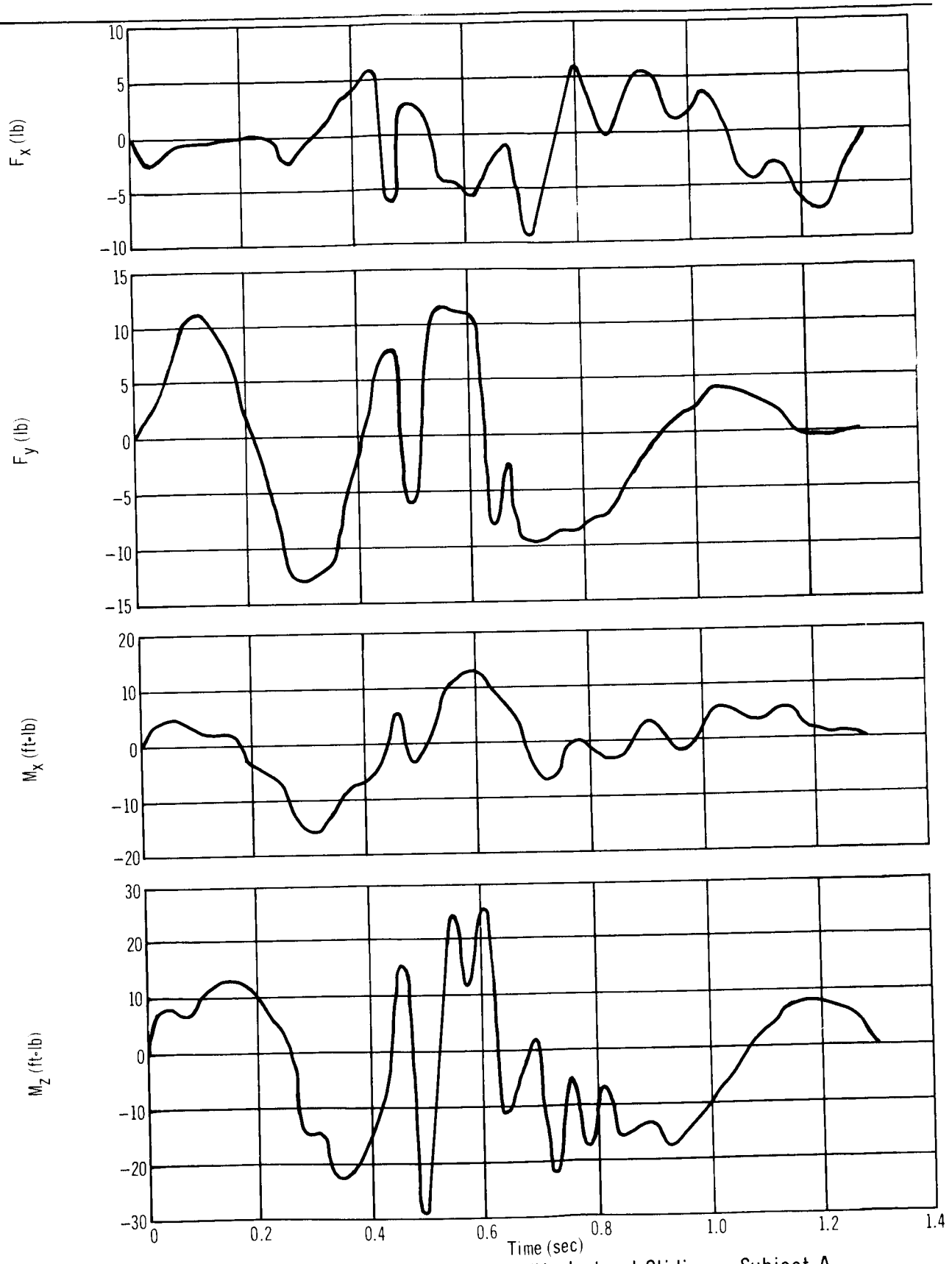

Figure 75. Console Operation Maximum Disturbance Profile Lateral Sliding – Subject A

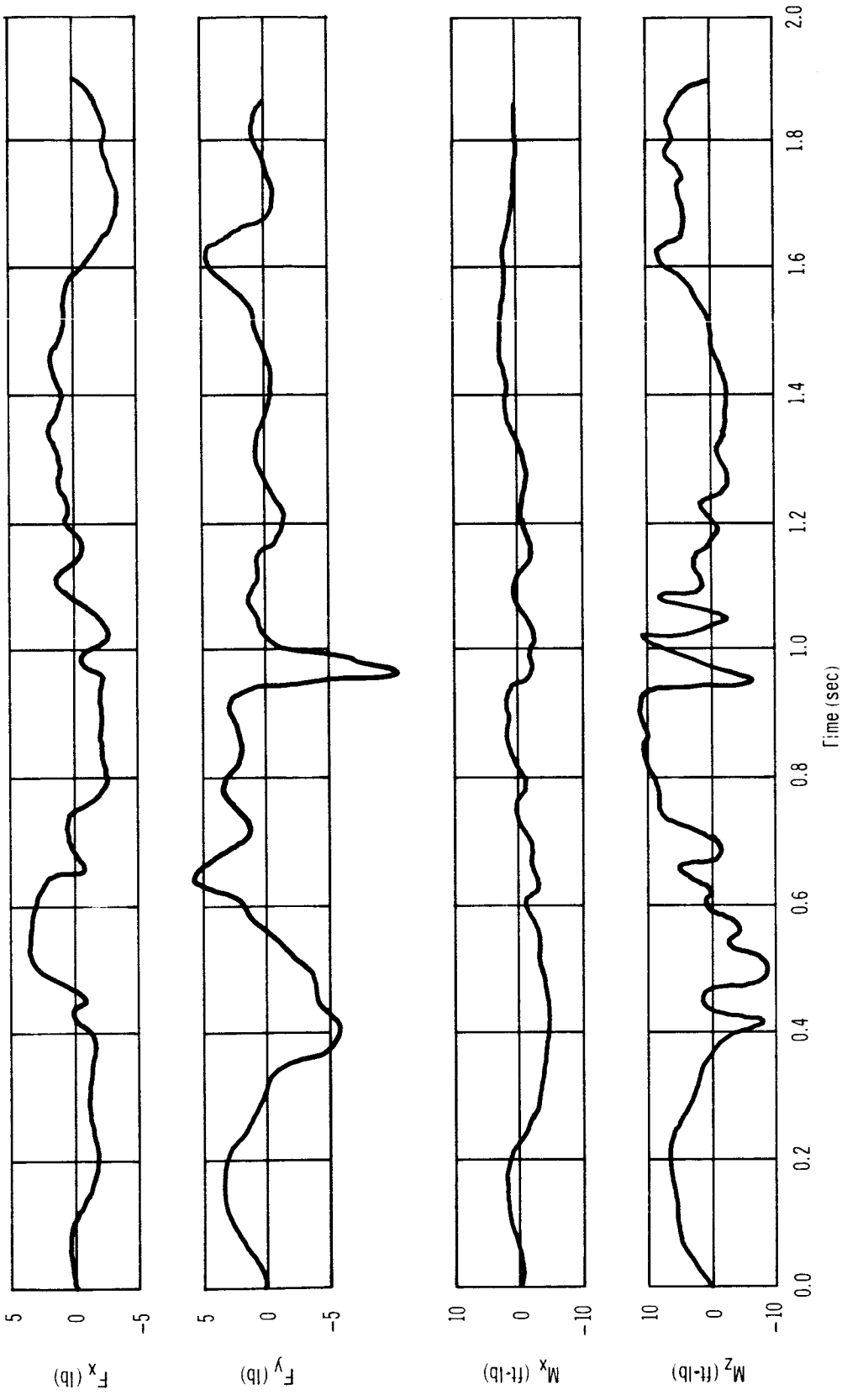

Figure 76. Console Operation Sliding Maximum Disturbance Profile – Subject B

Figs. 69 and 70 are for the maximum level of intensity. The maximum y axis forces produced are 9.6 lb and 8.6 lb for Subjects A and B, respectively.

Console Operation Sliding

The sliding console operation simulation is similar to the torquing operation. The subject initially has both hands resting on his thighs. He moves his left hand to the slide-bar handle. The subject grasps the handle and moves it first to the left as far as possible and then returns the handle to the original position. The handle is then released, and the subject returns his hand to the original position.

The nominal case is shown in figs. 71 and 72 for Subjects A and B, respectively. The force levels are compatible with the previous console operations. Subject A appears to be somewhat more facile in the console operation than Subject B.

The minimum case is shown in figs. 73 and 74. Again, there is very little difference between the magnitude of the forces for the nominal and minimum cases. The maximum force in the x and y axes for both cases is approximately 3 lb.

Figs. 75 and 76 illustrate the disturbances for the maximum intensity of the console sliding operation. The moment components, x and z, are given for this case along with the usual x and y forces. Again, Subject A is quite active and produces forces of 16 lb and moments of 29 lb-ft, while Subject B produces forces of 11 lb and moments of 11 lb-ft. Subject A performed the console operation in 0.4 sec less time than Subject B; hence, higher magnitudes of disturbances are to be expected.

CREW MOTION EXERCISES

Physical conditioning of the spacecraft crew is recognized as a primary requirement whenever extended periods of weightlessness are experienced. Accordingly, crew exercise activities are considered a major source of disturbance during a mission. The crew exercises simulated during this study include: (1) trunk bending exercise, (2) neck bending exercise, (3) rowing exercise, (4) pedal ergometer endurance exercise, (5) oscillating acceleration exercise, (6) full length body exercise, and (7) trunk rotation exercise. Each of these exercises has disturbance profiles which are referenced to the coordinate system shown in fig. 4. The test results for the crew exercise are discussed in the following paragraphs.

Trunk Bending Exercise

For the trunk bending exercise, the subject is in a standing position with his hands above his head. He then bends at the waist until his hands grasp the ankles, pulling his head toward his knees. This body segment motion is performed in the x-y plane (see fig. 4).

This exercise is similar to the waist bending motion, the only difference being that in the trunk bending exercise the hands are above the head and the torso is rotated through a greater angle. Hence, it is expected that the forces produced from the exercise will be larger than those of the waist bending motion.

Fig. 77 is a plot of the x and y forces for Subject A in performing the trunk bending exercise. The general shape of the curve of F_y is similar to that shown for the waist bending (fig. 17). The peak values of the x and y components of force are 16 lb and 44 lb, respectively, for the trunk bending exercise. Again, the x component is small because the upper and lower torso rotate in opposite directions. This exercise required 1.1 sec.

Fig. 78 shows the result of Subject B performing the trunk bending exercise. The maximum y-component force is approximately 16 lb, nearly a factor of three less than that of Subject A. The magnitude of F_y was roughly the same for all three cases that Subject B performed. It is noted that Subject B performed the exercise in 0.9 sec, compared to 1.1 sec for Subject A. Both subjects rotate the upper torso through the same angle. Hence, the most likely possibility of Subject B producing less disturbance is that he bent his knees while performing the exercise. From the area under the y component of force, it appears that Subject B motion was influenced by the gravity component of the pendulum support.

The equations derived for the forces are presented in Appendix C. The x component is omitted because it is small.

Neck Bending Exercise

For this exercise the helmet is removed from the subject. A head strap with a dynamometer attached is used. The free end of the dynamometer is grasped with the right hand fully extended. The exercise then consists of pulling the head against the constraining dynamometer.

No attempt was made to predict the disturbances resulting from this exercise. The dynamic description is dependent upon body muscles and not free swinging body segments.

The forces caused by this exercise are shown in figs. 79 and 80 for Subjects A and B, respectively. The body motion for this exercise is very small. Hence, it is not known whether the biasing of the y component of force for Subject A results from the pendulous gravity component. The forces exerted in either case are approximately 2 lb. Subject B appears to have a smoother action than that of Subject A.

The equations derived for the forces are presented in Appendix C.

Rowing Exercise

For this exercise, one end of the dynamometer is fastened to the left foot and the other end is grasped with the left hand. The dynamometer is pulled and the shoulder is rotated clockwise in the x-y plane. This exercise depicts a rowing motion.

The disturbances for Subjects A and B are shown in figs. 81 and 82, respectively. For Subject A, the maximum y component of force is approximately 13 lb, with a cyclic nature. The fundamental period is approximately 0.8 sec. Subject B exhibited a higher force, F_y, of 26 lb, with a shorter fundamental period.

Only the equation for the y component of force is presented in Appendix C because the x component is small.

Pedal Ergometer Endurance Exercise

For this exercise, the pedal ergometer is attached to the platform such that the pedaling motion is performed in the x-y plane. For the start of the test, the subject is pedaling at approximately 60 rpm with a load of 150 W. The disturbance profile for the acceleration to 60 rpm is not available.

Fig. 83 is a multiple-exposure photograph of Subject B performing the pedal ergometer exercise. Fig. 84 is a time history of the various body segment Euler angles. The torso and the arms remained nearly motionless while Subject B performed this exercise.

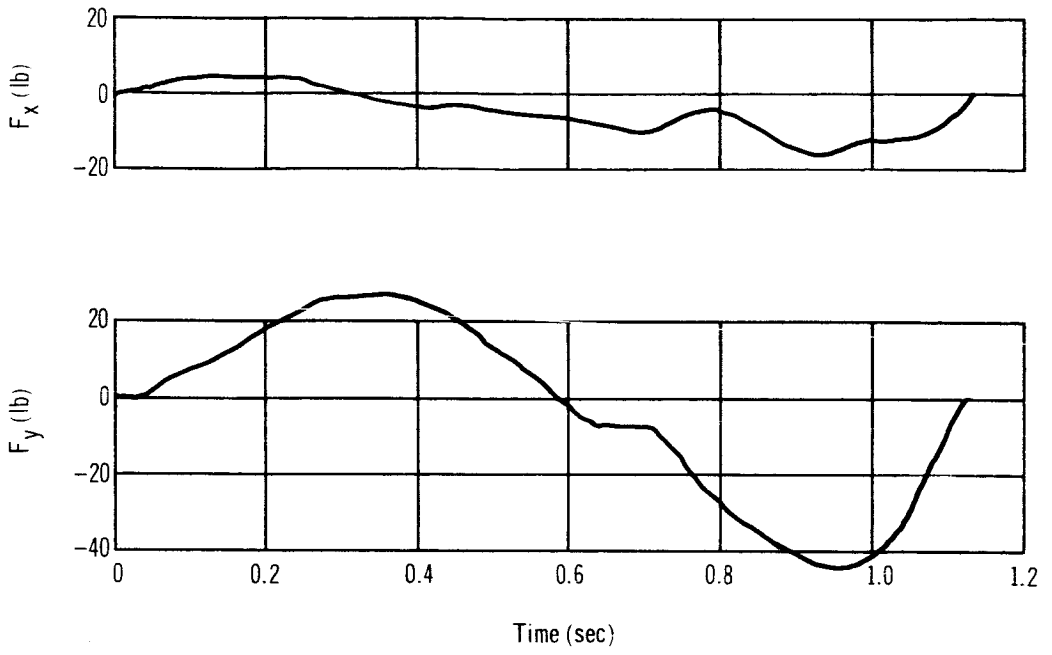

Figure 77 Trunk Bending Exercise Disturbance Profile – Subject A

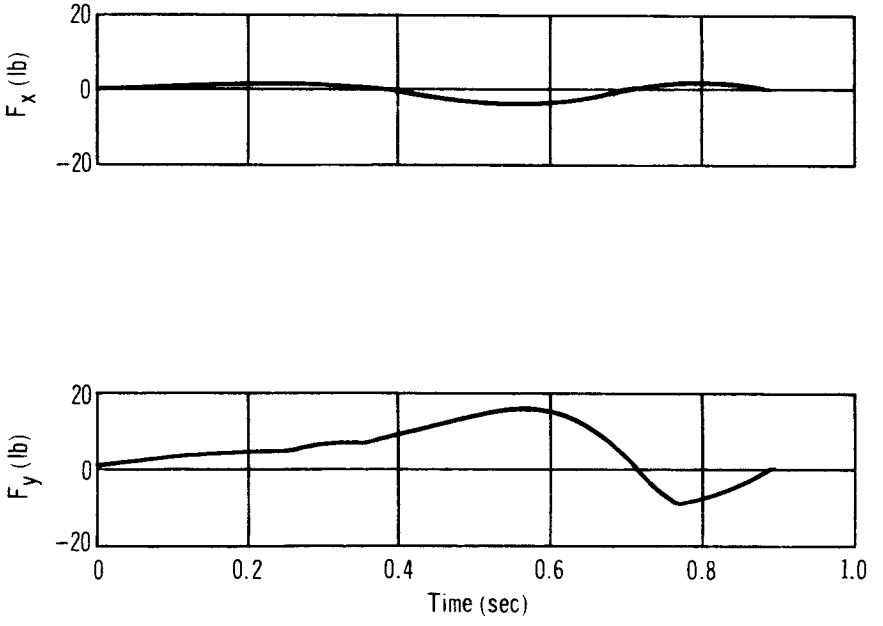

Figure 78. Trunk Bending Exercise Disturbance Profile – Subject B

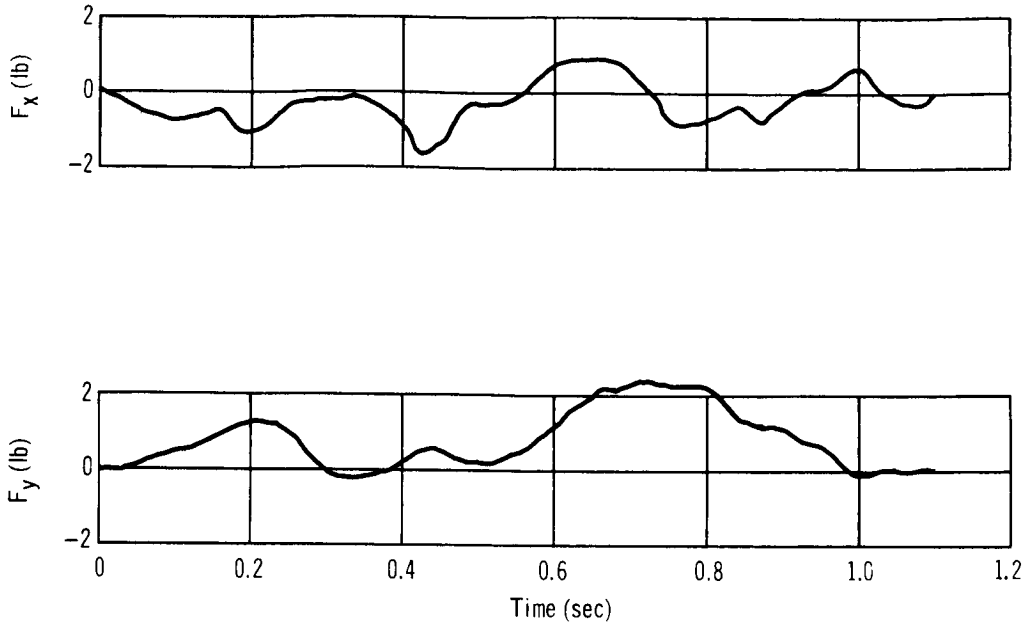

Figure 79. Neck Bending Exercise Disturbance Profile – Subject A

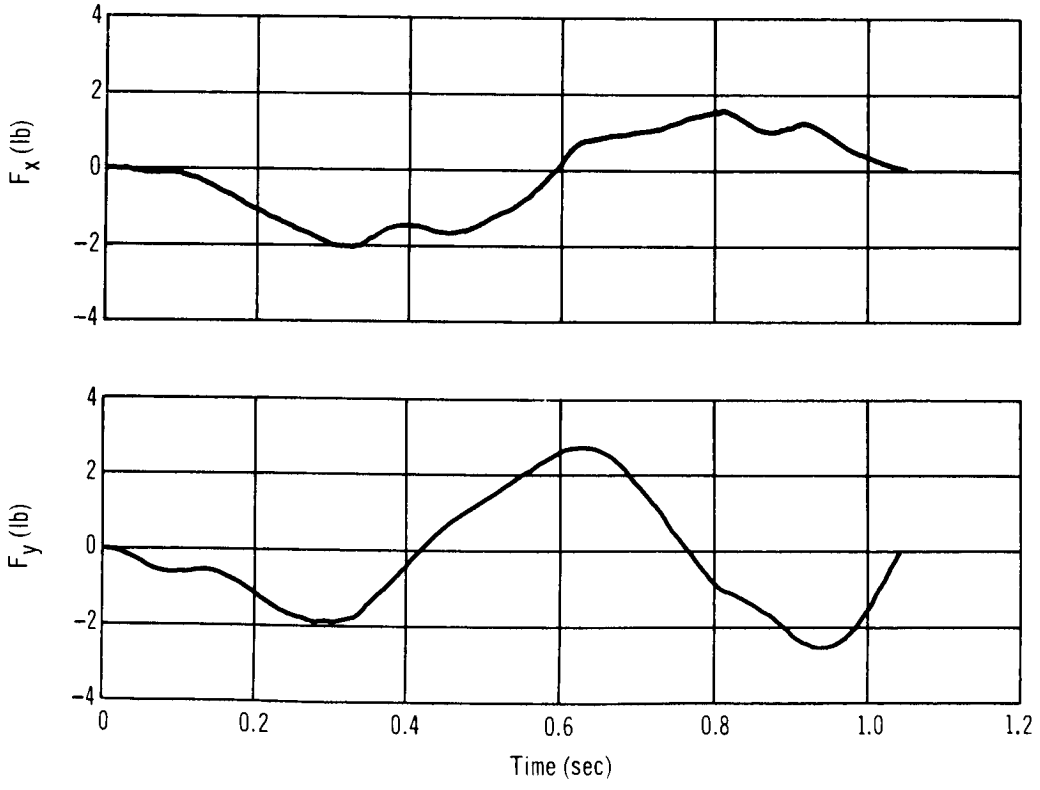

Figure 80. Neck Bending Exercise Disturbance Profile – Subject B

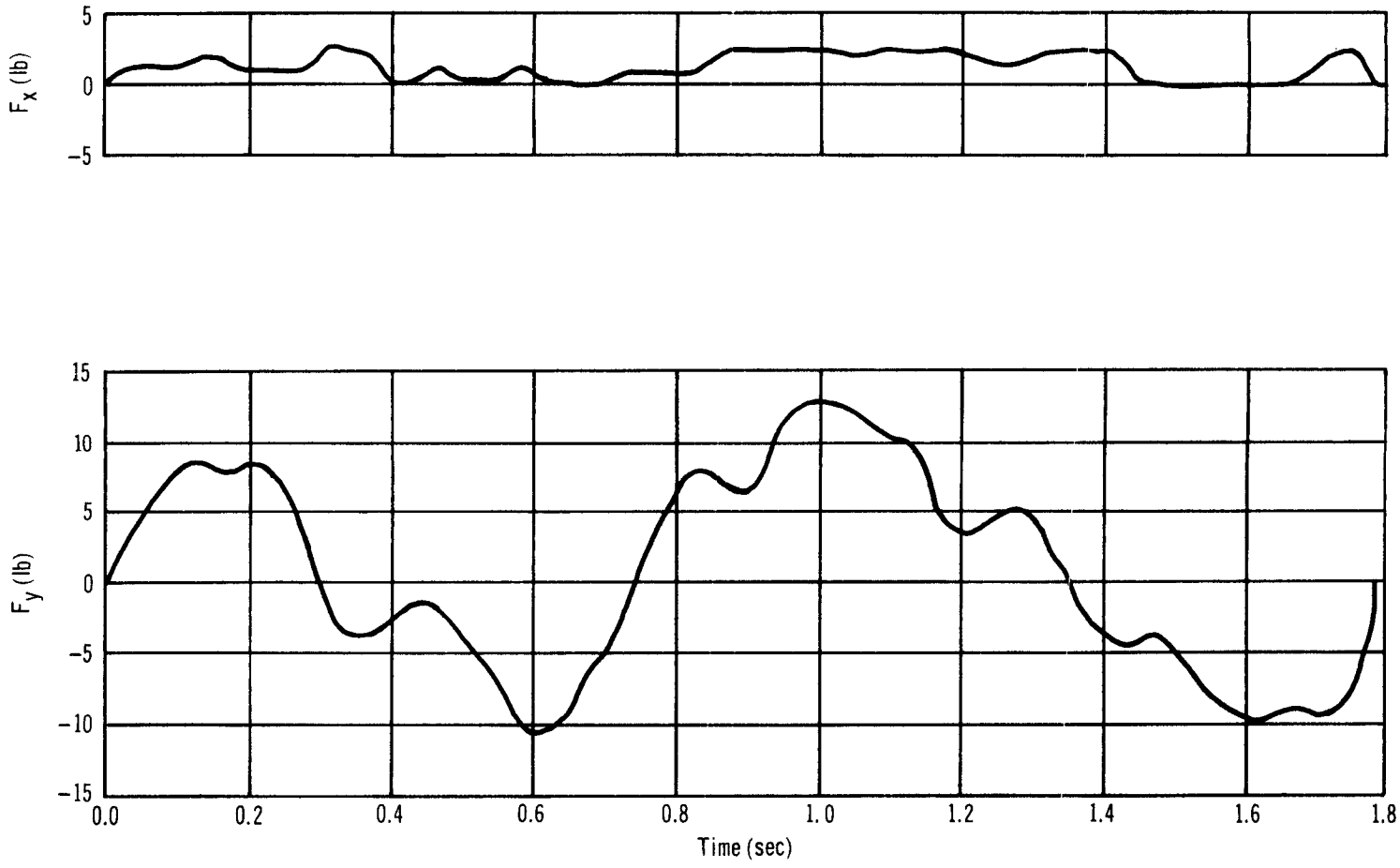

Figure 81. Rowing Exercise Disturbance Profile – Subject A

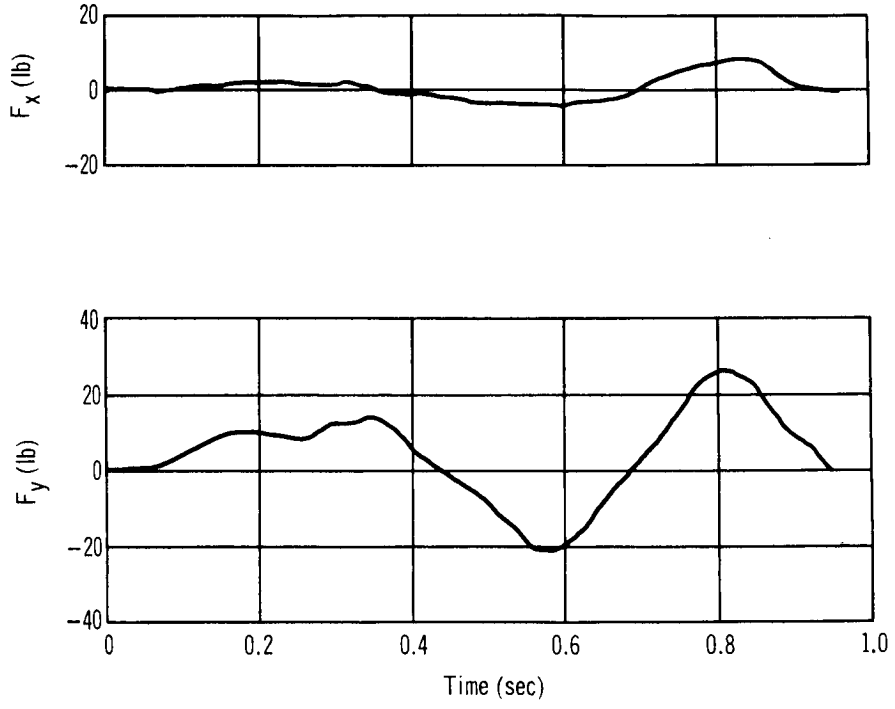

Figure 82. Rowing Exercise Disturbance Profile – Subject B

Figure 83. Pedal Ergometer Exercise

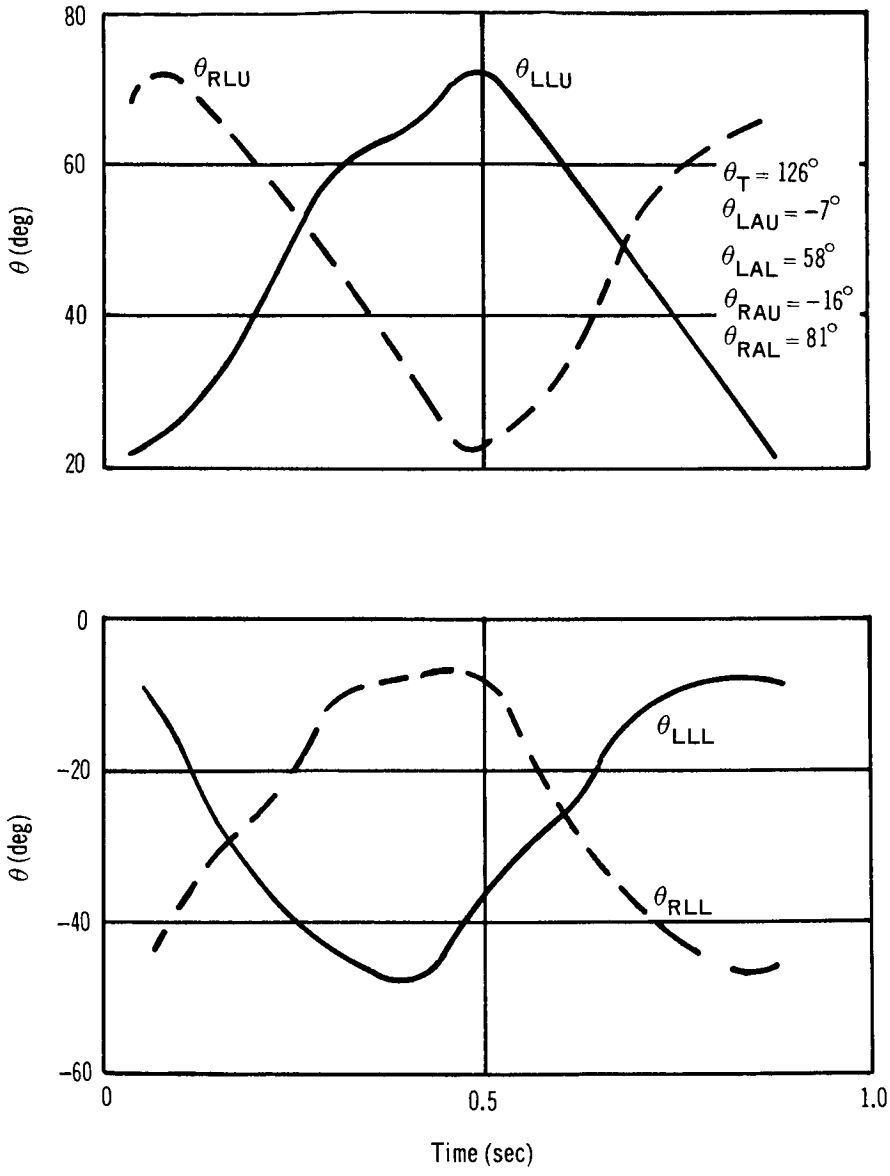

Figure 84. Pedal Ergometer Endurance Exercise Euler Angles – Subject A

Figs. 85 and 86 show the disturbances of the pedal ergometer exercise for Subjects A and B, respectively. Because the subjects were pedaling at approximately 60 rpm at the start of the test, the bias forces and moments were not obtained. Only the relative difference between the peaks of the force and moment components are representative for this disturbance. The forces and moments must integrate to zero over one full pedaling cycle because over one full cycle all body segments are at the same location as at the start of the cycle. Hence, the force and moment scales should be moved up or down to give equal areas on either side of the zero coordinate. In comparing figs. 85 and 86, Subject B performed a much smoother ride than Subject A. Both subjects induced approximately the same magnitude of disturbance.

The equations for the curves are presented in Appendix C.

Oscillating Acceleration Exercise

To perform the oscillating acceleration exercise, the subject springs off the force platform in the plus-y direction by straightening his legs, as in the free soaring. With his arms extended, he cushions the impact at the bounce board with his hands and pushes off the board to return to the force platform.

Fig. 87 is a multiple-exposure photograph of Subject A performing the oscillating acceleration exercise.

The body segment Euler angles for Subject A in performing the exercise are shown in fig. 88. This exercise required approximately 2.2 sec to complete. It should be noted that the subject's torso remained nearly erect throughout the exercise. Fig. 89 shows the displacement of the subject's head when performing the exercise. The y displacement is the vertical motion, which shows a maximum excursion of 41 in. The x displacement shows the distance the subject moved forward at the completion of the test.

Fig. 90 is a plot of the y component of force Subject A exerted while performing this exercise. The initial negative peak is produced when the subject pushes off the platform. The magnitude and time history of F_y is very similar to the nominal free soaring disturbance shown in fig. 33. This is to be expected, because the first part of these two tests is identical. The impact on the bounce board occurs approximately 0.57 sec after first motion, as shown in fig. 90. From this time until approximately 1.2 sec, the subject cushions his impact with his hands and then pushes off to return to the platform. The reason that the area under the positive force curve, or impulse, is greater than that for the negative force curve is that the subject reduces his initial velocity to zero (the velocity attained from pushing off the platform with his legs) and adds a velocity from pushing with his hands to return to the force platform. The peak forces exerted by the legs and arms are 85 and 106 lb, respectively.

The performance of Subject B is shown in fig. 91. The y component of force for both subjects is very similar. The major difference is that Subject B exerted more force with his legs than his arms. The x component of force is small compared to the y component.

The equations for the disturbances are presented in Appendix C.

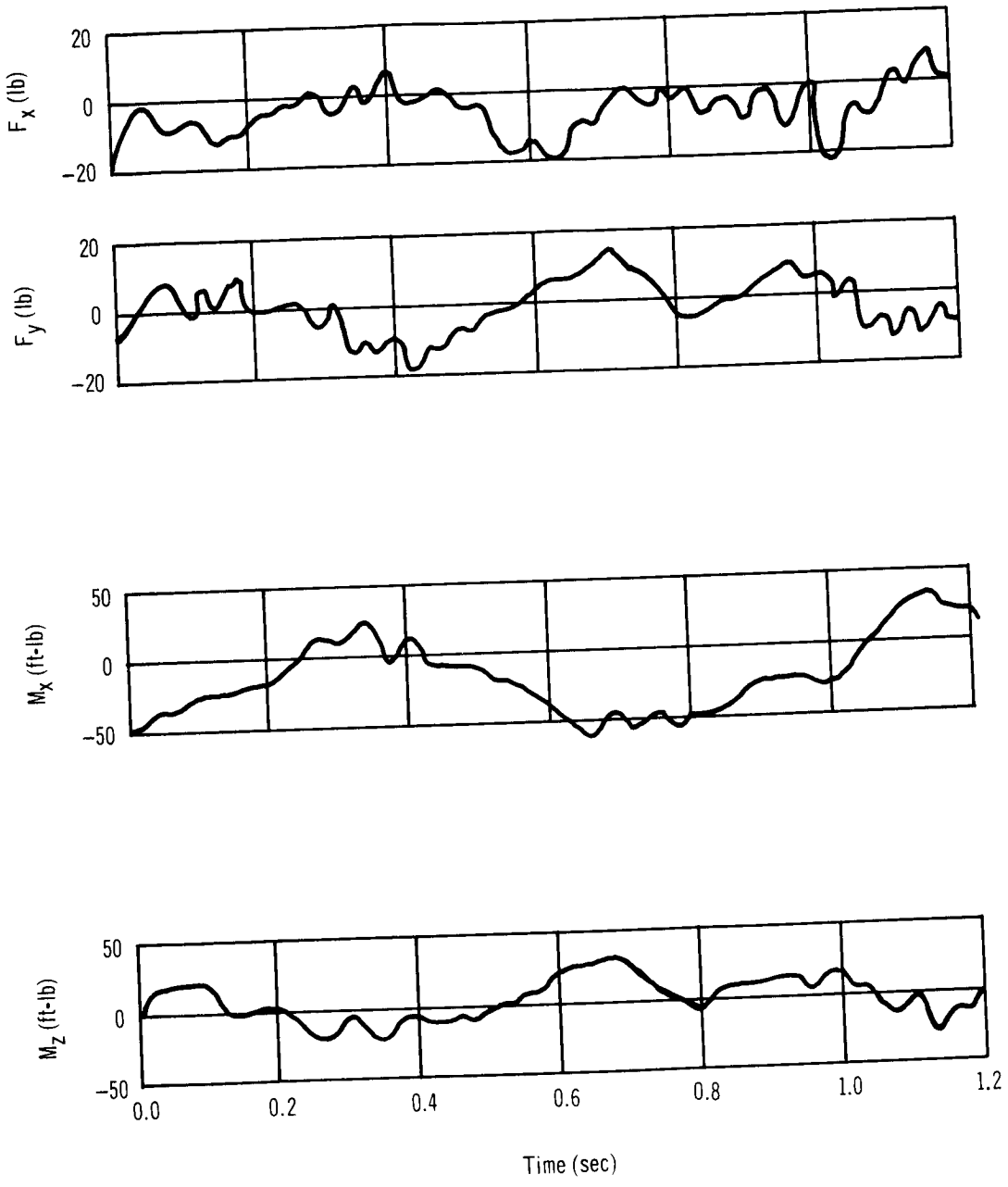

Figure 85. Pedal Ergometer Endurance Exercise Disturbance Profile – Subject A

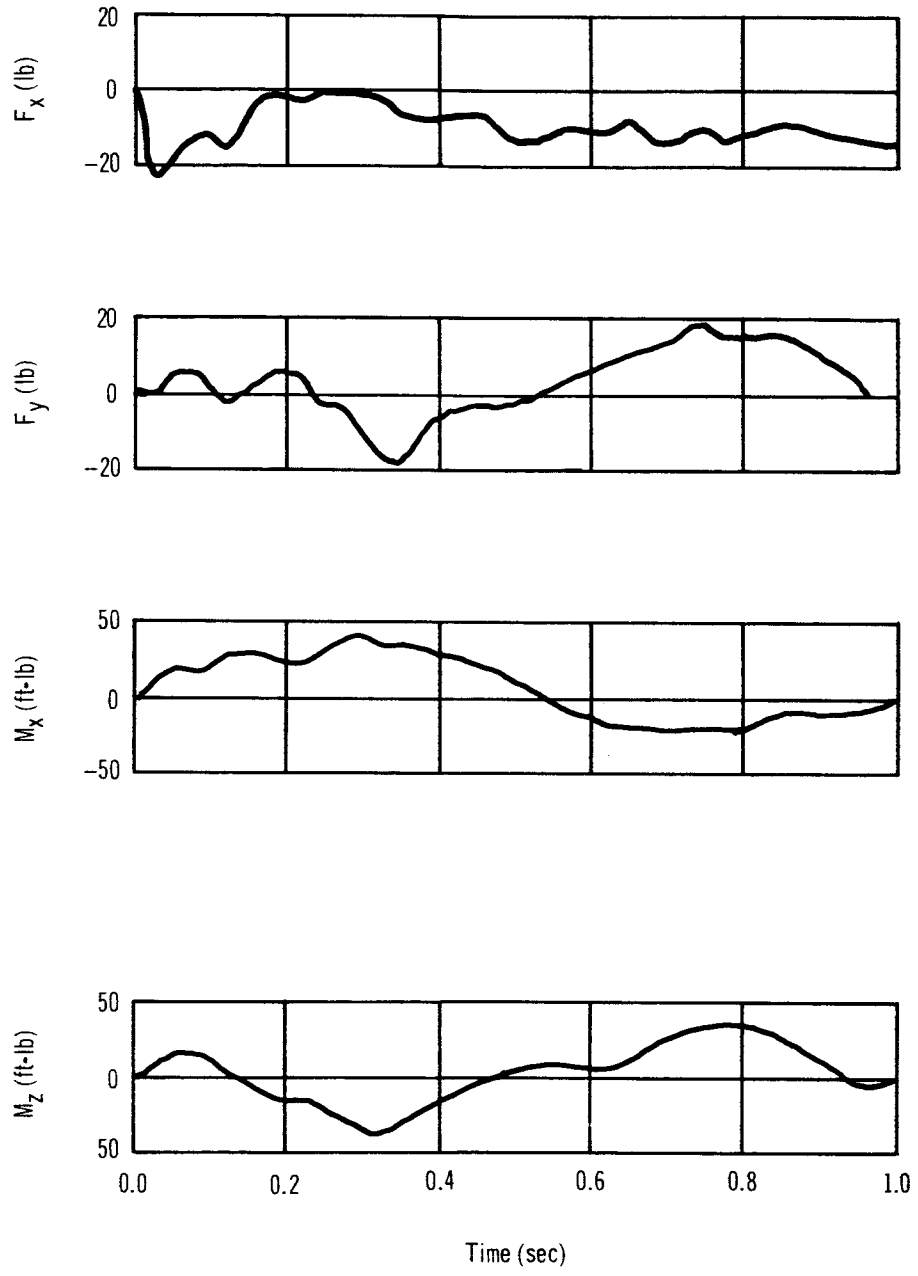

Figure 86. Pedal Ergometer Endurance Exercise Disturbance Profile – Subject B

Figure 87. Oscillating Acceleration Exercise

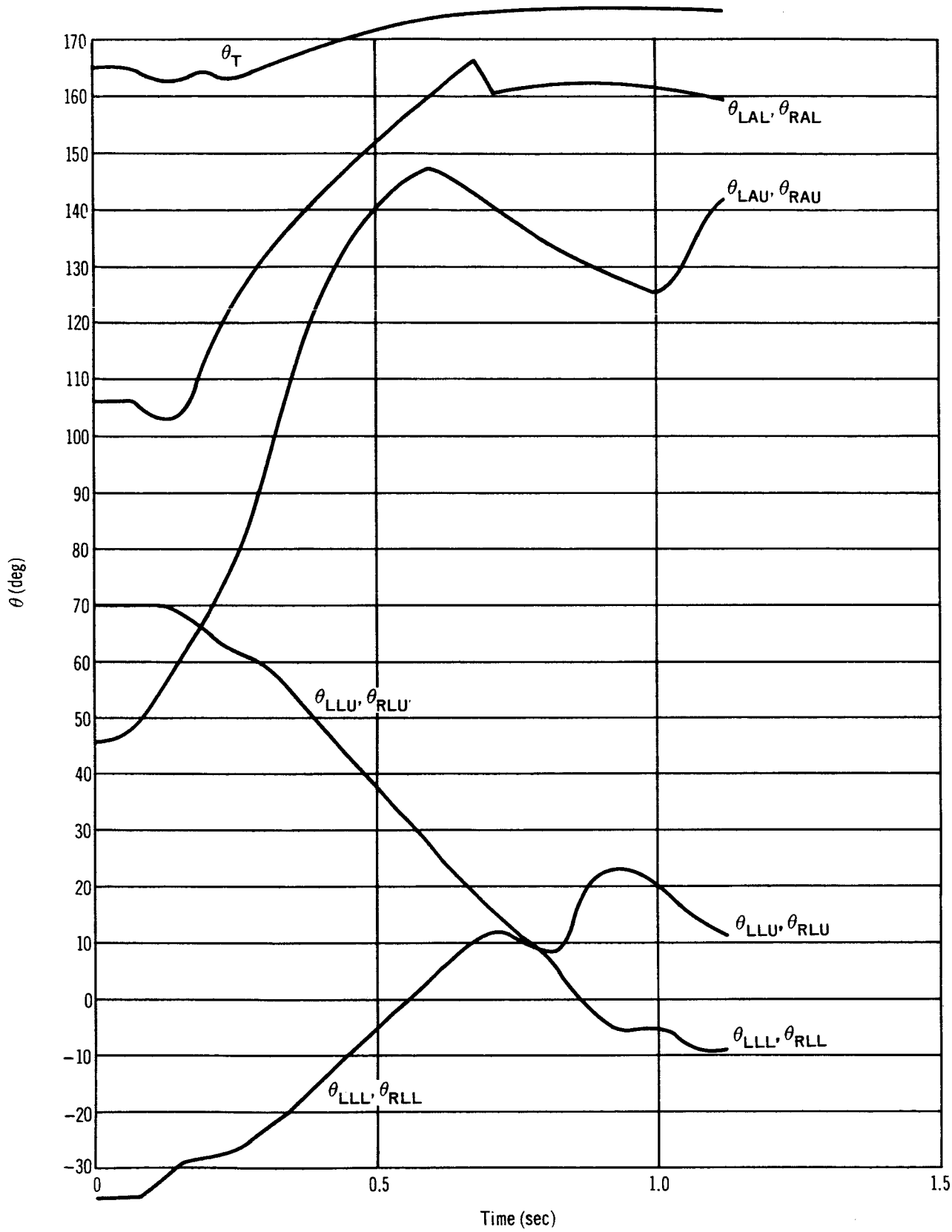

Figure 88. Oscillating Acceleration Exercise Euler Angles – Subject A

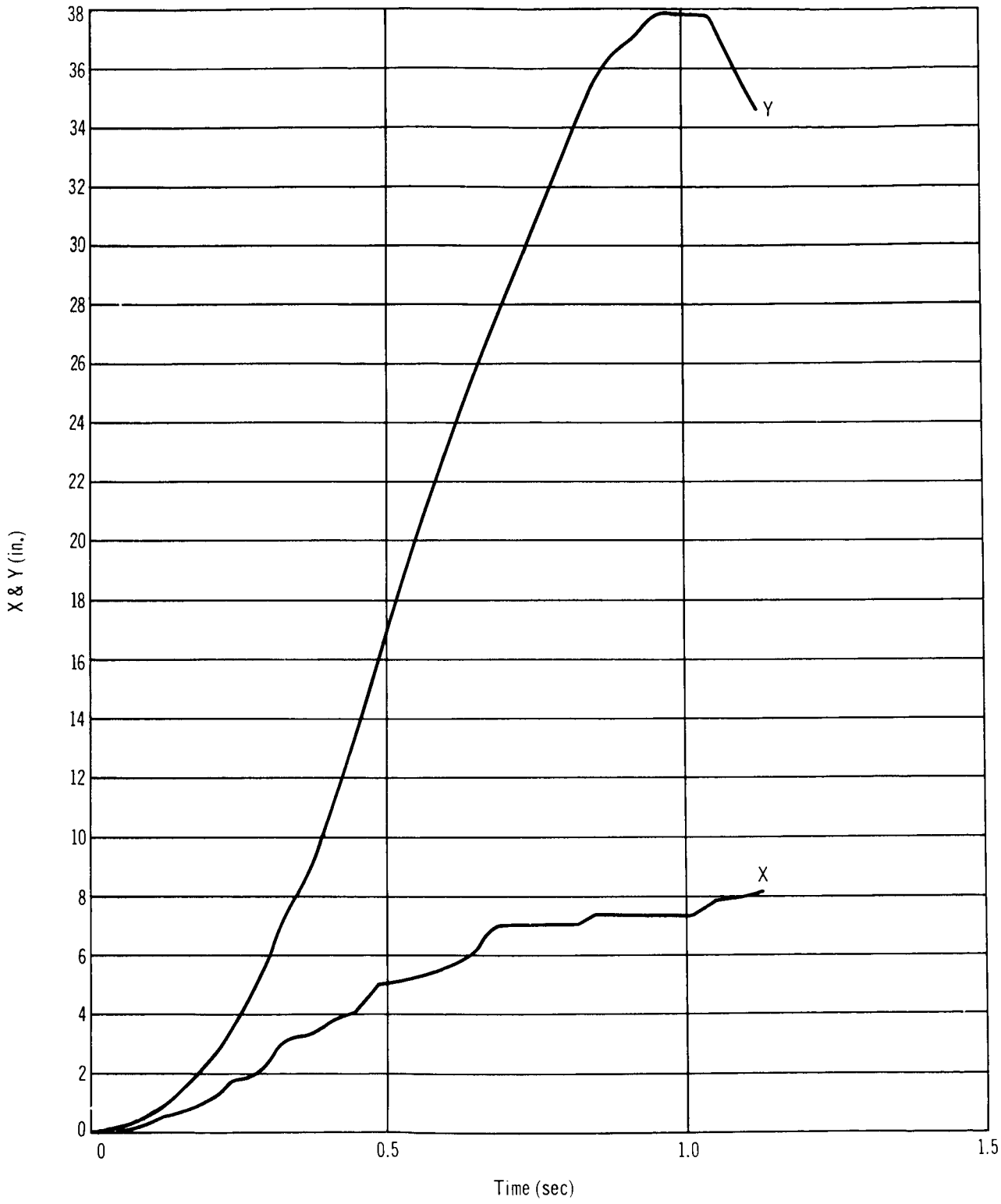

Figure 89. Oscillating Acceleration Exercise Displacement – Subject A

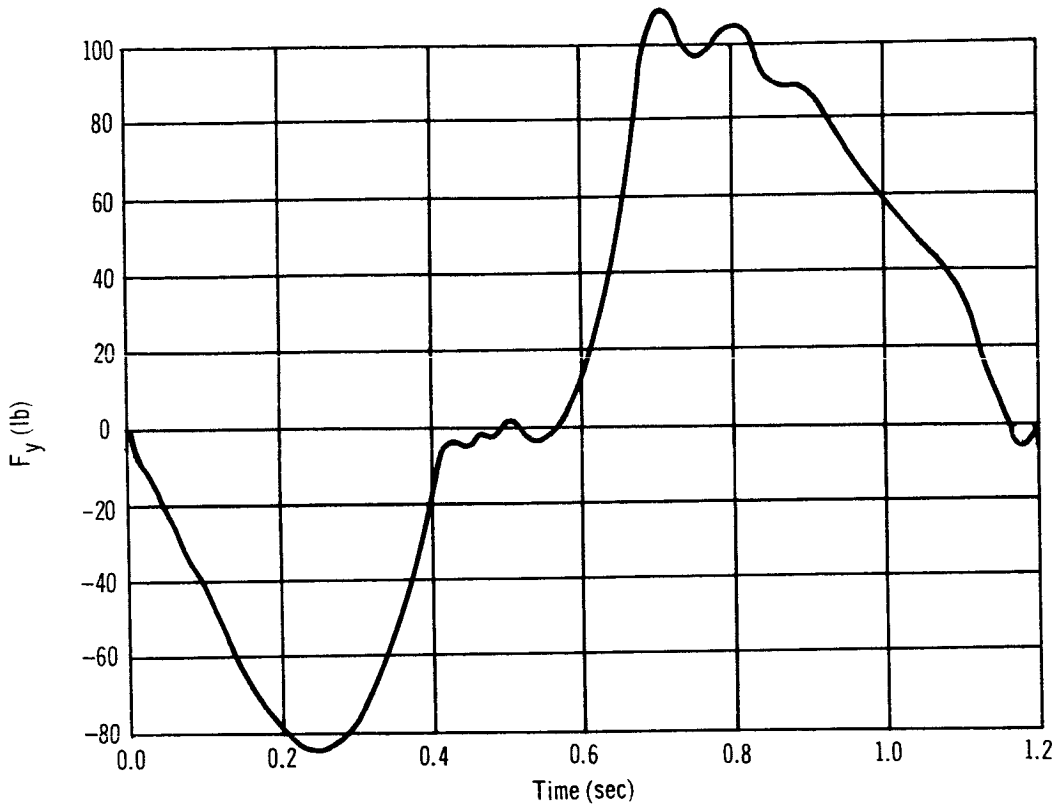

Figure 90. Oscillating Acceleration Disturbance Profile – Subject A

Full-Length Body Exercise

To perform the full-length body exercise, the subject places both feet in a foot-restraint assembly fixed to the platform. The exercise apparatus consists of a rod mounted on the platform parallel to the subject's longitudinal axis. A pair of handlebars attach to the rod so that they slide up and down it. Fixed to the handlebars are negator springs which require a force of 22 to 25 lb to slide the bars up the rod. The subject, in a crouching position, grasps the handlebars near the platform and moves them to the highest position in the plus-y direction, at which point he is in an erect position with the handlebars slightly above his head. The subject then returns to the crouching position with the handlebars.

The disturbances produced from the full-length body exercise for Subjects A and B are shown in figs. 92 and 93. In both figures, the initial negative portion of the y-axis force is produced as the subject accelerates from a crouched to an upright position. When F_y becomes positive, the subject is decelerating in a nearly upright position. The spike at approximately 1.4 sec of the F_y curve most likely is the result of the impact force of the handlebars reaching the mechanical limit on the rod. This limit is also noted in the moment plot for the z axis.

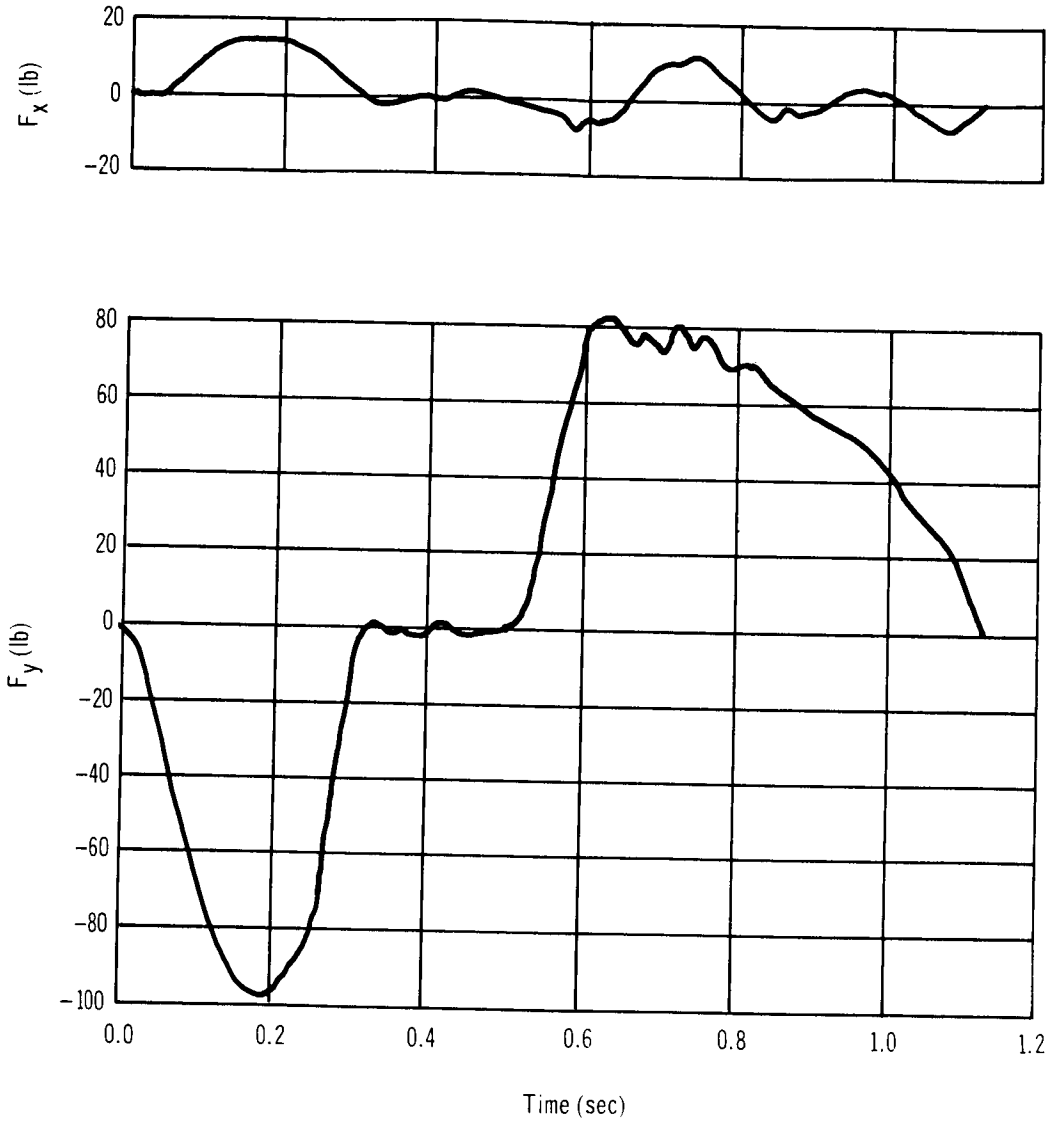

Figure 91. Oscillating Acceleration Exercise Disturbance Profile – Subject B

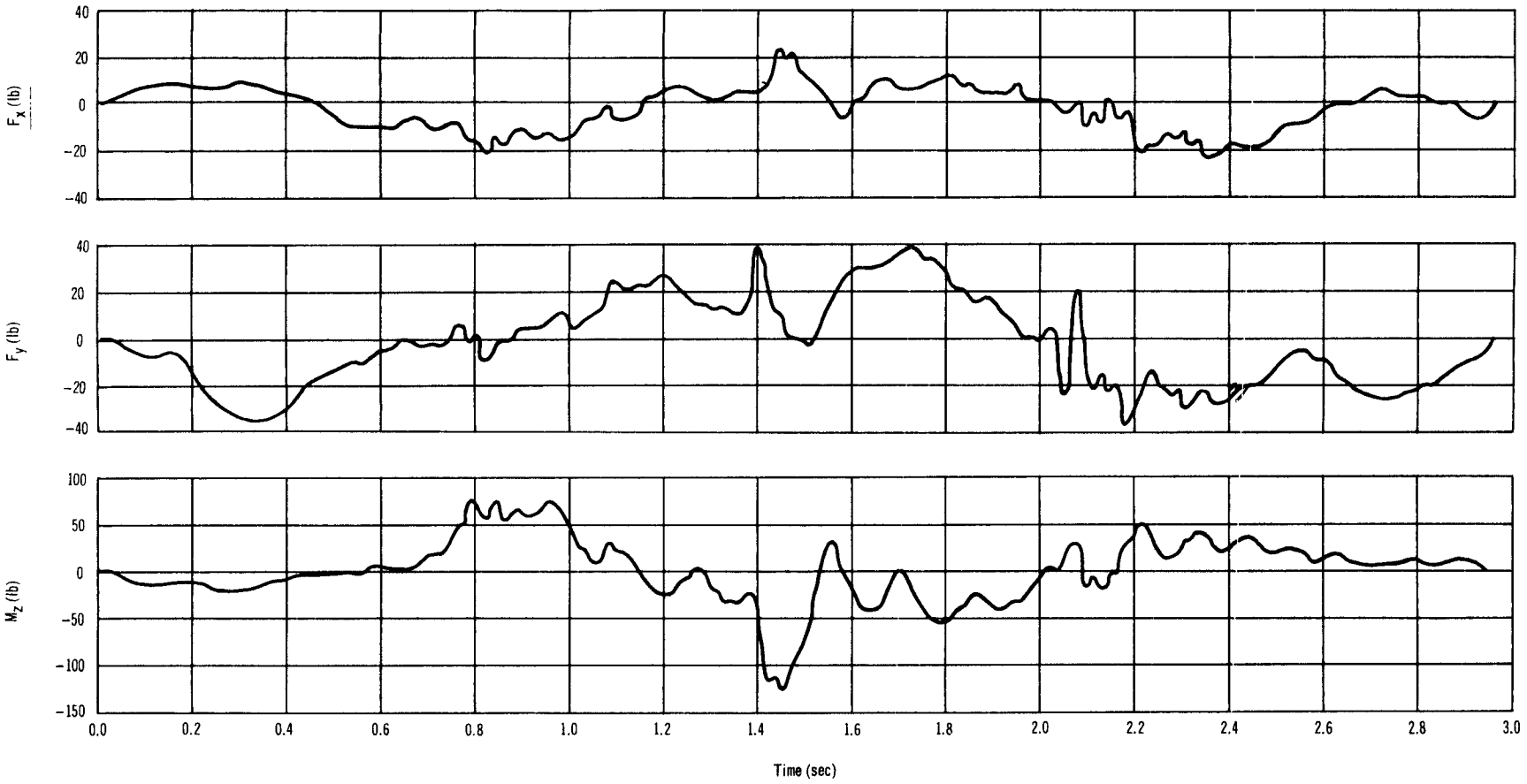

Figure 92. Full-Length Body Exercise Disturbance Profile – Subject A

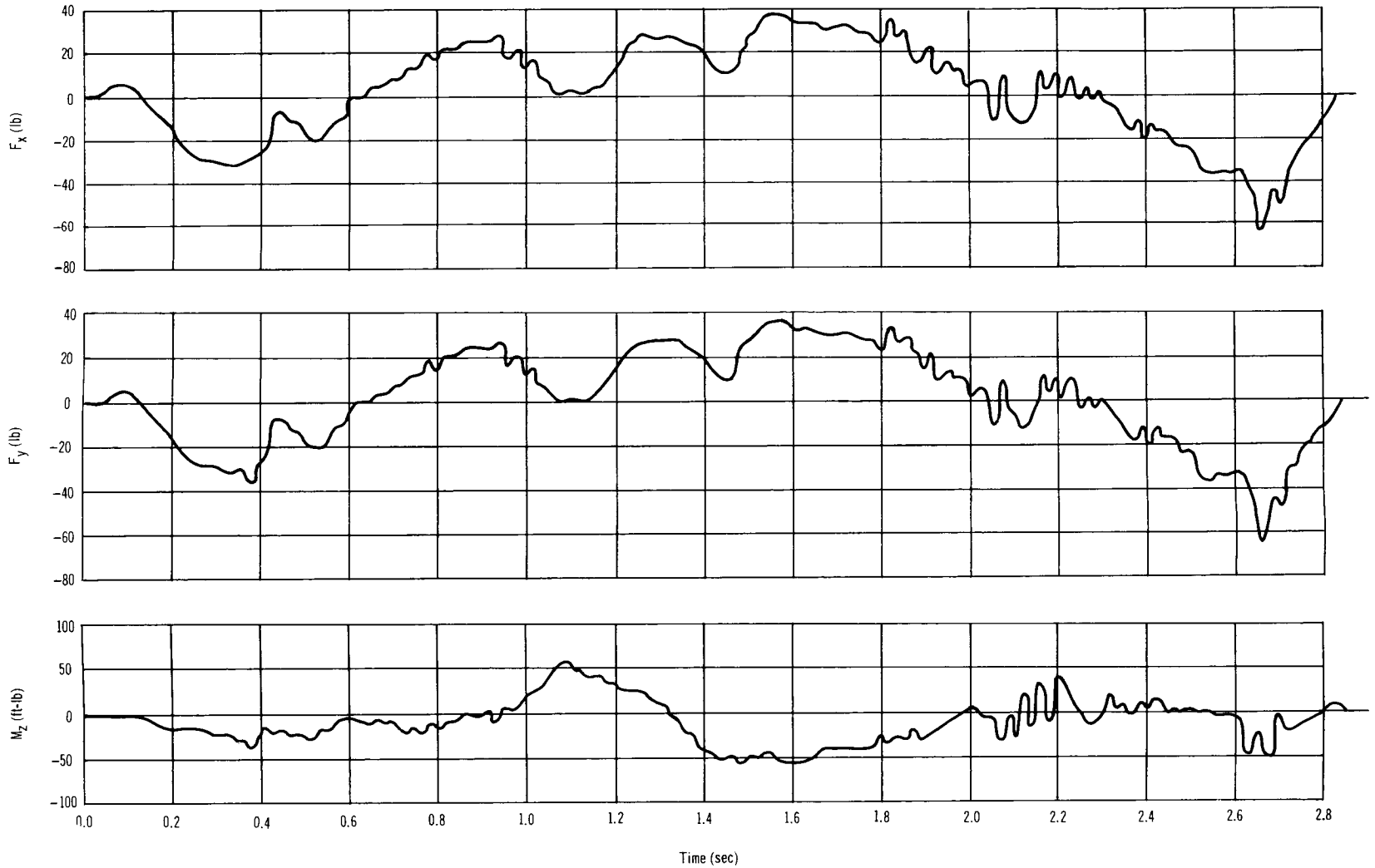

Figure 93. Full-Length Body Exercise Disturbance Profile – Subject B

The subject then accelerates from the standing position to a crouched position. The least negative portion of the curve indicates his deceleration in the crouching position. Total time required to perform this exercise is approximately 2.8 sec for both subjects. The moments about the x and y axis were small compared to the moments about the z axis; hence, they were omitted. This type of exercise can produce disturbing forces of 50 to 60 lb and moments of 100 lb-ft.

The equations for these disturbances are given in Appendix C.

Trunk Rotation Exercise

To perform this exercise, the subject places both feet in the foot restraint and grasps a longitudinal supporting bar from behind with both hands. The upper torso is then rotated in the x-z plane, first to the left, then to the right, and then returns to the starting position.

Figs. 94 and 95 show the disturbance for Subject A. This exercise is best depicted by the moment component, M_y. This component is fairly sinusoidal with nearly equal amplitudes. The initial negative value indicates a clockwise twisting of the torso. When the torso is completely turned to the left, the moment M_y is near its extreme negative peak, -52 lb-ft. This moment is primarily dependent upon the constraints of the arms behind the back grasping the bar and not the angular acceleration of the torso. As the torso twists to the right, the moment decreases. The moment goes to zero when the torso returns to the initial position. The positive portion of the moment is analogous to the negative side, only the torso is twisted to the right and then back. Forces noted for this subject's performance are complicated by the restraining geometry of the subject. Any type of twisting motion about the y axis contains the larger error source of the suspension system.

The performance of Subject B for this exercise is shown in figs. 96 and 97. Here again, the moment M_y best describes the test.

The equations for these disturbances are given in Appendix C.

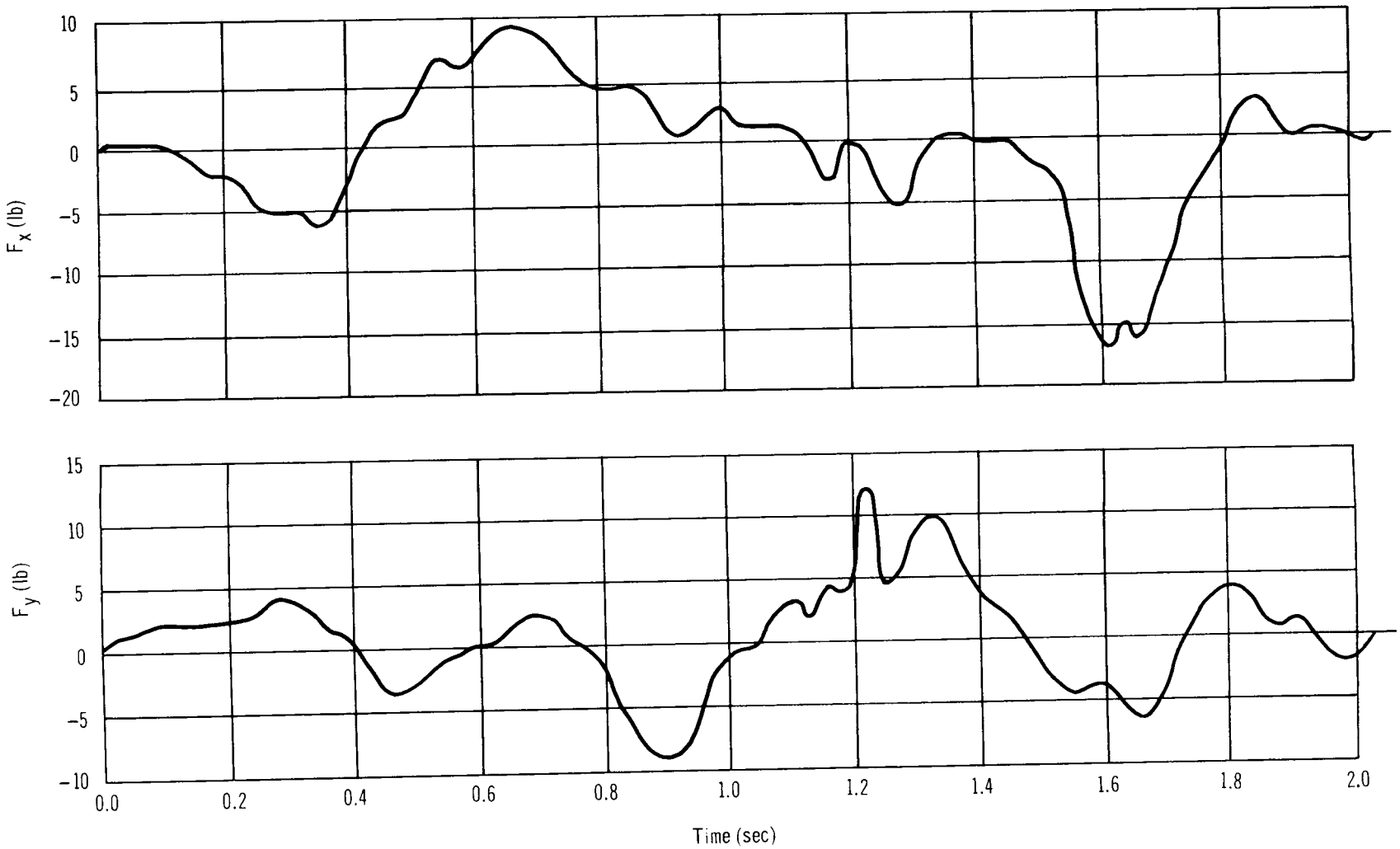

Figure 94. Trunk Rotation Exercise Disturbance Profile – Subject A

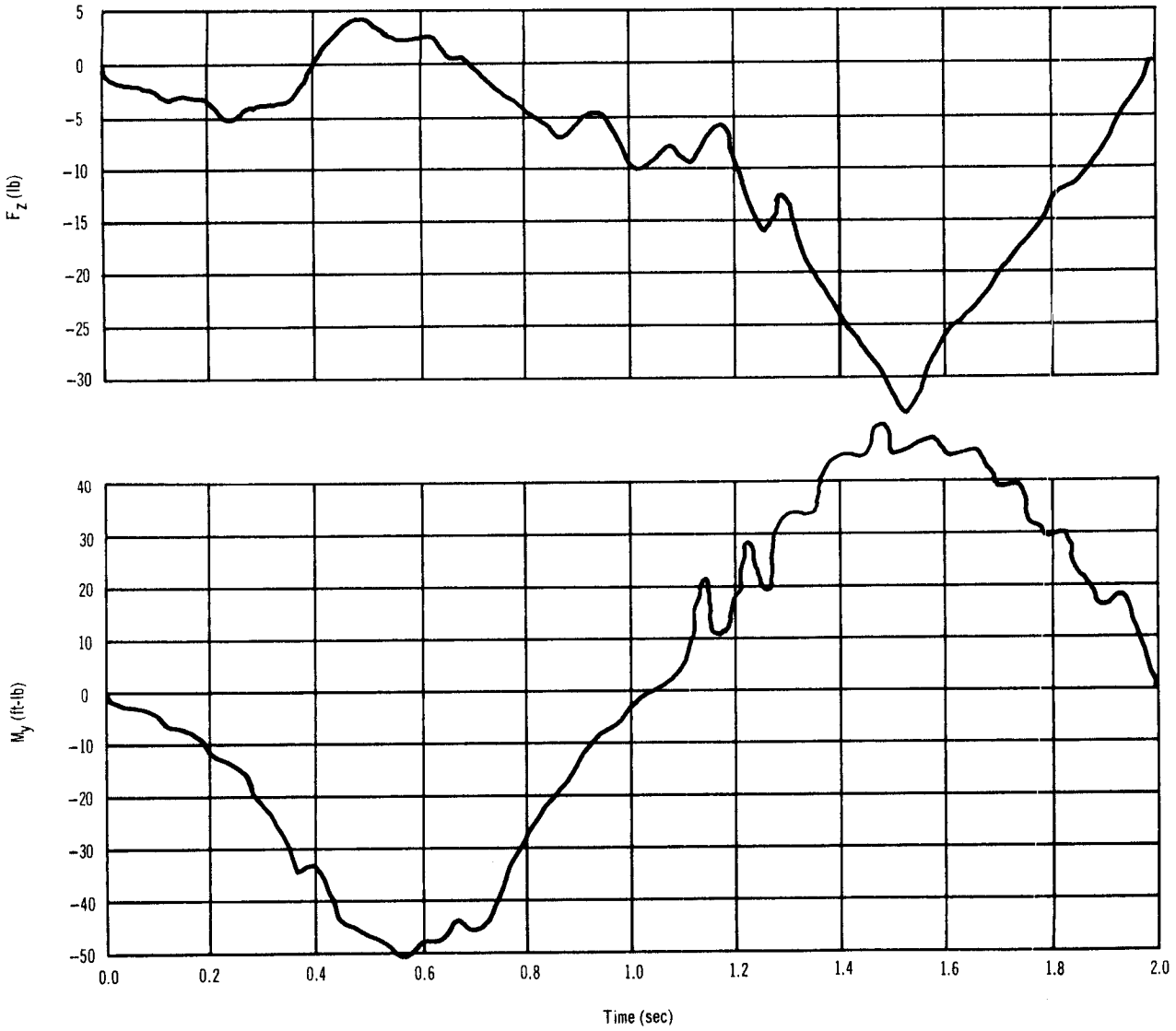

Figure 95. Trunk Rotation Exercise Disturbance Profile – Subject A

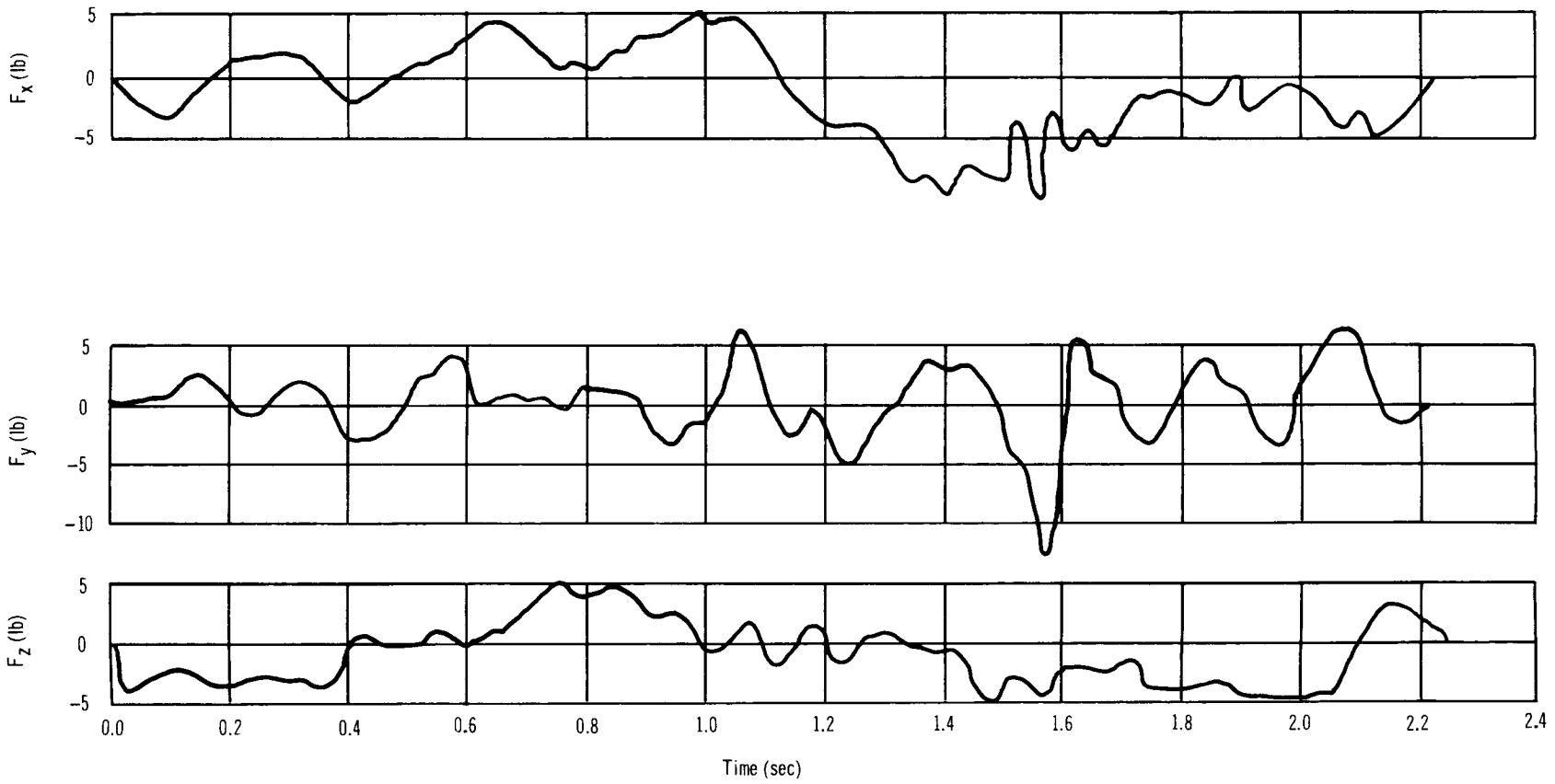

Figure 96. Trunk Rotation Exercise Disturbance Profile – Subject B

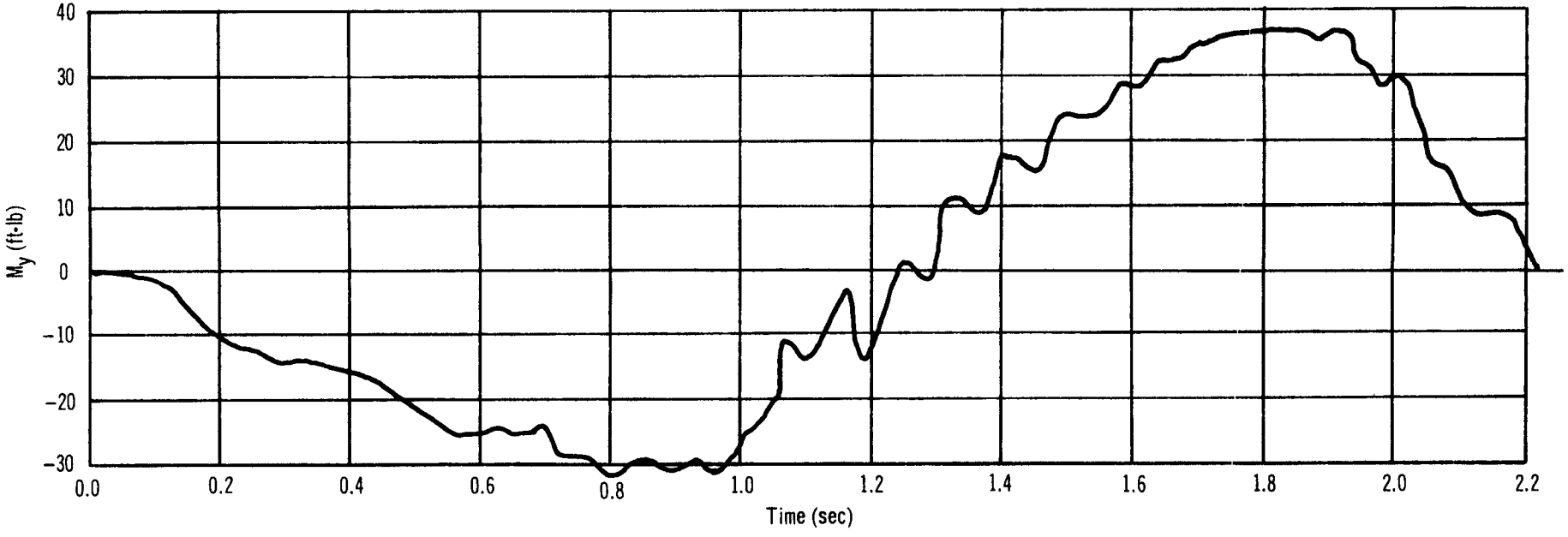

Figure 97. Trunk Rotation Exercise Disturbance Profile – Subject B

CONCLUSIONS

The disturbance profile of routine crew motions is one of the major disturbances acting on a space station. For a control system designed to evaluate the attitude hold and rate stabilization capability of the spacecraft, a complete knowledge of the disturbances must be obtained. This report provides a catalog of some of the crew motion disturbance profiles to be expected. Conclusions reached during this study are in the following general areas: (1) cyclic nature of the disturbance, (2) minimum disturbance threshold level attainable, (3) the transmissibility of certain components of force, (4) velcro walking feasibility, (5) effect on the MORL, and (6) performance of the simulation technique.

A majority of the tests indicate that the predominate frequency of the disturbances is in the range of 1 to 2 cps. To reduce the effect of these disturbances on a spacecraft to 10% of the original value, the response requirement of the control system would require a response capability of 20 cps. This is not practical with present momentum-storage concepts for large space stations, such as that for the MORL. However, it should be noted that this control capability only will be required during periods of ultrafine pointing requirements.

The minimum level of console operation for the three tasks (torquing, sliding, and push-pull) produce disturbing forces of approximately 2 lb, with a predominate frequency of 1 cps. This 2-lb force is the threshold level at which a crew member can perform the necessary tasks at a console. It is this threshold level that provides the disturbance profile during the short periods of fine pointing requirements. By properly designing the console, these threshold levels of disturbance can be reduced. The design should (1) minimize the travel of the operator's arm to perform the necessary console operations; (2) minimize the restraining forces of movable console hardware, (3) provide cushion areas which could receive impulse-like forces from the operator, and (4) place isolators in the restraining devices which would hold the operator at the console position to reduce the forces and moments applied in performing the console operation.

Some experiments may require fine attitude hold over long periods of time, such as one orbit period. During these experiments it may not be possible for the entire crew to remain at one station. Hence, the minimum level of locomotion will determine the magnitude of the disturbances during these experiments. The minimum force levels of locomotion noted from these tests are 9 lb for the velcro walk and 12 lb for the guided locomotion, with a predominate frequency of approximately 1 cps.

From several of the tests performed, it was noted that a particular force component was much less than predicted as compared to the other

force component. These are the tests during which the subject is standing with his feet restrained. When performing a body segment motion in this position, the other body segments tend to compensate for this motion, thereby reducing any change of angular momentum about the vertical (axis of suspension) direction. This results in transmission of smaller forces in a parallel direction to the standing surface than predicted. The mathematical model does not include this compensating characteristic of man.

Such compensating body segment motion has an adverse effect on the subject when he is velcro walking without hand holds. As the subject moves his foot forward, his torso moves in the opposite direction. To compensate for this effect, a moment must be produced by the flexure of the ankle so that the body is rotated in the walking direction. This induced moment appears to be so small that velcro walking without the use of a hand hold will be laborious if not impossible.

Table II shows the effect of a few of the basic crew motions on the attitude hold and rate stabilization errors of a MORL spacecraft. It is assumed that the MORL is uncontrolled because these disturbances, sinusoidal in nature, exhibit a much higher frequency than the present MORL control system can respond to. The present MORL control system (control moment gyros) response is 0.03 cps for the roll channel and 0.0067 cps for the pitch and yaw channel. The necessary parameters for the spacecraft are given in the table II. The equations of the disturbances for the first three motions are based on the fundamental term of the Fouries series derived for the motions in Appendix C. (The fundamental term for these motions performed by Subject A is large compared to the harmonics.) It is pointed out that the MORL attitude error resulting from the astronaut free soaring a distance of 20 ft with either a nominal or maximum effort is twice as large as the 0.13° assumed in the MORL Stabilization and Control System study. This maximum effort of free soaring, in which a soaring velocity of 7.7 ft/sec was attained, could be injurious to the crew member when terminating his motion.

The primary source of attitude error produced by crew locomotion is the astronaut's displacement. This displacement produces a rotation of the spacecraft body-axis inertia relative to the principle axis of inertia. It is because of this that the attitude errors for the nominal and maximum cases of free soaring are nearly the same. The small difference in the attitude errors is the result of the accumulation of attitude error during the push-off and impact-force profiles. Hence, the locomotion velocity or the particular means of locomotion, whether walking, soaring, or guided soaring, are practically independent of the attitude error accumulated for the total astronaut's moment. Different types of locomotion may produce higher transient attitude errors during the movement, but the total accumulated attitude errors will be nearly the same for a given astronaut displacement.

It should also be noted that the minor type of crew motion, such as the single pendulum arm motion, produces an attitude error of approximately 3 arc sec, with the assumed MORL parameters. For an attitude-hold

TABLE II

MORL RATE AND ATTITUDE ERRORS RESULTING FROM CREW MOTION DISTURBANCES

Motion	Max. force (lb)	Max. rate error (deg/sec)	Max. attitude error (deg)	Comments
Single pendulum arm motion	3.2	1.7×10^{-3}	0.9×10^{-3}	
Leg motion	7.6	4.7×10^{-3}	2.7×10^{-3}	
Bending at waist	9.0	9.0×10^{-3}	8.5×10^{-3}	
Free soaring				
nominal	92	36×10^{-3}	0.26	Distance traveled is 20 ft
maximum	350	96×10^{-3}	0.28	

Constants:

Subject A.
Motion 20 ft from spacecraft center of mass.
Spacecraft moment of inertia of 500 000 slug-ft^2 (MORL).

capability of meeting astronomical experiment requirements, for instance 0.1 arc sec, the MORL crew members must be isolated from the experiment platform, or a means of combating the high-frequency disturbances produced by crew motion will be required.

The primary disturbing moments induced on the spacecraft are a function of the crew motion disturbing forces acting at a nominal distance (6 to 8 ft) from the space station center of mass. The moments generated by the angular acceleration of the body segments are insignificant and can be neglected.

The counterbalanced pendulous simulation technique provides a method of recording the disturbance forces produced in the local horizontal plane with an accuracy of 6%, at reasonable expense. This simulation scheme also is readily adjustable to different subjects at a minimum of downtime. The subject assumes a normal position with the body segments because the counterbalanced segments can move easily in the vertical plane. However, this simulation technique is not recommended whenever large translations by the subjects are required. The counterbalance weights introduce an error into the simulation by moving vertically whenever the subjects translate in the horizontal plane.

RECOMMENDATIONS

Two areas of activity are recommended for additional study: (1) crew motion disturbances during extravehicular activity (EVA) and (2) design of isolators to minimize transmission of disturbances to the spacecraft.

The extravehicular crew motion study would be performed with the same simulation scheme used for this study with the subjects' wearing space suits. The space suit probably will restrict the deflections and rates of the subjects' body segments. Also, a new catalog of the subjects' motions would be required for a good representation of EVA. These data would be especially valuable for use in such programs as the orbital astronomy support facility.

The optimum location of compensators installed to eliminate unwanted disturbances is at the source of the disturbance. Accordingly, isolators placed between the astronaut and the spacecraft would reduce the amplitude of the crew motion disturbances to a level at which control systems might not be required to compensate for the crew motion. These isolators would not require any external power source and would be designed as an integral part of the shoes and restraint system.

The crew motion isolator study should include an investigation to identify various materials and mechanical devices suitable for use as isolators. It should include analytical analysis to specify and evaluate the characteristics of the isolators, design and fabrication of the best designs, and a test series to evaluate design characteristics.

APPENDIX A

Error Analysis

The primary errors associated with this zero-g simulation are of two basic types. The first consists of errors in the forces and torques induced on the platform because of differences in crew motion in a 1-g environment, compared with that of space. The second consists of errors in the measurement of the induced disturbances.

The errors in induced disturbance are caused by the following:

(1) Deviations of the supporting force point of application from the desired center of mass of the quasi-rigid body segment.

(2) Forces necessary to overcome the friction of the pulleys.

(3) Deviations in the alignment of supporting forces from the local vertical.

The errors in measurement of induced disturbances caused by the following:

(1) Platform accelerations.

(2) Imperfections in force balance and transformation matrix used in data reduction.

To determine the errors in induced disturbances, a previous example of crew motion will be illustrated. For this example, the man is comprised of two quasi-rigid parts with straight arm or leg motion.

The following figure represents the simplified crew motion used in determining the errors in induced disturbances.

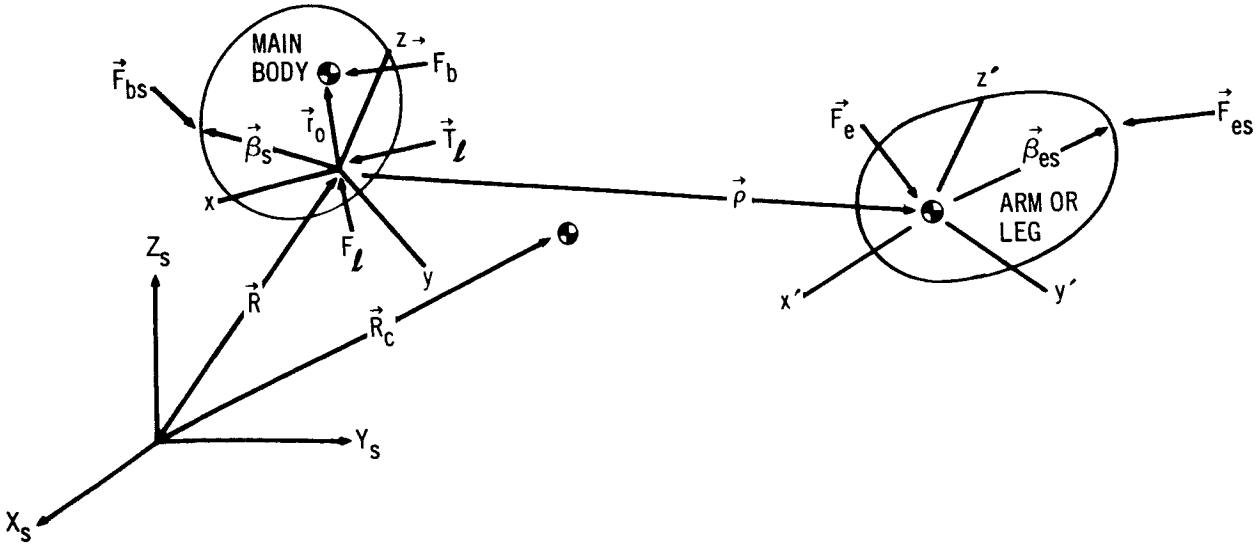

where

X_s, Y_s, Z_s	inertial axes
x, y, z	main body axes
x', y', z'	leg or arm axes
$\vec{R}$	radius vector from origin of inertial axes to main body axes
$\vec{R}_c$	radius vector from origin of inertial axes to instantaneous center of mass of men
$\vec{r}_o$	radius vector from origin of main body axes to main body center of mass
$\vec{\beta}_s$	radius vector from origin of main body axes to application point of support force
$\vec{\beta}_{es}$	radius vector from origin of arm or leg axes to application of support force
$\vec{\rho}$	radius vector from origin of main body axes to origin of arm or leg reference axes
$\vec{F}_{bs}$	support force of main body
$\vec{F}_{es}$	support force of arm or leg
$\vec{F}_b$	gravitational force on main body
$\vec{F}_e$	gravitational force on arm or leg
$\vec{F}_{\ell}$	force vector of platform on main body
$\vec{T}_{\ell}$	torque vector of platform on main body
M	mass of main body
m	mass of arm or leg

For the case of the zero-g simulation, the translational equation of motion of the center of mass of the man is given in vector form as follows:

$$\vec{F}_{\ell} + \vec{F}_b + \vec{F}_{bs} + \vec{F}_e + \vec{F}_{es} = (M + m)\frac{d^2 \vec{R}_c}{dt^2} \qquad \text{(A1)}$$

The acceleration is derived from the general equation defining the radius vector, which is as follows:

$$\vec{R}_c = \frac{1}{(M + m)} \left[M (\vec{R} + \vec{r}_o) + m (\vec{R} + \vec{\rho}) \right] \tag{A2}$$

For the zero-g simulation, the only variable on the right side of eq. (A2) is $\vec{\rho}$. This assumes the platform (laboratory) is not accelerated by crew motion. Hence, the acceleration term for eq. (A1) is given by

$$\frac{d^2 \vec{R}_c}{dt^2} = \left(\frac{m}{M + m} \right) \frac{d^2 \vec{\rho}}{dt^2} \tag{A3}$$

In the true zero-g environment, the translational equation of motion is given as

$$\vec{F}'_{\ell} + \vec{F}_b + \vec{F}_e = (M + m) \frac{d^2 R'_c}{dt^2} \tag{A4}$$

(The primes denote the difference between the true and simulated zero-g parameters.)

For the true zero-g environment, the vector $\vec{R}$ is no longer a constant, and the acceleration is given as the following equation:

$$\frac{d^2 \vec{R}'_c}{dt^2} = \left(\frac{1}{M + m} \right) \left[M \frac{d^2 \vec{R}}{dt^2} + m \left(\frac{d^2 \vec{R}}{dt^2} + \frac{d^2 \vec{\rho}}{dt^2} \right) \right] \tag{A5}$$

Ideally, the force measured in the simulation must be equal to the force imposed in the true zero-g environment, as

$$\vec{F}_{\ell} = \vec{F}'_{\ell} \tag{A6}$$

Substituting eq. (A3) into (A1) and eq. (A5) into (A4), the required constraint equation is obtained from eq. (A6), as follows:

$$\vec{F}_{bs} + \vec{F}_{es} + M\frac{d^2\vec{R}}{dt^2} + m\frac{d^2\vec{R}}{dt^2} = 0 \qquad \text{(A7)}$$

Because $d^2\vec{R}/dt^2 = \vec{g}$, the required magnitude and directions of the supporting forces are obtained as follows:

$$\vec{F}_{bs} = -M\vec{g} \qquad \text{(A8)}$$

$$\vec{F}_{es} = -m\vec{g} \qquad \text{(A9)}$$

For the counterbalanced zero-g simulation, eqs. (A8) and (A9) will also contain a small friction-force component. This friction force caused by the pulleys is approximately 5% of the bearing loading of the pulley. Because the loading of the pulleys is twice the segment mass, an error of 10% of the suspension forces is produced by them. The error resulting from pulley friction will result in a crew motion force error of approximately 0.5 lb in the x and y planes.

The required points of application of the supporting forces, $\vec{F}_{bs}$ and $\vec{F}_{es}$, are determined by applying Newton's second law of rotational motion. Again, for the zero-g simulation, $\vec{R}$ is constant and the following vector equation* is obtained.

$$\frac{d}{dt}(\vec{H}_T) = \vec{T}_{\ell} + \vec{r}_o \times \vec{F}_b + \vec{\beta}_s \times \vec{F}_{bs} + (\vec{\rho} + \vec{\beta}_{es}) \times \vec{F}_{es}$$

$$+ \vec{\rho} \times \vec{F}_e - m\vec{\rho} \times \frac{d^2\vec{\rho}}{dt^2} \qquad \text{(A10)}$$

where $\vec{H}_T$ is the total moment of momentum of the two-segment man model.

---

*Based upon derivation in "Active Satellite Attitude Control" in Guidance and Control of Aerospace Vehicles. Ed. C. T. Leondes, McGraw-Hill Book Company, Inc., New York, 1963.

In the true zero-g environment, the moment equation is obtained with $\vec{R}$ variable. The equation* is as follows:

$$\frac{d}{dt}(\vec{H}_T) = \vec{T}'_{\ell} + \vec{r}_o \times \vec{F}_b - M\,\vec{r}_o \times \frac{d^2\vec{R}}{dt^2} + \vec{\rho} \times \vec{F}_e - m\,\vec{\rho} \times \left(\frac{d^2\vec{R}}{dt^2} + \frac{d^2\vec{\rho}}{dt^2}\right) \tag{A11}$$

The torque from the simulation, $\vec{T}_{\ell}$, and the torque from the ideal case, $\vec{T}'_{\ell}$, must be equal.

$$\vec{T}_{\ell} = \vec{T}'_{\ell} \tag{A12}$$

From eqs. (A10) and (A11), the restraint is obtained as follows:

$$\vec{\beta}_s \times \vec{F}_{bs} + (\vec{\rho} + \vec{\beta}_{es}) \times \vec{F}_{es} + M\,\vec{r}_o \times \frac{d^2\vec{R}}{dt^2} + m\,\vec{\rho} \times \frac{d^2\vec{R}}{dt^2} = 0 \tag{A13}$$

With $\frac{d^2\vec{R}}{dt^2} = \vec{g}$ and eqs. (A8) and (A9), eq. (A13) is reduced to

$$(\vec{\beta}_s - \vec{r}_o) \times \vec{F}_{bs} + \vec{\beta}_{es} \times \vec{F}_{es} = 0 \tag{A14}$$

This equation is satisfied by the sufficient condition

$$\vec{\beta}_s = \vec{r}_o \text{ and } \vec{\beta}_{es} = 0$$

It has been illustrated that the ideal zero-g simulation of measuring the forces and torques produced by movements of a crew member to a space vehicle requires two conditions: (1) each quasi-rigid part of the man must be supported by a force equal in magnitude to its gravity force, and (2) each supporting force must be aligned with the -g vector through the center of mass of the part.

---

*Based upon derivation in "Active Satellite Attitude Control" in Guidance and Control of Aerospace Vehicles. Ed. C. T. Leondes, McGraw-Hill Book Company, Inc., New York, 1963.

Single Segment Leg Swing

Utilizing the notation in eq. (A14),

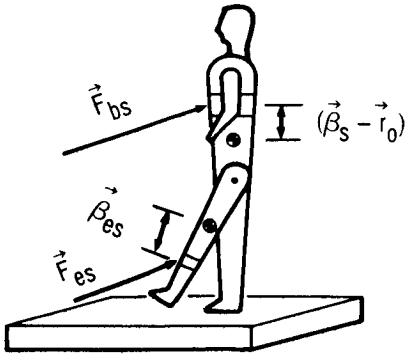

Total mass of crew member = 5.37 slugs

M (body mass) = 4.47 slugs

m (leg mass) = 0.9 slugs

$$(\vec{\beta}_s - \vec{r}_o) = 0.05 \text{ ft}$$

(This value assumes that the alignment of the body center of mass is within 0.05 ft of the support.)

$$\vec{\beta}_{es} = 0.6 \text{ ft}$$

(This value is based upon supporting the leg at the calf.)

The supporting forces are as follows:

$$F_{bs} = 4.47 \text{ g} = 145 \text{ lb}$$

$$F_{es} = 0.9 \text{ g} = 28.1 \text{ lb}$$

Substituting these values into eq. (A14), with the condition that $(\vec{\beta}_s - \vec{r}_o)$ and $\vec{\beta}_{es}$ are aligned with the local horizontal plane, the disturbance torque is obtained as:

$$\vec{T}_{erf} = 0.05 \times 145 + 0.6 \times 28.1 = 24.1 \text{ lb-ft}$$

This disturbance torque is in the local horizontal plane and is parallel to the surface of the platform. The torque will rotate the subject until his center of mass is aligned with an "equivalent single supporting cable." If the subject is attached to the platform, this initial disturbance torque will be transmitted to the force balance unit. This disturbance torque is analogous to a static error, which will be zeroed out by the force balance unit before the start of the test.

This large error torque indicates that each body segment should be supported as close to its center of mass as possible. For instance, if the leg is supported just above the knee instead of the calf, the error in the disturbance torque would be reduced to the following:

$$\vec{T}_{erf} = 0.05 \times 145 + 0.1 \times 28.1 = 10 \text{ lb-ft}$$

This error is still quite large and every measure of careful balancing should be taken to reduce it. The misalignment of the leg center of mass and supporting force alone produces a 5% error in the disturbance torques.

Single Segment Arm Swing

Parameters for the arm swing are as follows:

$$M = 5.06 \text{ slugs}$$

$$m = 0.31 \text{ slugs}$$

$$(\vec{\beta}_s - \vec{r}_o) = 0.05 \text{ ft}$$

$$\vec{\beta}_{es} = 0.3 \text{ ft}$$

The supporting forces are obtained as

$$F_{bs} = 5.06 \text{ g} = 163 \text{ lb}$$

$$F_{es} = 0.31 \text{ g} = 10 \text{ lb}$$

Again, with the aid of eq. (A14), the error in the disturbance torque is the following:

$$\vec{T}_{erf} = 0.05 \times 163 + 0.3 \times 10 = 11.2 \text{ lb-ft}$$

The misalignment of the arm center of mass and its supporting force alone produces a 10 to 12% error in the disturbance torques.

Thus, it has been illustrated that the supporting force must be aligned with the center of mass of the part to reduce errors in the torque disturbances.

The third primary source of error in induced disturbances is caused by deviations in the alignment of the supporting forces from local vertical. The counterbalance system for the zero-g simulation has a variable pendulum length as well as the usual pendulum swinging motion. A dynamic analysis of this counterbalance system for the zero-g simulation is presented in the following paragraphs to determine the errors associated with the suspension system.

From the following figure, the kinetic and potential energies are determined for motion in a single plane.

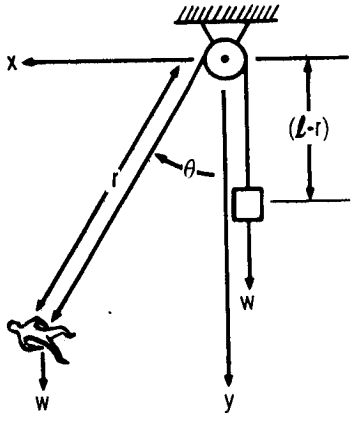

$$T = 1/2 \frac{W}{g} (\dot{r}^2 + \dot{\theta}^2 r^2) + 1/2 \frac{W}{g} \dot{r}^2$$

$$V = - W (\ell - r) - Wr \cos \theta$$

The Lagrangian is defined as

$$L = T - V = 1/2\ m (2\dot{r}^2 + \dot{\theta}^2 r^2) + mg\ell - mgr (1 - \cos \theta) \qquad (A15)$$

The equations of motion are obtained from

$$\frac{d}{dt} \left(\frac{\partial L}{\partial \dot{q}_i} \right) - \frac{\partial L}{\partial q_i} = 0 \qquad (A16)$$

and are given as follows:

$$\ddot{r} - \frac{\dot{\theta}^2}{2} r + \frac{g}{2} (1 - \cos \theta) = 0 \qquad (A17)$$

$$\ddot{\theta} + 2 \frac{\dot{r}}{r} \dot{\theta} + (g/r) \sin \theta = 0 \qquad (A18)$$

A digital computer program is utilized to solve these two nonlinear differential equations for the various initial conditions specified. However, before the results of the computer program are presented, an analytical probe will be made to determine what the characteristics of the two variables r and θ are like.

Assuming small angle approximations, eqs. (A17) and (A18) are rewritten as follows:

$$\ddot{r} - \frac{\dot{\theta}^2}{2} r + (g/4)\theta^2 = 0 \tag{A19}$$

$$\ddot{\theta} + 2\frac{\dot{r}}{r}\dot{\theta} + (g/r)\theta = 0 \tag{A20}$$

The crew motion used to study the dynamics of the suspension system is the free translation exercise. For this exercise the man pushes off the platform at some given velocity, $r\,\dot{\theta}_o$.

Making the usual substitution for removal of the first derivative term of eq. (A20), $\gamma = \theta e^{\int \dot{r}/r\, dt}$, the following is obtained:

$$\ddot{\gamma} + \frac{g - \ddot{r}}{r}\gamma = 0 \tag{A21}$$

If the free translation is to be performed at small velocities, say 1 to 4 ft/sec, then the linear acceleration, $\ddot{r}$, will be small compared to the gravitation acceleration, g. Hence, eq. (A21) can be approximated as a second-order differential equation with constant coefficients.

Solving eq. (A21) and substituting $\theta = \gamma e^{-\int \dot{r}/r\, dt}$ for the dummy variable, the following is obtained:

$$\theta = e^{-\int \dot{r}/r\, dt}(A \cos \beta t + B \sin \beta t) \tag{A22}$$

where

$$\beta = \sqrt{\frac{g - \ddot{r}}{r}} \cong \sqrt{g/r} \tag{A23}$$

Reducing eq. (A22) further and substituting the initial conditions of $\theta(0) = 0$, $r(0) = r_o$, and $\dot{\theta}(0) = \dot{\theta}_o$, the angular displacement is obtained:

$$\theta = (r_o/r)(\dot{\theta}_o/\beta) \sin \beta t \tag{A24}$$

On the assumption that $\ddot{r} \ll g$, the angular displacement is found to be a nearly sinusoidal function with a slightly decreasing amplitude.

For the second variable, eq. (A19) is multiplied by the factor $2(dr/dt) \cdot dt$ and integrated to obtain the following equation:

$$\dot{r}^2 = (dr/dt)^2 = 2\int \left[(\dot{\theta}^2/2)\, r - (g/4)\, \theta^2\right] dr + C_1 \tag{A25}$$

where C_1 is the constant of integration, performing the integration and rearranging as follows:

$$\frac{dr}{(1/2\ \dot{\theta}^2 r^2 - (g/2)\theta^2 r + C_1)^{1/2}} = dt \tag{A26}$$

With the initial condition of $r(0) = r_o$, the pendulum length, r, is obtained from eq. (A26) as follows:

$$r = r_o + R(t) \sinh(\dot{\theta}t/\sqrt{2}) \tag{A27}$$

With θ a sinusoidal function of time, t, the complexity of eq. (A27) needs no comment.

To substantiate some of the approximations made for the analysis, the results of a computer run using eqs. (A17) and (A18) are given in fig. A-1.

The parameters used in the computer run are a pendulous length of 54 ft for the man with an initial push-off velocity of 3.75 ft/sec, which corresponds to a $\dot{\theta}_o$ of 0.07 rad/sec. Only half of the period is illustrated, because the man impacts on the platform at this point. Fig. A-1 shows that the maximum angular excursion, θ, is approximately 5.5° for this relatively high translational velocity. In reducing the translational velocity by half, the angular excursion will be decreased by half. The other parameters of interest are the pendulum length and its derivatives. The plot of the pendulum length indicates that the man will drop approximately 3.5 in. during the

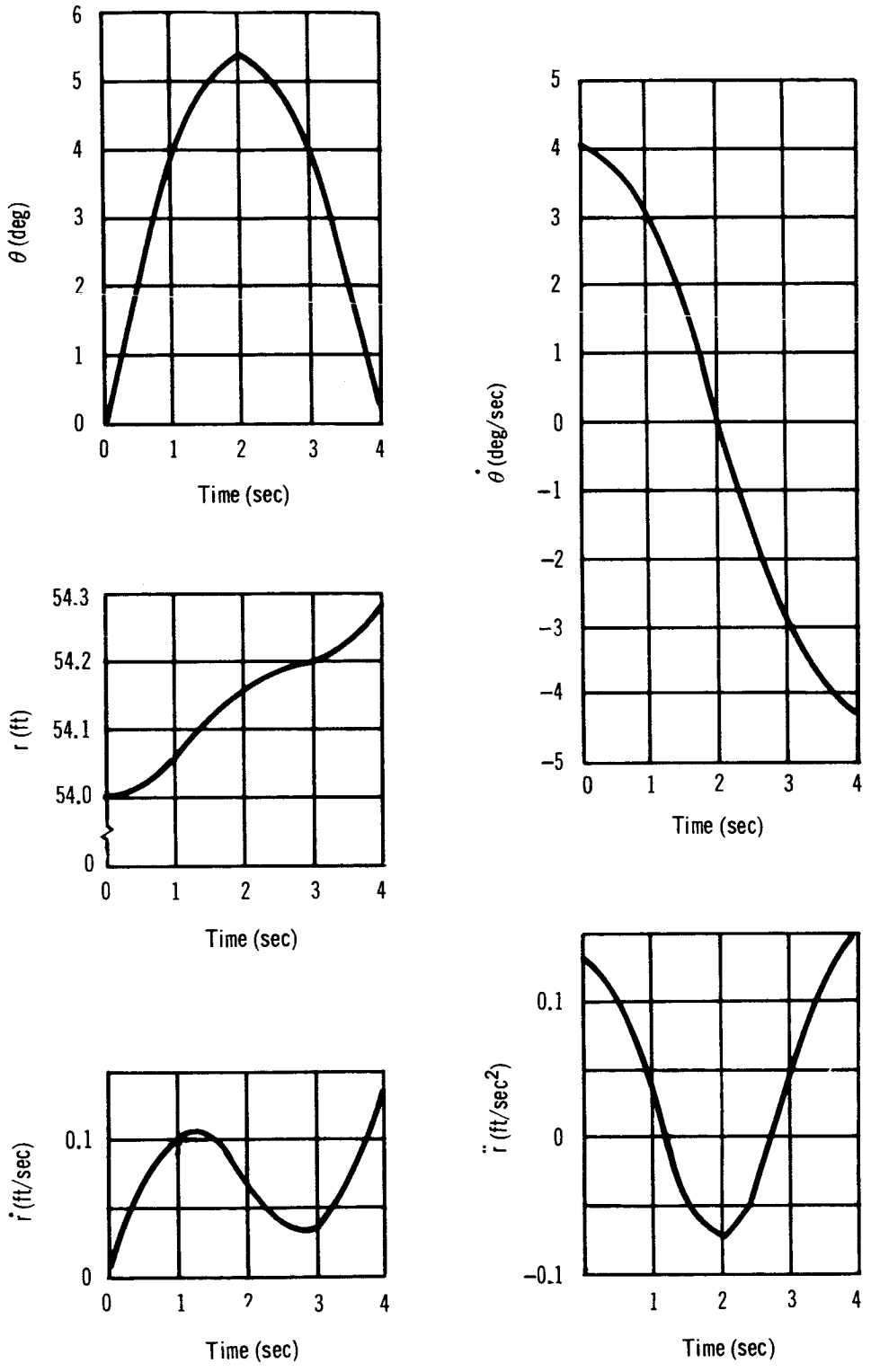

Figure A-1. Counter Balance Suspension System

swinging motion. Because the pendulum length changes very little, the assumption of $\ddot{r}$ and $\dot{r}$ being small is valid for this particular time period. Hence the counter balance suspension system is very nearly the same as a pendulum system.

The errors associated with the suspension system are directly proportional to the alignment of supporting forces from the local vertical. For the free translational motion (assuming 2 ft/sec velocity) the error in the force disturbances is approximately 5%, as obtained from ratioing the data given by the computer program.

For the leg motions with the leg support at the calf, the maximum support excursion is 2 ft, which produces an alignment error of 2/54 = 3.7%, where 54 ft is the suspension length. If the leg is supported just above the knee, the error in the disturbance force is 1.3/54 = 2.4%.

For the arm motions with the support at the biceps, the error in the disturbance force is 1.1%.

Some of the tests involve movements of several body segments. The error associated with the alignment of the supporting forces is then a combination of several cable alignments with different forces.

Platform accelerations and imperfections in the force balance are the two error sources in the measurement of induced disturbances. Analysis indicates that the platform natural frequency is high enough (150 to 300 cps) so that the platform accelerations will be negligible. On the basis of the analysis of the platform frequency, a disturbance error of less than 1% exists. The imperfections of the force balance are similar in nature to the platform accelerations. The force balance has six modes of vibration which are coupled into independently excitable groups. These modes of vibration are in the range of 34 to 850 cps. By orienting the force balance so that the lower mode is least excited, the lowest frequency associated with the force balance dynamics would be approximately 80 cps. The error associated with this dynamic mode for a 20-cps frequency is illustrated in the following paragraphs.

The dynamic equation is given as follows:

$$M\ddot{x} + Kx = F \sin \lambda t \qquad \text{(A28)}$$

where $\lambda \equiv$ frequency of input disturbance

$$\beta^2 = \frac{K}{m} \equiv \text{modal frequency of the force balance}$$

The solution to eq. (A28) is:

$$x = \frac{F}{m(\beta^2 - \lambda^2)}\left(\sin \lambda t - \frac{\lambda}{\beta} \sin \beta t\right) \qquad \text{(A29)}$$

From the ideal case of measuring the force, the error associated with the force balance can be obtained. This is found from eq. (A28) by lettering $m \rightarrow 0$. Hence, for the ideal case the following equation is given:

$$x = \frac{F}{K} \sin \lambda t \qquad \text{(A30)}$$

If the input frequency is 1/5 of the force balance-response frequency, the error in measuring the amplitude of the response frequency is 4%. [This is obtained from ratioing eqs. (A29) and (A30)]. There is also a component of the response which contains the force balance frequency. This component would be 20% of the amplitude of the input frequency. Because this component is a frequency five times higher than the input, its effect distorts the lower or input frequency of the output.

From the dynamic analysis of the crew motions presented in Appendix B, the input frequencies of the disturbances were found to be in the range of 1 to 15 cps. These, of course, were based upon assumed body segment profiles for the motion. Assuming disturbance input frequencies are in this range, an expected error of approximately 4% for a 15-cps input frequency will be associated with the lower mode of the force balance. Of course, the lower the input frequency, the smaller the error of measurement is. The instrumentation error is less than 2%.

A summary of the errors in the simulation for several crew motion exercises follows. Maximum errors are used for these conditions.

Free Translation Exercise (velocity of 2 ft/sec)

Suspension alignment	5%
Supporting force aligned with the center of mass	0
Force balance imperfections (based upon 12 cps input frequency)	2.3%
Instrumentation	2%
Platform Acceleration	1%
Total Error (RSS)	5.9%

Leg Motion Exercise
(based upon support above knee)

Suspension alignment	2.4%
Supporting force aligned with center of mass (based upon alignment of leg support to leg center of mass within 0.05 ft)	2%
Force balance imperfections	2.3%
Instrumentation	2%
Platform acceleration	1%
Total Error (RSS)	4.5%

Arm Motion Exercise
(based upon support above the elbow)

Suspension alignment	1.1%
Support force aligned with the center of mass (based upon alignment of arm support to arm center of mass within 0.1 ft)	4%
Instrumentation	2%
Force balance imperfection	2.3%
Platform acceleration	1%
Total Error (RSS)	5.3%

The crew motions which involve combination of arm and leg motion will have a total error equal to the average value of the individual errors. Thus, the simulation of crew motion activities is accurate to approximately 6% of the measured values.

APPENDIX B

Analysis of Body Segment Motions

The analysis for the specific crew motions considered are based upon the following four assumptions:

(1) Each quasi-rigid part of the man must be supported by a force equal in magnitude to its gravity force.

(2) Each such supporting force must be aligned with the -g vector through the center of mass of the part.

(3) The entire force and torque vectors resulting from the segment motion is transmitted to the platform (laboratory).

(4) There are no accelerations of the platform (laboratory) caused by body segment motions.

For the single-plane body motions considered (arm swing, leg swing, and body bending at the waist), a pendulum model is used to derive the equations for the forces and torques resulting from the segment motions. The magnitudes of these forces and torques are a function of the segment masses and inertias as well as the assumed rate profile for the various segment motions. The body segments mass and inertia are obtained from NASA's MAID Program.

To determine the resulting forces and torques on the platform (laboratory) from the crew motion, a generalized reference system is used to describe the location of the disturbing source with respect to the center of mass of the platform (laboratory).

The models, analyses, and reference systems used to describe the single-plane body motions are presented in the following paragraphs.

Double Pendulum Model

Arm, leg, and body bending motions. --The center of gravity displacements are given as follows:

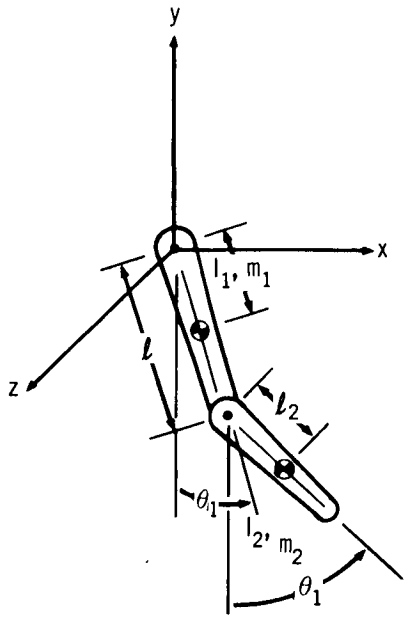

$$x_1 = \ell_1 \sin \theta_1 \tag{B1}$$

$$y_1 = -\ell_1 \cos \theta_1 \tag{B2}$$

$$x_2 = \ell \sin \theta_1 + \ell_2 \sin \theta_2 \tag{B3}$$

$$y_2 = -(\ell \cos \theta_1 + \ell_2 \cos \theta_2) \tag{B4}$$

The center of mass accelerations of the two segments are obtained from the above.

$$\ddot{x}_1 = \ell_1 (\ddot{\theta}_1 \cos \theta_1 - \dot{\theta}_1^2 \sin \theta_1) \tag{B5}$$

$$\ddot{y}_1 = \ell_1 (\ddot{\theta}_1 \sin \theta_1 + \dot{\theta}_1^2 \cos \theta_1) \tag{B6}$$

$$\ddot{x}_2 = \ell (\ddot{\theta}_1 \cos \theta_1 - \dot{\theta}_1^2 \sin \theta_1) + \ell_2 (\ddot{\theta}_2 \cos \theta_2 - \dot{\theta}_2^2 \sin \theta_2) \tag{B7}$$

$$\ddot{y}_2 = \ell (\ddot{\theta}_1 \sin \theta_1 + \dot{\theta}_1^2 \cos \theta_1) + \ell_2 (\ddot{\theta}_2 \sin \theta_2 + \dot{\theta}_2^2 \cos \theta_2) \tag{B8}$$

The forces acting through the center of mass of the second segment are as follows:

$$F_{x_2} = m_2 \ddot{x}_2 \tag{B9}$$

$$F_{y_2} = m_2 \ddot{y}_2 \tag{B10}$$

where $\ddot{x}_2$ and $\ddot{y}_2$ are given by eqs. (B7) and (B8) respectively.

The torque acting on the second segment is

$$T_{z_2} = I_2 \ddot{\theta}_2 \tag{B11}$$

Referencing the forces to the hinge point between the mass segments, the following expression for the torque is obtained:

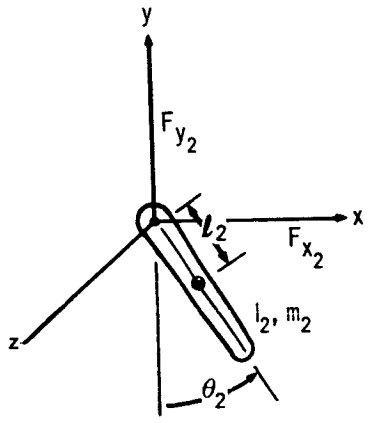

$$T_{zd_2} = T_2 + F_{x_2} \ell_2 \cos \theta_2 + F_{y_2} \ell_2 \sin \theta_2 \tag{B12}$$

The forces and torques on the first mass segment are obtained with the aid of the following diagram:

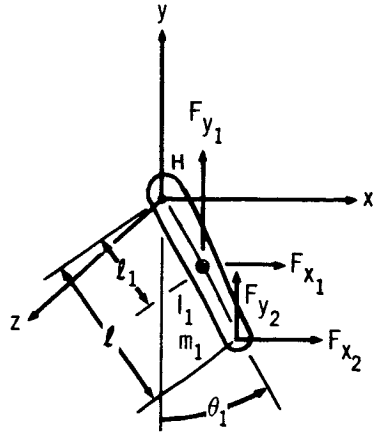

The total forces at the hinge point are as follows:

$$F_{xh} = F_{x_2} + F_{x_1} \tag{B13}$$

$$F_{yh} = F_{y_2} + F_{y_1} \tag{B14}$$

The total torque is given as follows:

$$T_{zt} = T_{z1} + T_{zd_2} + F_{x_2} \ell \cos \theta_1 + F_{y_2} \ell \sin \theta_1$$

$$+ F_{x_1} \ell_1 \cos \theta_1 + F_{y_1} \ell_1 \sin \theta_1 \tag{B15}$$

Substituting the expressions for eqs. (B13), (B14), and (B15), the total forces and torque are obtained as follows:

$$F_{x_h} = (m_1 \ell_1 + m_2 \ell)(\ddot{\theta}_1 \cos \theta_1 - \dot{\theta}_1^2 \sin \theta_1) + m_2 \ell_2 (\ddot{\theta}_2 \cos \theta_2 - \dot{\theta}_2^2 \sin \theta_2) \tag{B16}$$

$$F_{y_h} = (m_1 \ell_1 + m_2 \ell)(\ddot{\theta}_1 \sin \theta_1 + \dot{\theta}_1^2 \cos \theta_1) + m_2 \ell_2 (\ddot{\theta}_2 \sin \theta_2 + \dot{\theta}_2^2 \cos \theta_2) \tag{B17}$$

$$T_{zt} = (I_1 + m_1 \ell_1^2 + m_2 \ell^2)\ddot{\theta}_1 + (I_2 + m_2 \ell_2^2)\ddot{\theta}_2 + m_2 \ell_2 \ell (\ddot{\theta}_1 + \ddot{\theta}_2) \cos (\theta_2 - \theta_1)$$

$$- m_2 \ell_2 \ell (\ddot{\theta}_2 - \ddot{\theta}_1) \sin (\theta_2 - \theta_1) \tag{B18}$$

Eqs. (B16), (B17), and (B18) are used for the two-segment arm and leg swinging motions. The magnitudes are obtained from an assumed rate profile of the two segments.

In the case of the motion for body bending at the waist or straight arm or leg swings, eqs. (B16), (B17), and (B18) reduce to the following (this is the single-segment motion):

$$F_{x_{sh}} = m_e \ell_e (\ddot{\theta}_1 \cos \theta_1 - \dot{\theta}_1^2 \sin \theta_1) \tag{B19}$$

$$F_{y_{sh}} = m_e \ell_e (\ddot{\theta}_1 \sin \theta_1 + \dot{\theta}_1^2 \cos \theta_1) \quad \text{(B20)}$$

$$T_{zst} = (I_e + m_e \ell_e^2) \ddot{\theta}_1 \quad \text{(B21)}$$

where m_e is the mass of the single segment and ℓ_e is the length from the hinge point to the center of mass.

The coordinate system of the man referenced to the platform or floor of the laboratory is given to determine the forces and torques imparted. Because the man is fixed to the floor, his segment motions will appear as a reaction on the floor.

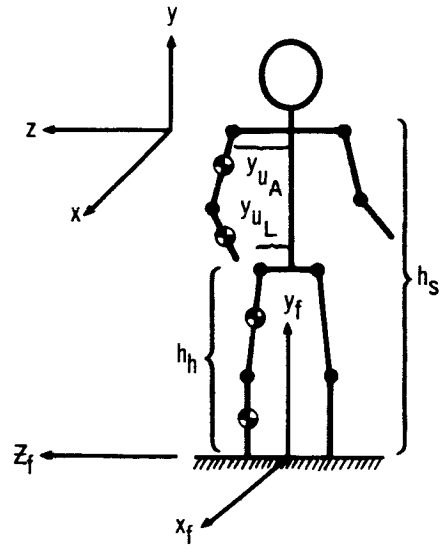

(x, y, z) = segment hinge coordinates

(x_f, y_f, z_f) = man coordinates with respect to floor or platform

h_s = shoulder height above floor

Y_{u_a} = shoulder width

y_{u_L} = hip width

h_h = height of hip joint above floor

The forces and torques imparted to the floor are given as follows:

$$F_{x_f} = - F_x \text{ [eqs. (B16) or (B19)]} \quad \text{(B22)}$$

$$F_{y_f} = - F_y \text{ [eqs (B17) or (B20)]} \quad \text{(B23)}$$

$$F_{z_f} = - F_z = 0 \quad \text{(B24)}$$

The torques for the arm segment motions are given by the following:

$$T_{x_f} = y_{u_a} F_y \text{ [eqs. (B17) or (B20)]} \quad \text{(B25)}$$

$$T_{y_f} = - y_{u_a} F_x \text{ [eqs. (B16) or (B19)]} \quad \text{(B26)}$$

$$T_{z_f} = - T_z \text{ [eqs. (B18) or (B21)]} + h_s F_x \text{ [eqs. (B16) or (B19)]} \quad \text{(B27)}$$

The torques for the leg motion or upper body bending are similarly derived.

$$T_{x_f} = y_{u_L} F_y \text{ [eqs. (B17) or (B20)]} \quad \text{(B26)}$$

$$T_{y_f} = - y_{u_L} F_x \text{ [eqs. (B16) or (B19)]} \quad \text{(B27)}$$

$$T_{z_f} = - T_z \text{ [eqs. (B18) or (B21)]} + h_h F_x \text{ [eqs. (B16) or (B19)]} \quad \text{(B28)}$$

To predict these forces and torques, it was mentioned that a segment profile is required. The total time for the motion can be assumed fairly accurate. The acceleration and rate profiles of the segments that tend to be obscure in the prediction of these forces.

An example of the single pendulum arm motion follows. A simple segment profile of constant acceleration/constant deceleration rotating through 90° will be used.

The arm parameters for the subject are given by the following:

$$m_e = 0.31 \text{ slugs (mass of arm)}$$

$$l_e = 1.01 \text{ ft}$$

$$I_e = 0.482 \text{ slug-ft}^2$$

From eqs. (B19), (B20) and (B21), the following expressions are obtained:

$$F_x = 0.315 (\ddot{\theta}_1 \cos \theta_1 - \dot{\theta}_1^2 \sin \theta_1) \quad \text{(B29)}$$

$$F_y = 0.315 (\ddot{\theta}_1 \sin \theta_1 + \dot{\theta}_1^2 \cos \theta_1) \quad \text{(B30)}$$

$$T_z = 0.482 \ddot{\theta}_1 \quad \text{(B31)}$$

The expressions for the segment profile are given by the following:

$$\ddot{\theta} = 2\pi \text{ rad/sec}^2 \text{ for } 0 \leq t \leq 0.5 \text{ sec}$$

$$\ddot{\theta} = -2\pi \text{ rad/sec}^2 \text{ for } 0.5 \text{ sec} < t \leq 1.0 \text{ sec}$$

Substituting the angular acceleration and its two derivatives into eqs. (B29) and (B30), the peak amplitudes for these two forces are approximately 2 lb in each case. The results of the simulation showed the maximum y components of force to be 3 lb and 2.6 lb for the two subjects. The maximum x components of force obtained from the simulation of the arm motion tests is approximately 1.4 lb. From the simulation data of the single pendulum arm motion, the acceleration of the arm appears variable. The slopes of the force curves at the start and end of the motion are small, indicating a small initial acceleration of the arm. The arm motion in the tests was completed in approximately 1 sec, which indicates higher accelerations later in the arm motion.

The x component of force computed is larger than that measured. This is the result of assuming a rigid model for the analytical expression. For any type of segment motion in which the crew member remains on a given point in the spacecraft, his transmission of force in a forward direction parallel to the surface will be small compared to the force he transmits normally to the standing surface. The reason for this is that the remaining body segments (other than the segment moved) tend to rotate in the opposite direction. Hence, the change in angular momentum for the total body is small, resulting in a small force transmitted parallel to the platform. From this it is noted that the model of the waist bending should be a double pendulum or two-segment model. The force derived from the single-segment model will be much higher than those of the simulation.

The basic use of the models for the segment motion is to size the force balance unit and to ensure the order of magnitude of the actual test data.

APPENDIX C

DISTURBANCE PROFILE DEFINITION

The analytical expression defining the disturbance profiles is presented in this appendix. A Fourier series is used to express the data, primarily because of the sinusoidal nature of the curves. The raw data, F(t), are used when evaluating A(N) and B(N).

$$A(N) = \frac{2}{t_f} \int_0^{t_f} F(t) \cos Nxt \, dt \text{ for } N = 0, 1, 2, \ldots i$$

and

$$B(N) = \frac{2}{t_f} \int_0^{t_f} F(t) \sin Nxt \, dt \text{ for } N = 0, 1, 2, \ldots i$$

A digital computer was used to evaluate the terms of the Fourier series. The Fourier series is of the form

$$f(t) = A_o/2 + \sum_{t=0}^{t_f} \sum_{N=1}^{7} \left[A(N) \cos (NX)\, t + B(N) \sin (NX)t \right]$$

where f(t) is the general form of the dependent variable F_x, F_y, F_z, M_x, M_y, or M_z. X is the fundamental frequency of the series, and t is the independent variable, time. N is the harmonic of the fundamental frequency, and A_o is the value of A(N) for N = 0. The series is valid for all values of time within the limits of 0 and t_f. The coefficients are to be multiplied by 10 to the power indicated by the number following the symbol E in the data columns.

SINGLE PENDULUM ARM MOTION

SUBJECT A

$X = 6.6$ $t_f = 1.05$

	FX		FY	
N	A[N]	B[N]	A[N]	B[N]
0	.5347938E 00	.0000000E 00	.3331490E 00	.0000000E 00
1	-.2097507E 00	-.7851553E 00	-.1009901E 01	-.2262812E 01
2	.2399528E-02	-.3938939E 00	.4370842E 00	.2310203E-01
3	-.1453359E-01	-.1707139E 00	-.6130150E 00	-.7869905E 00
4	.3452413E-01	.6381057E-01	.4277277E 00	-.3750472E 00
5	.3446670E-01	.8433963E-01	.2421799E 00	.2055070E-01
6	-.8575009E-01	.1314487E 00	-.5182676E-02	-.1825331E-01
7	.3666929E-01	.3741262E-01	.3997053E-02	-.6074831E-02

SUBJECT B

$X = 5.5$ $t_f = 1.2$

	FX		FY	
N	A[N]	B[N]	A[N]	B[N]
0	.6142760E 00	.0000000E 00	-.7682990E 00	.0000000E 00
1	.4361587E 00	-.2541772E 00	.1066694E 01	-.1240308E 01
2	.2104363E 00	-.1313119E 00	-.5265270E-01	-.3271884E 00
3	.1995187E-01	-.1553050E 00	-.2906438E 00	-.6161122E 00
4	-.1901245E-01	.1094145E 00	-.8282606E-01	.1814341E 00
5	.2351944E-01	-.4588781E-01	-.4776368E-01	-.1456081E 00
6	-.9507094E-02	-.1071385E 00	-.5572885E-01	-.2092909E-01
7	.3230487E-02	-.5720282E-01	-.5466113E-01	-.2745286E-01

DOUBLE PENDULUM ARM MOTION

SUBJECT A

$X = 7.62$ $t_f = .81$

	FX		FY	
N	A[N]	B[N]	A[N]	B[N]
0	.9735524E 00	.0000000E 00	.6633504E 00	.0000000E 00
1	.2253333E 00	-.6089527E 00	-.5424132E 00	-.1962490E 01
2	.2179341E 00	-.8025142E-01	.8901636E 00	-.8239609E 00
3	-.2491044E 00	.1151195E 00	.5664833E-01	-.4924668E 00
4	-.1141573E-02	-.1724538E-01	.1431812E 00	.1539153E-01
5	-.4171675E-01	-.3883245E-01	-.4049219E-01	.3620010E 00
6	.3396072E-01	-.1005272E 00	-.1176441E 00	.1005913E 00
7	.1484623E 00	-.2284355E-01	-.5242835E-01	.6298279E-01

SUBJECT B

$X = 5.57$ $t_f = 1.14$

	FX		FY	
N	A[N]	B[N]	A[N]	B[N]
0	.1270393E 01	.0000000E 00	-.1443474E 01	.0000000E 00
1	.5034773E 00	-.4894032E 00	-.9420566E 00	-.2159494E 01
2	-.2127560E 00	.8111178E-02	.1108952E 01	.1974578E 01
3	-.2120345E 00	.9447111E-01	.4229663E 00	-.1079459E 00
4	.7696829E-01	-.5173160E-01	.1870262E 00	-.1874070E 00
5	.1123761E-01	-.8065700E-01	-.4203364E-01	-.1825683E-02
6	-.6570225E-01	-.9859765E-01	-.5256250E-01	-.1074715E 00
7	-.2622251E-01	.5915477E-01	-.2765992E-01	-.1193700E 00

HEAD MOTION

SUBJECT A

$X = 6.86 \quad t_f = .93$

FX

N	A[N]	B[N]
0	-.4447346E 00	.0000000E 00
1	-.3047416E 00	.5755338E 00
2	.2843377E 00	-.3088696E 00
3	.8853082E-01	-.6708218E-01
4	.1596180E 00	.4232243E-01
5	-.2394451E-01	.3900198E-01
6	.1003005E 00	.5399260E-01
7	.8794077E-01	.6117100E-01

FZ

A[N]	B[N]
.2011759E 01	.0000000E 00
-.3993982E 00	-.4234483E 00
.1490741E 00	-.2211889E 00
.1727750E 00	.2495565E 00
.1726819E-01	.6882351E-01
.7351785E-01	-.5365642E-02
.3101464E-03	.9813739E-01
.4166010E-03	.1043563E 00

MY

N	A[N]	B[N]
0	-.2291528E 01	.0000000E 00
1	.3852250E 00	-.2163551E 00
2	-.5620783E-01	.1015998E 00
3	.7662382E-01	.7687129E-01
4	.1197401E-02	.6472280E-01
5	-.7628045E-02	-.3152970E-01
6	.1331861E-01	.1868627E-01
7	.2941550E-01	.4439292E-01

BENDING AT WAIST

SUBJECT A

$X = 3.34 \quad t_f = 1.88$

FX

N	A[N]	B[N]
0	-.3970205E 00	.0000000E 00
1	.1756022E 01	.3985060E 00
2	.5394433E-01	.5622934E 00
3	-.2610847E 00	-.3800677E 00
4	-.6770240E 00	-.2233066E 00
5	-.1051685E 00	.3330746E-01
6	.4513540E 00	-.9518288E-01
7	.8170574E-01	-.1690414E 00

FY

A[N]	B[N]
.3030851E 01	.0000000E 00
.2590438E 01	.6030340E 01
.4401490E 00	-.2240487E 01
-.1103157E 00	-.1949467E 01
-.9922137E 00	-.1225379E 01
-.8919521E 00	-.1461199E 00
-.4301755E 00	.2097650E 00
.1348687E 00	-.2056469E 00

SUBJECT B

$X = 3.5 \quad t_f = 1.8$

FX

N	A[N]	B[N]
0	-.1134649E 01	.0000000E 00
1	.9243648E 00	.1117271E 01
2	-.4483917E 00	.8707650E 00
3	-.1611000E 00	.1087109E 00
4	.7622484E-01	-.4068634E 00
5	-.2774272E 00	-.3036805E 00
6	-.1609994E 00	.2672575E 00
7	.2290771E 00	-.2526939E 00

FY

A[N]	B[N]
.8223613E 00	.0000000E 00
-.2237579E 01	.6678796E 01
.4308919E 00	.5942181E 00
-.2935701E 00	-.9002416E 00
.5253965E 00	.1424739E 01
.7674562E 00	-.4677687E 00
-.2188730E 00	.4543321E-01
-.3323107E-02	.5506130E 00

LEG MOTION

SUBJECT A

$X = 5.58 \quad t_f = 1.14$

	FX		FY	
N	A[N]	B[N]	A[N]	B[N]
0	.1260406E 01	.0000000E 00	.8793172E 00	.0000000E 00
1	-.3146733E 00	-.1875672E 00	-.1954883E 01	-.5375665E 01
2	.1750311E 00	.1028118E 00	-.1564932E 01	-.4140908E 00
3	-.1102115E 00	.2072002E-01	-.2472876E 00	-.1988911E 00
4	-.7418184E-01	.2226971E-01	.4215360E 00	.1242557E 00
5	.9125339E-01	.5793250E-01	.3678795E-02	-.8612069E-01
6	-.4990132E-01	.1534853E-01	.3517309E-01	-.1015206E 00
7	-.2818691E-01	-.1460504E 00	.1760296E 00	-.5914664E-01

SUBJECT B

$X = 5.17 \quad t_f = 1.32$

	FX		FY	
N	A[N]	B[N]	A[N]	B[N]
0	.3884201E 01	.0000000E 00	-.1283947E 01	.0000000E 00
1	-.2154848E-01	-.3010799E 00	.9389649E 00	-.1884738E 01
2	.7424384E-01	-.7962049E-01	.8721801E 00	-.1590553E 01
3	.7010458E-01	-.4540159E-01	.3069777E 00	-.4702741E-01
4	-.1899272E 00	-.2412426E 00	-.9554580E-01	-.2176563E 00
5	-.2189567E-01	-.5797547E-01	-.2353971E 00	-.1257925E 00
6	-.6036180E-01	-.7472420E-01	-.1024828E 00	-.1846410E 00
7	-.3633068E-01	-.7076696E-01	-.5481165E-01	-.1743982E 00

VELCRO WALKING (NOMINAL)

SUBJECT A

$X = 3.24 \quad t_f = 1.935$

	FX		FY	
N	A[N]	B[N]	A[N]	B[N]
0	-.2984092E 01	.0000000E 00	.2944797E 01	.0000000E 00
1	.3752976E 00	-.3556625E 01	.2206202E 01	.1766387E 01
2	.1396409E 01	.8646200E 00	-.2409724E 01	-.7397027E 01
3	-.1110557E 00	-.2412770E 01	.1917487E 01	-.3358776E 00
4	.7671601E 00	-.6065462E 00	-.6101578E-01	.6125341E 01
5	-.3578082E-01	.7347149E 00	-.9014402E 00	-.7347999E 00
6	.9421387E 00	.5630581E 00	-.1617618E 01	.3312499E 00
7	.2539841E-01	-.2344345E 00	-.3013862E 00	-.6162043E 00

SUBJECT B

$X = 4.24 \quad t_f = 1.485$

	FX		FY	
N	A[N]	B[N]	A[N]	B[N]
0	-.1485642E 01	.0000000E 00	-.1142032E 00	.0000000E 00
1	.2308258E 01	-.8047964E 01	.2252463E 01	.8143450E 00
2	.3289499E 01	-.1651677E 00	-.1836235E 01	-.6469110E 01
3	-.3320926E 00	-.1146938E 01	-.3103047E 01	.8927069E 01
4	-.1276401E 01	-.8174785E-01	-.5255217E 01	.3569779E 01
5	-.3770898E 00	.1425172E 00	-.8512428E 00	.1235059E 01
6	.2111466E 00	.2241555E 00	.4280859E 01	.1173129E 01
7	.1327652E 00	-.3319153E 00	.2150184E 01	.1566681E 01

VELCRO WALKING (MINIMUM)

SUBJECT A

$X = 2.48 \quad t_f = 2.05$

	FX		FY	
N	A[N]	B[N]	A[N]	B[N]
0	.1025494E 01	.0000000E 00	.5068502E 00	.0000000E 00
1	-.8145641E 00	-.9167104E 00	-.9664661E 00	.2583216E 00
2	-.2985942E 00	.3997574E 00	.7242835E 00	-.2364525E-01
3	.6643940E 00	.6150791E 00	.1419239E 01	.1750296E 01
4	-.7333443E-01	-.4282459E 00	-.7920840E-01	-.4225572E 00
5	.1070062E 00	.3678313E 00	-.2410167E 00	.1693612E 01
6	.5416143E 00	.8529007E-01	.1014208E 01	.3336440E 00
7	.2992456E 00	.7092971E-01	-.3154611E 00	-.2508742E-01

SUBJECT B

$X = 3.98 \quad t_f = 1.58$

	FX		FY	
N	A[N]	B[N]	A[N]	B[N]
0	-.2561985E 00	.0000000E 00	-.1571538E 01	.0000000E 00
1	-.4557920E 00	-.1085450E 01	-.9430437E 00	.1661606E 01
2	.1480369E 01	-.1070802E 01	.6005421E 00	-.1898435E 01
3	-.4535974E 00	-.4792401E 00	-.7300022E 00	.3794605E 01
4	-.3475812E 00	.2208505E 00	-.2176322E 01	.2757010E 01
5	-.4100415E-01	.1114873E 00	.1050392E 01	.5328085E 00
6	-.5181109E 00	.5569561E 00	.1855263E 00	.1046715E 01
7	.2265406E 00	.1614657E 00	.1247082E 01	.9196985E-01

VELCRO WALKING (MAXIMUM)

SUBJECT A

$X = 4.7 \quad t_f = 1.34$

	FX		FY	
N	A[N]	B[N]	A[N]	B[N]
0	-.1597732E 02	.0000000E 00	.7897145E 00	.0000000E 00
1	.7562990E 01	-.2608558E 02	.9502870E 01	.1220412E 02
2	.1005010E 02	.3462311E 01	-.1116967E 00	-.1200736E 02
3	-.1376615E 01	.1532092E 01	-.1370506E 02	-.8952207E 01
4	-.2596987E 01	-.3593374E 00	.9214915E 01	-.2148746E 01
5	-.4016032E 01	-.3587498E 00	.3737916E 01	.1423543E 01
6	.3438324E 00	-.3039994E 01	-.3444704E 00	.3336338E 01
7	-.3121967E 00	-.2049230E 01	.1877764E 01	.1756216E 01

SUBJECT B

$X = 4.31 \quad t_f = 1.17$

	FX		FY	
N	A[N]	B[N]	A[N]	B[N]
0	-.8702426E 01	.0000000E 00	-.2128674E 00	.0000000E 00
1	.4135239E 01	-.3688037E 01	.2859552E 00	-.3506012E 00
2	.8180687E 01	-.5545154E 01	-.2941876E 01	.6041139E 01
3	-.2290922E 00	-.2064008E 01	.4140738E 01	.4671296E 00
4	-.3764038E 00	.2195012E 01	.5021616E 00	.5682439E 01
5	.3418321E 01	-.4106494E 00	.3016467E 01	.1474678E 01
6	-.2977827E 00	-.2842589E 01	.1440552E 01	-.2334159E 01
7	-.9018631E 00	.4041647E 00	-.6116460E 01	.4688479E 00

FREE SOARING (NOMINAL)

SUBJECT A

$X = 3.52$ $t_f = 1.1$

FY

N	A[N]	B[N]
0	-.4368273E 01	.0000000E 00
1	-.4743719E 02	.1050248E 02
2	.1735516E 02	-.1461027E 02
3	.1144415E 02	.4126626E 01
4	.1895886E 02	-.1565734E 02
5	.9663008E 01	-.4899154E 00
6	-.3558198E 01	.5731945E 01
7	-.3381924E 01	.6520685E 01

SUBJECT B

$X = 14.45$ $t_f = .42$

FY

N	A[N]	B[N]
0	-.2671871E 02	.0000000E 00
1	.1285185E 02	.4996006E 01
2	-.6311774E 00	-.1103666E 01
3	.6110171E 00	-.3665049E-01
4	.4597444E 00	-.4482265E 00
5	-.3586187E-01	-.2117732E 00
6	-.2203613E 00	.6755207E-01
7	.1539082E 00	-.2452173E 00

FREE SOARING (MINIMUM)

SUBJECT A

$X = 11.9$ $t_f = .53$

FY

N	A[N]	B[N]
0	-.2823224E 02	.0000000E 00
1	.3259512E 01	.9704202E 01
2	.6430437E 01	.2403315E 01
3	.2129113E 01	-.1070147E 01
4	.4024284E-01	-.8364788E 00
5	-.8402458E-01	-.2355720E 00
6	.2405735E-01	.1929595E-02
7	.9198952E-01	-.6697180E-02

SUBJECT B

$X = 14.45$ $t_f = 0.43$

FY

N	A[N]	B[N]
0	-.4077669E 02	.0000000E 00
1	.1302447E 02	.1868841E 02
2	.3144408E 01	-.5089356E 01
3	.1961317E 00	.7853959E 00
4	.6647381E 00	-.1331724E 00
5	.8910207E 00	-.2735441E 00
6	.5532803E-01	.8942444E-02
7	.7004319E-01	-.1074635E 00

FREE SOARING (MAXIMUM)

SUBJECT A

$X = 24.6$ $t_f = 0.27$

FY

N	A[N]	B[N]
0	-.3115181E 03	.0000000E 00
1	.1789506E 03	-.4738038E 01
2	-.2796541E 02	-.1117432E 02
3	-.1677946E 02	-.3032743E 01
4	.5355444E 01	.6685662E 01
5	.2620034E 01	.6695000E 00
6	-.1116325E 01	-.3320149E 01
7	.4778403E 00	-.6474518E 00

SUBJECT B

$X = 27.9$ $t_f = 0.26$

FY

N	A[N]	B[N]
0	-.2035536E 03	.0000000E 00
1	.8671082E 02	.2148352E 02
2	-.1034839E 01	-.1384844E 02
3	-.5252486E 00	-.6099632E 01
4	-.5458473E 00	-.1596653E 01
5	-.2527763E 01	-.1233013E 01
6	-.1548226E 01	-.7301754E 00
7	-.1773650E 01	.4065411E-01

COMPRESSION WALKING (NOMINAL)

SUBJECT A

$X = 4.7$ $t_f = 1.3$

FX

N	A[N]	B[N]
0	-.2651304E 01	.0000000E 00
1	.3062271E 01	-.5664815E 01
2	-.1477295E 01	-.1022560E 01
3	-.1147332E 01	-.1777905E 01
4	-.8426733E 00	-.2072868E 00
5	.8988850E 00	.3207424E 00
6	-.8029875E 00	.6529028E 00
7	.5650178E 00	-.6163748E 00

FY

N	A[N]	B[N]
0	-.3383172E 01	.0000000E 00
1	.9515017E 00	-.1978340E 01
2	-.7996971E 01	-.7972940E-01
3	.4179123E 01	.1518050E 00
4	-.1659186E 01	.2001094E 01
5	.1817579E 01	.8504455E 00
6	.1641683E 01	.1591139E 01
7	.2295949E 01	-.1340044E 01

SUBJECT B

$X = 4.92$ $t_f = 1.28$

	FX		FY	
N	A[N]	B[N]	A[N]	B[N]
0	-.5761903E 00	.0000000E 00	.3282700E-01	.0000000E 00
1	.1431204E 01	-.5783451E 01	.1015831E 01	-.5047066E 00
2	.1193087E 01	-.3380235E 01	-.2618180E 01	.7673609E 01
3	-.1666497E 00	-.1127932E 01	.7952899E 01	-.1334981E 00
4	.7102268E 00	-.6743582E 00	.9085684E 00	-.4478544E 01
5	-.5904949E 00	-.9659121E 00	-.4037455E 01	-.8547818E 01
6	.4405956E 00	-.8109723E 00	-.3887557E-01	-.1143102E 01
7	-.9814637E 00	-.7013053E 00	-.3494548E 01	.3589091E 01

COMPRESSION WALKING (MINIMUM)

SUBJECT A

$X = 3.72$ $t_f = 1.7$

	FX		FY	
N	A[N]	B[N]	A[N]	B[N]
0	-.6493662E 00	.0000000E 00	.3403177E 01	.0000000E 00
1	.2185242E 00	-.2591763E 01	.3180819E 01	.8918942E 00
2	.1716506E 01	-.4626045E 00	-.1138306E 01	-.3821435E 01
3	.6639288E 00	-.4845764E 00	-.2544530E 01	-.5508096E 00
4	-.3143089E 00	-.1018633E 01	.9242956E 00	.1073218E 00
5	.8194746E 00	-.1641646E 00	-.1341561E 01	-.8715811E 00
6	.3198032E 00	-.6161295E 00	-.6052956E 00	.9951988E 00
7	.3420423E-01	.1226639E 00	.6678807E 00	-.8119346E 00

SUBJECT B

$X = 3.52$ $t_f = 1.78$

	FX		FY	
N	A[N]	B[N]	A[N]	B[N]
0	.2307836E 01	.0000000E 00	.1077108E 01	.0000000E 00
1	-.1395301E 01	-.5520921E 01	-.6641660E-01	.2139874E-01
2	.5444210E-01	-.2630544E 01	.3121466E 01	.2134642E 01
3	.9950081E 00	-.1398688E 01	-.2676151E 01	-.2703545E 01
4	.5519672E 00	-.4449504E 00	.1982867E 00	-.8547480E 00
5	.8427679E 00	-.9860238E 00	-.1787693E 01	-.3838449E 00
6	-.2377812E 00	.3296467E-01	-.8174999E-01	.5052196E-01
7	.1735168E 00	.5576596E 00	-.3164843E 00	.1915882E 00

COMPRESSION WALKING (MAXIMUM)

SUBJECT A

$X = 3.58$ $t_f = 1.13$

	FX		FY	
N	A[N]	B[N]	A[N]	B[N]
0	.2941668E 01	.0000000E 00	-.1136447E 01	.0000000E 00
1	.6395728E 01	-.1590169E 02	.1065724E 01	.1827655E 00
2	.3798976E 01	-.1566238E 01	-.6760640E 01	.1208908E 01
3	.3345731E 01	-.9342622E 00	.3543866E 01	-.5459562E 01
4	-.9351692E 00	-.2209703E 01	-.8777035E 01	.7542574E 01
5	-.2949520E 01	-.3101573E 01	-.1672106E 01	-.3642604E 01
6	-.8199343E 00	-.2922389E 01	.7186117E 01	.2610041E 01
7	.2741830E 00	-.1568599E 01	.8332809E-01	-.1162700E 01

SUBJECT B

$X = 4.82$ $t_f = 0.9$

	FX		FY	
N	A[N]	B[N]	A[N]	B[N]
0	-.5502832E 01	.0000000E 00	-.1709832E 01	.0000000E 00
1	.5420737E 01	-.5980257E 01	-.2905641E 01	.7458030E 00
2	.5630740E 00	-.3923436E 01	-.3885509E 01	-.1560409E-01
3	.3267644E 01	-.1725833E 01	-.3355633E 01	.1683548E 01
4	.1533050E 01	-.2680869E 01	.5008903E 01	.2532407E 01
5	.7633434E 00	.2371799E 01	-.1796701E 01	.5155357E 01
6	-.3283525E-01	-.7945254E 00	.7110216E 01	-.1098039E 00
7	-.1455365E 01	-.1638716E 01	-.2431972E 01	.7913927E 00

GUIDED LOCOMOTION NORMAL TO FORCE TABLE (NOMINAL)

SUBJECT A

$X = 3.24$ $t_f = 1.24$

	FX		FY	
N	A[N]	B[N]	A[N]	B[N]
0	.1154519E 01	.0000000E 00	-.6493018E 01	.0000000E 00
1	-.2258878E 01	.1026117E 01	.1566642E 01	-.6249859E 01
2	.1441323E 01	-.1309141E 01	-.1626396E 01	-.1379741E 01
3	.4538894E 00	.7108374E 00	.8364585E 00	.9945327E-01
4	.1590389E 00	.1478011E 01	.1792830E 00	-.2329063E-02
5	.1068048E 00	.1113517E 01	.1539098E 00	-.2001156E 00
6	.2041416E 00	.2110420E 00	.1727268E 00	.7439460E 00
7	-.4046899E 00	.1093760E 00	.5563018E 00	-.1641482E 00

SUBJECT B

	FX		FY	
N	A[N]	B[N]	A[N]	B[N]
0	-.2112203E 01	.0000000E 00	-.7480202E 01	.0000000E 00
1	.2113010E 01	.5764481E 01	.9714688E 00	-.6359005E 01
2	.1281966E 01	-.3343529E 01	.3187157E 01	-.1773959E 01
3	-.7796408E-01	-.3488744E 00	-.2208236E 00	-.5937741E 00
4	.1635654E-01	-.1320133E 01	-.1482055E 01	.9978831E-01
5	-.1186981E 01	-.2866194E 00	.1676125E 00	.9198791E 00
6	.4908008E-01	.2693163E 00	-.1870930E 00	-.5496896E-01
7	-.4644904E 00	-.2183502E 00	.2784258E 00	.6680117E 00

LOCOMOTION NORMAL TO FORCE TABLE (MINIMUM)

SUBJECT A

$X = 3.18$ $t_f = 2.5$

	FX		FY	
N	A[N]	B[N]	A[N]	B[N]
0	-.1812914E 01	.0000000E 00	-.6548926E 01	.0000000E 00
1	-.2243261E 01	.3284297E 01	.8857606E 00	-.3126337E 01
2	.1624093E 01	.4594444E 00	.3413766E 00	.3230416E 00
3	.4307883E-01	-.3842954E 00	.5491631E 00	-.3878394E-01
4	.1442238E 00	.8011239E 00	.2243961E 00	-.3291357E 00
5	.6645189E 00	-.5021731E-01	-.5699066E-01	-.2318179E-01
6	-.8756340E-01	.1056054E 00	.8749738E-01	-.1231415E 00
7	.1267302E 00	.3389775E 00	-.3479388E-01	-.1084412E 00

SUBJECT B

$X = 4.6 \quad t_f = 1.45$

	FX		FY	
N	A[N]	B[N]	A[N]	B[N]
0	-.1920759E 01	.0000000E 00	-.7778590E 01	.0000000E 00
1	-.1240214E 01	.4990186E 01	.2898573E 01	-.5797371E 01
2	.1843268E 01	-.2830540E 00	.3490118E 00	.1721321E 01
3	-.6341000E 00	.8460570E 00	.8570819E 00	-.9004872E 00
4	.7944557E 00	.5320297E 00	-.6561262E 00	-.8387426E 00
5	.6096210E 00	-.4321966E 00	.1296612E 00	-.1644055E 00
6	.3798334E 00	-.1724629E 00	-.7558011E-01	-.3822357E 00
7	.3971269E 00	-.2209996E 00	-.4151567E 00	.9194092E-01

GUIDED LOCOMOTION NORMAL TO FORCE TABLE (MAXIMUM)

SUBJECT A

$X = 7.45 \quad t_f = 1.13$

	FX		FY	
N	A[N]	B[N]	A[N]	B[N]
0	-.3049335E 01	.0000000E 00	-.2315705E 02	.0000000E 00
1	-.1002351E 02	.1056617E 02	.1285114E 02	-.1039566E 02
2	.4928512E 01	.3810138E 01	-.3980438E 01	-.9361406E 01
3	.7435930E 00	.6504396E 00	.2934274E 01	.2504205E 01
4	-.1593441E 01	.2327426E 01	.1223656E 01	-.2598337E 01
5	.1411773E 01	.5177279E 00	-.8926227E 00	-.8080523E 00
6	-.1331861E 01	.3709287E 00	.7270969E 00	-.7950934E 00
7	.2557952E 00	.1617266E 01	-.6562010E 00	-.8350112E 00

	MX		MZ	
N	A[N]	B[N]	A[N]	B[N]
0	-.3383323E 02	.0000000E 00	.4515687E 02	.0000000E 00
1	-.2122737E 01	.1467279E 02	.1965946E 02	-.4527214E 02
2	.9555891E 01	-.1100688E 02	-.1207921E 02	-.1244961E 02
3	-.5519992E 01	.4655364E 01	-.6065098E 00	-.2835937E 01
4	.4678769E 00	.5504453E 01	.3336315E 01	-.7309878E 01
5	.2122367E 00	.3460597E 01	-.7297088E 01	-.1309104E 01
6	.6910433E 00	.1464873E 01	.5573795E 01	-.4830017E 00
7	.1390507E 01	.2291040E 01	-.1606515E 01	-.5956065E 01

SUBJECT B

$X = 5.17 \quad t_f = 1.1$

	FX		FY	
N	A[N]	B[N]	A[N]	B[N]
0	-.5272596E 01	.0000000E 00	-.1487617E 02	.0000000E 00
1	-.2771837E 01	.9969639E 01	.9031545E 01	-.9586713E 01
2	.4884048E 01	-.3180262E 01	.2211790E 00	.3839308E 01
3	-.1936204E 01	.4766974E 00	-.3019861E 00	-.9499308E 00
4	.9738810E 00	-.9734548E 00	-.5288793E 00	.1132151E 01
5	-.1723362E 01	-.3469242E 00	.1222336E 01	-.6760228E 00
6	-.7248738E 00	.2174594E 01	-.2225538E 00	-.1799399E 01
7	.1324485E 01	.2560665E 00	-.5930427E 00	-.2502226E 00

	MX		MZ	
N	A[N]	B[N]	A[N]	B[N]
0	-.3633709E 01	.0000000E 00	.3047377E 02	.0000000E 00
1	.7780593E 00	.9083258E 01	.1135518E 02	-.4242104E 02
2	.5320083E 01	-.8224839E 00	-.1730846E 02	.8481395E 01
3	-.2588856E 01	-.1120508E 01	.4686021E 01	-.1319137E 01
4	.1259596E 01	-.6971446E 00	-.1562362E 01	.1638113E 01
5	-.1218999E 01	-.9048749E 00	.6934650E 01	.4463767E-01
6	-.1304375E 01	.2953992E 01	.5849269E 00	-.1032530E 02
7	.1924145E 01	.6813763E 00	-.5221751E 01	-.8194208E 00

GUIDED LOCOMOTION PARALLEL TO FORCE TABLE (NOMINAL)

SUBJECT A

$X = 3.46$ $t_f = 1.8$

	FX		FY	
N	A[N]	B[N]	A[N]	B[N]
0	-.2055685E 02	.0000000E 00	-.5379221E 01	.0000000E 00
1	.2038862E 01	-.5239771E 01	.9014704E 00	.5833899E 00
2	.3029337E 01	-.1372162E 01	.4913422E 00	-.4084594E 00
3	.1357756E 01	.1936747E 01	-.9671664E 00	-.5123311E 00
4	-.5635654E 00	.2297363E 01	.9469892E 00	-.6268588E 00
5	.3286967E 00	-.3594240E-01	-.5080005E 00	.5333002E 00
6	.4562611E 00	.2233418E 00	.7144379E-01	.5945033E 00
7	.1332937E 00	.1648562E 00	-.3337015E 00	.3186472E 00

SUBJECT B

$X = 4.92$ $t_f = 1.67$

	FX		FY	
N	A[N]	B[N]	A[N]	B[N]
0	.2326766E 01	.0000000E 00	.1977435E 00	.0000000E 00
1	.4729704E 01	-.6422900E 01	-.4602189E 01	.7852754E 01
2	.2473479E 01	.4903661E 00	-.6060071E 00	-.2236242E 01
3	-.9314035E-02	.1571416E 01	.7542299E 00	-.7684845E 00
4	.8056610E-01	-.1863652E 00	.1117647E 01	.4673610E 00
5	.2983579E 00	.1343420E 00	.2225856E 00	.9768291E 00
6	.9768651E-01	-.2102294E 00	.5359276E-01	.7460599E 00
7	.4286496E 00	.1521308E 00	-.3648238E 00	.1771758E 00

GUIDED LOCOMOTION PARALLEL TO FORCE TABLE (MINIMUM)

SUBJECT A

$X = 2.365$ $t_f = 2.24$

	FX		FY	
N	A[N]	B[N]	A[N]	B[N]
0	-.2080873E 02	.0000000E 00	-.4460965E 01	.0000000E 00
1	-.1324996E 00	.1330094E 01	.4435663E 00	-.3633992E 01
2	.1834322E 01	-.1775204E 01	-.2767587E 01	-.2905561E-01
3	.3939304E 00	.1978434E-01	-.1440252E 00	.3363884E 01
4	.1624201E 01	.1050530E 01	.1303608E 01	.1005585E 01
5	-.3092344E-01	.7680746E 00	.1274218E 01	-.2545558E 00
6	.2041851E 00	.1156105E 01	-.4268027E-01	-.8976498E 00
7	.6677179E-01	.4132654E 00	-.2434127E 00	-.2502869E 00

SUBJECT B

$X = 3.58$ $t_f = 1.78$

	FX		FY	
N	A[N]	B[N]	A[N]	B[N]
0	.4331689E 01	.0000000E 00	-.1595351E 01	.0000000E 00
1	.2049917E 01	-.4608225E 01	-.1725715E 01	.3147596E 01
2	.8494559E 00	-.2143765E 01	-.9439765E 00	.1579907E 01
3	.1073718E 01	-.1217841E 01	.4002767E 00	-.3594153E 00
4	.4676303E 00	-.2545418E 00	.6818175E 00	-.7365344E 00
5	.4015230E 00	-.3141885E 00	-.3109640E 00	-.2821619E 00
6	.2348753E 00	-.5230038E-02	.2298093E 00	-.3949293E 00
7	.1659994E 00	-.3280497E 00	.1169427E 00	.1474355E 00

GUIDED LOCOMOTION PARALLEL TO FORCE TABLE (MAXIMUM)

SUBJECT A

$X = 5.03$ $t_f = 1.28$

	FX		FY	
N	A[N]	B[N]	A[N]	B[N]
0	-.3835407E 02	.0000000E 00	-.4464001E 01	.0000000E 00
1	.1910968E 02	-.3802839E 02	-.2882392E 01	.1657685E 02
2	.4802261E 01	-.1802973E 02	.6138678E 00	.1546255E 02
3	.1509721E 01	.1312505E 01	-.8342885E 00	.7887003E 00
4	-.2928430E 01	.5053823E 01	.2441564E 01	-.4562110E 01
5	.6760193E 01	.2886588E 01	-.3376858E 01	.1228058E 00
6	-.4061611E 00	.5604239E 00	.2621464E 00	-.1092457E 01
7	-.8450725E 00	-.1524376E 01	.1234750E 00	-.1821351E 00

	MY		MZ	
N	A[N]	B[N]	A[N]	B[N]
0	-.5360984E 01	.0000000E 00	.5615919E 02	.0000000E 00
1	.1443373E 01	-.8613154E 01	-.2716552E 02	.1757790E 02
2	-.1907350E 01	.2756855E 01	-.1090915E 02	.1797547E 02
3	.7118297E 00	.2761771E 01	.3996375E 01	.8746623E 01
4	.3281039E 01	-.7014497E 00	.1186933E 02	-.7271857E 01
5	.1366626E 01	.4259190E 01	-.7022076E 01	-.9919562E 01
6	.8018554E 01	-.6956692E 01	-.2833242E 01	-.5788703E 00
7	-.3863475E 01	-.5454413E 01	.5250765E 00	.2585769E 01

SUBJECT B

$X = 4.15$ $t_f = 1.5$

	FX		FY	
N	A[N]	B[N]	A[N]	B[N]
0	.5993165E 01	.0000000E 00	-.9220953E 00	.0000000E 00
1	.1585175E 01	-.3074820E 02	.3626344E 01	.1984822E 02
2	.7153278E 01	.3082317E 01	-.4863005E 01	-.1344635E 01
3	.5153784E 01	.5274905E 01	-.2773319E 01	-.2689172E 01
4	.2159038E 00	-.2229556E 01	.1137947E 01	-.3697907E 01
5	-.2074535E 01	.6976777E 00	.2693649E 01	.7414591E 00
6	-.1177708E 01	.1016248E 00	.1112824E 01	-.1996208E 01
7	-.4161872E 00	-.9252185E 00	.4746299E 00	.1334782E 01

CONSOLE OPERATION TORQUING (NOMINAL)

SUBJECT A

$X = 2.535$ $t_f = 2.7$

FX

N	A[N]	B[N]
0	.4975722E 00	.0000000E 00
1	-.1549055E 00	.3257868E-01
2	-.3841524E 00	-.7498177E 00
3	-.4732652E 00	-.6000315E 00
4	.8315595E-01	-.5499738E 00
5	.3074934E 00	.1380874E 00
6	.3261996E 00	.4317187E 00
7	.8804560E-01	-.1229186E 00

FY

N	A[N]	B[N]
0	-.1086166E 01	.0000000E 00
1	-.5446934E 00	.3681894E 00
2	-.2815520E 00	.1338226E 01
3	.5160708E 00	.2426776E 00
4	-.3724050E-01	-.8309208E 00
5	.6269817E 00	-.1195300E 00
6	.4380985E 00	.8836404E-01
7	-.2697679E-01	.1933342E-02

MZ

N	A[N]	B[N]
0	-.2784482E 01	.0000000E 00
1	-.9071628E 00	.4835484E 00
2	.3548563E-01	.3977746E 01
3	.3308625E 01	.1701341E 01
4	.3680013E 00	-.1469480E 00
5	-.2415759E 00	-.4332826E 00
6	-.4057074E 00	-.8690703E 00
7	.4228498E 00	.4689086E 00

SUBJECT B

$X = 2.56$ $t_f = 2.4$

FX

N	A[N]	B[N]
0	.2393860E 00	.0000000E 00
1	-.1238533E 01	-.7878757E-02
2	-.6745269E 00	.6296440E 00
3	.2364176E-01	-.8567600E 00
4	.4466782E 00	.4729329E 00
5	.6017929E 00	.3121532E-03
6	-.5086377E 00	-.1564204E 00
7	.3954022E 00	-.2403853E-01

FY

N	A[N]	B[N]
0	.3973947E 00	.0000000E 00
1	.4146677E 00	-.1567215E 00
2	-.4456560E 00	-.2653566E 00
3	.9745690E-02	.2609362E 00
4	-.1275774E 01	.2176839E 00
5	-.1818723E 00	.3101005E 00
6	-.2524250E 00	-.7883326E 00
7	.8693282E-01	-.8722497E-01

CONSOLE OPERATION TORQUING (MINIMUM)

SUBJECT A

$X = 2.8$ $t_f = 2.81$

FX

N	A[N]	B[N]
0	.4847631E 00	.0000000E 00
1	-.4128945E 00	-.2191499E 00
2	-.1251314E 01	-.7841033E 00
3	-.2873731E 00	-.1465349E 00
4	.9654880E 00	.1508133E 00
5	.1265864E 00	.4395269E 00
6	.1319580E 00	-.9160830E-01
7	.1376946E 00	.1607685E 00

FY

N	A[N]	B[N]
0	-.9699578E 00	.0000000E 00
1	-.3722530E 00	.5188973E 00
2	.3800705E-01	.9075926E 00
3	-.4416411E-01	-.6237981E 00
4	-.5622514E 00	-.4954639E-01
5	.2788325E 00	.2851733E 00
6	.4737856E 00	-.3241290E 00
7	.4347515E-01	.5651189E 00

SUBJECT B

$X = 2.84$ $t_f = 2.56$

	FX		FY	
N	A[N]	B[N]	A[N]	B[N]
0	.3561652E 00	.0000000E 00	.1127748E 00	.0000000E 00
1	-.3500270E 00	-.2932903E 00	.3297527E 00	.1009104E 00
2	-.7170542E 00	-.1730822E 00	.1264670E 00	-.1785953E 00
3	.1168438E 01	-.1353958E 01	.8544379E-01	.5530443E 00
4	.1674159E 00	-.4020696E 00	.4208834E-01	-.1050830E 00
5	-.7114554E 00	-.5501717E 00	-.3384188E 00	-.2884815E 00
6	.2343953E-01	-.3038217E-02	.1575764E 00	-.4484854E 00
7	.2116757E 00	.7733783E-02	-.9391799E-01	.1101126E 00

CONSOLE OPERATION TORQUING (MAXIMUM)

SUBJECT A

$X = 3.4$ $t_f = 1.86$

	FX		FY	
N	A[N]	B[N]	A[N]	B[N]
0	.8911247E-01	.0000000E 00	-.2744247E 00	.0000000E 00
1	-.2914669E 01	.4524555E 00	.1799209E 01	-.1270666E 01
2	-.2703741E 01	.7362071E 00	-.8379875E 00	.1507045E 01
3	.1829127E 01	.4184902E 00	-.9235439E 00	.2723633E 01
4	.9978729E 00	-.1373970E 01	-.3665467E 00	-.4616981E 00
5	.5870147E 00	-.3489771E 00	.8666056E-01	-.1251866E 01
6	.1082857E 01	-.8838822E 00	.8762929E 00	-.1313973E 01
7	-.3246131E 00	-.5189457E 00	-.1050416E 01	-.6277033E 00

	MX		MZ	
N	A[N]	B[N]	A[N]	B[N]
0	-.1416935E 02	.0000000E 00	-.1032615E 01	.0000000E 00
1	.2296929E 01	-.2428927E 01	.9340785E 01	-.3934462E 01
2	.4174525E 00	-.3340944E 01	.3312006E 01	.3599400E 00
3	.5282714E 00	.4784813E 01	-.3394381E 01	.3597623E 01
4	-.1706918E 01	-.1201698E 01	-.4913049E 01	.2130839E 01
5	.1643526E 01	-.2763171E 00	-.5285888E 00	-.3498157E 01
6	-.1366976E 01	.6834641E 00	.3347674E 00	.1587394E 01
7	.8690342E 00	-.5824371E-01	-.3316372E 00	.8732331E 00

SUBJECT B

$X = 3.52$ $t_f = 1.96$

	FX		FY	
N	A[N]	B[N]	A[N]	B[N]
0	-.3716462E 00	.0000000E 00	.3906628E 00	.0000000E 00
1	-.2538841E 01	.2946049E 00	.8965195E 00	-.6996477E 00
2	-.4473630E 00	.9305342E 00	-.6914660E 00	.7877573E-01
3	.1481686E 01	-.1310558E 01	.4903006E 00	.7171678E 00
4	.7580810E 00	.1304596E 01	-.6117320E 00	.4887936E 00
5	-.3936681E 00	-.2039023E 00	-.4604894E-01	-.3614166E 00
6	.5057876E 00	-.7676052E 00	-.2545445E 00	-.8879658E-01
7	.1995938E 00	.8183849E 00	-.2360894E 00	.7257999E 00

	MX		MZ	
N	A[N]	B[N]	A[N]	B[N]
0	-.1081710E 02	.0000000E 00	.2464295E 01	.0000000E 00
1	.1082901E 01	-.4850710E 00	.6857815E 01	-.2209306E 01
2	.1287189E 01	-.1796058E 01	-.2688625E 01	-.9410902E 00
3	-.1121815E 01	.3099339E 01	-.5631912E-01	.2069283E 01
4	.5211179E-01	-.8041293E 00	-.3477156E 01	-.9193837E 00
5	-.3580416E 00	.1127324E 01	.1407840E 01	-.1217614E 00
6	-.9434872E 00	-.8649886E 00	-.2071265E 01	.4385039E 00
7	.1245490E 01	.9762147E 00	.6327723E 00	-.6271310E-02

CONSOLE OPERATION PUSH-PULL (NOMINAL)

SUBJECT A

$X = 2.92 \quad t_f = 2.13$

	FX		FY	
N	A[N]	B[N]	A[N]	B[N]
0	.4230584E 00	.0000000E 00	.6680955E 00	.0000000E 00
1	-.1762021E 00	.2661564E 00	-.7018184E-01	.1068193E 00
2	-.5358211E 00	.2460704E 00	-.2121920E 00	.4991289E 00
3	-.9538861E 00	-.3530969E 00	-.2864740E 00	.1183928E 01
4	.1277274E 00	-.6510442E 00	-.8497513E 00	.6658584E 00
5	.6059671E 00	-.4274842E 00	.3944391E 00	-.3458730E 00
6	.3016764E 00	.3826277E 00	.5316048E 00	.4156757E 00
7	.4023122E 00	.8565233E-01	.8866207E 00	-.3426881E 00

SUBJECT B

$X = 2.92 \quad t_f = 2.15$

	FX		FY	
N	A[N]	B[N]	A[N]	B[N]
0	-.1533984E 01	.0000000E 00	.1552690E 01	.0000000E 00
1	.1376420E-01	-.1371208E 00	.6012606E 00	.7662183E-01
2	-.5085240E 00	-.9485731E-01	.1076887E 01	.5183808E 00
3	-.5334656E 00	.5713519E 00	-.4118560E 00	-.5549913E 00
4	.1609510E 00	-.2030606E 00	-.2429898E 01	-.2145611E-01
5	.5120423E-01	-.5021293E 00	-.7228688E 00	-.3429375E 00
6	.5378070E 00	-.6651955E 00	.1328708E 01	-.2179960E 00
7	.4820691E-01	.3157633E-01	-.3661815E 00	-.4231972E 00

CONSOLE OPERATION PUSH-PULL (MINIMUM)

SUBJECT A

$X = 2.63 \quad t_f = 2.2$

	FX		FY	
N	A[N]	B[N]	A[N]	B[N]
0	.1604052E 00	.0000000E 00	.1596124E 01	.0000000E 00
1	.4079365E-01	.1280123E 00	.4067538E 00	-.2589123E-01
2	-.2895018E 00	.1565548E 00	-.1739714E 00	.3830954E 00
3	-.7381916E 00	-.5594058E 00	.2304510E 00	.4282029E 00
4	.4920755E 00	-.7781403E-01	-.4682534E 00	-.2301686E 00
5	.2718817E-01	.7499476E-01	.2360024E 00	-.4517572E 00
6	-.8139684E-01	-.9298816E-01	.2760467E 00	-.2309515E 00
7	-.6271916E-01	.1420565E 00	-.7053417E-01	.7214082E-01

SUBJECT B

$X = 2.7$ $t_f = 2.34$

	FX		FY	
N	A[N]	B[N]	A[N]	B[N]
0	-.6219727E 00	.0000000E 00	.9745178E 00	.0000000E 00
1	.2914166E 00	.3040396E-02	-.5654093E-01	-.1055652E 00
2	.1395956E 00	.4192671E-01	.1378757E 00	.5207876E 00
3	-.9025703E-01	-.9493132E-01	.1274663E 00	.6354273E 00
4	.4600002E 00	-.7581009E 00	.3996126E 00	.1083362E 01
5	-.2138101E 00	-.1450243E 00	.4655025E 00	.4999541E 00
6	.2944083E-02	-.6373166E 00	.6272645E 00	-.1372993E 00
7	-.6387823E 00	-.4823944E-01	-.2885658E 00	-.7265870E 00

CONSOLE OPERATION PUSH-PULL (MAXIMUM)

SUBJECT A

$X = 2.88$ $t_f = 1.62$

	FX		FY	
N	A[N]	B[N]	A[N]	B[N]
0	.1036145E 01	.0000000E 00	.1967875E 01	.0000000E 00
1	.3780306E 00	-.1377774E 00	.7068440E 00	-.3956871E 00
2	.8076762E-01	-.4891636E 00	.1992987E 01	-.6441462E 00
3	-.1349265E 01	-.8386754E 00	.1982489E 01	-.6519628E-01
4	-.6657740E 00	.7385821E-01	-.4781821E 00	-.3311516E 00
5	.1867914E-02	.9571597E-01	-.1829295E 01	.2294314E 01
6	-.9904251E-01	-.1141618E 00	-.6437448E 00	.1667748E 01
7	-.4026307E 00	.6115231E-01	-.1294971E 01	.4500886E 00

SUBJECT B

$X = 3.98$ $t_f = 1.56$

	FX		FY	
N	A[N]	B[N]	A[N]	B[N]
0	-.4449978E 00	.0000000E 00	.9087906E 00	.0000000E 00
1	-.5592332E 00	.1616336E 00	.2569581E 00	-.7807639E-01
2	-.9067089E 00	.4345633E 00	-.6265159E 00	.8843118E 00
3	.1448088E 00	.1664608E 00	-.1926193E 01	.1061298E 01
4	.3068412E 00	.3966077E 00	-.1068006E 01	.7616063E 00
5	.5419348E 00	-.3581920E 00	-.2366423E 00	.5543879E 00
6	-.1115327E 00	-.3685055E-01	-.6508216E 00	.7099592E 00
7	-.1733162E-01	.2385054E 00	-.2258275E 00	.1363475E 01

CONSOLE OPERATION LATERAL SLIDING (NOMINAL)

SUBJECT A

$X = 3.45$ $t_f = 1.71$

	FX		FY	
N	A[N]	B[N]	A[N]	B[N]
0	-.3119516E 00	.0000000E 00	.1721521E 01	.0000000E 00
1	.1783940E 00	.4419596E 00	.7520241E 00	-.2023869E 00
2	-.8939352E 00	-.6443154E 00	-.4855642E 00	.9393659E 00
3	.4899981E-01	.1219392E 00	.1047453E 00	.4798139E 00
4	-.2430217E 00	-.9212003E 00	-.9061832E 00	.1247810E-02
5	.7620350E-01	.3117406E-02	-.5728505E 00	-.1782151E 00
6	.2574755E 00	.8739058E-01	.3300283E 00	.4377698E 00
7	.9616847E-01	-.1509580E 00	.6655612E 00	.1267969E 00

SUBJECT B

$X = 2.565 \quad t_f = 2.45$

	FX		FY	
N	A[N]	B[N]	A[N]	B[N]
0	.5662682E 00	.0000000E 00	.9454294E 00	.0000000E 00
1	-.2583278E 00	-.7195874E-02	.3685179E 00	-.5659093E-01
2	-.7404530E 00	.1547578E 00	.5079191E 00	-.2567055E 00
3	-.1039905E 01	-.1469452E-01	.2033413E 00	-.3596716E 00
4	.9371350E-01	-.5311835E 00	-.2570281E 00	.2490112E 00
5	.3103614E 00	.1239918E 00	-.8182161E 00	.4970954E 00
6	.1856452E 00	-.6311475E-01	-.2704733E-01	.2230506E 00
7	.1880523E-01	.1623861E 00	-.1449853E 00	-.3097999E 00

CONSOLE OPERATION LATERAL SLIDING (MINIMUM)

SUBJECT A

$X = 2.47 \quad t_f = 2.4$

	FX		FY	
N	A[N]	B[N]	A[N]	B[N]
0	-.2503401E 00	.0000000E 00	.1006255E 01	.0000000E 00
1	.2548376E 00	.2379242E 00	.2595349E 00	-.1934790E 00
2	-.6810334E 00	.2685624E 00	.1433520E 00	.1064565E 00
3	-.6734311E 00	-.8297293E 00	.7252058E-01	.6994772E 00
4	.2539362E 00	-.2051709E 00	-.4543169E 00	.2103666E-01
5	.3268480E 00	-.2568143E 00	-.2811817E 00	.1313928E 00
6	.1800862E 00	.1226115E 00	-.1024593E 00	-.1816853E 00
7	.1453150E 00	-.1671153E 00	.1615935E 00	.5051457E-01

SUBJECT B

$X = 2.56 \quad t_f = 2.55$

	FX		FY	
N	A[N]	B[N]	A[N]	B[N]
0	.7499605E-01	.0000000E 00	.1321463E 01	.0000000E 00
1	-.3463165E-01	-.3771595E-02	.2579118E 00	-.4077998E-01
2	-.4730709E 00	-.1055113E 00	.1148763E 01	-.8066753E-02
3	-.3660092E 00	-.5288100E 00	.3523820E 00	-.4304611E-01
4	.4413229E 00	.2959789E 00	-.2036997E 00	.1031998E 00
5	.4130372E-01	.1082605E 00	-.4214625E 00	.1823793E-01
6	.1014237E 00	.1326940E-01	-.3057134E 00	.2618308E-01
7	.2333330E 00	-.8305025E-01	.4689673E 00	.6041536E-01

CONSOLE OPERATION LATERAL SLIDING (MAXIMUM)

SUBJECT A

$X = 4.55 \quad t_f = 1.32$

	FX		FY	
N	A[N]	B[N]	A[N]	B[N]
0	-.5106240E 00	.0000000E 00	.5684875E 00	.0000000E 00
1	-.9006091E 00	-.4473447E-01	.2744150E 01	.5094649E 00
2	-.3045731E 01	.6507767E 00	.1582462E 01	-.2525104E 01
3	.1867832E 01	.1490275E 01	-.2334868E 01	.7659358E 01
4	-.2829503E-01	.5032808E 00	-.1609284E 01	-.1017729E 01
5	-.2856713E-01	-.2186201E 00	-.1353142E 01	-.4198066E 00
6	.6343102E 00	-.4609938E 00	.7194221E 00	-.1384430E 01
7	.1728534E 00	.5415954E 00	.2327537E 00	.1062718E 01

	MX		MX	
N	A[N]	B[N]	A[N]	B[N]
0	.1245957E 01	.0000000E 00	-.2393470E 01	.0000000E 00
1	.2279634E 00	-.3098680E 01	.6184350E 01	.2711695E 01
2	.4278223E 01	-.1645901E 01	.7903197E 01	-.2111751E 01
3	-.1798010E 01	.4572724E 01	-.6409788E 01	.4265535E 01
4	-.1265874E 01	-.1205090E 01	-.3192008E 01	-.3513579E 01
5	-.1505335E 00	.9505473E 00	-.3777822E-01	.6652820E 00
6	.5431726E 00	-.1107214E 01	.1748138E 01	-.1921639E 01
7	.5331947E 00	.9985580E 00	-.5530174E 00	.2786580E 01

SUBJECT B

$X = 3.19 \quad t_f = 1.96$

	FX		FY	
N	A[N]	B[N]	A[N]	B[N]
0	-.7776873E 00	.0000000E 00	.1227857E 01	.0000000E 00
1	-.5005503E 00	.1490955E 00	.1214674E 00	-.2357372E 00
2	-.1343537E 01	.5498495E 00	.4482379E 00	-.7999026E 00
3	.1085830E 01	-.1608781E 00	.4345695E 00	.1646821E 01
4	.9649921E 00	.4054941E 00	-.7506671E 00	.1050241E 01
5	-.6463884E-01	-.5049246E-01	-.2924297E 00	-.9649210E-03
6	-.1434358E 00	-.1730646E 00	-.1975238E 00	-.2753805E 00
7	.1735793E 00	-.1535725E 00	.2330752E 00	-.3859580E 00

	MX		MZ	
N	A[N]	B[N]	A[N]	B[N]
0	-.2142536E 02	.0000000E 00	.3666901E 01	.0000000E 00
1	.5117357E 00	-.1458323E 01	.5782695E 00	-.2885308E 00
2	.7544682E 00	-.6000921E 00	.3405979E 01	-.2036859E 01
3	.3884096E 00	.1640776E 01	-.1730021E 01	.2177055E 01
4	.1325570E 00	.6182872E 00	-.2002997E 01	.8855493E-01
5	-.1453462E 00	.1642372E-01	.1797266E 00	.1553757E 00
6	-.2832396E 00	-.3270110E 00	-.7213131E 00	-.4085675E 00
7	.3487589E 00	.2572037E-02	.4099787E 00	-.2175668E 00

TRUNK BENDING EXERCISE

SUBJECT A

$X = 5.43$ $t_f = 1.1$

	FX		FY	
N	A[N]	B[N]	A[N]	B[N]
0	-.4653311E 01	.0000000E 00	-.3753295E 01	.0000000E 00
1	.2102031E 01	.7146199E 01	-.7283694E 01	.3035166E 02
2	.6681940E 00	.4009931E 01	.3637924E 01	.3623810E 01
3	.1194092E 01	.1105762E 01	.6133996E 01	-.6043183E 00
4	.3634614E 00	-.1289353E 01	.1219109E 01	-.1462908E 01
5	-.3780017E 00	.8988452E 00	.1461100E 01	-.2256296E 00
6	.8189174E 00	.6081158E 00	-.1136850E 00	-.1611839E 01
7	.5937725E 00	-.5352114E 00	-.6021212E 00	.2900781E 00

SUBJECT B

$X = 4.91$ $t_f = 0.9$

	FX		FY	
N	A[N]	B[N]	A[N]	B[N]
0	.2892810E 00	.0000000E 00	.6077995E 01	.0000000E 00
1	.1804618E 01	.1856716E 01	-.6772755E 01	.5688486E 01
2	-.1329146E 01	.1246549E 01	.2440927E 01	-.6322109E 00
3	.8770047E 00	-.1215083E 00	-.2998311E 01	.1853529E 01
4	-.5580182E 00	-.1976851E 00	.2232867E 01	.1095996E 01
5	-.1113097E 00	.8116340E 00	-.3777876E-01	-.1569268E 01
6	.1125474E 00	.4691311E 00	-.9563962E 00	.1381986E 00
7	.1577979E 00	.1165222E 00	.3877607E-01	.6687436E 00

NECK BENDING EXERCISE

SUBJECT A

$X = 5.57$ $t_f = 1.1$

	FX		FY	
N	A[N]	B[N]	A[N]	B[N]
0	.1641549E 01	.0000000E 00	.1014912E 01	.0000000E 00
1	-.7192818E-01	-.3229925E 00	-.4108682E 00	-.5526764E 00
2	.2675666E 00	.2095827E-01	-.3176432E 00	.6987659E 00
3	-.2017672E 00	-.4515343E 00	.1142874E-01	.8986612E-02
4	.3807424E-01	.2977571E 00	-.1076036E 00	-.1349771E 00
5	-.6188004E-01	.5641398E-01	.1844995E 00	-.8440260E-01
6	-.4279752E-01	.4378244E-02	.7681123E-01	.7516109E-01
7	.1556571E 00	.7954814E-01	-.3726115E-01	-.6617342E-01

SUBJECT B

$X = 5.74$ $t_f = 1.3$

	FX		FY	
N	A[N]	B[N]	A[N]	B[N]
0	.1169358E 01	.0000000E 00	-.4766573E 00	.0000000E 00
1	.2505734E 00	-.1419519E 01	-.1180917E 01	-.3751384E 00
2	-.6042474E-01	.3612164E 00	.1392877E 01	.8787441E 00
3	.6655348E-01	.9398648E-01	.2877853E 00	-.7346694E-01
4	-.1167124E 00	.3295487E-01	.7308721E-01	-.1644435E 00
5	.3536612E-01	-.1831744E 00	.2945124E 00	-.2390118E 00
6	-.5992501E-01	.1801803E-01	.5734877E-01	-.2283950E 00
7	-.2158562E-01	-.5942792E-01	-.2281672E-01	-.1880663E 00

ROWING EXERCISE

SUBJECT A

$X = 3.52$ $t_f = 1.79$

	FX		FY	
N	A[N]	B[N]	A[N]	B[N]
0	.2395224E 01	.0000000E 00	.1334484E 01	.0000000E 00
1	-.2865462E 00	-.2003585E 00	-.3709956E 01	-.1004392E 01
2	.2123107E 00	.8160800E 00	.4280145E 01	.6996166E 01
3	-.7921944E-02	.9565362E-01	-.1071739E 01	.2146986E 01
4	.4378669E 00	-.7220135E-01	.1102169E 01	.1254983E 01
5	.9954999E-01	-.3239700E 00	.1717184E 00	.1525585E 01
6	.7389744E-01	-.1505252E 00	-.1260879E 01	.3548464E 00
7	-.1880231E 00	.2470926E 00	.1211011E 01	-.5572349E 00

SUBJECT B

$X = 7.9$ $t_f = 0.95$

	FX		FY	
N	A[N]	B[N]	A[N]	B[N]
0	-.3129101E 00	.0000000E 00	.7970937E 01	.0000000E 00
1	.3053973E 01	-.2822633E 01	.1182168E 02	-.4001603E 01
2	-.2203795E 01	-.1784629E 00	-.1190422E 02	-.6405299E 00
3	-.7440490E 00	.1430636E 01	-.1124160E 01	.2978814E 01
4	.3651592E 00	.4638482E 00	-.3076431E 00	.7915040E 00
5	-.5321434E-01	.2258575E 00	.1699148E 01	.1062842E 01
6	.2121029E 00	.1981375E 00	-.2166921E 00	.5675473E 00
7	.3319220E-01	.2482690E 00	.3101212E-01	.9718500E 00

PEDAL ERGOMETER ENDURANCE EXERCISE

SUBJECT A

$X = 5.3$ $t_f = 1.2$

	FX		FY	
N	A[N]	B[N]	A[N]	B[N]
0	-.6454114E 01	.0000000E 00	.4387904E 00	.0000000E 00
1	.8702507E 00	.2107053E 01	-.2569807E 00	-.3828413E 01
2	-.2649793E 01	-.9523686E 00	.6765625E 00	.5683725E 01
3	.5020317E 01	-.3766690E 00	-.4933611E 01	.4354070E 00
4	-.4574409E 00	-.8578671E 00	.2015966E 00	.4014875E 01
5	.1886795E 01	-.3500426E 00	.2616226E 01	.1152078E 01
6	-.1133604E 01	-.1501313E 01	-.6646753E 00	-.2982785E 00
7	-.1151673E 01	-.7067355E 00	.3785031E 00	.4962097E 00

	MX		MZ	
N	A[N]	B[N]	A[N]	B[N]
0	-.3953363E 02	.0000000E 00	.1406144E 02	.0000000E 00
1	.1189437E 02	.1638774E 02	-.3858227E 01	-.9584289E 01
2	-.4792751E 01	-.2065207E 02	.7442406E 01	.7905856E 01
3	.4226995E 01	-.1022797E 02	-.6514701E 01	.3877757E 01
4	.2429237E 01	-.8047095E 01	.1008618E 01	.9916173E 01
5	-.2655233E 01	-.4594117E 01	.1692274E 01	.4201356E 00
6	-.5871464E 01	-.9106304E 01	-.4584998E 00	.4296494E 01
7	-.5552261E 01	-.2339170E 01	.6105527E-01	.1801748E 01

SUBJECT B

$X = 6.07 \quad t_f = 1.04$

FX

N	A[N]	B[N]
0	-.1665100E 02	.0000000E 00
1	-.1749597E 01	.3149104E 01
2	-.3634891E 01	-.1470585E 01
3	-.1059948E 01	-.1793541E 01
4	-.6320751E 00	-.6703763E 00
5	.1091856E 01	.2743142E 00
6	.1340024E 00	-.8000125E 00
7	.5148973E 00	.4138961E 00

FY

N	A[N]	B[N]
0	.3638695E 01	.0000000E 00
1	.3014324E 01	-.9746566E 01
2	-.2532038E 01	.4304681E 01
3	-.2802482E 01	.1487085E 01
4	.6363374E-01	-.1532484E 01
5	.1640885E 01	.1215727E 01
6	-.7459349E 00	.1700290E 01
7	.1468050E 00	-.2719134E-01

MX

N	A[N]	B[N]
0	-.9205212E 02	.0000000E 00
1	-.1619420E 01	.2690422E 02
2	-.3891380E 00	-.3473823E 01
3	.2712718E 00	.2910083E 01
4	-.8634468E 00	.2960495E 01
5	-.1496719E 01	.8573466E 00
6	.5831086E 00	-.9346094E 00
7	.1004144E 01	-.4092773E-01

MZ

N	A[N]	B[N]
0	.5578960E 02	.0000000E 00
1	.2606103E 01	-.2193533E 02
2	.2655880E 00	.6824752E 01
3	-.2603744E 01	.1028643E 02
4	.2650694E 01	.6949837E 00
5	-.1061847E 00	.1863009E 01
6	-.2369817E 00	.2797257E 01
7	-.5608253E 00	-.7678898E 00

OSCILLATION ACCELERATION EXERCISE

SUBJECT A

$X = 4.6 \quad t_f = 1.3$

FY

N	A[N]	B[N]
0	.2937158E 02	.0000000E 00
1	-.1366861E 02	-.7498413E 02
2	.3025355E 01	.1734293E 02
3	.5866945E 01	.1049039E 02
4	-.1353158E 02	.7755100E 00
5	.6892747E 01	.2977746E 01
6	-.4552339E 01	.1481385E 01
7	.2291455E 01	.1976046E 01

SUBJECT B

$X = 5.44 \quad t_f = 1.16$

FX

N	A[N]	B[N]
0	.6365990E 01	.0000000E 00
1	.1343426E 01	.2700417E 01
2	-.4060874E 01	.4604527E 01
3	-.1243756E 01	.1762246E 00
4	-.3089433E 01	-.3070748E 01
5	.3079563E 00	.2331340E 01
6	.1528478E 01	.1959721E 00
7	-.2558666E 00	-.5043245E 00

FY

N	A[N]	B[N]
0	.2677897E 02	.0000000E 00
1	-.2761800E 02	-.6527632E 02
2	.7503447E 01	-.1008291E 02
3	.1553714E 02	-.7872280E 01
4	-.4147637E-01	.1428776E 02
5	-.4288768E 01	-.2430093E 01
6	-.8050275E 00	.1443995E 01
7	.2517707E 01	-.1494025E 01

FULL LENGTH BODY EXERCISE

SUBJECT A

$X = 2.142 \quad t_f = 2.95$

FX

N	A[N]	B[N]
0	-.2179188E 01	.0000000E 00
1	-.1798941E 01	-.1331539E 01
2	.9923074E 01	.4764136E 01
3	.8881088E 00	.3881004E 00
4	-.2134950E 01	-.2660507E 01
5	-.2125266E 01	.9251130E 00
6	-.1854840E 01	.1281823E 00
7	-.8624830E 00	.4162422E 00

FY

N	A[N]	B[N]
0	.2852597E 01	.0000000E 00
1	-.2103657E 02	.2298971E 01
2	.7152745E 01	.2692807E 00
3	.4837608E 01	-.6168667E 01
4	-.2163232E 01	.1349338E 01
5	.6441236E 01	.3466966E 01
6	-.2860598E 00	.4901683E 01
7	.3006380E 01	.2482070E 01

MZ

N	A[N]	B[N]
0	-.1707763E 01	.0000000E 00
1	.1332291E 02	.6043429E 01
2	-.2574010E 02	-.2210112E 02
3	.9981321E 01	-.5099652E 01
4	.1438547E 01	.1163176E 02
5	.2865155E 00	-.7635361E 01
6	-.1641641E 01	-.1395039E 01
7	.9815287E 01	-.1239450E 01

SUBJECT B

$X = 2.34 \quad t_f = 2.85$

FX

N	A[N]	B[N]
0	.1041143E 01	.0000000E 00
1	.3773960E 01	-.5972038E 00
2	.5549457E 01	.4876529E 01
3	.1086306E 01	-.1580282E 01
4	.1750366E 01	.6852106E 00
5	-.2477706E 01	-.8813784E 00
6	-.7530832E 00	-.4297938E 01
7	-.6277880E 00	-.1872496E 01

FY

N	A[N]	B[N]
0	.4724964E 01	.0000000E 00
1	-.2706411E 02	.1278229E 01
2	-.4066340E 01	.3938680E 01
3	.2242984E-01	-.4100423E 01
4	.5136558E 01	.3738527E 01
5	.5166363E 01	.3622083E 01
6	.1162195E 01	-.2343123E 01
7	.4794323E 01	-.6570245E 00

MZ

N	A[N]	B[N]
0	-.3339137E 01	.0000000E 00
1	.7890869E 00	.2771584E 01
2	-.1143414E 02	-.2488643E 02
3	.7155954E 01	.1264808E 02
4	-.7536326E 01	-.4408976E 01
5	.7325454E 01	-.1546311E 00
6	-.5007548E 00	.5244460E 01
7	.1014437E 01	.1337367E 01

TRUNK ROTATION EXERCISE

SUBJECT A

$X = 3.29 \quad t_f = 2.02$

FX

N	A[N]	B[N]
0	-.1725784E 01	.0000000E 00
1	-.3710578E 01	.3529522E 01
2	.9350233E 00	-.5591683E 00
3	.4231871E 01	.1477246E 01
4	.2578079E 01	.8228019E 00
5	.7015887E 00	-.1738171E 01
6	-.8887808E 00	-.1063894E 01
7	-.7093167E 00	-.4506140E 00

FY

N	A[N]	B[N]
0	.1624842E 01	.0000000E 00
1	.5234984E 00	-.1267677E 01
2	-.1361199E 01	.3090933E 01
3	.3236063E 01	.4856399E 00
4	-.1175162E 01	-.9385418E 00
5	.2536487E 00	-.2060329E 01
6	-.4014846E-02	.5073482E 00
7	-.8574238E-01	-.6886214E 00

FZ

N	A[N]	B[N]
0	-.2029173E 02	.0000000E 00
1	-.3490144E 01	.1204977E 02
2	.2575961E 01	.3441768E 01
3	.4438971E 01	-.5322719E 00
4	.5968688E 00	.2908233E 00
5	-.4879673E 00	.7347250E 00
6	-.1274730E 00	.5724920E 00
7	.2729360E 00	.3804122E 00

MY

N	A[N]	B[N]
0	-.1885521E 01	.0000000E 00
1	.1708530E 02	-.4210506E 02
2	.2324636E-01	-.1759498E 00
3	-.4923665E 01	-.1077845E 01
4	-.5409638E 00	-.2560934E 01
5	-.8081694E 00	-.1431017E 01
6	-.4109435E 00	-.1792155E 01
7	-.6082773E 00	-.1837685E 00

SUBJECT B

$X = 2.77 \quad t_f = 2.15$

FX

N	A[N]	B[N]
0	-.1965801E 01	.0000000E 00
1	-.1225564E 01	.3439548E 01
2	.1587734E 01	-.1776896E 01
3	-.1698869E 01	-.2241450E 00
4	.2342322E 00	.6438887E 00
5	-.3006903E 00	-.7110833E 00
6	.1014197E 01	.2673981E 00
7	-.1701345E 00	.6758626E 00

FY

N	A[N]	B[N]
0	-.1410419E 00	.0000000E 00
1	.5576442E 00	-.2169632E 00
2	-.1229128E 00	-.2981391E 00
3	.5905105E 00	-.1492954E 00
4	.1542112E 00	-.1160318E 00
5	-.6111764E 00	.2892516E 00
6	-.4342091E 00	-.7574520E 00
7	-.6386356E 00	.6152685E 00

FZ

N	A[N]	B[N]
0	-.1689664E 01	.0000000E 00
1	-.1757709E 01	.1861426E 01
2	.5584679E 00	-.1146035E 01
3	.1207037E 01	-.2512233E 00
4	.2940262E 00	-.1560595E 00
5	.9359537E 00	-.1052257E 01
6	-.1098047E 00	-.2465255E 00
7	-.3558562E 00	-.3489330E 00

MY

N	A[N]	B[N]
0	-.1303854E 01	.0000000E 00
1	.1155289E 02	-.2870932E 02
2	-.6303835E 01	.8539168E-01
3	-.2027953E 01	-.1241338E 01
4	-.6801019E 00	.1411270E 01
5	-.6278677E 00	.5762237E 00
6	.7009234E 00	.5604274E 00
7	-.6292745E 00	.7757660E 00

APPENDIX D

PHYSICAL BODY MEASUREMENTS

The following measurements taken of the two subjects are the inputs for the MAID program written by NASA at Langely Research Center. The results of this program give the various segment inertias and center of mass locations used in the analytical work for obtaining the forces of some of the simple segment motions.

Fig. D-1 shows the model of the various body segment pivot points and mass centers. It should be pointed out that the reference axis for the man model is not the same as used for the tests. To make both the reference systems compatible requires a simple translation of the origin with a rotation of 90° about 1 axis.

Because the man model is assumed to be symmetrical, only the parameters to describe the segment pivot points and mass centers of the right arm and leg are given. The pivot points and segment mass centers are assumed to be contained in the Y_{MI} - Z_{MI} plane.

Tables D-I and D-II present the segment masses and inertias obtained from the MAID program. The segment numbers correspond to the numbering given in fig. D-1.

Physical Body Measurements of Subject A

The physical body measurements of Subject A are as follows:

		Values
(1)	Ankle circumference: minimum circumference of right ankle	6 in.
(2)	Axiallary arm circumference: arms lowered, upper arm circumference at arm pit	13.5 in.
(3)	Buttock depth: depth at level of greatest rearward protrusion	10.2 in.
(4)	Chest breadth: measured at level of nipples	14.1 in.
(5)	Chest depth: measured at level of nipples	10.6 in.
(6)	Elbow circumference: measured with arm extended	10.75 in.

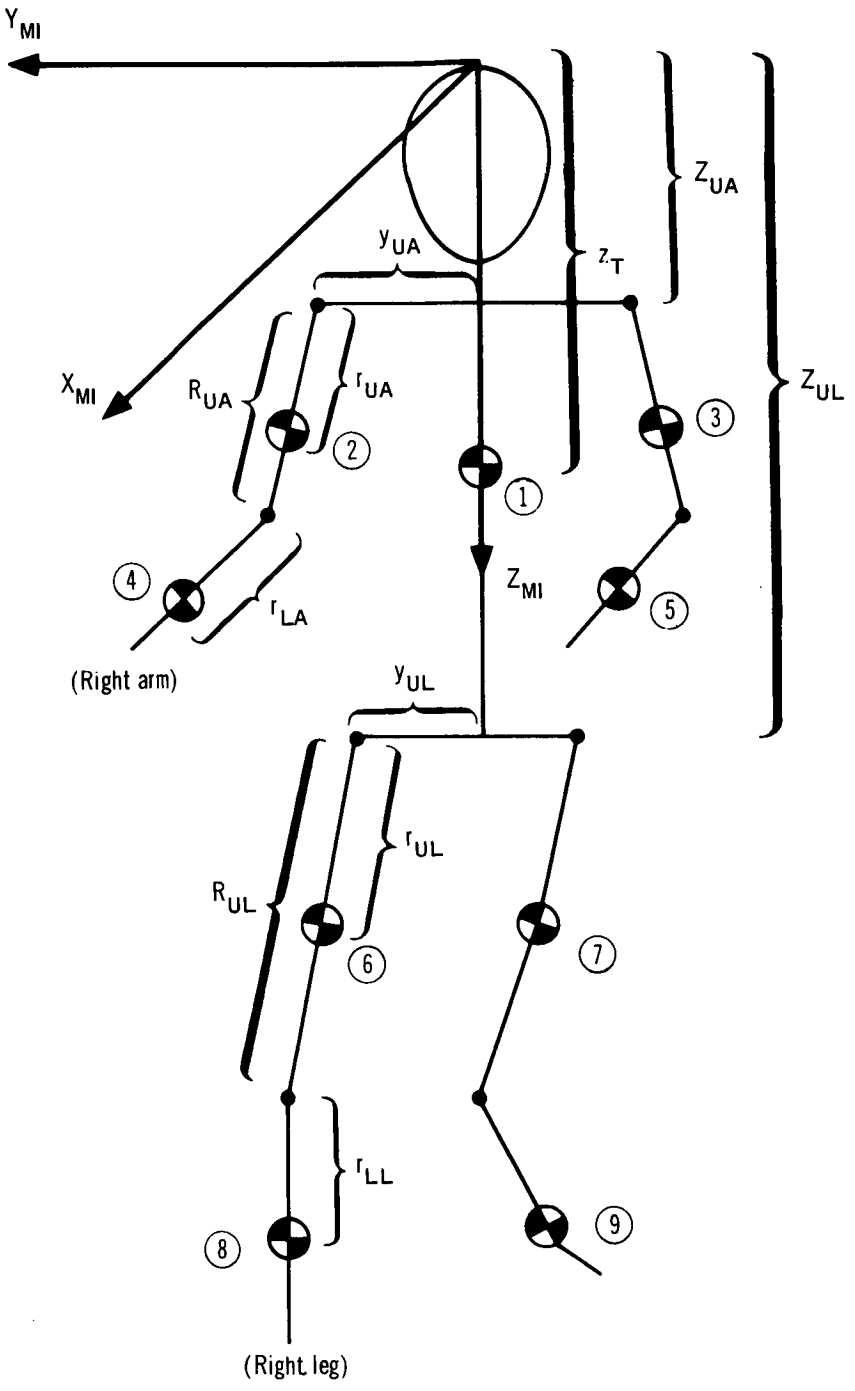

● Segment Pivot Points

Segment Mass Centers

$z_T \equiv$ Torso segment radial (1)

$r_{UA} \equiv$ Right upper arm segment radial (2)

$r_{LA} \equiv$ Right lower arm segment radial (4)

$r_{UL} \equiv$ Right upper leg segment radial (6)

$r_{LL} \equiv$ Right lower leg segment radial (8)

$R_{UA} \equiv$ Right upper arm segment length (2)

$R_{UL} \equiv$ Right upper leg segment length (6)

$y_{UA} \equiv$ Shoulder pivot displacement (Y_{MI} axis)

$Z_{UA} \equiv$ Shoulder pivot displacement (Z_{MI} axis)

$y_{UL} \equiv$ Upper leg pivot displacement (Y_{MI} axis)

$Z_{UL} \equiv$ Upper leg pivot displacement (Z_{MI} axis)

Figure D-1. Segment Pivot Points and Mass Centers

TABLE D-I

SEGMENT MASS AND MOMENT OF INERTIA CALCULATION OF SUBJECT A

	1	2	3	4	5	6	7	8	9
Segment hinge points (ft)									
Y	0.00000	0.77072	-0.77072	0.77072	-0.77072	0.22506	-0.22506	0.22506	-0.22506
Z	0.00000	1.16238	1.16238	2.10833	2.10833	2.73333	2.73333	4.15000	4.15000
Segment masses (slugs)	2.94102	0.17201	0.17201	0.13939	0.13939	0.54107	0.54107	0.34783	0.34783
Segment volume (ft^3)	1.58741	0.09215	0.09215	0.05644	0.05644	0.27758	0.27758	0.11628	0.11628
Specific gravity	0.95564	0.96279	0.96279	1.27379	1.27379	1.00541	1.00541	1.54288	1.54288
Segment length (ft)	2.73333	0.94595	0.94595	1.22171	1.22171	1.41667	1.41667	1.50000	1.50000
Segment radial (ft)	1.72297	0.34195	0.34195	0.58260	0.58260	0.67636	0.67636	0.64825	0.64825
I_X (slug-ft^2)	1.72768	0.01904	0.01904	0.02004	0.02004	0.07885	0.07885	0.08423	0.08423
I_Y (slug-ft^2)	1.63509	0.01904	0.01904	0.02004	0.02004	0.07885	0.07885	0.07987	0.07987
I_Z (slug-ft^2)	0.32577	0.00228	0.00228	0.00112	0.00112	0.02022	0.02022	0.00827	0.00827

TABLE D-II

SEGMENT MASS AND MOMENT OF INERTIA CALCULATION OF SUBJECT B

	1	2	3	4	5	6	7	8	9
Segment hinge points (ft)									
Y	0.00000	0.71977	-0.71977	0.71977	-0.71977	0.29495	-0.29495	0.29495	-0.29495
Z	0.00000	1.11143	1.11143	2.10833	2.10833	2.94167	2.94167	4.37500	4.37500
Segment masses (slugs)	2.98937	0.17603	0.17603	0.14194	0.14194	0.55030	0.55030	0.35444	0.35444
Segment volume (ft^3)	1.91271	0.09147	0.09147	0.05822	0.05822	0.26149	0.26149	0.13951	0.13951
Specific gravity	0.80615	0.99261	0.99261	1.25742	1.25742	1.08549	1.08549	1.31049	1.31049
Segment length (ft)	2.94167	0.99690	0.99690	1.25542	1.25542	1.43333	1.43333	1.50000	1.50000
Segment radial (ft)	1.83056	0.38421	0.38421	0.60325	0.60325	0.69818	0.69818	0.69230	0.69230
I_X (slug-ft^2)	2.12995	0.02095	0.02095	0.02185	0.02185	0.08239	0.08239	0.08361	0.08361
I_Y (slug-ft^2)	2.03813	0.02095	0.02095	0.02185	0.02185	0.08239	0.08239	0.07844	0.07844
I_Z (slug-ft^2)	0.35819	0.00221	0.00221	0.00115	0.00115	0.01875	0.01875	0.00959	0.00959

		Values
(7)	Fist circumference: measured with tape passing over thumb and knuckles	11.5 in.
(8)	Forearm length: measured between radiale and stylion	11 in.
(9)	Foot length: longest foot dimension (standing)	10.4 in.
(10)	Knee circumference: measured at mid-patella level (standing)	14.75 in.
(11)	Head circumference: maximum circumference of head (above brow ridges)	23 in.
(12)	Hip breadth: maximum breadth of hips (standing)	13.2 in.
(13)	Shoulder (acromial) height: vertical distance from floor to right acromion (standing)	56 in.
(14)	Sitting height: subject sitting in chair with knees bent at right angles (distance measured from sitting surface to top of head)	34.5 in.
(15)	Sphyrion height: vertical distance from floor to sphyrion (subject standing with legs slightly apart)	3.5 in.
(16)	Stature: subject standing, vertical distance from the floor to top of the head	67.75 in.
(17)	Substernale height: vertical distance from floor to substernale point at lower edge of breastbone (standing)	47.75 in.
(18)	Thigh circumference: circumference of thigh just below lowest point in gluteal furrow (standing)	24.5 in.
(19)	Tibiale height: vertical distance from floor to right tibiale (standing)	18 in.
(20)	Trochanteris height: vertical distance from floor to trochanterion on right side (standing)	35 in.
(21)	Upper arm length: length of upper arm between acromion and radiale	13.5 in.
(22)	Weight: nude weight	172 lb

	Values
(23) Waist breadth: minimum horizontal distance between points marking the most lateral indentation in the abdominal region (standing)	11.4 in.
(24) Waist depth: anterior to posterior distance of the abdomen at the level of the most lateral indentation waist points (standing)	9.65 in.
(25) Wrist circumference: minimum circumference of wrist, measured with tape just proximal of the styloid process of the ulna.	7.25 in.

Physical Body Measurements or Subject B

Following are the physical body measurements of Subject B:

	Values
(1) Ankle circumference: minimum circumference of right ankle	8.75 in.
(2) Axiallary arm circumference: arms lowered, upper arm circumference at arm pit	12.75 in.
(3) Buttock depth: depth at level of greatest rearward protrusion	10.8 in.
(4) Chest breadth: measured at level of nipples	13.2 in.
(5) Chest depth: measured at level of nipples	10.8 in.
(6) Elbow circumference: measured with arm extended	11.0 in.
(7) Fist circumference: measured with tape passing over thumb and knuckles	11.25 in.
(8) Forearm length: measured between radiale and stylion	11.5 in.
(9) Foot length: longest foot dimension (standing)	11.2 in.
(10) Knee circumference: measured at mid-patella level (standing)	15 in.
(11) Head circumference: maximum circumference of head (above brow ridges)	23.5 in.

		Values
(12)	Hip breadth: maximum breadth of hips (standing)	14.3 in.
(13)	Shoulder (acromial) height: vertical distance from floor to right acromion (standing)	59.25 in.
(14)	Sitting height: subject sitting in chair with knees bent at right angles (distance measured from sitting surface to top of head)	37 in.
(15)	Sphyrion height: vertical distance from floor to sphyrion (subject standing with legs slightly apart)	3.5 in.
(16)	Stature: subject standing, vertical distance from the floor to top of the head	70.5 in.
(17)	Substernale height: vertical distance from floor to substernale point at lower edge of breastbone (standing)	48.5 in.
(18)	Thigh circumference: circumference of thigh just below lowest point in gluteal furrow (standing)	23 in.
(19)	Tibiale height: vertical distance from floor to right tibiale (standing)	18 in.
(20)	Trochanteric height: vertical distance from floor to trochanterion on right side (standing)	35.25 in.
(21)	Upper arm length: length of upper arm between acromion and radiale	14 in.
(22)	Weight: nude weight	175 lb
(23)	Waist breadth: minimum horizontal distance between points marking the most lateral indentation in the abdominal region (standing)	12.8 in.
(24)	Waist depth: anterior to posterior distance of the abdomen at the level of the most lateral indentation waist points (standing)	10.4 in.
(25)	Wrist circumference: minimum circumference of wrist, measured with tape just proximal of the styloid process of the ulna	7.25 in.